^PREDICTABILITY OF EAST AFRICAN SEASONAL RAINFALL WITH SEA SURFACE TEMPERATURE GRADIENT MODES *lj*

By

WILLIAM OGALLO NYAKWADA
DEPARTMENT OF METEOROLOGY,
UNIVERSITY OF NAIROBI,
P.O. BOX 30197,
NAIROBI, KENYA

A THESIS SUBMITTED IN FULFILLMENT OF THE REQUIREMENT FOR THE DEGREE OF DOCTOR OF PHILOSOPHY (PHD) IN METEOROLOGY,
UNIVERSITY OF NAIROBI,
KENYA.
JANUARY 2009

DECLARATION

This thesis is my original work and has not been presented for a degree at any other University. / T l f ^ /

Signature: _____ Dat*q*-^*JaJj*^^*X*

William Nyakwada
Department of Meteorology,
University of Nairobi

Signature: _____ Da *vjgjbd&s&l—*

Professor Liglhan A. Ogallo
Department of Meteorology,
University of Nairobi

Signature: 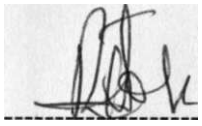 Da, t r & b k s Z l

Dr Raphael E. A. Okoola
Department of Meteorology,
University of Nairobi

DEDICATION

I dedicate this dissertation to my late Father William Nyakwada whom I was not able to meet and share with as a parent, and my mother Wilkister Akinyi Nyakwada who built in me the spirit of determination to achieve my vision of life.

ACKNOWLEDGMENTS

I wish to express, from the depth of my heart, my appreciation for the guidance and useful suggestions provided by my two supervisors, Prof. Laban A. Ogallo and Dr. Raphael E. A. Okoola. Their words of encouragements and guidance throughout the period of my study gave me the energy to soldier on. My sincere gratitude also goes to the Government of the Republic of Kenya who provided me with the financial support to enable me undertake this study. I wish also to appreciate the support, words of encouragement and suggestions I received from Dr. Joseph Romanus Mukabana, the Director of Kenya Meteorological Department. I also wish to record my appreciation to my colleagues Mr. M. Gondwe, Ben Owuor, P.A. Omondi, Mr. Z. O. Owiti, W. Gitau and. Samuel M Mwangi who were available to share their experiences on various software packages used in this Study.

I would not have completed my work if I did not have adequate comfort. I wish to extend my special appreciation to the support I received from my family especially my two wives Anjeline A. Nyakwada and Sylvia Nyakwada, who continued to encourage me throughout the period of my study, and my children who accommodated my late working hours and reduced availability to give the desired parental love.

Finally, I wish to appreciate the contribution of my secretary Catherine Nyaga who was available to assist in typing most of the chapters of this thesis.

TABLE OF CONTENTS

LIST OF FIGURES

LIST OF TABLES

LIST OF ACRONYMS

1	a.m.s.l	Above mean seal level.
2	ACMAD	African Centre for Meteorological Application and Development
3	AGCMs	Atmospheric General Circulation Models
4	AIOD	Atlantic-Indian Ocean Dipole
5	AMSL	Mean Seas Level
6	ANN	Artificial Neural Networking
7	ANOVA	Analysis of Variance
8	ARMEX	Arabian Sea Monsoon Experiment
9	CA	Composite Analysis
10	CCA	Canonical Correlation Analysis
11	COLA	Center for Ocean-Land-Atmosphere
12	CPC	Climate Prediction Center
13	CRED	The centre for research on epidemology of Disastes
14	DIA	Dar es Salaam International Airport
15	DJF	December-January-February
16	DMC	Drought Monitoring Centre
17	EMS	Esselte Map Service
18	ENSO	El Nino Southern Oscillation
19	EOF	Empirical Orthogonal Function
20	FA	Factor Analysis
21	GCM	General Circulation Model
22	GHA	Greater Horn of Africa
23	GOC	Great Ocean Conveyor
24	HFA	Hyogo Framework of Action
25	ICPAC	IGAD Climate Prediction and Applications Centre
26	IDRC	International Development Research Centre
27	IGAD	Intergovernmental Authority on Development
28	IMTR	Institute for Meteorological Training and Research
29	IOD	Indian Ocean Dipole
29	IPCC	Intergovernmental Panel On Clmate Change
30	ISDR	International Strategy for Disaster Reduction
31	ITCZ	Inter-Tropical Convergence Zone
32	KMD	Kenya Meteorological Department
33	LEV	Natural Logarithm Method
34	MAB	Meridional SST gradient modes for the Atlantic Ocean
35	MAM	March - May
36	MIB	Meridional SST gradients modes for the Indian Ocean
37	MISO	Monsoon Intraseasonal Oscillation
38	MJO	Madden-Julian Oscillation
39	NAO	North Atlantic Oscillation
41	NCAR	National Center for Atmospheric Research
42	NCEP	National Centers for Environmental Prediction
43	NMHS	National Meteorological/Hydrological Service

44	NMS	National Meteorological Service
45	OOSDP	Ocean Observing System Development Panel
46	OFDA	The office of U.S Foreign Disaster Assistance
47	OLR	Outgoing Long-Wave Radiation
48	OND	October - November - December
49	OP	Office of the President of the Republic of Kenya
49	PCA	Principal Component Analysis
50	QBO	Quasi-Biennial Oscillation
51	RA	Regression Analysis
52	SADC	Southern Africa Development Community
53	SLP	Sea Level Pressure
54	SOND	September-December
55	SPARC	Stratospheric processes and their role in climate
56	SSTG	Sea Surface Temperature Gradients
57	SST	Sea Surface Temperature
58	TMA	Tanzania Meteorological Agency
59	UMD	Uganda Meteorological Department
60	UNEP	United Nations Environment Programme
61	WCRP	World Climate Research Programme
62	WMO	World Meteorological Organization
63	ZAF	Zonal SST gradient mode for the combined Indian-Atlantic
64	ZIND	Zonal SST gradient mode based on IOD
65	ZPAC	Zonal SST gradient mode for the Pacific Ocean

ABSTRACT

The overall objective of this study is to improve the skills of seasonal rainfall prediction in East Africa through the use of sea surface temperature gradient modes. The sea surface temperature data used to generate the sea surface temperature gradient modes were for the period 1960-2006. The sea surface temperature gradient modes were generated for the Indian, Atlantic and Pacific oceans separately, and for the Indian and Atlantic oceans combined. The study assumed that the combined Indian and Atlantic Ocean sea surface temperature modes could provide other unique predictors that cannot be picked by the Principal Component Analysis modes of the individual oceans. Other data used in the study included monthly station rainfall, global wind and satellite derived outgoing long-wave radiation for the same period 1960-2006. The satellite derived outgoing long-wave radiation data is, however, only available from 1974-2004. The data were quality controlled and normalized using standard methods before they were used in the study.

The methods used in the study included Correlation Analysis, Composite Analysis, Regression Analysis, Canonical Correlation Analysis and Artificial Neural Networks.The sea surface temperature gradient predictors were searched from all standard seasons of the year, namely December-February, March-May, June-August, and September-November, since the best predictor is that associated with sea surface temperature variability that leads seasonal rainfall. Rainfall prediction studies were, however, restricted to the main rainfall seasons of the region that are concentrated within March-May and September-December months.

Quality control analyses indicated that most of the data used in the study were of acceptable quality. The time series analyses of the standardized data indicated inter-annual recurrences of large and low values of anomalies in all records. The large SST anomalies are evident during the El Nino/Southern Oscillation and Indian Ocean dipole years. The extreme high and low rainfall values, on the other hand, reflected the major flood and drought years.

The results from Principal component Analysis of sea surface temperatures indicated that both the Atlantic and Indian Oceans have significant influence on regional rainfall. The first four Principal Component Analysis modes of variability that formed major sources of influence of sea surface temperature on regional rainfall represented ocean wide warming, and zonal and meridional sea surface temperature variability associated with El

Nino/Southern Oscillation, Indian Ocean Dipole, interhemispheric Dipole in the Atlantic Ocean, and the Atlantic-Indian Ocean Dipole.

The extreme phases of the modes are associated with some climate extremes affecting the region linked to El Nino/Southern Oscillation, Indian Ocean Dipole and the Atlantic-Indian Ocean Dipole, among other regional climate systems. There are unique modes that compliment the major modes of variability for the individual seasons. The major modes of sea surface temperature variability for the Atlantic, Indian and Pacific Oceans were used to develop sea surface temperature gradient modes for the individual oceans and the combined Indian-Atlantic Oceans. The study documented for the first time a dipole for the combined Atlantic-Indian Ocean, which may be referred to as Atlantic-Indian Ocean Dipole, which has useful linkage with regional rainfall.

The results from Correlation Analysis indicated that the use of sea surface temperature gradient modes as predictors has advantage over grid point sea surface temperatures and Principal Component Analysis modes, and has the potential to improve seasonal rainfall forecasts for both seasons especially for the March-May season. The highest value of correlation observed with September-December rainfall, and grid-point sea surface temperatures and Principal Component Analysis modes was 0.74 compared to 0.85 observed with the sea surface temperature gradient modes. The September-December rainfall continues to have higher potential of predictability than March-May. The predictors from the Atlantic and Pacific Oceans have longer lead-time than those associated with the Indian Ocean, which achieve peak relationships within the seasons. The use of predictors from the Indian Ocean may require that they be predicted. The relationships observed with rainfall for the months making March-May season are not similar. The zonal modes have stronger relationships with rainfall compared to meridional modes. This may be attributed to the strong influence of the zonal gradients to low-level tropical circulation and convergence in the tropics, and the meridional orientation of the area of study, which favours the incursion of moisture from the easterly/westerly air currents associated with the Indian Ocean/Congo Basin.

Results from composite analysis of rainfall, sea surface temperature, wind and satellite derived outgoing long wave radiation indicated significant linkages amongst some of the extreme phases of sea surface temperature gradient modes and rainfall Principal

component Analysis modes over eastern Africa. The sea surface temperature gradient modes effectively delineated rainfall, wind and satellite derived outgoing long wave radiation indicating that the observed relationships are through their influence on the general circulation, moisture transport and convection. The sea surface temperature gradient mode associated with the Atlantic-Indian Ocean Dipole had the highest capability to delineate March-May rainfall while September-December rainfall could be delineated effectively by the zonal modes associated with both Atlantic-Indian Ocean Dipole and the Indian Ocean Dipole.

The results from regression analysis indicated that the use of sea surface temperature gradient modes would improve the prediction of seasonal rainfall in the region especially for March-May rainfall season. The Heidke Skill Score associated with the models based on sea surface temperature gradient modes was >0.20 indicating the models had useful skills.

Canonical Correlation Analysis results further indicated that the major sources of influence of sea surface temperature on seasonal rainfall were the zonal and meridional sea surface temperature variability, and the basin wide warming/ cooling associated with El Nino Southern Oscillation, Indian Ocean Dipole and interhemispheric dipole in the Atlantic Ocean. The zonal surface temperature variability in the Indian Ocean together with the Interhemispheric Dipole in the Atlantic Ocean provided the highest influence on September-December rainfall but was secondary for March-May. The ocean-wide warming/cooling formed the highest source of sea surface temperature influence on March-May but was secondary for September-December. The results also indicated higher prediction skill for September-December rainfall compared to March-May.

The results from Artificial Neural Networks showed marked improvements in the skills of the models especially for March-May rainfall season compared to regression and canonical correlation analysis methods. The Heidke Skill Score in the training period for both seasons was >0.90 indicating high capability in fitting the models. The Heidke Skill Score for the March-May and September-December models for the verification period were >0.24 indicating the ability of Artificial Neural Networks method in improving the predictability of rainfall especially the March-May season.

This study has developed prediction tools that have improved the skill of seasonal rainfall forecasts for both seasons, especially the major (long) rainfall season of March-May

that most previous studies have had major difficulties in providing operational skilfull seasonal early warning products as observed from the improvements in the values of Heidke Skill Scores.These tools were derived from sea surface temperature gradient modes, as well as the inclusion of some more powerful Artificial Neural Networks and canonical correlation analysis methods. The skillful seasonal forecasts would be useful in reducing and managing the risks associated with seasonal rainfall extremes.They would further provide useful inputs to the improvement of early warnings of extreme rainfall events and contribute to disaster risk reductionand sustainable socio-economic development in the region. Such results would not only provide new climate risk management tools for coping with past and current climate extremes, but also experiences and lessons that can be extended to addressing climate change adaptation challenges.

CHAPTER ONE

1. INTRODUCTION

1.1 BACKGROUND

The availability of water, energy, food and other socio-economic needs in East Africa, like other parts of the world, is influenced by daily weather, and monthly, seasonal, annual and inter-annual climate variability. Most of the natural hazards that often translate into disasters affecting East Africa are related to extreme climate events. Anomalous rainfall events such as droughts and floods are among the extreme climate events with adverse effects on the society and economy of the region. The adverse effects resulting from a single anomalous event can linger on for a long period (ISDR 2006, WMO 2006). The climate anomaly that is most devastating and has widespread impacts is drought as demonstrated in Figures la and lb, and Table 1.

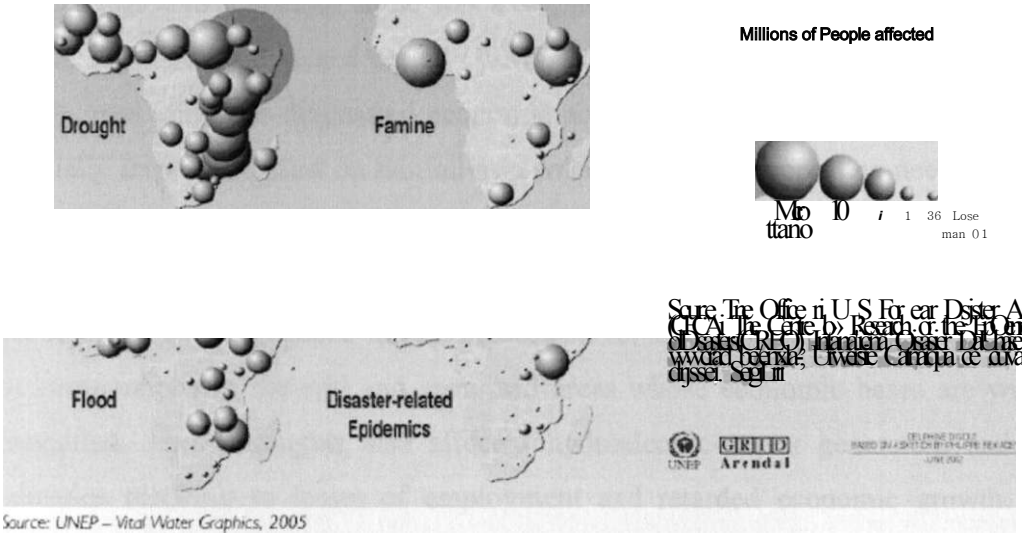

Figure la: People affected by natural disasters in the period 1971-2000 (source: OFDA/CRED, 2006).

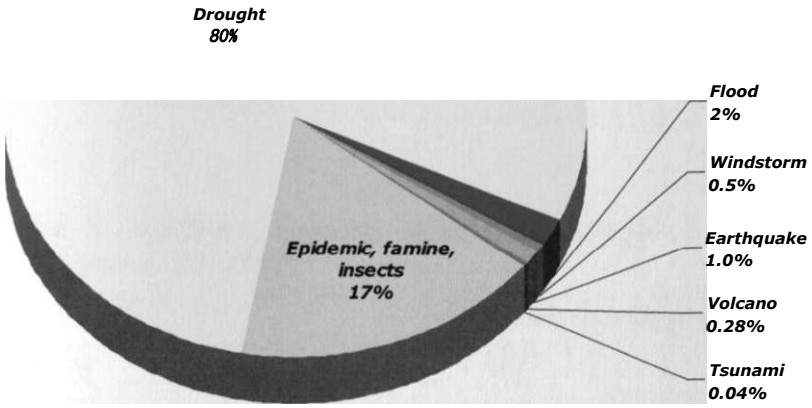

Figure lb: Losses of human life worldwide during the period 1980-2005. (Source: OFDA/CRED 2006).

The analysis of losses of life associated with natural disasters during the period 1980-2005 indicated that drought alone was associated with 80% of the losses of life worldwide (Figure lb) during the stated period (WMO 2006). The groups most vulnerable to drought are the ones with less diversified economic activities leading to weak economic bases and especially those dependent on rainfall as a source of all life supporting needs (Pothergill and Peek 2004).

The droughts of 1983/84, 1999-2000 and 2005-2006 that affected parts of the region, had severe negative impacts, which lingered on for a long time and most adversely affected the communities in the arid and semi-arid areas whose economic bases are weak and not diversified. These droughts also affected hydroelectric-power generation and agro-based industries resulting to losses of employment and retarded economic growth. The social vulnerability to drought is increasing largely because of population growth leading to increased demand and competition for limited water and other natural resources (UNEP 1992). The rapid accumulation of climate-related risks in recent decades and the associated patterns of losses indicate ineffectiveness and even breakdown in spontaneous adaptation and coping (UNDP 2002).

Table 1: Number of people affected by drought in Kenya during the period 1975—2006*(Source: OP 2007)*

Year	**Number of people affected**
1975	16 000
1977	20 000
1980	40 000
1984	200 000
1992	1.5 million
1995-6	1.4 million
1999-2000	4.4 million
2004-6	2.5 million initially to 3.5 million currently estimated

Another natural hazard with adverse effects in the region is floods. The recent heavy rains and the associated floods affecting parts of the region were observed in 1961/62, 1970, 1972, 1977, 1978, 1980, 1982, 1989, 1992, 1994, 1997-1998, 2003/2004, and 2006(0p 2007). These extreme wet conditions have devastating effects on the economy, society and infrastructure of the region as was observed in the listed years when there was extensive damage to property, infrastructure and settlements.

Extreme climate events cannot be stopped from occurring. However, the associated impacts can be mitigated (Namias 1985). The prediction of seasonal climate events is an important component of an early warning. The warnings formulated from the skillful seasonal forecasts may contribute significantly to the prevention of climate related natural disasters, enhanced productivity in sectors dependent on climate (Meza et al. 2008) and efficient management of the institutions dependent on weather and climate (Georgakakos and. Graham 2008). The warnings may also help to reduce the vulnerability of the communities and sectors frequently affected by weather and climate related hazards. The

improvement of the skill of seasonal forecasts is useful in the mitigation of climate related risks and for taking advantage of the positive aspects of the climate extremes.

Most attention to address disasters in the region related to natural hazards has been given to disaster response and relief. Such a reactive approach is not sustainable and cost effective. There is a need to develop systems that are able to forewarn the people in the vulnerable areas to create preparedness and reduce the losses of lives and property.

Some efforts have been made in the region to provide seasonal rainfall forecasts. Most of the past seasonal rainfall prediction efforts for the region have been based on empirical methods using gridpoint sea surface temperature (SST) data (Black et al. 2003; Clark et al. 2003;; Hastenrath 1990,1995; Mutemi 2003; Omondi 2005; Owiti 2005). Even these empirical prediction methods have low prediction skill during the main rainfall season of March-May (MAM) compared to October-December (OND)(Owiti 2005). Some skill for the March-May season with empirical methods was, however, reported by Njau (2006) using tropospheric circulation indices, and Indeje and Semazi (2000) using Quasi-Biennual Oscillation (QBO).

Some studies have used dynamical prediction methods to predict the climate of East Africa (Gorddard and Graham 1999; Goddard et al. 2000; Indeje 2000). Both empirical and dynamical studies have shown good prediction skills mainly during the short rainfall period (October-December months) within the equatorial sector. The models, however, had good skill only at some selected locations in the region. The details of the objective of this study are discussed in the next section.

1.2 OBJECTIVE OF THE STUDY

The overall objective of this study is to improve skills of seasonal rainfall prediction in East Africa through the use of sea surface temperature gradients (SSTG) modes. Improvements in the prediction of seasonal rainfall over the region will contribute to disaster risk reduction and sustainable development efforts of the countries in East Africa.

1.2.1 SPECIFIC OBJECTIVES

In order to accomplish this objective, several specific objectives were developed namely to:

i. Determine SST gradient (SSTG) modes that have significant relationships with rainfall for the specific seasons and locations in East Africa.

ii. Study space-time characteristics and linkages between SSTG modes and seasonal rainfall extremes.

iii. Examine the global/regional climate systems that may be associated with (ii).

iv. Use results from (i) to (iii) to improve seasonal rainfall prediction and early warning tools for the region.

1.3 JUSTIFICATION AND SIGNIFICANCE OF THE STUDY

In this section the climate associated problem that motivated this study and the research questions together with the hypothesis, assumptions and limatations of this study are discussed. The climate associated problem that motivated this study is the significant influence of climate extreme events on the socio-economic activities in East Africa. Most of the social and economic activities in the region are dependent on rainfall. The day-to-day and seasonal characteristics of rainfall, therefore, influence almost all socio-economic sectors of the region. Hence the ability to provide skilful seasonal forecasts is important for disaster preparedness and for enabling the communities to take advantage of the good times. As more evidence confirms the potential of climate change (IPCC 2007; Lee et al. 2006; Wood and Overland 2006), climate forecasts will be important tools for the prevention and mitigation of negative impacts of climate extremes and adaptation to climate shifts (Stewart et al. 2004; Usman et al. 2005).

The sectors such as agriculture and food security, energy, water resources and many others depend on climate and therefore need timely forecasts for efficient management to reduce the impacts of climate extremes, which always snowball to affect many other sectors of the economy. In some cases, droughts are followed by floods, or vice versa, with far reaching implications. Table 2 gives examples of the effects of drought and floods experienced in Kenya during the period 1965 to 2006. It can be observed from Table 2 that droughts and floods are frequent and affect a large number of populations in the country. This example for Kenya represents frequent experiences by other countries in the region and beyond. Rainfall variability plays a major role in agro-based industries as was observed in some studies in India where rainfall accounted for over 50% of groundnut yield (Challinor et. al. 2003).

Climate extremes have also been associated with the outbreak of human and animal diseases as demonstrated in Figures la and lb discussed in section 1.1 above. A number of times the impacts of climate extremes go beyond the capability of an individual country to accommodate leading into a disaster. The region recently experienced El Nino related floods in 1997/98 and 2005/2006. The region also experienced severe droughts in the years 1984, 1999-2000 and 2004-2005, which were very devastating. Some of the regional climate extreme events are associated with teleconnections with processes in the neighbouring global oceansandbeyond.lt is possible to predict climate extreme events (Namias 1985) since some precursor signals are often observed before the occurrence.

Table.2: Number of people in Kenya requiring relief in flood and drought disasters since 1965*{(Source: OP 2007)*

Year	Number of People Needing Relief	Type of Disaster	Year	Number of People Needing Relief	Type of Disaster
1965	260 000	Drought	2000	125 000	Floods
1971	130 000	Drought	2000	2 740 000	Drought
1979	40 000	Drought	2001	3 400 000	Drought
1984	600 000	Drought	2002	60 000	Floods
1992	2 700 000	Drought	2003	45 000	Floods
1993	1 200 000	Drought	2005	3 500 000	Drought
1997	212 000	Floods	2006	Records not yet available	Drought January-August 2006
1998	539 000	Floods	2006	Records not yet available	Floods September-December 2006

Many recent studies have shown significant teleconnections between the Indian and Atlantic Oceans, and East African rainfall (Black et al. 2003; Goddard and Graham 1999; Hastenrath and Polzin 2004; Indeje 2000; Nicholson 1986; Shreck and Semmazzi 2004; Owiti 2005; Omondi 2005). There have been some changes in SST variability and other general circulation parameters that may have far reaching implications on the space -time patterns of the regional extreme rainfall events (An and Wang 2000; Baines and Folland 2007; Harrison and Carson 2007; Wang and An 2001). The climate regime shift of 1976-77 has been associated with the changes in the evolution of El Nino especially with regard to the period, amplitude, spatial structure and temporal characteristics (An and Wang 2000;

Harrison and Carson 2007; Wang and An 2001). The oceans have experienced cooling and warming in the period 1950-2000 (Harrison and Carson 2007; Mokhov et. al. 2004). These shifts in the SST regimes may influence relationships based on specific model training periods due to possible changes in some model statistics. These climate shifts may also influence the characteristics of the global and regional climates.

The continued population growth will force more people to settle in the high disaster prone areas. Parts of the region that are prone to natural disasters such as the lake Victoria Basin have population density as high as 1000 people per square kilometer (Oyaya 1999). Such high population densities need efficient early warning systems to reduce disaster risks and enhance resilience of the communities. Hyogo Framework of Action on Disaster Risk Reduction (HFA) recognizes the importance of early warning systems to disaster risk reduction (ISDR 2005).

This study assumes that the the improvements in seasonal climate forecasts may help in reducing losses of life and property, and risks in sectors dependent on rainfall since the climate forecast is an important component of an early warning system (Alusa 2003; Greenfield and Fisher 2003; Ogallo et al. 2000; Singhrattna et al 2005; WMO 2004). The seasonal climate forecasts remain the most important tools not only for the mitigation of natural climate related disasters, but also for efficient exploitation of natural resources for the improvement of the well-being of the society. However, the skills of seasonal forecasts are generally low especially for the major rainfall season of March-May.

Various efforts have been made in the region to develop models that may be used to forecast seasonal rainfall. Despite these efforts rainfall continues to be the most difficult meteorological element to predict in the East African region due to the complex topography and the large water bodies, which have a strong influence on the temporal and spatial distribution of rainfall (Asnani and Kinuthia 1979). The use of more powerful methods such as Artificial Neural Networks (ANN), whose performance is not dependent on the knowledge of the characteristics of the region of study (Hsieh 2004), may help in improving the forecasts.

Most of the models that are currently being used in the region are based on grid point SST values, which have several limitations including under/over estimation of the extremes and poor performance in some years and at some locations. Several recent studies have

presented significant skill in the use of SST based models. The skills of such models are weak in some areas and seasons. The season with relatively high prediction skill over some parts of the region and for years with large SST anomalies is October -December (OND) (Black et al. 2003; Clark et al. 2003; Omondi 2005; Owiti 2005). The limitations to simulate cross equtorial flow add to the difficulties of predicting rainfall over the region from dynamical models. The efforts to improve the skill of seasonal rainfall forecasts need to be encouraged. The increased frequency and severity of severe weather and climate extreme events such as droughts and floods and the high potential for the occurrence of climate extremes in the region need long lead-time skilful forecasts to enable the policy-makers to make decisions to prepare the communities for the anticipated events. The suffering and damages associated with the 1983/84, 1998-2000 and 2004-2005 droughts, and 1961, 1997/98 and 2006 floods are still fresh in the memories of most of our population. Accurate forecasts would minimize the suffering associated with extreme climate anomalies.

This study recognizes that the sea surface temperature gradients together with the associated pressure gradients have a strong influence on the atmospheric and oceanic circulation Barry and Chorley 1968; Lindzen and Nigam 1987; Shukla 1991).The SST gradient influence the Walker circulation together with the intensities of the individual cells(Lindzen and Nigam 1987). The temperature gradients and the associated pressure gradients are key factors in determining pressure gradients, wind patterns, moisture transport, moisture convergence and divergence patterns, and many other regional circulation patterns that determine rainfall anomalies (Goddard et al 2000; Lindzen and Nigam 1987).

The study hypothesis is that the sea surface temperature gradient modes, through their influence on pressure gradients, and atmospheric and oceanic circulations (Lindzen and Nigam 1987; Stone and Chervin 1984), would better represent the influence of atmospheric and oceanic circulation on seasonal rainfall over the region than the often used grid point SSTs and lead to improvements in relationships between rainfall and SST based predictors. The study also assumes that horizontal atmospheric flows in response to meridional and zonal temperature gradients, which are stronger than the vertical flows(Byers 1959), would account for most of the influence of the general circulation on seasonal rainfall over the region. These assumptions are motivated by the findings of the previous studies, which have shown that meridional and zonal gradients have the highest influence on the general

circulation in the tropics (Lindzen and Nigam 1987; Ward 1998). A more detailed discussion of the properties of SST gradient modes that motivated this study is presented in section 2.2.1.4.

The improvements in the skill of seasonal forecasts would contribute to the desired shift in disaster response with emphasis on disaster risk reduction incorporating preparedness, mitigation and prevention within the context of sustainable development and towards reducing risks and vulnerability to natural disasters (Briceno 2004; ISDR 2005). The importance of seasonal forecasts could be revealed by the increased demand among the rural communities since majority were aware of the risks associated with climate variability (Tarhule and Lamb 2003). An adequate warning leads to preparedness and reduced negative impacts. Timely and accurate climate forecasts together with appropriate coping systems can significantly reduce the vulnerability of a community (Usman 2005) by facilitating easy shifts to new climate condtions and preparedness.

The limitations of the assumptions in this study include the influence of climate change on the developed tools and inability to transfer the models from location to location without calibration.

A review of the literature relevant to this study is discussed in in the next chapter starting with the climatology of the rainfall over East Africa.

CHAPTER TWO

2.0 LITERATURE REVIEW

In this chapter, the literature relevant to this study is reviewed starting with the climatology of rainfall of East Africa.

2.1 THE CLIMATOLOGY OF RAINFALL OVER EAST AFRICA

East Africa has complex spatial and temporal patterns of daily and seasonal precipitation due to the influence of topography and the distribution of water bodies (oceans and lakes) discussed later in section 3.1. Lake Victoria with an area of about 70 000 square kilometers is known to have a strong influence on the climate of the region especially the areas in its neighbourhood (Anyah et al 2006; Asnani and Kinuthia 1979). These areas have a low pressure trough over them throughout the year caused by differential heating between the lake and land, located over the land and lake at daytime and night respectively (Asnani and Kinuthia 1979). The presence of the trough renders these areas to have no distinct season of rainfall and have rainfall almost throughout the year. The two major rainfall seasons of the region are March-May (MAM) and October-December (OND). The average amount of rainfall received in MAM is higher than in OND at most locations (Hastenrath et al 1993). However, OND exhibits higher interannual variability than MAM (Agumba 1985; Behera et al. 2005; Black et al. 2003; Clark et al. 2003; Hastenrath et al 1993). The IGAD Climate Prediction and Applications Centre (ICPAC) include the month of September in operational seasonal forecasts to have the season as September-December (SOND) (ICPAC 2006), which was adopted in this study.

There are also marked differences in the potential of experiencing climate extreme events in both seasons with the potential for experiencing the deficient and excess rainfall being highest at most locations during OND rainfall season (Nyakwada 2003). The differences in the average rainfall amounts associated with MAM and OND seasons have been attributed to the differences in the sea surface temperatures of Indian Ocean associated with the two seasons (Figure 4) with OND being cooler than MAM due to persistent cold SSTs in the western Indian Ocean during September-October-November (Behera et al.2005) as a result of coastal upwelling linked to northern summer monsoons.

The major synoptic features that influence the weather of the region are the Inter-tropical Convergence Zone (ITCZ), subtropical anticyclones (Mascarene, Azores, Arabian and St Helena), the tropical easterly/westerly waves, monsoons and the tropical depressions/cyclones (Ogallo 1993). The climate of the region is also affected, through teleconnections, by sea surface temperature (SSTs) over the global Oceans, El Nino/ Southern Oscillation (ENSO), Quasi-Biennial Oscillation (QBO) and the Madden-Julian Oscillation (MJO) (Ogallo 1988b; Ogallo et al 1988;1994; Omeny 2006). The Brewer-Dopson circulation discussed in section 2.1.9, through its influence on Hadley circulation and tropical convection (Salby and Callaghan 2005), may have significant influence on regional rainfall. Figures 2a and 2b give the mean atmosperic circulation for the months of January and July/August together with the associated synoptic systems.

Recent studies (Anyah et al. 2006; Black et al. 2003; Owiti 2005; Saji et al. 1999) observed significant relationships between regional rainfall and the Indian Ocean Dipole (IOD). The SOND rainfall over most parts of the region is likely to be enhanced during the positive phase of IOD (Black et al. 2003; Owiti 2005). El Nino/Southem Oscillation (ENSO) influences the rainfall over the region (Wang and Eeltahir 1999; Ogallo and Suleiman 1987; Roplewski and Halpert 1989). The region also experiences non-ENSO related climate extremes (Behera et al.2005; Saji and Yamagata 2003) as was observed in 1961 that may be associated with anomalous surface and mid-tropospheric flow from northwestern Atlantic Ocean and eastern flow from the Indian ocean (Anyah and Semazzi 2006).

The details of the effect of Sea surface Temperature (SST), El-Nino-Southern Oscillation (ENSO), Quasi-biennual Oscillation (QBO) and Madden-Julian Oscillation (MJO) are discussed later in this chapter after discussing the major synoptic features affecting the climate of the region.

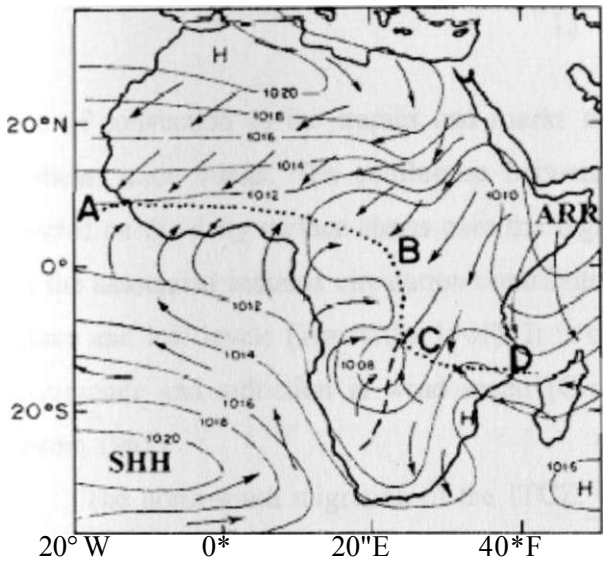

Figure 2a: The mean atmospheric circulation for the month of January (ARR-Arabian Ridge, SHH-St Helena High Pressure, H over north Africa-Azore High, and H over the southern Indian Ocean -Mascarine High pressure systems) (Adopted from Okoola 1996)

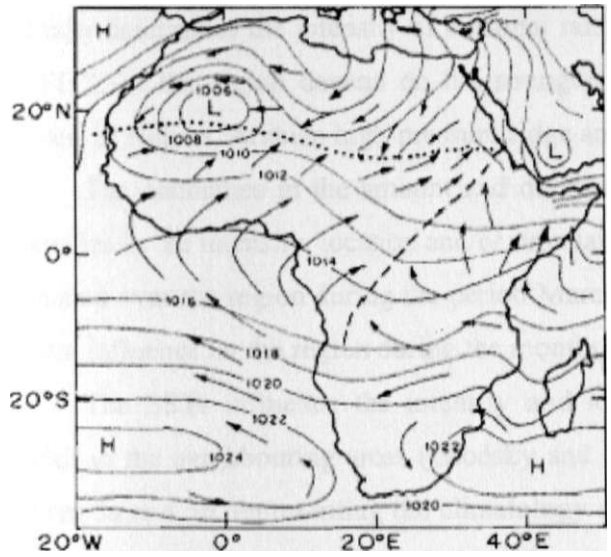

Figure 2b: The mean atmospheric circulation for the months of July/August (Adopted from Okoola 1996)

2.1.1 INTER-TROPICAL CONVERGENCE ZONE

The Inter-Tropical Convergence Zone (ITCZ) is the single most important system controlling the seasonal rainfall of East Africa(Asnani 1982; 1993). The ITCZ is a prominent

zone of convection in the tropics and marks the convergence between the northeast and southeast trade winds. The confluence between these winds is diffuse and may not be detected on the daily surface charts over the region. The complex topography, water bodies and the associated induced circulation contribute to the diffuse structure of the ITCZ at the surface and low levels (Trawartha 1961). It is observed as a narrow band of surface wind convergence and reduction in wind speed (Grodskey and carton 2003; Thompson 1957; Sansom 1965).

The north-south migration of the ITCZ, which lags the sun by three to four weeks, makes parts of the regions near the equator to have two rainfall seasons and those far from the equator to have one rainfall season (EAMD 1962; Griffith 1958; Ogallo 1987b). The abrupt migration of the ITCZ has- been associated with the nonlinear meridional advection of angular momentum by the circulation and ocean thermal inertia (Xian and Miller 2008). Its intensity determines the intensity of seasonal rainfall. The surface location and intensity of the ITCZ in the region depend on the strengths of the subtropical high-pressure systems, Azores, St Helena, Arabian high-pressure ridge and the Mascarine.

The anomalies in the amount and distribution of rainfall have been associated with anomalies in the intensity, location and/or orientation of the ITCZ (Ogallo 1987b). The ITCZ is located over the region during the period March- May and October-December and has the highest influence on the region during the months of April and November (Anyamba 1993).

The SSTs influence the intensity and location of ITCZ over the oceans and the rainfall in the neighbouring areas (Grodsky and Carton 2003; Hastenrath and Heller 1977). Figures 3a and 3b, representing the climatology of the SST over the Equatorial Atlantic and Indian Ocean, indicates that the periods when the ITCZ is located over the region and has maximum influence on rainfall coincide with the peaks in the SST variability in the equatorial Atlantic and Indian Ocean. The largest peaks in the SSTs for both oceans are observed in the months of April and November, which are the peak rainfall months for the March-May and October-December rainfall seasons, respectively. It can be observed from Figure 3 that, for both oceans, the period March-May is warmer than October-December. Sadler et al. (1987) made similar observations. Behera et al. (2005) attributed the differences in seasonal SSTs for the western Indian Ocean to coastal upwelling associated to northern summer monsoons over the Indian Ocean.

The north-south migration of the ITCZ involves the alternate advancing and retreating of monsoon winds. It is located furthest north and south during the periods June-August and December-February respectively. The ITCZ has the maximum influence over the region in the months of April and November (Anyamba 1993).

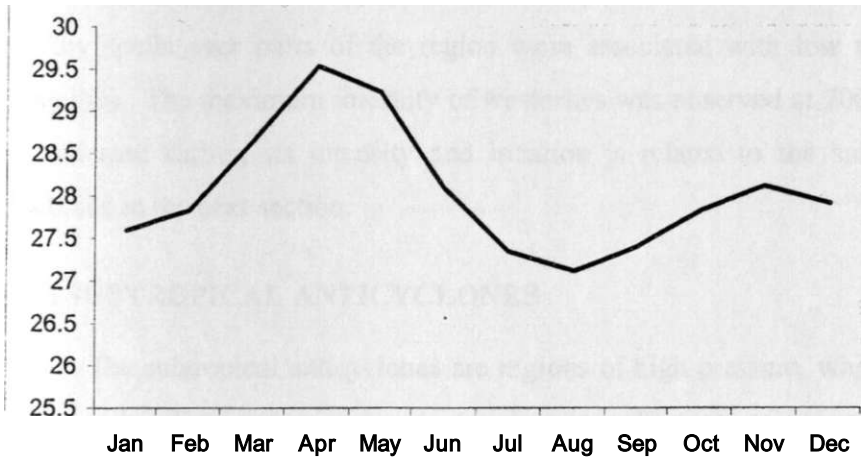

Figure 3a: Long-term mean monthly sea surface temperature over the equatorial Indian Ocean generated from NCEP/NCAR reanalysis sea surface temperature data for the period 1960-2006 for the region 5°N-5°S, 40°E-70°E.

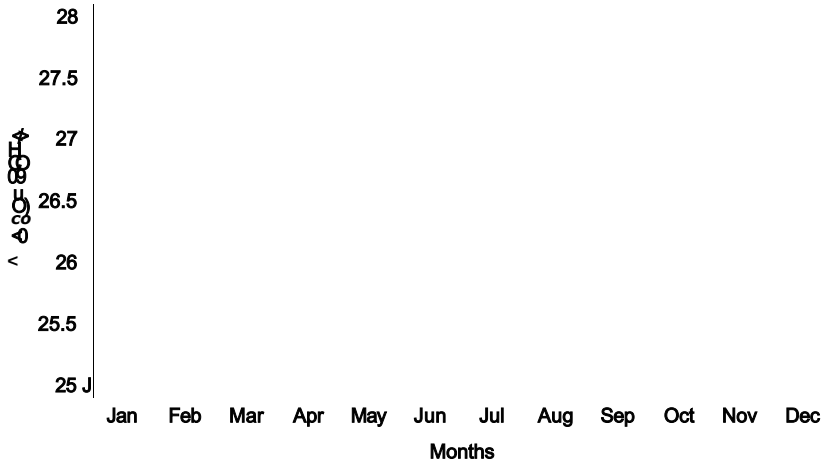

Figure 3b: Long-term mean monthly sea surface temperature over the equatorial Atlantic Ocean generated from NCEP/NCAR reanalysis sea surface temperature data for the period 1960-2006 for the region 5°N-5°S, 35°W-15°W.

The annual oscillation of ITCZ causes the onset and withdrawal of seasonal rains in the region. The intensity, location and the date of arrival of the ITCZ influence the seasonal rainfall performance. There are large inter-annual variations in the position and intensity of the ITCZ leading to large variations in seasonal rainfall. The study of Okoola (1996) concentrated on March - May rainfall season and the results indicated that the anomalously wet/dry spells over parts of the region were associated with low to mid-level westerlies /easterlies. The maximum intensity of westerlies was observed at 700hPa level. However, as indicated earlier, its intensity and location is related to the sub-tropical anticyclones discussed in the next section.

2.1.2 SUBTROPICAL ANTICYCLONES

The subtropical anticyclones are regions of high pressure, which form the sources of trade winds. They act as pumps of moisture into the areas of convergence. Their location and intensity influence the seasonal rainfall performance in a region. The subtropical anticyclones with significant influence on the climate of the region include the Azores (in the Northern Atlantic Ocean), St. Helena (in the Southern Atlantic Ocean), the Mascarine (in the Southern Indian Ocean) and the Arabian High Pressure Ridge (in the Arabian Sea)(Figure 2a). It should be noted that the Arabian High Pressure Ridge is an extension of the Siberian High Pressure. The location of the Arabian High Pressure Ridge oscillates between the African continent and the Arabian Sea. The Maritime location is favourable for rainfall occurrence in the region. The Arabian Ridge is fully developed during southern summer in the period December-February. It is mainly associated with the difluence flow over the region creating mainly dry conditions in the eastern sector of the region.

The Mascarine high pressure is a major pump of moisture into the region. It is at its strongest during the Southern Winter (June-August) when it is associated with the East African High Pressure Ridge, which render the wind flow over Eastern Africa mainly diffluent at lower levels. It is also associated with the East Africa Low Level Jet (Findlater 1969a, 1969b, 1974). The sea surface temperature anomalies over the south East Indian Ocean in southern summer associated with the Mascarine pulses have been suggested to be the precursors of ENSO events (Terray and Dominiak 2005).

The St. Helena High Pressure is an important pump of moisture into the region from the Congo Basin. The Congo Basin is an important source of moisture for Uganda and the Western parts of Kenya and Tanzania. These areas receive significant rainfall during the period June-August when the subtropical Anticyclones in the southern hemisphere are fully developed.

The Azores High Pressure is useful in the enhancement of the convergence in the region. The dry northwesterly winds associated with the Azores subtropical anticyclone converge with the north easterlies from a maritime Arabian Ridge and enhance moisture convergence and rainfall in the meridional arm of the Inter-tropical Convergence Zone. All these anticyclones are influenced by the fluctuations in the surface temperature that affect the density of the overlying air.

The sub-tropical anticyclones and the ITCZ influence the mean wind flow in the region. The intensities, orientation and locations of the subtropical anticyclones together with the locations of the convergence zones dictate the mean flow of the air currents. The Azores and the Arabian ridge are generally associated with dry and continental air currents. However, at times the Arabian Ridge is located over the ocean and enhances moisture incursion into the region. St. Helena and Mascarine are associated with moist air currents. The intensification of Mascarine and St. Helena is associated with enhanced rainfall activity in the region (Ogallo 1987b). Seagar et al. (2003) using idealized model indicated that the subtropical anticyclones form as a response to monsoon heating over land but need further amplification to bring them up to the observed strengths. When the subtropical anticyclones are well developed during the local winter, the equator ward flow to the east of the anticyclone tends to cool the sea surface temperature and the pole ward flow on the western parts tends to warm the SSTs (Seagar et al 2003). The amplifications of the anticyclones through air-sea interactions contribute to there strengthening to the observed seasonal strengths (Seagar et al 2003). The South Indian Ocean Anticyclone is amplified in the developing El-Nino phases and decays toward the mature phase of El Nino (Wang et al 2003).

The monsoons associated with the subtropical anticyclones and the location of the ITCZ are discussed in the next section

2.1.3 MONSOONS

The climate of the region is influenced by the northeast and southeast monsoons, which are experienced during southern and northern summer respectively. During the period March-May and October-December both southeast and northeast monsoon exist with one withdrawing and the other advancing. The northeast monsoons are generally continental, dry, shallow and diffluent (Anyamba 1983; Findlater 1971). They enter the region in a northeasterly direction. They, however, develop into two air currents over northern Kenya. One air current flows southward along the East African Coast. The other air current flows into Uganda, Southern Sudan and Eastern parts of the Democratic Republic of the Congo(Anyamba 1983; 1993). The southeast/southwest monsoon is stronger than the northeast monsoon. It enters the region as southeasterly air current and leaves as southwesterly air current. It develops into two air currents over the Coastal Plains of Kenya and Tanzania.

The air current flowing to the west over Tanzania meets the Congo Basin air current over the western parts of Tanzania. The westward air current over Kenya meets with the Congo Basin air current over the western Highlands. The east-west fluctuations of the surface location of the Congo Basin air current boundary reflect the fluctuations in the intensities of the Atlantic and Indian Ocean anticyclones (Anyamba 1983; 1993). Anyamba (1983) gives a detailed analysis of the monsoon air currents affecting the region.

The southeast monsoon, which occurs during northern summer, is associated with the East African Low Level Jet (Findlater 1969a; 1969b), which is a major feature of this air current. The Jet plays a significant role in the northward transport of mass and energy (Findlator 1969b). It originates from around Mauritius and Madagascar, and continues northward along the East African Coast to Somalia and then towards Indian Subcontinent. The location of the core is about 1.5km above mean seas level (AMSL) with the mean speeds of 12.5ms^{-1}. The Jet is estimated to be 200-400km wide 500-1000m long and 1km in depth. It has large diurnal and seasonal variations. The afternoon speeds are about two thirds of the morning speeds (Ngara 1977).

The full establishment of the northeast and southeast monsoons is generally associated with the dry weather conditions over the region due to the low-level difluence associated with the Arabian and east African high-pressure ridges. However, some parts of

western Kenya, eastern Uganda and Coastal areas receive significant rainfall (Tomsett 1969). Some parts of Western Kenya and Uganda benefit from the incursion of the Congo basin air mass. The coastal areas benefit from the convergence in the coastal trough. The Indian Ocean Monsoon unlike those in the Atlantic and Pacific Oceans are characterized with a complete reversal in inter-hemispheric temperature gradients and cross-equatorial airstreams between the winter and summer hemispheres.

During the transition period, surface westerly airstreams dominate the central Indian Ocean associated with the east-west pressure gradient (Hastenrath and Polzin 2004). The east-west pressure gradient in the Indian Ocean is strongest during the period June-August and influences the latitude of curvature of monsoon wind current making the periods March-May and September-November to be Favourable for the development of equatorial westerlies in the central Indian Ocean associated with flooding a long the cost of East Africa in October-December (Hastenrath and Polzin 2004).The studies of Asia-Austria monsoons (Wang et al 2003) have indicated that the intensity of monsoon over the Indian ocean are influenced by ENSO events with El-Nino/La-Nina leading to the weakening /enhancement of the monsoons.

The strongest weakening of the low level winds and vertical motion is observed in the fall of El Nino (Wang et al 2003). From the development to the decay of El Nino the largest variability of Asian-Australian Monsoon system shifts from the tropical southern Indian Ocean to the Western North Pacific (Wang et al 2003). Anomalous sea level pressure 850hPa winds and 500 hPa vertical motion are experienced in the region 10°S-10°N, 40°E" 160°E during the summer of El-Nino development and are reversed in the summer of El-Nino decay (Wang et al 2003). Monsoon regimes are associated with large-scale ascent and higher humidity that may lead to more frequent but weaker cloud cells (May and Ballinger 2007) and are influenced by the atmosphere-ocean interactions (Fu et al. 2002). Rao (2005) gives an overview of the Arabian Sea Monsoon Experiment (ARMEX) and one of the observations from the analysis was that the ocean plays a key role in regulating the monsoon but is at the same time impacted on by it through the influence on SST.

Recent studies indicate that climate change may lead to variations in the monsoon patterns and the associated climates (Fu et al. 2007; Patricola and Cook 2007). Such changes may have far reaching social and economic impacts especially in the countries where climate

plays a major role in economic development. However, climate change may not influence monsoon-ENSO relationships (Annamalai et al. 2007). The predictability of monsoon intraseasonal oscillation (MISO) is higher over the Indian Ocean (10°S-30 °N, 60°E -160°E) than over the Pacific Ocean (Fu et al. 2007) and MISO could be predicted up to 35 days using atmospheric ocean coupled model.More information on the monsoons of East Africa may be obtained from Anyamba (1983); Asnani (1982); Findlator (1969a; 1969b; 1971) and Okoola (1996).

In the next section, the easterly and westerly waves are discussed.

2.1.4 EASTERLY AND WESTERLY WAVES

The easterly waves are westward propagating wavelike perturbations within the easterly current. They are observed equator-ward of the subtropical high-pressure belts in the neighbourhood of the ITCZ and associated with the origin of tropical cyclones. Their conditions at a specific location will depend on whether it is the location of origin, enhancement or decay. Easterly waves forming in the Pacific have been observed to cross the Indian Subcontinent into the Arabian Sea and weaken towards the Western Arabian Sea (Asnani 1993). The arrival of an easterly wave is recognized by the disturbance of the weather condition and changes in the surface pressure.

While most studies have addressed northern summer easterly waves, it is believed that easterly waves also occur in Southern Hemisphere (Asnani 1993). Asnani (1993) gives a detailed discussion of tropical easterly waves. They have been observed in the Indian Ocean (Cadet and Olory-Togbe 1977). The easterly waves are known to influence the weather of the region. Most of the influence is felt along the coast (Fremming 1970; Gichuiya 1970; Lumb 1966; Njau 1982).

Eastward and westward propagating waves have been observed along the equator in the Atlantic and the westward propagating waves are associated with the meridional oscillation of the equatorial undercurrent about the equator presumably induced by a tropical instability waves (TIW) (Kate 1997). The TIW have also been observed in the Pacific Ocean and have a strong influence on wind currents and rainfall (Jochum et al. 2007).

Another westerly wave with significant influence on rainfall is the Madden-Julian Oscillation (MJO). The MJO, which consists of pulses of strong winds and pressure surges,

has a-strong influence on regional rainfall (Burroughs 1999; Matthews 2000; Omeny 2006). The MJO is at its strongest during the months of December and May (Burroughs 1999). Enhanced MJO activity in Western Pacific in spring is associated with an eastward-expanded warm pool and low frequency westerly surface zonal wind anomalies, which favour the development of El Nino (Hendon et al. 2007). The most favoured location for formation of primary MJO is the Indian and maritime continent of western Pacific oceans (Matthews 2008).

The next subsection discusses tropical cyclones, which are amongst the synoptic features with significant influence on the rainfall of the region.

2.1.5 TROPICAL CYCLONES

Tropical Cyclones affecting the region form in the Arabian and southwestern Indian Ocean. They form in the Arabian Sea region during the period March-May) and in the southern Indian Ocean during the period December-February. The tropical cyclone days over Indian Ocean contains prominent decadal cycles, higher frequencies linked to QBO and had positive relationships with SSTs over the entire south west Indian Ocean from September to March (Jury et al. 1999). Burroughs (1999) suggested the possibility of association between the occurrence of tropical cyclones and the Madden-Julian Oscillation (MJO). The MJO has a strong influence on the development of tropical cyclones in the Australian region (Hall et al. 2001). The increase in SSTs and reduction in the vertical wind shear in areas where tropical cyclone form may lead to increased Tropical Cyclone activities (Eisner 2003). The tropical cyclones are associated with the devastating impacts over southern Africa. Even though no significant trend has been observed in the occurrence of tropical cyclones, there has been a significant increase in the impacts of the hazards associated with tropical cycle, which may be attributed to the increase in population (Raghavan and Rajesh 2003).

The effects of tropical cyclones on weather and climate of the region depend on the time of the year, location of the cyclone and the associated large-scale flow (Anyamba 1984, 1993). The cyclones in the Arabian Sea enhance rainfall along the coast of Kenya. The cyclones that move to the Mozambique Channel can have adverse effects on weather and climate of the region in March-May as was observed in 1984 when deficient seasonal rainfall was attributed to the occurrence of tropical cyclones in the channel (Anyamba 1993).

The cyclones in the Mozambique Channel during March-May season induce low-level diffluent flow in the region (Anyamba 1993). However, the cyclones in the Mozambique Channel during the months of December and January tend to enhance rainfall and are often associated with floods affecting the region during the period. They are characterized with the increase in pressure gradient between northern Africa and Atlantic Ocean and Southwest Indian Ocean resulting to moist westerlies convergence over the region as was observed in 1961/62 and 1992/93 (Anyamba 1993).

It can, therefore, be concluded that the influence of the tropical cyclones on rainfall of the region depends on the season, track and location of the cyclones. The tropical cyclones can either enhance or reduce rainfall depending on the above characteristics. The observed increases in the trends of occurrence of tropical cyclone over the southern Indian ocean with central pressure < 945hPa (Kuleshov et al. 2008), may have signiginfiant impact on the rainfall over the region. The previous section had discussed the synoptic systems that influence the rainfall of the region. It should be noted that the global SSTs have a strong influence on the rainfall of the region.

The SSTs over the global oceans, which influence the occurrence of tropical cyclones and climates of the region, respond to El Nino - Southern Oscillation (ENSO) phenomenon discussed in the next section.

2.1.6 EL NINO /SOUTHERN OSCILLATION

El Nino/Southern Oscillation (ENSO) is the single most prominent mode of climate variability at seasonal to interannual time scales that influence the global atmospheric circulation and its impacts on regional climates depend on the region and season, and the strength and spatial distribution of the associated SST anomalies (Clark et al. 2003; Colberg and Reason 2004; Gorddard et al. 2000; Kane 1998; Lau 1985; Wassila et al 1999; Wolter 1989). The influence of ENSO on climate is associated with its disruption of the general circulation and influence on sea surface temperatures (SST) (Annamalai et al.2007; Chevrin and Druyan 1984; Colberg and Reason 2004; Krishnamurthy and Kirtman 2003; Kug et al. 2006; Kug and Kang 2006; Ort and Yienger 1996; Rao et al. 2007; Schreck and Semazzi 2004; Tanaka et al. 2004). ENSO has a strong influence on trade winds (Colberg and Reason 2004) and climate of the region (Ogallo and Suleiman 1987; Ogallo 1987b; Ropelewski and

Halpert 1987; Wassila 1999; Wang and Eltahir 1999). El Nino has been observed to weaken the Hadley circulation (Colberg and Reason 2004; Rao et al. 2007).

ENSO has significant influence on rainfall over Eastern Africa (Indeje 2000; Indeje et al 2000; Korecha and Barnston 2007; Nicholson and ECim 1997; Schreck and Semmazzi 2004). El Nino is associated with enhanced seasonal rainfall over the region especially during the OND season (Indeje 2000; Nicholson and Kim 1997; Njau 1987; Ogallo and Suleiman 1987; Ropelewski and Halpert 1989; Schreck and Semmazzi 2004) and the cold phase (La Nina) is associated with deficient seasonal rainfall over parts of the region (Ropelewski and Halpert 1989). ENSO also influences the onset, secession and the peaks of seasonal rainfall (Indeje 2000).

The magnitude, seasonal timing, duration and consistency of the response of rainfall to ENSO varied from place to place and from episode to episode (Nicholson and Kim 1997). Njau (1987) observed that most of the severe droughts over Kenya were experienced in March-May rainfall season preceding El-Nino event and rarely in March-May following El-Nino peak in December.The Southern Oscillation, which is the atmospheric component of ENSO, is associated with changes in sea surface pressure gradients that influence the climate of the region (Hastenrath et al. 1993).

The high SO phase is associated with high and low pressure over the western and eastern Indian Ocean, respectively (Hastenrath et al. 1993) resulting to enhanced westerly and cooling over the western parts of the ocean. The negative phase has the opposite effect leading to enhanced rainfall over the western Indian Ocean and East Africa (Hastenrath et al. 1993).

ENSO is linked to the Indian Ocean variability through the modulation of walker circulation (Krishnamurty and Kirtman 2003; Kug et al. 2005; 2006; Xie et al. 2002). The SSTs over the southern Indian Ocean during the DJF have been observed, since the 1976-1977 climate shift in the Indian and Pacific Oceans, to be good predictors of El Nino (Terray and Dominiak 2005). Kug et al (2006) using a Center for Ocean-Land-Atmosphere Studies (COLA) interactive ensemble coupled model observed that El Nino events accompanied with anomalously warm Indian Ocean terminated and translated to La Nina rapidly due to upwelling in the western Pacific Ocean resulting from anomalous easterlies induced by anomalous warm Indian ocean.

The low-level circulation pattern associated with the above-normal rainfall over the region is dominated by easterly inflow from the Indian Ocean and westerly inflow from the Congo tropical rain forest into the positive rainfall region (Anyah and Semazzi 2006; Indeje 2000; Schreck and Semazzi 2004).The significant influence of ENSO on climate has motivated studies exploring its use as a predictor of climate in the region and beyond. The approaches that use ENSO as a predictor start by forecasting ENSO and follow it with possible impacts, which depend on the strength of ENSO (Colberg and Reason 2004; Leetmaa 2003; Wassila et al. 1999; Wang and Eltahir 1999; Zebiak 2003).

Another SST related phenomenon with marked influence on the climate of the region is the Indian Ocean Dipole (IOD) discussed in the next section.

2.1.7 INDIAN OCEAN DIPOLE

The Indian Ocean Dipole (IOD) and the related Indian Ocean Zonal Mode are SST modes that have been observed to have significant influence on rainfall over the region and other areas neighbouring the Indian Ocean (Ajayamohan and Rao 2008; Behera et al. 2005; Black et al. 2003; Clark et al. 2003; Meyers et al. 2007 ;Owiti 2005; Omondi 2005). The IOD is caused by air-sea interactions in the tropical Indian Ocean leading to the warming/cooling of western/eastern tropical Indian Ocean during the positive/negative phases resulting into the reversal of Sea Surface temperature gradients and changes in the zonal wind currents (Black et al. 2003; Behera et al. 2005; Clark et al. 2003; Murtugunde et al. 2000; Owiti 2005; Saji et al. 1999; Saji and Yamagata 2003; Webster et al. 1999; Yu and Riennecker 2000).

The warm/cool western/eastern Indian Ocean is associated with enhanced/deficient OND seasonal rainfall over the region (Behera et al. 2005; Black et al. 2003; Clark et al. 2003; Owiti 2005; Saji and Yamagata 2003) resulting from the anomalous changes in Walker circulation that lead to anomalous moisture transport and convergence (Behera et. 2005). The influence of the IOD on rainfall over the region is much higher than that associated with ENSO (Behera et al. 2005), is strongest with the OND rainfall (Owiti 2005) and outweighs that of ENSO (Behera et al. 2005). However, ENSO events that co-occur with IOD events are stronger than those that occur independently (Saji and Yamagata 2003; Song et al. 2007). Similarly the IOD events that co-occur with ENSO events are stronger than those that occur

independently (Song et al. 2007). Behera et al.(2005) suggested a possibility of a secondary influence on short rains from a regional mode located near the East African Coast

The processes associated with the occurrence of IOD and the ENSO linkages have generated a lot of research (Meyers et al. 2007; Tozuka et al. 2007). Some studies have indicated that the IOD is not related to ENSO (Saji and Yamagata 2003; Song et al.2007) while some have indicated some relationships (Huang and Shukla; 2007; Tozuka et al. 2007) and some have indicated that some events are independent from ENSO but some co-occur with ENSO (Ihara et al. 2008). The Indian Ocean Dipole (IOD) is another SST related predictor of seasonal rainfall that has given useful skill over parts of the region (Behera et al. 2005; Owiti 2005).

The spatial and temporal variations of the global SSTs are influenced by, amongst other systems, the Great Ocean Conveyor and Ocean Waves discussed in the next section.

2.1.8 THE GREAT OCEAN CONVEYOR AND OCEAN WAVES

Wave patterns dominate the movement of water mass and heat energy, and may influence global climate (Burroughs 1999; Katz 1997; WMO 1999). The wave - induced mixing influence SSTs and may play an important role in regulating temperature distribution in the upper ocean and the evolution of ENSO (England and Huang, 2005; Nagura et al. 2008; Qiao et al. 2004). The amount of heat transported around by atmospheric and oceanic currents plays an important role in determining the mean climate of any region on earth (Shukla 1991; Wunsch and Heimbach 2006) and the ocean waves have significant influence on Sea Surface Temperatures (SSTs) (Hashizume et al. 2003; Jochum et al. 2007; Qiao et al 2004; Marmorino et al. 2004; Valsala and Ikeda 2007 ; Zang and Gottschalk 2002).

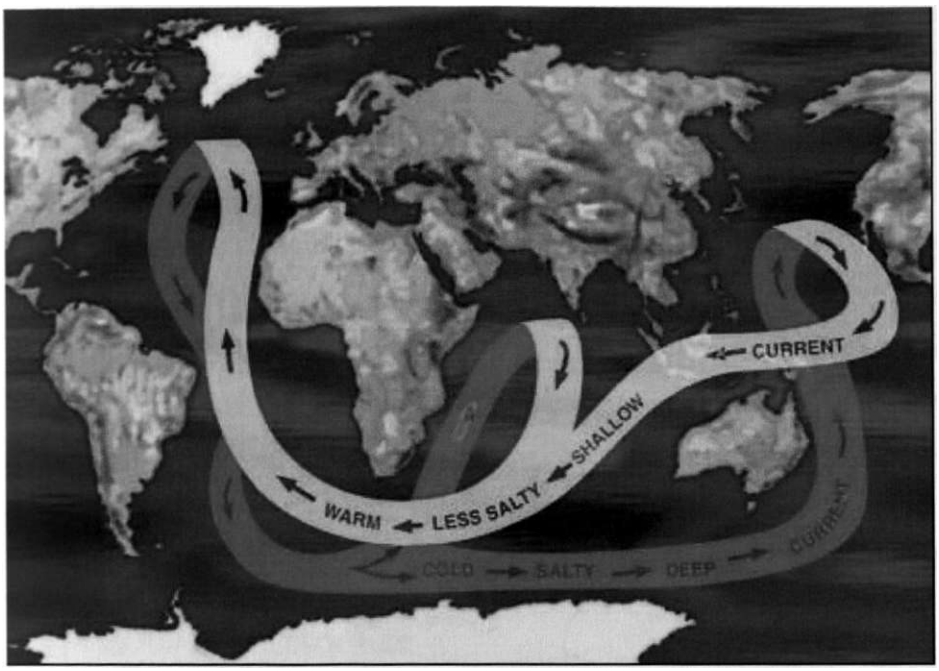

Figure 4: The great ocean conveyor showing warm waters moving from the Indian and Pacific Oceans and cold waters moving from the northern Atlantic Ocean to the Indian and Pacific Oceans (Gross 1972).

Figure 4 gives a representation of the Great Ocean Conveyor (GOC). The GOC consists of ocean currents (large-scale movements of water) caused mainly by wind currents, and unequal heating and cooling of ocean waters (Gross 1972; Saenko et al. 2002). The GOC transports warm and low salinity water from the tropical Pacific and Indian oceans round South Africa to north Atlantic near Iceland (Burroughs 1999). The Atlantic carries more heat northward than does the Pacific and the Indian Ocean (Burroughs 1999) and the southern Atlantic Ocean has significant influence on the SSTs of tropical Atlantic Ocean (Hickey and Weaver 2004). The Indian Ocean makes negligible contribution to heat transport because it extends only a short distance northward (Burroughs 1999).

The GOC and the associated currents influence the global climate patterns through ocean-atmosphere interactions and any change in the path or strength of the GOC may influence the climate around the world (Burroughs 1999; Dong and Kelly 2004; Stouffer et al. 2007; WMO 1999). Similarly, the changes in climate may affect the GOC (Cai and Cowan 2007; Keller et al. 2007) since the ocean currents are highly influenced by surface wind currents (Fratantoni et al. 2000). The ozone depletion may lead to the strengthening of

ocean currents (Cai and Cowan 2007) with possible impacts on the general circulation and climate.

The strong association between ocean currents and climate has stimulated research to establish their influence on regional climates (Burhanuddin 2004; Cai and Cowan 2007; Keller et al. 2007; Valsala and Ikeda 2007). This study emphasizes the importance of the ocean currents and the associated SST gradients in the study of climate variability and prediction. Significant linkages have been observed between the processes in the strasphere and climate.

In the next section a brief review of Brewer-Dobson Circulation climate linkage are discussed.

2.1.9 BREWER-DOBSON CIRCULATION.

The residual mean circulation of the stratosphere also referred to as the Brewer-Dobson circulation (BD), involves downwelling over the winter pole and upwelling at subpolar latitudes (Brewer 1949; Salby and Callaghan 2005). The intensification of BD has been associated with enhanced Hadley Circulation and organized convection (Salby and Callaghan 2005). The enhanced vertical motion associated with DB is achieved through anomalous divergence in the tropical upper troposphere and downwelling in the Arctic stratosphere. Tropical circulation in response to the processes in the stratosphere leads to organized convection in the tropics and account for about 40% of the interannual variance of tropical divergence.

The BD, through interactions with processes in the troposphere and its influence on ozone transport has significant influence on climate including its predictability (Salby and Callaghan 2005; Weber et al. 2007; WCRP 2005). These likages have motivated more research to better understand the process and its contribution to climate prediction (WCRP 2005).

The methods used in climate prediction may be classified into three major categories namely statistical, dynamical and statistical-dynamical (hybrid) (Barnston et al. 1994; Carson 1998; Goddard et el. 2000; Hastenrath 1986; 1995; Tang et al. 2000). The next section discusses statistical methods.

2.2 STATISTICAL METHODS

Statistical methods are the most frequently used in seasonal climate prediction in the region (Anderson et al 1999; Carson 1998; Eldaw et al. 2003, Folland et al 2001; Indeje and Semazzi 2000; Kinuthia et al. 1988; Mungai and Mukabana 2003; Nicholson and Kim 1997; Ntale et al.2003; Stockdale et al. 2006; Swiers and Storch 2004). These methods have played a key role in forecasting weather and climate on timescales ranging from hours to several seasons and are moderately successful in parts of the world where there are teleconnections between the ocean surface and the atmosphere (Zwiers and Von Storch 2004). Statistical methods are not deterministic but provide an estimate of atmospheric seasonal anomaly that is likely to occur (Carson 1998; Greischar and Hastenrath 2000). The use of these methods is motivated by simplicity, the ability to address only a component of a climate system and inability to conduct a laboratory experiment with the earth system (Swiers and Storch 2004).

The major assumption of statistical methods is that the past statistical relations inherent in the training data sets will be maintained in the future. This assumption may not be sustained in event of climate change leading to a challenge in the application of prediction tools developed from these methods. The methods start by identifying relationships between a predictor and predictand. The functional relationships are then developed for cases of significant relationships. These methods are capable of giving skillful forecasts but may miss events with amplitudes not represented in the training period (Carson 1998; Greischar and Hastenrath 2000). They need high quality long records of data to ensure that most events are represented (Carson 1998; Greischar and Hastenrath 2000).

The major challenge for using these methods is the possibility of variations in the performance of the predictors over a time period (Black et al 2003; Hastenrath 1995) and the need of quality long records that may not be available at some locations. Some of the required data for the predictors are observations over the oceans where observations networks are inadequate and data quality may not be assured. The methods also suffer from sampling errors that increase with the number of predictors on which the regression equation is developed (Delsole and Shukla 2002). Some of the statistical methods frequently used to predict rainfall include regression analyses, canonical correlation analysis (CCA), and Artificial Neural Networking (ANN) (Tang et al. 2000).

The regression analysis and CCA methods are linear and ANN is non-linear. It is expected that the capability of ANN to simulate complex non-linear variability (Fabbian et al. 2007) would improve the skills of forecasts issued using this method since the climate system involves many nonlinear processes, such as convection in the atmosphere and upwelling in the equatorial oceans. However, some studies have indicated that these methods have comparable skills in situations where the relationships are linear (Barnston et al. 1994; Tang et al. 2000).

Under the regression methods the first step is to determine the association between the predictand and predictor using measures of association. The method often used to measure association is simple correlation analysis discussed in section 3.3.4. The inclusion of a few predictors that account for most of the variance of the predictand is essential since the increase in the number of predictors may lead to an increase in regression error (Mo and Straus 2002). The most frequently used predictors include Quasi-biennual oscillation (QBO) Sea level Pressure Wind, sea surface temperature (SST), El Nino /Southern Oscillation (ENSO), Madden-Julian Oscillation (MJO) and sea surface temperature gradients (SSTGs). Auto-regression models are based on the relationships within the predictand to predict its future conditions.

There have been attempts to use auto-regression to predict rainfall in the region (Matari 1993). Matari (1993) observed a correlation of 0.7 between rainfall onset date and the length of growing season indicating that the rainfall onset date accounted for 49% of the variance of length of the growing period. Statistical methods are still the most reliable in seasonal climate prediction (Hwang et al. 2001; Shabbar and Barnston et al. 1996; Zwiers and Von Storch 2004) and can over perform dynamical methods in some cases (Hastenrath 1995).

The advances in dynamical methods may not bring to an end the use of these methods despite their limitations (Anderson et al 1999; Folland et al 2001). Through the efforts of African Centre for Meteorological Application and Development (ACMAD), IGAD Climate Prediction and Application Centre (ICPAC) and Southern Africa Development Community (SADC) Drought Monitoring Centre (DMC) capacity in the use of statistical methods to predict seasonal rainfall has improved significantly in majority of the countries in Africa. This study employs all the statistical methods listed above to compare their skills in the

prediction of seasonal rainfall over the region. The details of each of statistical methods used in this study are discussed in chapter 3.

The next subsections discuss studies on the most frequently used predictors of seasonal rainfall starting with Quasi- biennual oscillation (QBO).

2.2.1 STATISTICALLY DERIVED PREDICTORS

2.2.1.1 QUASI- BIENNUAL OSCILLATION

Quasi- biennual oscillation (QBO) is a process in the troposphere and stratosphere with a period of about 28 months involving a quasi-periodic reversal of zonal wind from easterly to westerly. The phases of QBO have distinct linkages with seasonal rainfall over many parts of the tropics (Bhalme et al 1987; Claud and Terry 2007; Collimore 2003; Indeje 2000; Indeje and Semazzi 2000; Ogallo et al. 1994) .The Westerly/Easterly phases of QBO have been associated with enhanced/depressed rainfall and convection in tropical areas (Collimore et al 2003; Indeje 2000; Indeje and Semazzi 2000; Ogallo et al 1994). The westerly phase of QBO has been associated with the higher than normal tropopause enabling deep convection (Collimore et al 2003).

Studies of the relationships between QBO and seasonal rainfall over the region have indicated strong relationships (Indeje 2000; Indeje and Semazzi 2000; Ogallo et al. 1994). The values of correlation as high as +0.80 were concentrated over the western parts of the region and were strongest for relationships between MAM rainfall and QBO for the month of June preceding the season. The relationships between MAM rainfall and QBO were lowest for December-February preceding the onset of MAM rainfall (Indeje and Semazzi 2000). The contingency analysis indicated 60% likelihood for the occurrence of above normal MAM rainfall during the western phase of QBO and 63% likelihood of below normal MAM rainfall during the eastern phase of the QBO (Indeje and Semmazzi 2000). QBO was not related to MAM rainfall in some years as was observed in the years 1966, 1973 and 1983, which were associated with strong and prolonged ENSO events (Indeje and Semmazzi 2000). Most of the high Indian Ocean Dipole (IOD) events correspond to the easterly phase of QBO (Indeje and Semmazzi 2000).

In the next section, studies using sea level pressure and wind as predictors are discussed.

2.2.1.2 SEA LEVEL PRESSURE AND WIND

The use of sea level pressure (SLP) and wind as predictors is motivated by the notion that the pressure gradient influences wind current, the transport of moisture and sea surface temperature (Camberlin 1997; Hastenrath and Polzin 2004; Lamb 1978). The wind currents influence the sea surface temperature through atmosphere - ocean interactions (Behera et al. 2005; Hashizume et al. 2002; Nilson 2000; Scott 2003) and by extension the climate regimes of the areas in the neighbourhood of water bodies. The interactions between surface wind and SSTs contribute significantly to the space-time structures of tropical climate and its variability (Hashizume et al. 2002; Neetin et al. 1998).

The anomalous wet / dry MAM rainfall seasons have been associated with low to mid-level westerlies /easterlies (Okoola 1996). Indeje (2000) associated wet years over the region with the deceleration of mid-troposphere easterlies and dry years with strong mid-troposphere westerly wind anomaly. The wind currents also influence ocean currents (Rodrigues et al. 2007), which influence global climate. The winds at low-and upper -levels have been associated with enhanced forcing and frontogenesis (Stuart and Grumm 2007).

The anomalous seasonal rainfall over the region during OND has been associated with the changes in sea surface pressure gradients in the tropical Indian ocean caused by ENSO and IOD (Behera et al. 2005; Hastenrath and Polzin 2003; Saji and Yamagata 2003). Various attempts have been made to predict rainfall from SLP (Lamb 1978; Sansom 1955). Sansom (1955) achieved multiple correlations of 0.46 for long rains (March-May) and 0.42 for short rains (October-December) with SLP and developed functional relationships between rainfall over parts of Kenya and SLP at various points over Africa and neighbouring oceans.

The North Atlantic Oscillation (NAO), which is a seesaw in surface pressure between the high and midlatitudes, always represented with the normalized pressure difference between Iceland and the Azores, exhibits interannual and multidecadal variability (Latif et al 2006) and has been observed to have useful relationships with climate variability in the neighbouring areas and beyond (McGregor and Phillips 2004; Pire and Perdigao 2007; Riviere and Orlanski 2007; Watanabe 2004). The phases of NAO are highly dependent on the waves coming from the eastern Pacific Ocean (Riviere and Orlanski 2007). Reason (2004) observed that the trade winds from warm ocean waters to relatively cool ocean waters

tend to weaken. Kanemba (1993) observed that the migrating low-pressure systems (troughs) in the region 30°S-50°S influence rainfall over the region during the JJA period.

The other most frequently used predictors are ENSO and SSTs discussed in the next section.

2.2.1.3 SEA SURFACE TEMPERATURE AND EL NINO /SOUTHERN OSCILLATION

Sea surface temperatures (SSTs) of the global oceans are the most frequently used predictors of seasonal rainfall (Eldaw et al. 2003; Federove et al. 2003; Goddard and Graham 1999; Ininda 1998; Koster et al. 2000; Li and Zeng 2008; Mutai et al. 1998; Palmer 1986; Ward, and Folland 1991; Zwiers and Von Storch 2004).

The use of SSTs and the related processes such as ENSO, IOD and gradients as predictors is motivated by their slow variability and strong influence on atmospheric circulation (Brankovic et al 1994; Chang 1998; Carson 1998; Frederiksen et al. 2001; Frankignoul and Sennecheal 2007; Goddard and Graham 1999; Lamb 1978; Lau et al. 1997; Lau 1997; Livezy et al. 1996; ; Losada et al. 2007; Mo et al. 1994; Namias 1978; Nobre and Shukla 1996; Ort and Yienger 1996; Pauluis 2004; Reason 2004; Ward 1998; Vidyunmala et al. 2007). The SSTs also contribute to most of precipitation variance in the tropics (Koster et al.2000; Ward and Folland 1991). In the dynamic models SST fields are used as predictors and in statistical methods, the anomalies of SSTs are used (Hastenrath 1990; Repelli and Nobre 2004).

The East African seasonal rainfall variability is related to SST over the Atlantic, Indian and Pacific Oceans (Frederiksen et al. 2001; Goddard and Graham 1999; Ogallo 1988a; Okoola 1996; Omondi 2005; Owiti 2005). The processes associated with SST such as El Nino/Southern Oscillation (ENSO) discussed in section 2.1,6, Indian Ocean Dipole (IOD) discussed in section 2.1.7 and Atlantic interhemispheric SST gradient have significant influence on rainfall over the region and beyond through their interaction with the general circulation of the atmosphere and oceans (Clark et al 2003; Firth et al 2005; Hu and Huang 2006; Kushnir et al. 2006; Loyah 1986; Moura and Shukla 1981; Nagura and Konda 2007; Ogallo 1988a; Okoola 1996; Omondi 2005; Owiti 2005; Rasmusson and Carpenter 1982; Sutton and Hodson 2007). The interhemispheric mode in the northern tropical Atlantic

during the period March-May (northern spring) influences the development of ENSO events in the Pacific Ocean in subsequent months (Wu et al. 2007).

Various efforts have been made to determine useful relationships between SST and seasonal rainfall over the region and other parts of the tropics that could be used to predict seasonal rainfall over the region (Black et al. 2003; Clark et al 2003; Hastenrath et al. 1993; Mutai et al. 1998; Mutai and Ward 2000; Nicholson and Entekhabi 1987; Nyakwada 2003; Sansom 1955; Mutai 2003; Ogallo 1988a; Omondi 2005; Owiti 2005; Tschuck et al. 2004). The SSTs of parts of global oceans are highly related to rainfall over parts of the region (Black et al. 2003; Clark et al 2003; Mutai 2003; Nicholson and Entekhabi 1987; Nyakwada 2003; Ogallo. 1988a; Omondi 2005 Owiti 2005;Tschuck et. al. 2004). Mutai et al (1998) observed .that July - September sea surface temperature (SST) explained 30 to 60% of the average OND seasonal rainfall variance over the region.

The enhanced/ depressed seasonal rainfall over the region has been associated with the warming/cooling over the western Indian Ocean (Barnston et al. 1996; Beltrando and Cadet 1990; Clark et al 2003; Nicholson and Entekhabi 1987; Okoola 1996; Owiti 2005) and the cooling over the eastern Indian Ocean (Behera et al. 2005; Black et al 2003; Clark et al. 2003; Owiti 2005). Okoola (1996) observed that wet/dry seasons over the region were closely associated with distinct anomalously warm/cool SSTs over parts of the western Indian/eastern Atlantic Oceans.

The significant relationships observed between SST and seasonal rainfall over the region has motivated efforts to develop functional relationships to predict seasonal rainfall over the region. Some recent attempts include the works of Clark et al. (2003); Mutai et al. (1998); Mwale and Gan (2005); Ntale et al (2003); Owiti (2005); Omondi (2005) and regular preseason capacity building workshops conducted since 1998 by ICPAC among others.

The SST based models have been observed to give climate outlooks for the region with useful skills (Mutai et al. 1998; Mwale and Gan 2005; Ntale et al. 2003; Wang and Eltahir 1999; Sun et al.2007; Wassila et al. 1999). The skills of the forecasts are, however, influenced by the statistics of the weather within the season, which are dependent on internal chaotic variations (Zebiak 2003). The major challenge in the use of SSTs as predictors is that the relationships with SSTs in the immediate neighbouring oceans do not have adequate lead-time (Mutai et al. 1998), the locations of predictors have a tendency to change with time

(Firth et al 2005) and the relationships would lapse in some years as was observed for the period 1983-1993 (Clark et al.2003). The other challenge is the climate regime shift that has been observed in the SSTs of the global oceans (Harrison and Carson 2007; Wang and An 2001). The variations in correlation between rainfall and SSTs are a major challenge to empirical methods since they are based on persistent relationships.

The inclusion of SSTs from oceans far from the region is useful for forecasts with long lead-time (Kleemam 2007). The long lead-time climate prediction can be achieved by predicting the SSTs of the global oceans. The SSTs over the Atlantic Ocean can be predicted with useful skill 3-4 months ahead using SSTs from the Pacific and Indian Oceans (Repelli and Nobre 2004; Stockdale et al. 2006). Most of SST variability in the equatorial and southern Atlantic is not dependent on ENSO but on local forcing (Huang et al. 2002).

Another predictor frequently used in the region and beyond is El Nino - Southern Oscillation (ENSO) discussed in section 2.1.6. The SSTs and ENSO are the most frequently used predictors of seasonal rainfall at ICPAC (Ntale et al. 2003), which serves the region and the neighbouring countries that are members of the Intergovernmental Authority on Development (IGAD). The forecasts based on SSTs and ENSO have shown useful skills in the region. The major weakness in SST and ENSO based models of seasonal forecasting is that the highest relationships with some global oceans are achieved very close to the onset of the season (Korecha and Barnston 2007; Mutai 2003) and the centres of teleconnection of ENSO with atmospheric and ocean processes may shift between El Nino and La Nina years (An et al.2007).

The predictability of ENSO for the period March-May is generally weak since the period forms a transition in the phases (Annamalai et al. 2007; Korecha and Barnston 2007; Zebiak 2003). The weaknesses observed in the predictors discussed in the previous sections have led to the need for other predictors that would improve the predictability of seasonal rainfall.

In the next section the approaches based on sea surface temperature gradients as predictors are discussed.

2.2.1.4 SEA SURFACE TEMPERATURE GRADIENTS

Atmospheric motions are dominated with the gradients in temperature and the associated pressure gradients (Barry and Chorley 1968; Shukla 1991). Hence the use of sea surface temperature gradients could improve the representation of the driving forces of the general circulation. The use of sea surface temperature gradients is motivated by their influence on the atmospheric circulation (Bjerkness 1969; Chang 1998; Chervin and Druyan 1984; Chu 1989; Gill 1980; Lamb 1978; Lindzen and Nigam 1987; Nobre and Shukla 1996; Ort and Yienger 1996; Pauluis 2004; Ward 1998; Vidyunmala et al. 2007). Lindzen and Nigam (1987) observed that sea surface temperaure gradients together with the associated pressure gradients have a significant influence on the wind and precipitation patterns in the tropics. Significant relationships have been observed between rainfall and SST gradients (Clark et al. 2003; Moura and Shukla 1981). The SST gradients influence wind currents and the associated moisture transport (Chu 1989; Lindzen and Nigam 1987).

Walker circulation and the intensity of the individual cells is highly dependent on SST gradients (Chervin and Druyan 1984). The north-south migration of the sun results into seasonal variations in the strengths of meridional SST gradients, and the intensity and position of southeast trade winds (Yu and Rienecker 2000). The intensity and location of the inter-tropical convergence zone is highly dependent on temperature gradients through their influence on pressure gradients (Vidyunmala et al. 2007).

Some of the SST gradients that have been documented to influence climate of the region and beyond include the Zonal SST gradients in the Indian ocean associated with the IOD (Behera et al.2005; Clark et al 2003; Owiti 2005; Saji et al. 1999; Singhrattna et al 2005; Webster et al. 1999;Yu and Riennecker 2000); the zonal SST gradient in the pacific (Bjerkness 1969); and the zonal and meridional SST gradients in the Atlantic ocean(Moura and Shukla 1981; Nobre and Shukla 1996; Wang 2002; Xie 1999). The meridional and zonal SST gradients are linked through teleconnections with large-scale atmospheric circulation such as the Walker and Hadley cells (Wang 2002).The zonal and meridional SST gradients have a strong signature on the climate of the tropical areas (Lindzen and Nigam 1987; Ward 1998). In the tropics the zonal gradients are generally smaller than the meridional gradients

but are more important in forcing low level tropical circulation and convergence than the meridional gradients (Lindzen and Nigam 1987). However, the zonal SST gradients have been observed to have no influence on the southern Atlantic anticycone (Richter et al. 2008).

Meridional sea surface temperature gradients in the Atlantic Ocean have been observed to have significant influence on rainfall over the Atlantic ocean and the neighbouring areas (Chang 1998; Folland et al. 1986; Hastenrath and Heller 1977; Hastenrath 1995; Lamb 1978; Moura and Shukla 1981; Nobre and Shukla 1996; Parker et al. 1988). The improvement in the skill of predictions of seasonal rainfall over Brazil was attributed to the inclusion of the inter-hemispheric temperature gradient over the Atlantic as a predictor (Moura and Shukla 1981). Recent studies have indicated linkages between the onset of ENSO and. the inter-hemispheric dipole in the Atlantic Ocean with the dipole leading ENSO onset with some months (Li et al. 2007; Wu et al. 2007). The inter-hemispheric dipole has its maximum amplitute in spring (Wu et al. 2007). Most of the attempts to predict seasonal rainfall over the region have used grid point SST or time coefficients of sea surface temperature principal component modes. However, the mean climate contains strong spatial and temporal gradients of pressure, temperature, salinity, velocity and water vapour (Shukla 1991).

The studies discussed in section 2.1.7 that use IOD as a predictor of seasonal rainfall over the region represents major attempts to predict seasonal rainfall from SST gradients (Behera et al. 2005; Black et al. 2003; Clark et al. 2003; Owiti 2005; Saji et al. 1999;Webster et al. 1999; Yu and Riennecker 2000). However, in addition to zonal gradients such as IOD, meridional gradients play an important role in the modulation of atmospheric circulation and climate (Hastenrath and Heller 1977; Moura and Shukla 1981). The zonal and meridional SST gradient modes, have significant influence on climate (Clark et al. 2003; Lindzen and Nigam 1987; Ward 1998) and would represent both meridional and zonal circulation of the atmosphere that dominate horizontal moisture transport (Bjerkness 1969; Chang 1998; Chervin and Druyan 1984; Lindzen and Nigam 1987; Nobre and Shukla 1996; Ort and Yienger 1996; Pauluis 2004; Vidyunmala et al. 2007; Ward 1998; Webster et al. 1999).

The other category of methods used to predict seasonal rainfall is dynamical methods discussed in the next section.

2.3 DYNAMICAL METHODS

The use of dynamical methods involves the simulation of the atmosphere-land-ocean interactions to predict the future state of the atmosphere. Atmospheric general circulation models (AGCMs) have reasonable skills in seasonal prediction during some seasons and parts of the tropics and subtropics (Janowiak 1992; Shongwe 2005) but the skill is generally low in areas where local features have significant influence on climate (Frederiksen et al. 2001). In situations where the relationships are linear the skills of statistical and dynamical methods are comparable (Gorddard et al. 2000; Kumar and Hoerling 2000).

The sources of errors in dynamical methods include ocean initial conditions, unpredictable nature of the synoptic atmospheric variability and coupled model errors (Barnston et al. 2000;Vialard et al 2005). The weaknesses in the prediction of atmosphere's natural variations has been singled out as a major cause of low level of seasonal forecast skill since the seasonal average is a function of individual weather events (Barnston et al. 2000; Wang and Chang 2004). The chaotic nature of the atmospheric processes also pauses major difficulties for the use of dynamical methods in long-range weather prediction (Lorenz 1963). However, some components of atmospheric processes influenced by external forcing may be predictable with a lead-time beyond the deterministic prediction limits ((Shukla 1981). They have shown potential predictability of ENSO events (Kirtman et al. 1997) but do not adequately represent diurnal variation of rainfall in the tropics (Janowiak 1992) and the model skills depend on seasons (Shongwe 2005).

The limitation of AGCMs in areas where local features have significant influence on climate may limit their use in the region where the local features such as the water bodies and topography have strong signature on climate. The AGCMs have a tendency to overpredict convection over eastern Africa due to complex toporography (Richter et al. 2008).

Sea surface temperatures are potential predictors for the achievement of long-range climate prediction from dynamical methods especially in parts of the tropics where the relationships are strong (Shukla 1998). The potential of long-range predictability using SSTs has motivated studies in the use of AGCMs in seasonal prediction (Mo and Straus 2002; Shukla et al. 2000). Improvements in the skills of seasonal forecasts from dynamical methods have been observed from the use of a two-tier approach (two AGCMs) (Livezy et al. 1996). The use of ensemble methods, which involves the integration of a AGCM with various initial

conditions to obtain probabilistic information about future states and to provide an estimate of the natural variability inherent in the atmosphere, has shown further improvements in the skills of seasonal prediction from dynamical methods (Mason et al. 1999; Peng and Kumar 2005; Shukla et al. 2000). The skill of seasonal forecasts based on a combination of AGCMs (multimodel ensemble), is higher than that of a single model (Barnston et al. 2003; Goddard et al. 2000; Kumar and Hoerling 2000).

Recent studies have indicated that seasonal predictability by the Atmospheric General Circulation Models (AGCMs) varied from model to model (Shukla et al 2000) and the influence of identical SST may result into more than one state of the atmosphere (Druyan et al 2002; Kumar and Hoerling 2000). The understanding of the causes of the differences in the performance of the various models was essential for the improvement of seasonal forecasts from AGCMs (Shukla et al. 2000). The skillful SST and better AGCM circulation and humidity predictions would improve the skills of the AGCMs to predict seasonal climate (Druyan et al. 2002). However, perfect SST or observed atmospheric forcing do not translate into consistently realistic precipitation distribution (Druyan et al. 2002).

The use of dynamical methods need compensation for biases in the model climatology (Folland et al 2001), which requires several decades of simulations or hind-cast for the climatological reference period using the same number of ensemble members as used in real-time forecasts. The AGCMs tend to have high skills in years when the SST anomalies are strong and during ENSO (Livezy et al. 1996; Shukla et al 2000). The AGCM models gave a skilful forecast of the extremely wet conditions over eastern Africa associated with the 1997/98 El Nino events (Frederiksen et al. 2001). The model performance in areas where intraseasonal variations are strong depends on the ability to represent them (Frederiksen et al. 2001).

Phelps et al. (2004) using NCEP/CPC seasonal Forecast System observed that atmospheric initial conditions had little effects on the model monthly and seasonal means for lead times of one month or more and the model was more skilful on seasonal than monthly predictions. The AGCMs have also been used in the detection and attribution of climate change (Kettleborough et al. 2007; Stone et al. 2007). Dynamical methods can give erroneous results if the model does not reproduce the predictand field adequately (Misra and Zhang 2007).

Another approach to improve the skills of dynamical method is to run a system that combines dynamical and statistical methods. This approach is discussed in the next section.

2.4 STATISTICAL-DYNAMICAL (HYBRID) METHODS

Statistical-dynamical methods are some of the models frequently used in long-range prediction (Hastenrath 1995). The first step in this hybrid method involves the prediction of potential predictors using AGCMs that are used as inputs in the statistical prediction models to give a forecast (Hastenrath 1995; Mo and Straus 2002). The selection of potential predictors is facilitated by diagnostic studies using the AGCMs to reproduce the conditions related to a specific anomaly (Folland et al. 1991; Gowariker et al. 1989; Hastenrath 1995; Ramirez et al. 2007). A combination of statistical and dynamical methods improves the skills of AGCMs and has capability to correct systematic errors (Mo and Straus 2002). However, the regression schemes may not be successful for situations where SST-forced signals are very weak or not easily separated from noise (Mo and Straus 2002). Misra (2007) proposed a method for reducing systematic errors in regional climate models. Statistical, dynamical, and statistical - dynamical models including the complex coupled models with sophisticated data assimilation and initialization procedures have similar and modest capability for long-range prediction of El Nino (Zebiak 2003).

Statistical methods were employed in this study due to their simplicity, capability to operate on personal computers and observed capability for long-range prediction.

The next chapter discusses the area of study, and data and methods used in this study.

CHAPTER THREE

3.0 DATA AND METHODOLOGY

This chapter discusses the area of study, and the data and methods that were used in the study to address the overall and specific objectives starting with the presention of the area of study.

3.1 THE AREA OF STUDY

3.1.1 EAST AFRICAN COUNTRIES AND THEIR PHYSICAL FEATURES

The area of this study is East Africa (Figure 5) consisting of three countries namely Kenya, Uganda and Tanzania. The region is within Latitude 6°N and 12°S and Longitudes 28°E and 42°E. It has complex topography. The physical features contributing to the complex topography of the region include the high mountains Kilimanjaro (5895m), Kenya (5195m), Elgon (4321m), Ruwenzori Range (5110m), Mufumbiro (4510m), Meru (4565), Elgon (4321m), Aberdare Ranges (3906) and Mau Escarpment (3098m) above mean seal level (a.m.s.l).

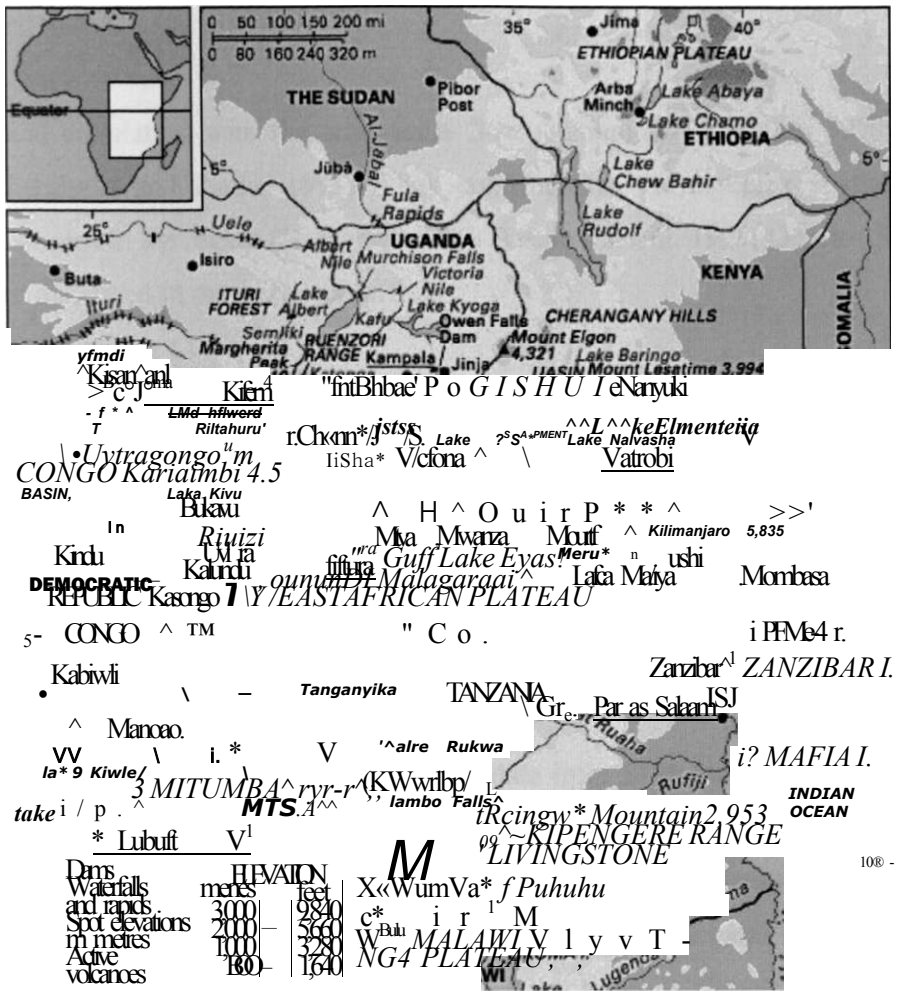

Figure 5: Domain of the study region depicting the physical features (source: Indeje 2000).

Mt Kilimanjaro and Kenya are unique having snow at their tops thoughout the year despite being located in the warm equatorial region. The variations in the characteristics of these snowcaps can be useful indicators of regional climate change. The high mountains are the sources of the majority of the major rivers in the region. Also the Great Rift Valley and the low lands dominating the eastern part of the region contribute to the complex topography of the region. The mountains are associated with gravity waves that influence large-scale flow (Martin and Lott 2007) and climate.

The large water bodies, Lake Victoria and Indian Ocean, are among the other physical features influencing the climate of the region. These physical features have significant influence on the climate of the region through the interactions of the associated

local circulation with the large-scale flow (Asnani and Kinuthia 1979; Anyah et al. 2006; Mukabana and Pielke 1993). They contribute to the complex spatial patterns of rainfall observed in the region (Basalirwa 1999; Basalirwa et al. 1999; Ogallo 1989).The data used are discussed in the next section 3.2.

3.2 DATA USED IN THE STUDY

The data used in this study include rainfall, sea surface temperature (SST), outgoing long-wave radiation (OLR) and reanalyzed wind data. The detail discussions of these data are presented in the next subsections.

3.2.1 RAINFALL

This study used monthly rainfall data from 59 stations (Table 3a) for the period 1960-2006 available at the IGAD Climate Prediction and Application Centre (ICPAC) formerly known as the Drought Monitoring Centre (DMC), Nairobi obtained from the Kenya Meteorological Department (KMD), Tanzania Meteorological Agency (TMA) and Uganda Meteorological Department (UMD). The homogeneous climate zones used in this study are those presented in Figures 6a and 6b developed over the years by ICPAC through pre-season capacity building workshops from principal component analysis (PCA) using the same data(ICPAC 1999). The same zones are used for operational purposes and capacity building workshops at ICPAC (ICPAC. 1999). Many recent studies including Komutunga (2006); Njau (2006); Omondi (2005) and Owiti (2005) used the same homogenous zones in order to reduce the number of rainfall stations used in examining teleconnections between regional rainfall and global scale circulation variables.

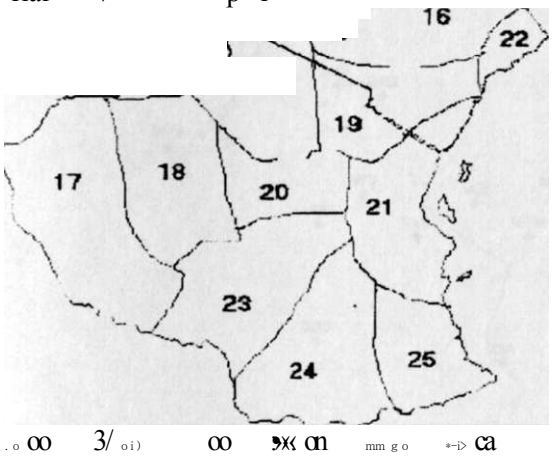

Figure 6a: Homogeneous climatic zones for March-May season used in the study (source: ICPAC. 1999)

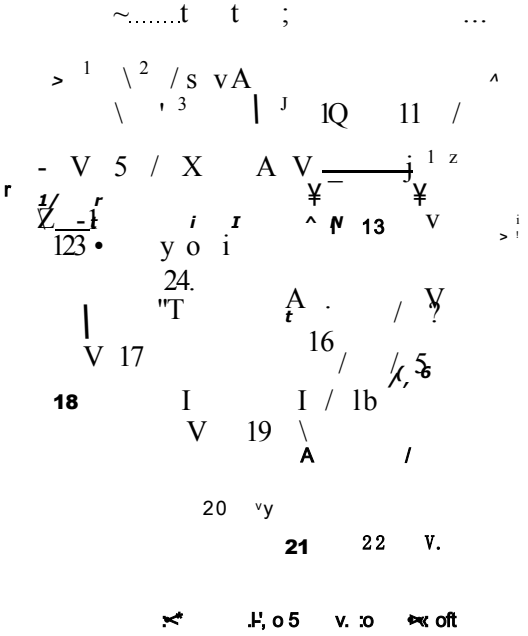

Figure 6b: Homogeneous climatic zones for September-December season used in the study (source: ICPAC. 1999)

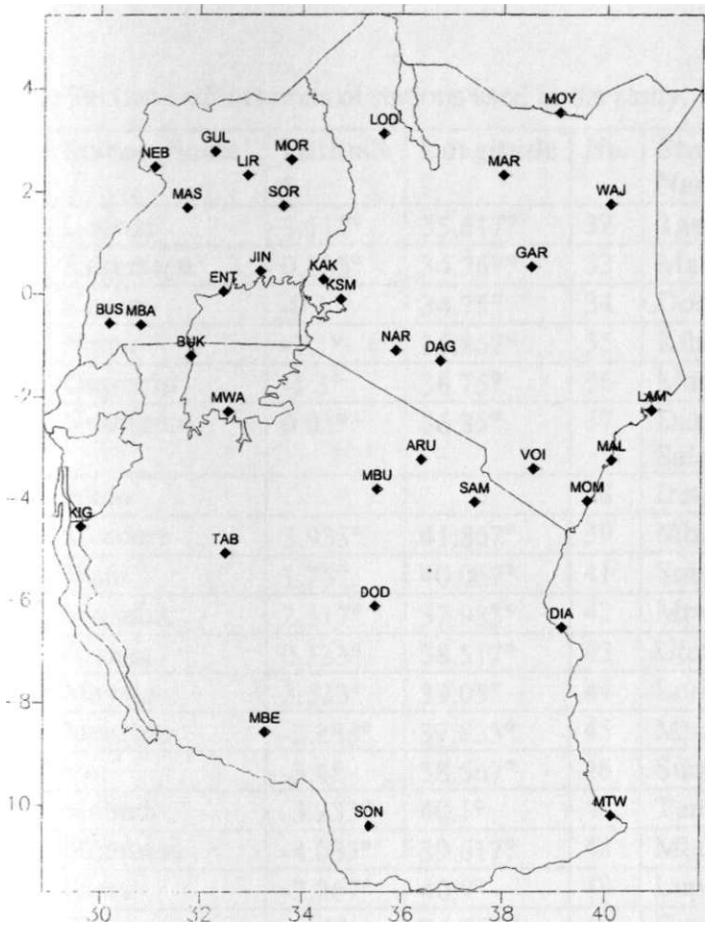

Figure 6c: The distribution of the stations representing homogeneous rainfall zones over the study region with the names represented with the first three letters.

The stations presented in Figure 6c, Tables 3b and Table 3c that had the highest loadings with the Principal Component (PC) modes dominant in specific zones and high correlation with most stations within the respective zones were used to represent the zones in developing functional relationships to predict rainfall.

Table 3a: List and locations of stations used in the study.

No.	Station Name	Latitude o	Longitude	No.	Station Name	Latitude	Longitude
1	Lodwar	3.117°	35.617°	32	Tanga	-5.05°	39.04°
2	Kakamega	0.283°	34.767°	33	Mahenge	-8.6°	36.7°
3	Kisumu	-0.1°	34.75°	34	Dodoma	-6.1°	35.46°
4	Narok	-1.1°	35.867°	35	Kibondo	-3.5°	30.8°
5	Dagoretti	-1.3°	36.75°	36	Matombo	-7°	37.7°
6	Nyahururu	0.03°	36.35°	37	Dar es Salaam(DIA)	-6.52°	39.12
7	Isiolo			38	Iringa	-7.38°	35.46°
8	Mandera	3.933°	41.867°	39	Mbeya	-8.56°	33.28°
9	Wajir	1.75°	40.067°	41	Songea	-10.4°	35.35°
10	Marsabit	2.317°	37.983°	42	Mtwara	-10.21°	40.11°
11	Garissa	0.533°	38.517°	43	Utete	-8.01°	38.75°
12	Moyale	3.533°	39.05°	44	Loliondo	-2.03°	35.62°
13	Makindu	-2.283°	37.833°	45	Mpanda	-6.2°	31.05°
14	Voi	-3.4°	38.567°	46	Sumbawanga	-8.6°	31.2°
15	Malindi	-3.233°	40.1°	47	Tunduru	-11.1°	37.3°
16	Mombasa	-4.033°	39.617°	48	Mbulu	-3.8°	35.5°
17	Lamu	-2.267°	40.9°	49	Luponde	-9.4°	34.6°
18	Elgon	1.15°	34.767°	49	Gulu	2.78°	32.28°
19	Kerugoya	-0.5°	37.267°	50	Lira	2.32°	32.93°
20	Monieri	-0.65°	35.067°	51	Morulem	2.62°	33.77°
21	Nanyuki	0.05°	37.033°	52	Soroti	1.72°	33.62°
22	Maralal	1.1°	36.7°	53	Tororo	0.68°	34.17°
23	Bukoba	-1.2°	31.49°	54	Entebbe	0.05°	32.45°
24	Musoma	-1.3°	33.48°	55	Masindi	1.68°	31.72°
25	Mwanza	-2.28°	32.55°	56	Mbarara	-0.6°	30.68°
26	Arusha	-3.22°	36.38°	57	Nebbi	2.48	31.08
27	Moshi	-3.21°	37.2°	58	Bushenyi	-0.57	30.17
28	Ilonga	-6.7°	37.1°	59	Jinja	0.45	33.18
29	Kigoma	-4.53°	29.4°				
30	Same	-4.05°	37.44°				
31	Tabora	-5.05°	32.5°				

KEY: Negative sign preceeding a litude implies 'South"

Table 3b: Rainfall stations used to represent March - May climatic zones

Zone	Representative Station	Zone	Representative Station	Zone	Representative Station
1	Nebbi	10	Bushenyi	19	Same
2	Lira	11	Jinja	20	Dodoma
3	Masindi	12	Bukoba	21	Mombasa/Malindi
4	Soroti	13	Mbulu	22	Lamu
5	Kakamega	14	Dagorreti	23	Mbeya
6	Lodwar	15	Moyale	24	Songea
7	Wajir	16	Garissa	25	Mtwara
8	Marsabit	17	Kigoma	26	Kisumu
9	Mbarara	18	Tabora	27	Mwanza

Table 3c: Rainfall stations used to represent September-December climatic zones

Zone	Representative Station	Zone	Representative Station	Zone	Representative Station
1	Gulu	9	Mbarara	17	Tabora
2	Lira	10	Marsabit	18	Kigoma
3	Morulem	11	Wajir	19	Dodoma
4	Narok	12	Garissa	20	Mbeya
5	Dagoretti	13	Voi	21	Songea
6	Masindi	14	Lamu	22	Mtwara
7	Entebbe	15	Mombasa/Malindi	23	Bukoba
8	Kisumu	16	Same	24	Mwanza

In the next section, the Sea Surface Temperature (SST) data are discussed.

3.2.2 SEA SURFACE TEMPERATURE

Sea surface temperatures are widely used as a key predictor in most climate prediction models due to the long period of persistence of the SST anomalies (Kirtman et al. 1997; Okoola 1996; Omondi 2005; Owiti 2005; Smith and Reynold 2004). The major sources of errors in SST records are missing observations, instruments and methods used to make the measurements, and analysis methods (Smith et al. 2008). The SST data used in this study were obtained from the National Center for Environmental Prediction/Climate Prediction Center (NCEP/CPC). Several efforts have been made to improve the quality of SST records due to their value in climate prediction (Smith and Reynold 2004; Smith et al. 2008). Kanamitsu et al (2002); McPhaden et al. (1998); Reynolds et al. (2002); Smith and Reynolds (2002; 2004), and Smith et al. (2008), among other authors, have discussed the details of these data.

The data used were for the period 1960 to 2006 for 10°x10° latitude/longitude boxes located over both Indian and Atlantic oceans. The quality of SST data to the south of 30°S may not be good (Weare 1977).

In the next subsection the wind data used in the study are discussed.

3.2.3 NATIONAL CENTER FOR ENVIRONMENTAL PREDICTION / NATIONAL CENTER FOR ATMOSPHERIC RESEARCH REANALYSIS WIND DATA

The wind often represent atmospheric circulation, which is a bridge linking SST changes with the atmosphere in different parts of the world oceans (Lau 1997). The wind data used in the study were from the United State of Merica National Center for Environmental Prediction / National Center for Atmospheric Research (NCEP/NCAR) reanalysis database (Kalnay *et al.* 1996). Details of these data that were constructed through a process involving the recovery of land surface, ship, rawinsonde, pibal, aircraft, satellite, and other data together with data quality control and assimilation over the period 1957-1996 may be obtained from Kalnay et al. (1996), Kanamitsu et al (2002) and Poccard et al. (2000), among other authors.

The 2.5° x 2.5° latitude/longitude grid points wind data for the period 1960-2006 were used in this study. The meridional and zonal components of wind data were analyzed in

this study in order to establish the physical reality of the relationships observed between rainfall and sea surface temperature gradients discussed in section 3.3.3. The NCEP/NCAR data, which cover a period of over 50 years, has been used in various climate studies (Indeje 2000; Owiti 2005). In the region, Indeje (2000) and Owiti (2005) among many other authors have used the same database to investigate linkages between wind patterns associated with climate extremes and the phases of the Indian Ocean dipole respectively. The wind data used in this study is for the period 1960 to 2006

The next section discusses OLR data used in this study.

3.2.4 SATELLITE DERIVED OUTGOING LONG-WAVE RADIATION

The satellite derived outgoing long-wave radiation (OLR) is a good proxy for rainfall especially over parts of the tropics where the small spatial variation of temperature makes its interpretation easy. The low and high OLR values, which correspond to low and high cloud top temperatures, generally correspond to deep convection and cloudless areas, respectively (Janowiak 1992; Liu et al. 2007; Nyakwada 1992; Nyakwada et al 1995). These properties have made the use of OLR data in studies looking at the onset and cessation of rainfall, and properties of ITCZ (Franchito et al. 2008). The data was available for the period 1974-2004. Many authors have used OLR data to infer convection and rainfall patterns (Franchito et al. 2008; Motel l and Weare 1987; Nyakwada 1992; Nyakwada et al. 1995; Okoola 1996). The OLR data, averaged over 2.5° x 2.5° latitude/longitude were used in this study to infer the convention patterns associated with the phases of the SSTG modes.

In the next section the methods used in this study are discussed.

3.3 METHODOLOGY

In this section, the various methods used in this study are discussed. These include the methods used to organize the data to meet the needs of the study such as estimating missing records, generating areal rainfall estimates, data standardization, and lastly examination of the quality of the records used in the study.The other methods focused on the specific objectives of the study that included determination of SSTG modes that have some prediction potentials to seasonal rainfall for the specific seasons and regions of East Africa; delineation of the major space-time characteristics and linkages between SSTG and seasonal rainfall extremes; examination of the global/regional climate systems that may be associated

with the observed linkages between SSTG modes and seasonal rainfall extremes; finally the determination of the improvement in the predictability of East African seasonal rainfall with SSTG modes.

The key methods that were used for investigating relationships within the variables include correlation analysis, Regression Analysis (RA), Canonical Correlation Analysis (CCA), Artificial Neural Network (ANN) and composite analysis. The RA and ANN methods were used to determine improvements in the predictability of regional seasonal rainfall with SSTG modes to provide new early warning tools for regional seasonal rainfall extremes such as droughts and floods.

The methods used for addressing data challenges of the study are discussed in the next section.

3.3.1 DEVELOPMENT OF QUALITY DATA BASE FOR THE STUDY

In order to ensure that well representative and high quality data base was available for the study, several analyses were undertaken that included estimation of missing records, generating areal rainfall estimates, standardization of available data, and finally assessing the quality of all records used in the study. Details of these methods are provided in the following sections.

3.3.1.1 ESTIMATION OF MISSING RECORDS

Most climatological records have gaps, which must be filled before such data may be used for the continuous studies like in the case of time series analysis. The methods commonly used to estimate missing data include isopleth, isopercentile, correlation, arithmetic mean, regression, Thiessen polygon and Empirical Orthogonal Function (EOF) methods. Only a brief account of arithmetic mean method, which was used in this study, is included here. The details of the other methods can be obtained in many references including Basalirwa (1979); Grimmer (1963); Nyakwada et al. (1992); Shaw (1988); Thiessen (1911); and WMO (1960; 1965; 1966) among other authors. It is, however, important to note here that the choice of stations used was restricted to those with a maximum of 10% missing data, provided the missing data were not for consecutive years, to avoid dilution of the records (WMO 1970; 1974).

The estimation of missing data by arithmetic mean method requires the knowledge of a neighbouring station best correlated to the station with missing data. Hence, under this method, the first step is to identify a neighbouring station, which has the highest correlation with the station with missing records. Correlation coefficient can quantify the degree of relationships between pairs of variables. In this study simple correlation coefficient (r), discussed in section 3.3.4, was used to determine the neighbouring stations best related to the stations with missing data. If r is significantly different from zero, then the pair of variables is significantly correlated.

The neighbouring station with the highest correlation coefficient (r) and reliable record is used to estimate the missing records as shown in equation (1).

$$X_{Aj} = \frac{X_{BJ}}{X_{Bb}} X_{Aa} \qquad (1)$$

X_{Aj} is the missing record of station A in the j^{th} year, X_{Bj} the record for station with reliable records (B) in year y, and X_a and X_b are the long-term averages for stations A and B, respectively based on the period of records available at A. This method generally requires long period of records in order to generate stable averages for individual stations. It also requires relatively homogeneous distribution of station in the catchments. Such a network could include all the best-correlated neighbouring stations, which are required to estimate the missing records.

A part from using point records from the locations, knowledge of arealaverage estimates over certain latitude and longitudinal boundaries are sometimes required.

The technique used for areal averaging in this study is presented in the next section.

3.3.1.2 AREAL ESTIMATE

In this study both point and areal averaged records are used to examine the relationships between SSTG modes and rainfall. A part from using time coefficients of the dominant PCA modes, simple areal averaging of SST over say 10°x10° latitude/longitude grid boxes was also included. Ogallo (1980b) has discussed the details of PCA derived areal indices.

In the next section the methods used to assess and correct the quality of the records are discussed.

3.3.1.3 QUALITY OF THE RECORDS

Most climatological records, including those estimated or derived from areal estimates are characterized by inconsistencies, which may be caused by the adopted methods, changes in the location and exposure of the rain gauge, technology, instrument type and microclimate. Errors associated with the methods used to estimate missing records, data collection, transmission and processing may also introduce heterogeneity into the records. It is ,therefore, necessary to check for the quality of climatological records before such data are used in any climatological analysis. The quality of the estimated data was also investigated in this study. The most commonly used methods of testing the quality of data include the run test, mass and residual mass curves methods. Only a brief account of mass curves analysis, which was used in this study, is included here. The details of the various methods may be obtained in various references including Ogallo (1981 a); Thom (1966) and WMO (1966).

Mass curve analysis involves the plotting of cumulative climatological records against time. The patterns of these graphs can be used to test for the quality of the records. A single straight line is obtained for nearly error free (homogeneous) records. Other patterns indicate heterogeneity in the records. For the heterogeneous records, the next step would be to correct for heterogeneity. The method commonly used to adjust heterogeneous records is the double mass curves. The principles of the double-mass curves analysis are similar to those of mass curves. Double-mass curves analysis, however, plots the cumulative values of the heterogeneous records against the cumulative values of records from a homogeneous station or parameter.

Further details of the methods used for data quality control can be obtained in many references including Chow (1964); Kohler (1949) and WMO (1970; 1974; 1983)

In the next section the methods used to standardize the data for ease of comparison are discussed.

3.3.1.4 DATA STANDARDIZATION

The complex topography has a high signature on the amount and variability of rainfall in the region (Trewartha 1961). There are large spatial variation in the means and standard deviations. The mean and the variance are the most frequently used parameters to standardize data. This study has used the same approach to standardize the records used in

the study. The computation of standardized anomalies (z) involves the subtraction of the sample mean from the records and dividing the result by the standard deviation.

The mathematical expression of this process is given below in equation 2

$$z = \frac{}{S_x} = \frac{}{S_x} \quad \text{----------}$$

where X is the observed data, X is the mean, ^ is the anomaly and S_x the standard deviation. The standardization of records ensures that the mean of the standardized records is zero (0) and the standard deviation is unit (1).

This approach reduces the influence of the mean and variance on the average rainfall over a homogeneous rainfall zone (Nicholson 1986). The standardized anomalies have been widely used in many past studies including those by Frankignoul and Sennechael (2007); Korecha and Barnston (2007); Indeje and Semazzi (2000); Nicholson (1986); Omondi (2005); Owiti (2005) and Stuart and Grumm (2007) among many other authors. Various efforts to study the variability of rainfall in the region have used this approach (Nicholson and Entekhabi 1987; Nicholson 1986; Ogallo and Suleiman 1987; Ogallo 1980a; 1986; Okoola 1996; Omondi 2005 and Owiti 2005).

The standardized point and areal records were subjected to several analyses including Principal Component Analysis (PCA), Artificial Neural Networks (ANN), Canonical Correlation Analysis (CCA), Regression Analysis (RA) and Composite Analysis (CA). In the next section, the methods used to establish the dominant modes in SST records are discussed.

3.3.2 PRINCIPAL COMPONENT ANALYSIS

Principal Component analysis (PCA) and factor analysis (FA) are the most frequently used multivariate techniques in atmospheric sciences to reduce data sets while retaining maximum variability contained in the original data, establish similarities in spatial and temporal climate variability, and identify the dominant modes of variability in statistical fields (Barnston and Livezy 1987; Karl et al. 1982; Wilks 2006; Von Storch and Zwiers 1999).. The PCA and FA belong to the family of Empirical Orthogonal solutions, which are derived from the concept of the variance. The first step involves the calculation of a measure

of association for the set of variables, followed by the construction of a set of orthogonal functions that can represent the measured variables. Factor analysis, unlike PCA, takes into consideration the unique variance accounted for by the common set of orthogonal functions (factors) and defines the orthogonal functions as exact mathematical linear transformation of the original data.

The PCA and FA translate data sets containing large numbers of variables into few new variables while ensuring that the highest variability in the original data set is retained. The new variables are called factors in FA and Principal Components (PCs) in PCA.

The factors and PCs are linear projections of the standardized measured variables in the orthogonal vector space. The factor coefficients represent the ordinates of a point representing a variable in this space.

Factor analysis (FA) represented by M common empirical orthogonal functions (factors) and n unique factors can be expressed in a mathematical model as:

$$Z, = a_n F_x + a_{i2} F_2 + \ldots + a_{im} F_m + dp, \quad / = 1,2,\ldots\ldots M \qquad (3)$$

Where Z, is the variable *i* in the standardized form, F_L represents the common orthogonal function (factors), u_t the unique factor for variable *i, aij* the standard multiple regression coefficient of the variable *i* on the common factor *j* and *d*is the regression loading of the unique factor, which is often very difficult to estimate for physical variables. The regression coefficients (loadings) can be obtained from the correlation and covariance matrices of the variables (Harman 1967; Richman 1981; vonStorch and Zwiers 1999; Wilks 2006).

The correlation matrix was used in the study to derive the regression weights (loadings). The advantages of using correlation matrix include:

- Equal weighting of all stations or grid points to avoid bias positioning of the synoptic centres,
- Assigning perfect position correlation between a variable and itself by setting the diagonal of the input matrix to unity and
- The loadings can be regarded as correlation coefficients of the grid points (locations) with a specific orthogonal function (Barnston and Livezy 1987;Richman 1981; Karl et al. 1982; von Storch and Zwiers 1999; Wilks 2006).

Principal Component Analysis (PCA) is used in this study since the unique properties of the individual variables/locations are extremely difficult to estimate mathematically. The value of diUi in equation (3) was, therefore, set to zero in this study. The extraction of the factors or PCs in the descending order ensures that the first few factors or PCs, representing most of the variability in the original data set, are retained (Hsieh 2004; von Storch 1999; Wilks 2006). The variables that are related cluster together onto similar vector spaces or factors. Many authors have used PCA to examine complex relationships between large numbers of variables (Basalirwa 1999; Basalirwa et al. 1999; Dyer 1975; Gregory 1975; Grimmer 1963; Janowiak 1988; Mungai 1984; Mutai and Ward 2000; Richman 1981; Ogallo 1980a; 1986; 1988b; 1989; Wolter 1989). ICPAC has used this approach to establish rainfall homogeneous zones in the Greater Hone of Africa (GHA).

Some of the unique properties of the PCA and other Empirical Orthogonal functions (factors) that have made them the most preferred methods to study complex relationships between many variables include:

- The ability to reduce the large volume of data by replacing the measured variables and inter-correlated variables by a smaller number of uncorrelated variables (Principal Components),
- The capability to reveal the spatial and temporal patterns of the physical processes inherent in the data.
- The orthogonality in time (statistically independence) of the Principal components (PCs) and their coefficients.
- No requirement for equidistant points of the observations unlike most of the other orthogonal functions (Kutzbach 1967).

The PCA concept is used in this study to establish the dominant modes in the SST data that could be used to develop SSTG modes to predict seasonal rainfall over the region. The PCA was also used in preparing the data for use in canonical correlation analysis (CCA) discussed in section 3.3.6. The spatial patterns of the dominant modes observed in the SST fields would help in developing SSTGs modes to represent the influences of the Atlantic, Indian, and Pacific Oceans. The use of the principal component analysis, however, requires the identification of the number of factors, which must be included in the solutions.

The methods commonly used to determine the number of the PC's to include in the solutions are discussed in the next section.

3.3.2.1 DETERMINATION OF THE NUMBER OF SIGNIFICANT PRINCIPAL COMPONENTS

There are always as many factors (eigenvectors) as the number of variables in the data set involved in the analysis. Since the aim of PCA is to establish new variables representing the highest portion of the variance in the original data, it is expected that some of the variability of individual variables may be redundant. It is, therefore, essential to identify modes (principal components) that effectively represent most of the variance (70%</?^{2}>90%) (Jolliffe 2002; Wilks 2006) of the original data and the underlying physical phenomena. The inclusion of very few principal components (underfactoring) or very many PCs (over factoring) can distort the map patterns obtained from rotated principal components (RPC's).

The most frequently used methods to determine the number of significant factors include Kaiser's criterion (Kaiser 1960), Scree test (Catell 1966), the natural logarithm method (LEV) (Craddock and Flood 1969; Craddock and Flintoff 1970) and the use of sampling error in the eigenvalues (North et al. 1982). All of these methods ensure that only a few factors, extracting substantial amount of the total variance that may not be considered as noise, are retained in the solutions. The next subsections present brief discussions of these methods. More details of the methods used to determine the number of PCs to retain in the models may be obtained in Jolliffe (2002); North ct al., (1982) and Wilks (2006), among other authors.

3.3.2.2 SCREE TEST

The Scree test method involves the plotting of eigenvalues against the corresponding ordinate eigenvector numbers. The point where the graph becomes a straight line forms the truncation point (Cattel 1966).

3.3.2.3 NATURAL LOGARITHM METHOD

The suggestion of Natural Logarithm Method (LEV) by Craddock and Flood (1969) was on recognition that in meteorology noise eigenvalues are in geometric progression. The LEV involves the plotting of the natural logarithms of the eigenvalues against the ordinate numbers of their principal components. The truncation value is near the point where the graph becomes a straight line.

3.3.2.4 SAMPLING ERRORS

The use of sampling errors of the eigenvalues to determine the number of significant principal components (factors) was suggested by North et. al. (1982). In this approach, the sampling errors for the eigenvalues are compared with the separation in the neighbouring eigenvalues. It is recommended that the eigenvalues be separated by at least one or two times the sampling error of the eigenvalue (Barring 1987). The sampling error (SE) of eigenvalue may be expressed in a mathematical equation as:

SE=kV2^V.....(4)

Where k and /V represent the eigenvalue and total number of records, respectively.

3.3.2.5 KAISER'S CRITERION

This approach retains all eigenvectors with eigenvalues greater than one (Kaiser 1959). All the four methods of identifying significant factors give comparable results (Ogallo 1989). In this study, Kaiser's criterion and scree tests were used since they were readily available in the software used in the analysis.

The principal of orthoganality in the extraction of eigenvectors (PCs) dictates that PCs are orthogonal to one another and only the first eigenvector that extracts most of the variability in the original data set is in the direction of the variation of the data. Since the underlying physical processes are not independent, the orthogonality of the PCs may not be realistic (North 1984; Wilks 2006). It is recommended that if the study is aimed at interpreting the physical processes contributing to the variability, a subset of the eigenvectors be rotated to simplify the interpretation (North 1984; Richman 1986; Wilks 2006).

The rotation does not affect the total variance explained by the eigenvalues. A brief account of the rotation is given in the next section.

3.3.2.6 **ROTATION OF PRINCIPAL COMPONENTS**

The methods frequently used in the rotation of eigenvectors (Factors) are the varimax (orthogonal) (Kaiser 1959) and oblique rotations. The varimax method retains orthogonality of the eigenvectors, which are rotated through ninety degrees (90°). The oblique rotations, which include oblimax, oblimin and promax, relax the orthoganality discussed in Varimax and allows some correlation between the factors (Richman 1981; 1986). The oblique rotation is more powerful than Varimax (Richman 1981) but the difficulty to estimate the degree of associations between the clustered variables is a hindrance to the use of the methods. The varimax solution, which has been widely used by many authors, was adopted in this study.

3.3.2.7 **PHYSICAL REALITY OF THE PRINCIPAL COMPONENTS**

The determination of physical reality and climatological stability of the loading patterns derived from Principal component analysis (PCA) is essential. The methods frequently used to establish physical reality and climatological stability of the PCA loadings patterns include inter-station correlations, PCA for a subgroup of the data, (e.g the only locations/variables that had been clustered together, PCA for sub-period of records) and vector plotting the variables into the vector space of the dominant factor(s).

The methods that use subgroup data are developed on the assumption that all stations/variables that were clustered together when all stations were subjected to PCA should have similar temporal variations and cluster on one factor. The sub-period method divides the period of the study into two or more sub-periods and conduct PCA on each sub-period. It is expected that the PCA map patterns for the sub-periods are comparable to those obtained from the complete record if the map patterns are stable.

The vector plotting approach involves the use of the regression weights on pairs of factors to cluster variables into the vector space of the dominant factors. The clusters depict the map patterns of the PC's with variables clustering near the axis of the respective dominant PC.

Inter-station correlation method compares the map patterns obtained from the correlations between the stations and spatial patterns of the dominant PCA modes. The map patterns should be comparable if the PCs are physically realistic. The details of these methods can be obtained in many references including Barnston and Livezy (1987); Hsieh (2004); North et al.(1982); Richman (1986); Rinne and Jarvanoja (1979) among other authors.

In this study, inter-station correlation was used to determine the stability and consistency of the PC patterns.

3.3.2.8 SIGNIFICANCE OF FACTOR LOADINGS

The testing of significance of factor loading borrows from the methods used to test correlation by recognizing the similarities between factor loadings and correlation coefficients. For samples greater than **100,** loading values of at least **0.31** are considered significant. For higher factors, however, it is recommended to adjust the level of significance as presented in equation 5 below.

$$SE\ of\ loading = SE\ of\ correlation\ \ 4n/n + i\text{-}m \quad (5)$$

SE is Standard Error, *n* the number of variables and m the factor member.

The standard errors of correlations may be obtained from the Table given by Child (1990). Significant loadings have coefficients greater than thrice the SE of the loading. Details of this method can be obtained from many authors including Burt (1952). This method was used in the study to determine the levels of significance of the loadings for the various eigenvectors. Once the dorminat SST modes are established, the next step is to develop SST gradient modes discussed in the next section.

3.3.3 **Development of Sea Surface Gradient Gradient Modes**

The meridional and the zonal components of the global circulation system largely influence the transport and convergence of moisture in the atmosphere. The circulation patterns are dependent on the distribution of temperature (heat energy.) The gradients of sea surface temperatures would be a realistic representation of the processes behind the

circulation, and moisture transport and convergence. The gradients are developed from the major SST PC modes.

Both zonal (Hast-West) and meridional (North-South) SST gradient (SSTG) modes were developed to represent the influence on rainfall associated with the zonal and meridional components of atmospheric circulation. The gradients and rainfall indices generated for the whole period of study were used for further analyses. A general representation of SSTG mode at time *t* is presented in equation 6.

$$SSTG(t) = A(t)_{ij} - B(t)_{u} \quad (6)$$

Where *A* and *B* represent standardized anomalies of SST averages over areas A and B representing respective PC modes or time coefficients of the respective dominant PCA modes that are centred at latitude (i) and longitude (j). The zonal and meridional Gradients were computed in the direction of the arrows as shown in Figure 39 in section 4.3.3

Correlation analysis used to quantify the relationships between SST based predictos and rainaffall are discussed in the next section.

3.3.4 CORRELATION ANALYSIS

The correlation coefficient (r) is the most frequently used index for quantifying the degree of relationships between pairs of variables. The correlation coefficient is a good measure of relationships and can be used to identify predictors (Singhrattna et al 2005). Correlation (r) at time lag *k* can be expressed in a mathematical equation as:

$$r_k = \frac{\sum_{t=1}^{N-|k|}(X_t - \bar{X})(Y_{t+k} - \bar{Y})}{\sqrt{\left\{\sum_{t=1}^{N}(X_t - \bar{X})^2\right\}\left\{\sum_{t=1}^{N}(Y_t - \bar{Y})^2\right\}}} \quad (7)$$

Where *X,* and *Y,* are rainfall and SST gradients for the specific regions at times *t,* and, $\bar{X}$ and $\bar{y}$ arithmetic means of X_t and *Y,* at time *t,* respectively. *N* is the length of records. The simple correlation coefficient is obtained from equation (7) by setting k to zero. When the variables are significantly related the simple correlations coefficient r is significantly different from zero, *r* is positive or negative when the variables are positively or negatively correlated and |r| = 1 when the variables are perfectly correlated. The statistical significance of *r* may be estimated, using the standard *t* - test, as indicated in equation (8).

N-2

(8)

t_{N-2} is the student *t* - distribution value with *N-2* degrees of freedom and *N* is as defined in equation (7) above.

The details of *t* - test can be obtained in many standard references including (Battacharyaa and Johnson 1977; Wannacott and Wannacott 1985; WMO 1983).Once a significant correlation has been determined between variables, the next step would be to develop functional relationships.

In the next section regression analysis is discussed.

3.3.5 REGRESSION ANALYSIS

For any pair of rainfall and SSTG modes, which have significant correlation coefficient (r), the next step is to establish the nature of the relationships. This is achieved by determining the best regression equation governing the relationship. A multiple linear regression model which expresses rainfall at any specific time t (Y_t) as a function of SST gradients at time lag k (X_{it+k}) may be expressed as:

$$Y_t = a + b_1 X_{1t+k} + b_2 X_{2t+k} + \ldots + b_n X_{nt+k} \quad (9)$$

for zero lagged relationships the equation becomes:

$$Y_t = a + b_1 X_{1t} + b_2 X_{2t} + \ldots + b_n X_{nt}$$

Where a_t and are regression constants. The regression constants, *a* and *b,* can be estimated from available records.

The major challenges of multiple regression methods include the large number of predictors to be included into the model, computation of several regression coefficients and the possibility of interrelationships among predictors. The interrelationships among predictors may lead to unstable regression coefficients (Mo and Straus 2002). Regression Models based on two to three predictors have been observed to produce better forecasts than those using large numbers of predictors (Delsole and Shukla 2002). Sun et al. (2007) used linear regression models relating a weather index, measuring drought severity and flooding, and SST to predict corn yield over parts of Brazil with useful skill. The multiple regression

methods are the most frequently used in the region and have provided seasonal forecasts with useful skills (Korecha and Baraston 2007).

In this study functional relationships between rainfall and SST gradients are developed using forward stepwise multiple regression method available in the Systat Software Version 8.0 package readily available (Wilkinson 1998). The functional relationships (regression equations) were developed only for locations where the correlations coefficients (r) were statistically significant. The statistical significance of the regression constants, together with the variance of rainfall accounted for by SST gradients was estimated from the Analysis of Variance (ANOVA) principals. Details of ANOVA together with other regression principles can be obtained from Battacharyaa and Johnson (1977); Fisher (1958); Madden (1976); Wannacott and Wannacott (1985) and Wilks (2006), among other authors.

The model performance was assessed using two methods. In the first approach a subset of the data that was excluded in the development of the model (training) period was used to test the model skill. The training period was 1961-1990 and the period used to assess the model skill was 1991-2006.

Another method used to estimate prediction skills of models was cross validation. The cross validation method leaves out a section of the data to construct a model to predict the period that was left out. The window of the data left out is moved forward and each time a model is constructed to predict the period not included in the model development. The advantage of this method is that no training data is required. The predictions from the windows are then used to form a time series of the predictions, which are compared to the predictand. A simple correlation between the predictor and predictand time series or the root mean square error could be used to estimate the skill. The cross validation may give unrealistic skills if there is high inter-annual relations in seasonal rainfall (Barnston et al 1996). Many authors have used this method to assess skills of models (Barnston et al 1996; Omondi 2005; Owiti 2005). More details of this method could be obtained from various authorsincluding Barnston et al. (1996); Battacharyaa and Johnson(1977); von Storch and Zweirs(1999), and Wannacott and Wannacott (1985);.

The Heidke Skill Score (HSS), derived from the elements in the contingency table was used to establish the performance of the models. It gives the accuracy of the forecast

relative to random chance and measures the fraction of correct forecasts after eliminating the forecasts correct due purely to random chance. The mathematical expression of HSS is given in equation 10 as:

$$Hoo = \frac{(hits + correctnegative) - (expected\ correct)random}{N - (\exp ected\ correct)random} \quad (11)$$

where expected correct(random) (EC) may be expressed as:

$$EC = \frac{(H + M)(H + F) + (CN + M)(CN + F)}{N} \quad (12)$$

N is the number of forecasts, H is hits, M is misses, F is false alarms, and CN is correct negatives.

Regression methods do not show the source of influence. A superior multivariate linear method, canonical correlation analysis, which is able to relate data fields and identify the sources of relationships, is discussed in the next section 3.3.6.

3.3.6 CANONICAL CORRELATION ANALYSIS

Canonical Correlation Analysis (CCA) is a multivariate linear statistical model that defines predictive relationships between the predictors and predictands. It has been found to have skill and to offer some insight into the physical basis of the relationships used to derive the predictions. Unlike regression, which tries to study how each Y-is related to X, variables, the CCA examines how the entire Y field is related to the X field (Hsieh 2004; Wilks 2006). The holistic view has made CCA popular (Barnett and Preisendorfer 1987; Rajeevan et al 1999; Shabbar and Barnston 1996). In CCA, a set of loadings for the predictor elements is related to a similar set of loadings for the predictand elements. These loading patterns may be interpreted as indicators of the underlying physical processes. The method may also be considered as a special form of empirical orthogonal function (EOF) analysis with the correlation structure between predictor and predictand datasets described more completely with each successive CCA mode. If X(t) is a matrix composed of independent data set $x_{(}$(t) at time t and **Y**(t) is a matrix composed of data set y . (t) at time t dependent on X(t), the CCA establishes linear combinations

"(t)= a.X(t) ..... (13)

and

v ***(t)=b.Y(t)***.....(14)

such that the canonical variate^ u and v have maximum correlation. This condition is achieved through the choice of appropriate weight vectors a and b that ensure that cor(w.v) is maximized. The weights vectors, a and b, are also referred to as the map patterns (Hsieh 2004).

The first step of CCA involves data reduction and orthogonalization through separate EOF analysis for the predictor and predictand data sets. The time modes of the dominant modes in the separate data sets are then correlated and only correlations between the predictors and predictands are used. The resulting cross correlation matrix is the input for the actual CCA. The CCA produces modes each containing,eigenvectors (loading patterns) for predictors and predictands, an amplitude time series for each (showing years specific patterns occurred) and eigenvalues (showing the importance of the relationship).

The advantages of CCA include ability to operate on full fields of information and to objectively define the most highly related pattern of predictors and predictands, and the capability to define both the space and time evolution of the predictor dataset that best predicts an associated pattern of a predictand. The disadvantages of CCA include the estimation of the reverse matrices needed in CCA, which may be impossible for highly inter-correlated data fields since the matrices may be degenerative. The transformation of the variables into orthogonal variates helps reduce the problems associated with inter-relationship in the data sets (Repelli and Nobre 2004). The CCA can also be unstable if the records are not long enough or if there is noise in the data.

Details of this method may be obtained in Bamston et al. (1996); Barnston and Smith (1996); Barnett and Preisendorfor (1987); Barnett (1981); Glahn (1963); Hsieh (2004); von Storch and Zweirs (1999), and Wilks (2006), amongst other authors. The method is used in this study to develop relationships between rainfall and sea surface temperature that would be used to predict seasonal rainfall. The method is further used to determine the space-time evolution of the prime predictors of seasonal rainfall.

Both regression and canonical correlation analyses are linear methods and only correctly extract the linear structures of the data (Hsieh 2004). Atmospheric processes have non-linear components that may not be captured by linear methods.

In the next section, Neural Network method, which can capture complex non-linear structures of the data, is discussed.

3.3.7 ARTIFICIAL NEURAL NETWORKS

An artificial neural network (ANN) is a data processing system that can learn the relationships between a pair of one or multidimensional data sets (Hsieh 2004; Long et al 2005; Statsoft 2007; Zwiers and Von Storch 2004). The development of Artificial Neural Networks (ANN) borrows from the way the brain works (Rajeevan et al. 2000). The network consists of interconnected neurons (processing elements) that work in parallel to solve a specific problem. Each neuron is a specialized cell, which can propagate signals when activated beyond the threshold. The neurons are trained to fire for only specific thresholds of the signal and to remain inactive when the threshold is not achieved. The networks leam by example and cannot be programmed to perform specific tasks.

The performance ANN models is highly dependent on the examples in the data set used to train the network. The ability of the network to establish a solution to any problem is a major weakness of ANN method since some solutions may not be useful. The ANN learns the relationships by minimizing the error resulting from the estimation of the output(s)(predictand(s)) from the input(s)(predictor(s)). The processing of estimates is also referred to as training. The training involves the implementation of a function *fix)* that transforms the input X into output Ysuch that:

$$f : X \backslash\text{->} Y \qquad (15)$$

Where X is input and Y is output. The ANN models are referred to networks since the function f(x) is composed of other functions $P^{-}(*)$ in the form:

$$/\ W\ \hat{}\ I\ w\ \hat{}\ W \qquad (16)$$

Where yy is the weighting sum, K is a transfer function which is predefined, ***g*** is a collection of functions, which is sometimes referred to as a vector and is presented as:

$$s^{=} \ldots\ldots £_n \qquad (17)$$

The most frequently used transfer functions are hyperbolic tangent and logistic functions. Only the logistic function used in this study is discussed. The logistic function is expressed as

$$\hat{} = \frac{}{l + e} \quad \text{.....C8)}$$

Where x is the input and y is the output.

The use of logistic function (sigmoid function) in a single-layer neural network model makes it identical to the logistic regression model. The logistic function is the most frequently used in statistical modelling due to its capability to accommodate backpropagation networks, which are more powerful than the feedforward networks. For logistic function the controls or threshold are 0 and 1. Hence the neuron is trained to fire (activated) when the signal reaches 1 and not to fire (remain dormant) when the signal is zero. These thresholds ensure that only neurons associated with the inputs that contribute at a given time are activated. The use of logistic function is also motivated by its continuous and easy to calculate derivative. The network used in our study is a backpropagation called "BrainCom 1.2" ,which is described in details by BrainCom (2007).

ANN method has a higher capability to fit non-linear processes than observed for linear regression models and may over perform dynamical methods (Ramirez et al. 2007). The advantages of ANN in forecasting rainfall include the high capability to simulate non-linear relationships, represent complex relationships, ability to generate forecasts for any location without prior knowledge of the factors that may influence the relationships such as topography, distribution of water bodies etc (Hsieh 2004; Ramirez et al. 2007; Zwiers and Von Storch 2004).

The limitations of ANN method, like other statistical analysis techniques, is the need for a training dataset that suitably represents the behaviour of the system to avoid a situation where the technique may learn spurious relationships that are peculiar to the training data, and may conceal more general and robust relationships. The other limitations of ANN method include convergence at various levels, over-fitting, and the need for test data set independent from that used in developing the model (Hsieh 2004). For poor data set (eg.

short noisy data records) the problems with convergence and over-fitting may render ANN methods incapable of offering advantage over linear methods (Hsieh 2004).

ANN methods have skills comparable to linear methods in situations dominated by linear relationships (Tang et al 2000). ANN methods showed improvements in the estimation of wind speeds, SST, and sea surface air temperature from the Special Sensor Microwave Imager (SSM/I) observations (Meng et al. 2007). The method has also shown improvements in the predictiction of seasonal rainfall (Mauget and Ko 2008). Details of the method can be obtained from Frankel et al (1995), French et al (1992); Hsieh (2004); Hsu et al. (1997); Kuligowski and Barros (1998) and McCann (1992) amongst other authors. Useful information on this method may also be obtained at the Internet websites indicated in the list of references.

This method was used in this study to establish its capability to improve relationships between seasonal rainfall and SSTG modes that may be used to predict seasonal rainfall. In the next section composite analysis method is discussed.

3.3.8 COMPOSITE ANALYSIS

Composite analysis is a simple method used to study atmospheric processes influencing specific phenomena. The first step of the method involves the choice of a basis for developing composites. The second step involves the selection of the cases that meet a specific category of the decided base. The selected cases are then averaged to set a mean pattern of the element in response to the behaviour of the selected base (Drbohlav et al. 2007; Kayano et al. 2007; Nobre and Shukla 1996; Krishnamurthy and Shukla 2007; Malony and Shaman 2008). This approach was used in this study. The SSTG modes formed the basis for composite analysis.

In cases where emphasis on contrast is required, the use of the difference between the mean patterns created by contrast signals are recommended since it enhances the contrast (Nobre and Shukla 1996).

Many authors have used this method to study the responses of various meteorological elements to some anomalies in the general circulation (De and Mukhopathyay 1999; Kayano et al. 2007); Mo et al 1997; Njau 2006; Okoola 1996; Owiti 2005) used this approach to study the behaviour of eastern Africa monsoons associated with wet and dry years. Kayano et

al. (2007) used the method to determine the response of rainfall in South America to ENSO and Pacific inter-decadal oscillation. De and Mukhopathyay (1999) used the method to determine the response of sea surface temperature to ENSO and observed that during ENSO (EL-Nino years), the SST anomalies both over the Arabian Sea and the Bay of Bengal were positive in the months of October to December, and the reverse occurred during La Nina years. Mo et al (1997) used the method to study the evolution of persistent wet and dry events over the central United States. Owiti (2005) used this method to investigate the relationships between IOD and OND rainfall. Njau (2006) used this method to study rainfall patterns associated with the upper tropospheric warm and cold thermal regimes and observed significant teleconnection between 300hPa geo-potentials and temperature, and seasonal rainfall. The Wet/dry seasonal conditions were associated with warm/cold temperatures at 300hPa level (Njau 2006).

The advantages of the method are that the composites can reveal the relationships that might not be captured by simple correlations. In this study, composite analysis was used to determine the responses of rainfall to specific characteristics of the zonal and meridional gradients. The method was also used to determine the evolution of rainfall characteristics associated with specific signals in the SSTG modes from the OLR, wind, and other reanalysis data.

The results of the study are discussed in Chapter 4.

CHAPTER FOUR

4.0 RESULTS AND DISCUSSIONS

This chapter presents the results that were obtained from the various methods that were presented in chapter 3. It should be recalled that the overall objective of this study is to improve seasonal prediction skills of rainfall in the region through the use of sea surface temperature gradients (SSTG) modes. The first step in achieving this objective involves determining the dominant modes of variability in seasonal sea surface temperatures for the Indian and Atlantic Oceans from Principal Component Analysis (PCA) that could be used to derive sea surface temperature gradients (SSTG) modes that have prediction potentials to seasonal rainfall for the specific seasons and regions of East Africa. However, before the data could be subjected to the various analyses it was important to subject them to quality analyses. The results from quality analyses are discussed in the next section

4.1 DATA QUALITY CONTROL ANALYSIS

The first most important step in any analysis is to determine the quality of the data. Figures 7a and 7b give examples of mass curves that were used to test for the homogeneity of the records. It can be observed from Figures 7a and 7b that there was no significant trend in the rainfall data for Gulu in Uganda and Dar es Salaam International Airport (DIA) in Tanzania for the period 1961-2006. Similar results were observed with the other data sets.
Only the records that passed the quality control tests were used in this study, and they formed the foundation for all analyses that were undertaken in this study. The time series analyses of the standardized data indicated inter annual recurrences of large and low values of anomalies in all records. The large SST anomalies are evident during the El Nino/Southern Oscillation and Indian Ocean dipole years. The extreme high and low rainfall values, on the other hand, reflected the major flood and drought years. In the next section, the results from principal component analysis are discussed.

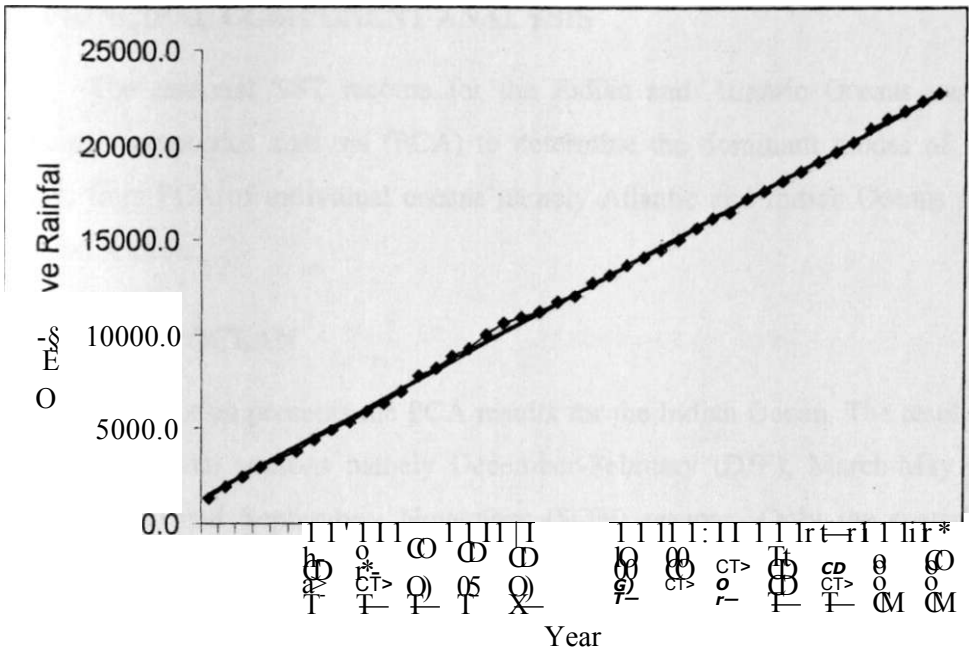

Figure 7a: Cumulative mass curve of September-December rainfall for Gulu station in Uganda

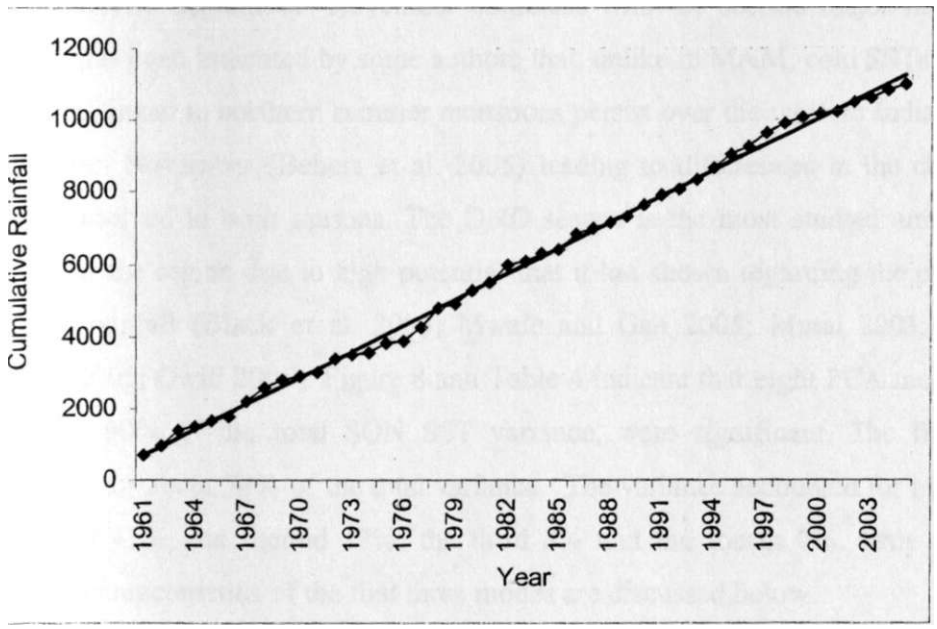

Figure 7b: Cumulative mass curve of September-December rainfall for Dar es Salaam International Airport station in Tanzania

4.2 PRINCIPAL COMPONENT ANALYSIS

The seasonal SST records for the Indian and Atlantic Oceans were subjected to principal component analysis (PCA) to determine the dominant modes of variability. The results from PCA of individual oceans namely Atlantic and Indian Oceans are presented in the next section.

4.2.1 INDIAN OCEAN

This section presents the PCA results for the Indian Ocean. The results are presented for the individual seasons namely December-February (DJF), March-May (MAM), June-August (JJA) and September- November (SON) seasons. Only the spatial and temporal characteristics of the first three modes that accounted for most of the seasonal total SST variance are presented.

4.2.1.1 SEPTEMBER-OCTOBER-NOVEMBER

In this section, the results from PCA of September- November (SON) SST are discussed. The September- November coincides with the second major rainfall season of OND. It has been indicated by some authors that, unlike in MAM, cold SSTs associated with upwelling linked to northern summer monsoons persist over the western Indian Ocean during September- November (Behera et al. 2005) leading to differences in the characteristics of rainfall received in both seasons. The OND season is the most studied among the rainfall seasons of the region due to high potential that it has shown regarding the predictability for seasonal rainfall (Black et al. 2003; Mwale and Gan 2005; Mutai 2003; Ogallo 1988a; Omondi 2005; Owiti 2005). Figure 8 and Table 4 indicate that eight PCA modes, accounting for about 90% of the total SON SST variance, were significant. The first four modes accounted for about 74% of the total variance. The variance accounted for by the first mode was about 41%, the second 17%, the third 8% and the fourth 7%. Only the spatial and temporal characteristics of the first three modes are discussed below.

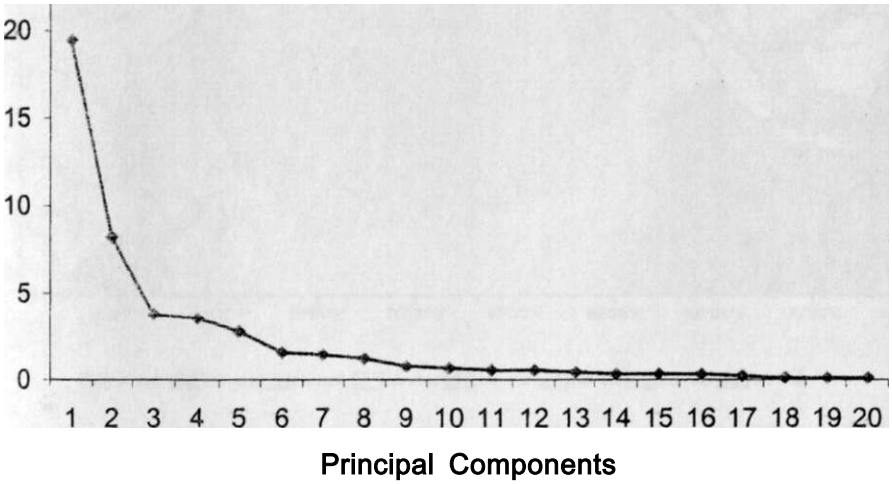

Figure 8: Results of scree test for principal component analysis of September-November sea surface temperatures for the Indian Ocean

Table 4: The significant principal component analysis modes of September-November sea surface temperatures for the Indian Ocean based on Kaiser's criterion and the associated sea surface temperature variance

PCA mode number	Eigenvalues	% of Total Variance	Cumulative % of Total Variance
1	19.39	41.26	41.26
2	8.22	17.48	58.74
3	3.83	8.16	66.90
4	3.51	7.47	74.37
5	2.81	5.99	80.36
6	1.59	3.38	83.74
7	1.50	3.18	86.92
8	1.23	2.61	89.53
9	0.93	1.97	

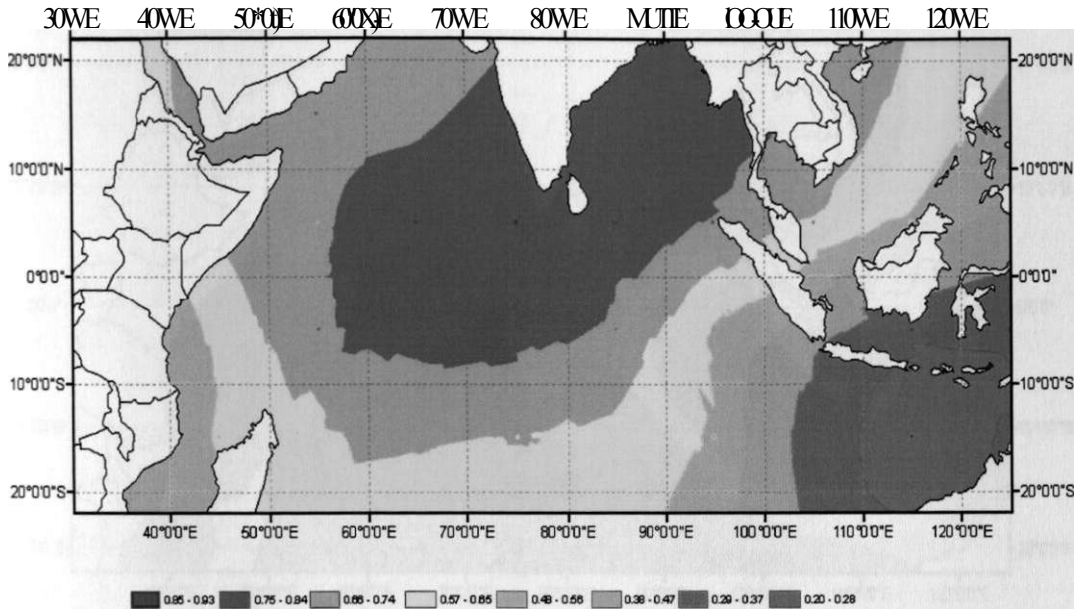

Figure 9a: The spatial patterns of the loadings of the first principal component analysis mode of September-November sea surface temperatures for the Indian Ocean

Figure 9 gives the spatial patterns of the loadings of SON PC modes. Figure 9a indicates that the first PC mode had high positive loadings with the same sign over the entire Indian Ocean with the highest loadings concentrated in the area between latitudes 20°N and 20°S. This mode seems to represent the mean seasonal patterns of SST over the ocean (Behera et al. 2005; Chambers et al. 1999; Schreck and Semazzi 2004; Terray and Dominiak 2005; Tozuka et al. 2007; Ward and Folland 1991; Yu and Rienecker 1999). The spatial patterns of the loadings of the second PCA mode are given in Figure 9b. Figure 9b indicates that the second PCA mode displays a dipole characteristic with a positive pole located in the eastern (20°N-30°S, 90°E-130°E) and a negative pole located in the western (20°N-30°S, 40°E-90°E) parts of the Indian Ocean. The dipole patterns of the second PCA resembles the Indian Ocean Dipole (IOD), which has received a lot of attention with regard to the associated SST variability and regional rainfall patterns (Black et al. 2003; Behera et al.2005; Huang and Shukla 2007; Meyers et al. 2007; Owiti 2005; Owiti 2005; Saji and Yamagata 2003; Tozuka et al. 2007; Yu and Rienecker 2000;).

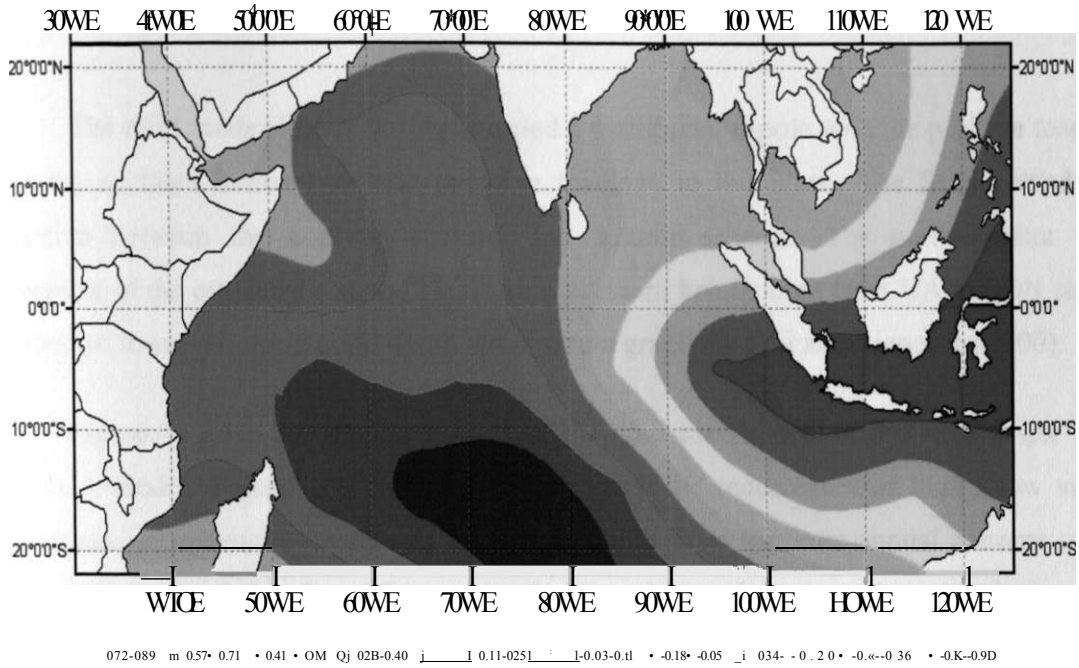

Figure 9b: The spatial patterns of the loadings of the second principal component analysis mode of September-November sea surface temperatures for the Indian Ocean

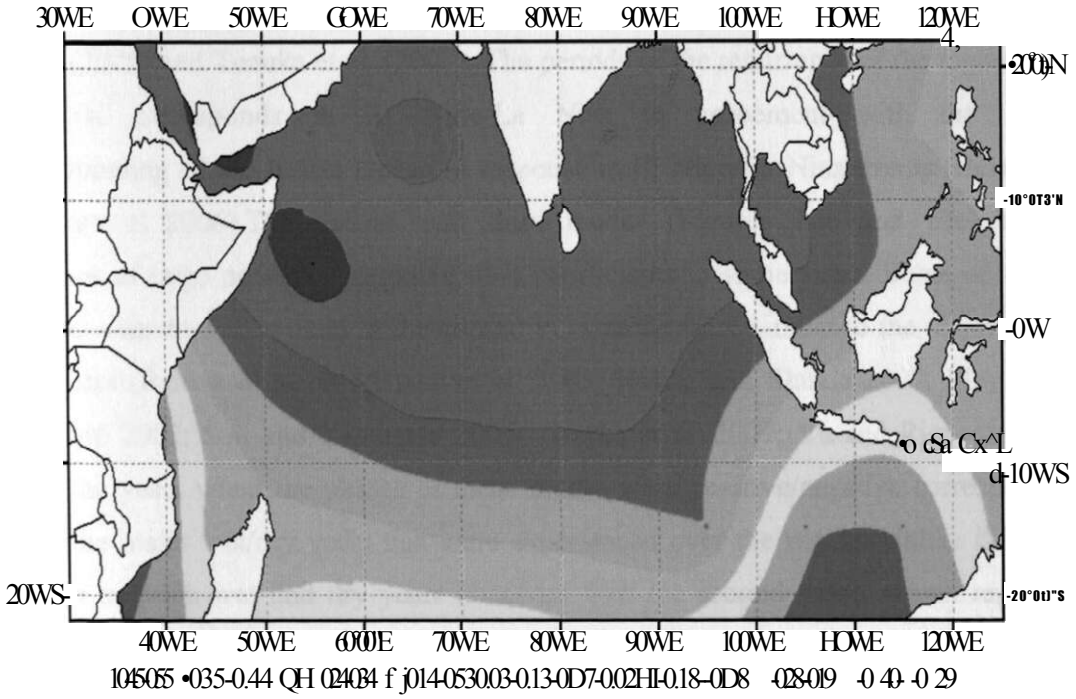

Figure 9c: The spatial patterns of the loadings of the third principal component analysis mode of September-November sea surface temperatures for the Indian Ocean

The third mode (Figure 9c) represented a meridional dipole with the positive loadings over the southern hemisphere and negative loadings to the north. The SON period is a transition between the northern summer and autumn seasons. The north-equator ward movement of the overhead sun and ITCZ from northern hemisphere from JJA to SON season is expected to induce some north-south temperature gradients (Yu and Rienecker 2000).

Figure 10 gives the graphical plots of the time coefficients of the three major SON SST PCA modes. Figure 10a indicates that although the recurrences of high / low values were common, increasing trend was quite discernible from the inter-annual patterns of the time coefficients of the first PCA mode. Similar observations have been made in some previous studies including An and Wang (2000); Harrison and Carson (2007); Ihara et al.(2008); and Wang and An (2001). This trend is in agreement with the observed changes in the temperatures of the global oceans (IPCC 2007). Some of these studies have indicated that these trends could be associated with the shifts on the evolution and characteristics of ENSO. This mode has significant inter-decadal variability similar to those observed by Omondi (2005) and Tozuka et al. (2007). The periods of the recurrence of the highest/lowest coefficients corresponds to El Nino/La Nina in agreement with the expected warming/cooling of the Indian Ocean in response to El Nino/La Nina events (Behera et al. 2005; Kug et al. 2006).The second and third modes (Figures 10b and 10c) also had recurrences of large positive / negative time coefficients in some years. Some of the years associated with the recurrences in the second PCA mode were similar to the major IOD and ENSO years (Behera et al.2005;Black et al. 2003; Huang and Shukla 2007; Meyers et al. 2007; Owiti 2005; Saji and Yamagata 2003; Tozuka et al. 2007; Yu and Rienecker 2000). Most of the years when the phases of these modes were positive/negative corresponded to some of the major wet/dry years that were experienced over the region. Unlike the distinct separation between wet and dry years observed with the second mode, which represented zonal SST variability, some of the low/high coefficients of the third PCA were not associated with large-scale rainfall anomalies over the region. It should be noted that the third PCA mode accounted for only 8% of Indian Ocean SST variability.

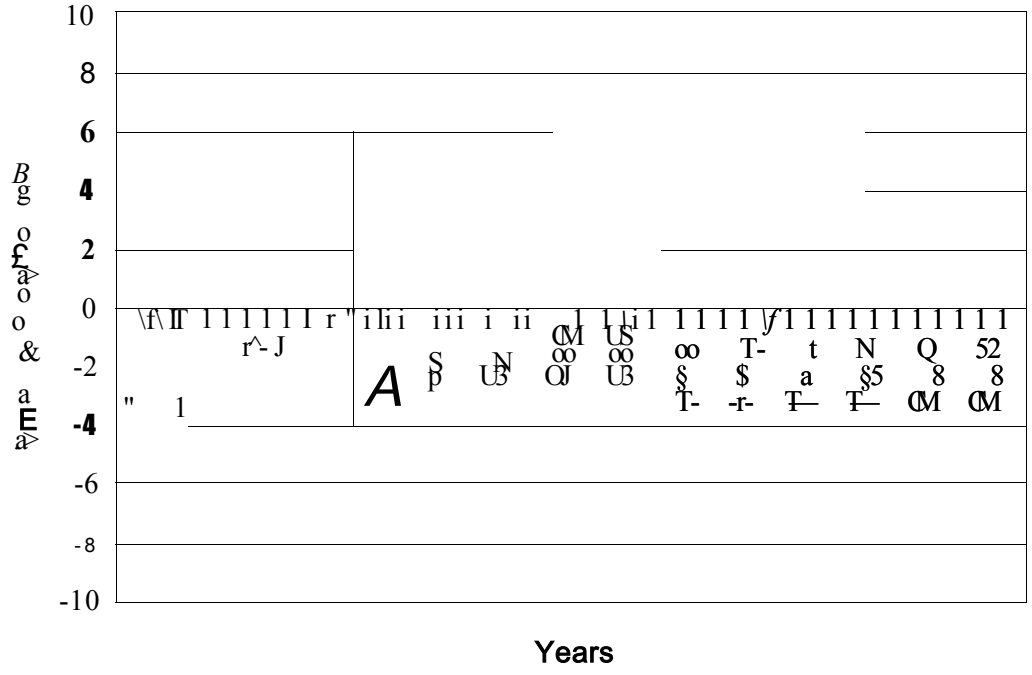

Figure 10a: The graphical plot of the time coefficients of the first principal component analysis mode of September-November sea surface temperatures for the Indian Ocean

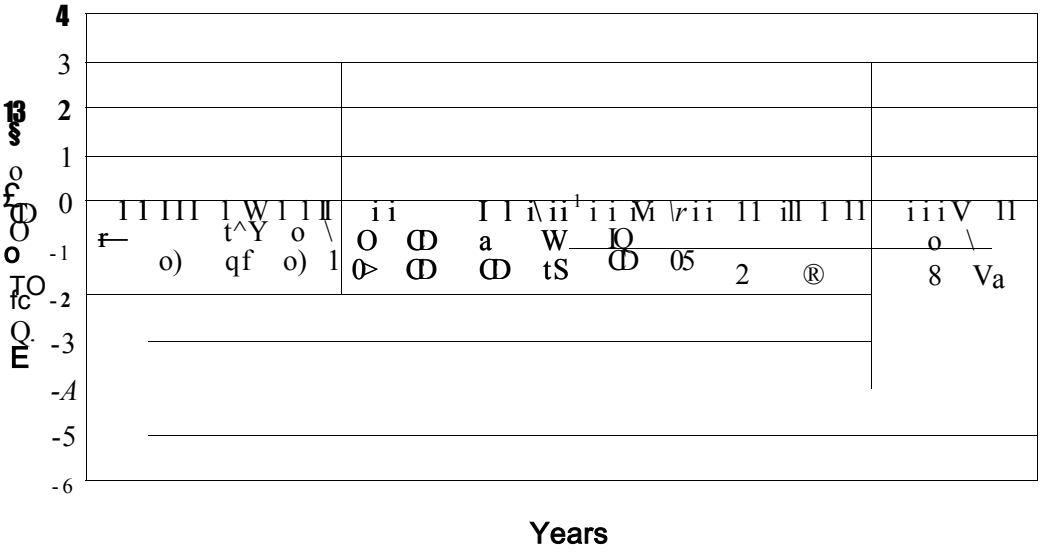

Figure 10b: The graphical plot of the time coefficients of the second principal component analysis mode of September-November sea surface temperatures for the Indian Ocean

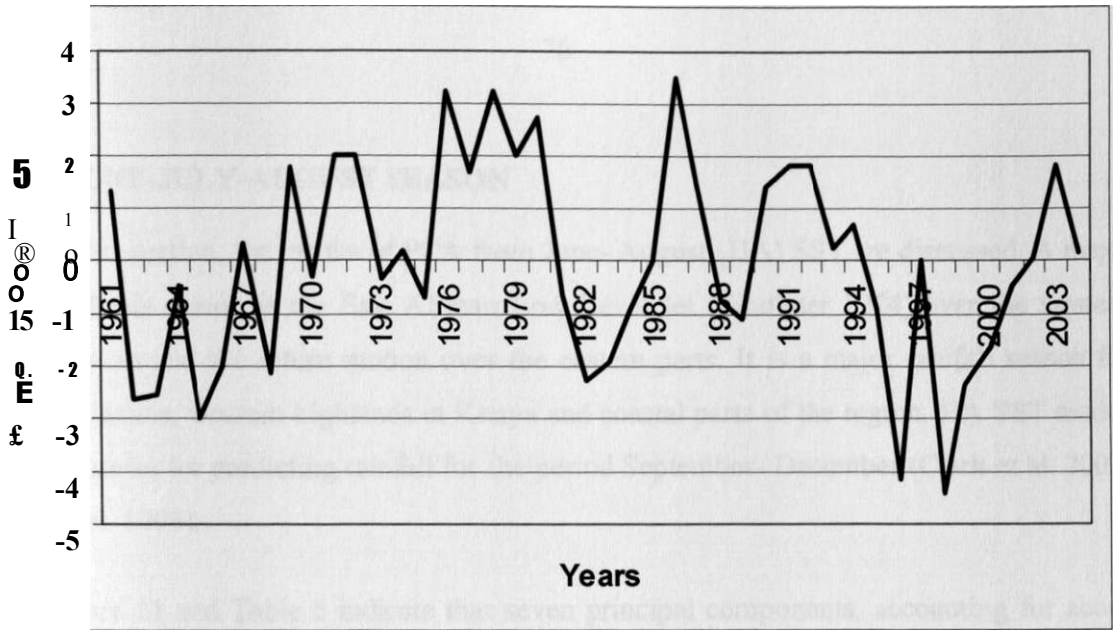

Figure 10c: The graphical plot of the time coefficients of the third principal component analysis mode of September-November sea surface temperatures for the Indian Ocean

The third PCA mode also reflected meridional SST variability that is expected to have relatively weaker influence on the climate of the region compared to the modes representing zonal SST variability in agreement with the findings of Lindzen and Nigam (1987). It can, however, be used to represent unique localized characteristics at some specific locations.

The spatial and temporal characteristics of the modes observed in this season indicate that the zonal SST variability dominate in the Indian Ocean. In general, the negative/positive coefficients of the major first two PCA modes representing zonal SST variability corresponded to some of the major wet/dry years associated with positive IOD and El Nino / negative IOD and La Nina events as listed by Behera et al. (2005); and Black et al. (2003); Clark et al. (2003); Owiti (2005); and Saji and Yamagata (2003) among other authors. In the next section the results from PCA of June- August SST are discussed.

4.2.1.2 JUNE-JULY-AUGUST SEASON

In this section, the results of PCA from June- August (JJA) SST are discussed. A major feature of this season is the East African Low Level Jet (Findlater 1974) over the western Indian Ocean and the return motion over the eastern parts. It is a major rainfall season for most of Uganda, western highlands in Kenya and coastal parts of the region. JJA SST modes are very useful for predicting rainfall for the period September- December (Clark et al. 2003; Mutai et al. 1998).

Figure 11 and Table 5 indicate that seven principal components, accounting for about 89%. of the total JJA SST variance, were significant in the JJA SST. The first four modes accounted for about 75% of the total variance. The first, second, third and fourth mode accounted for about 44%, 15%, 9% and 7% of the total JJA SST variance, respectively. The spatial characteristics of most of the JJA PCA modes were quite similar to those of SON. There are, however, some differences in the magnitudes and spatial spread of areas under high positive / negative loadings and variances accounted for by each mode compared to SON. For example, the variance accounted for by the second mode dropped from about 17% in SON to 15% in this season. The unique dipole mode over equatorial western Indian Ocean is now represented by the third PCA mode (Figure 12). It had a positive pole located in the western (0°-10°S, 30°E-60°E) and a negative pole in central (0°S-30°S, 70°E-90E°) Indian Ocean. This mode represents a zonal variation in SST similar to IOD but displaced eastward. Behera et al. (2005) indicated the existence of a secondary zonal mode near the coast of East Africa that compliments the IOD in enhancing OND rainfall during the positive IOD phases. This unique PCA mode was only observed during JJA.

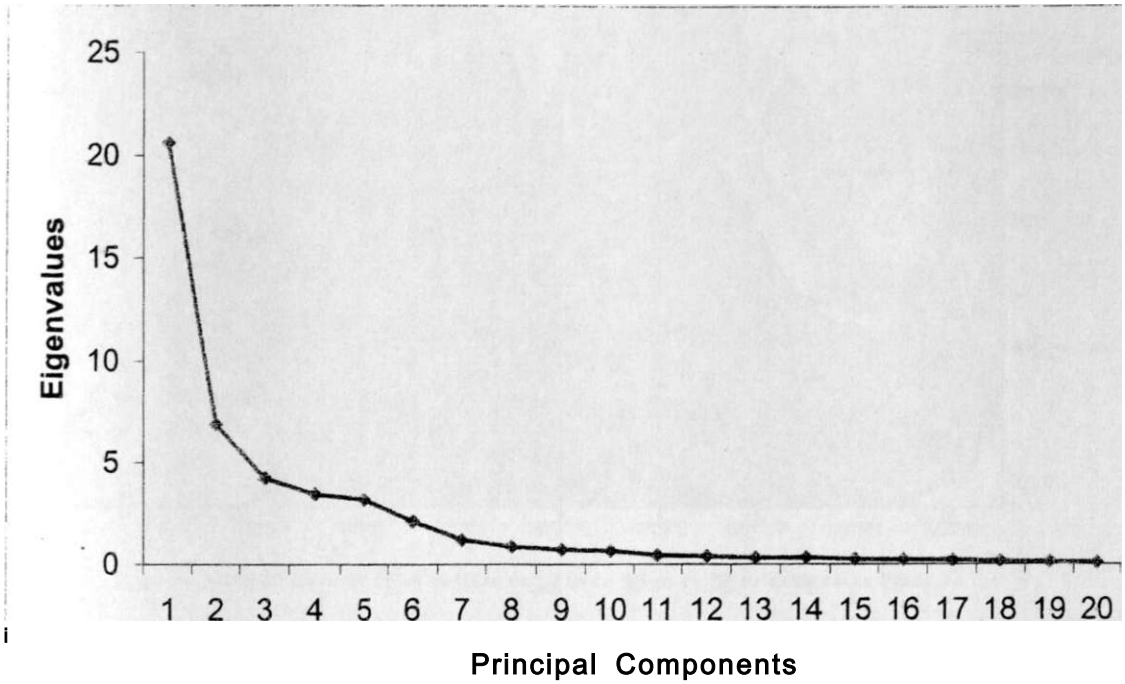

Figure 11: Results of scree test for principal component analysis mode of June-August sea surface temperatures for the Indian Ocean

Table 5: The significant principal component analysis modes of June-August sea surface temperatures for the Indian Ocean based on Kaiser's criterion and the associated variance

PCA mode Number	Eigenvalues	% Of Total Variance	Cumulative % of Total Variance
1	20.58	43.79	43.79
2	6.89	14.66	58.45
3	4.25	9.04	67.49
4	3.46	7.36	74.85
5	3.19	6.79	81.64
6	2.14	4.55	86.19
7	1.23	2.62	88.81

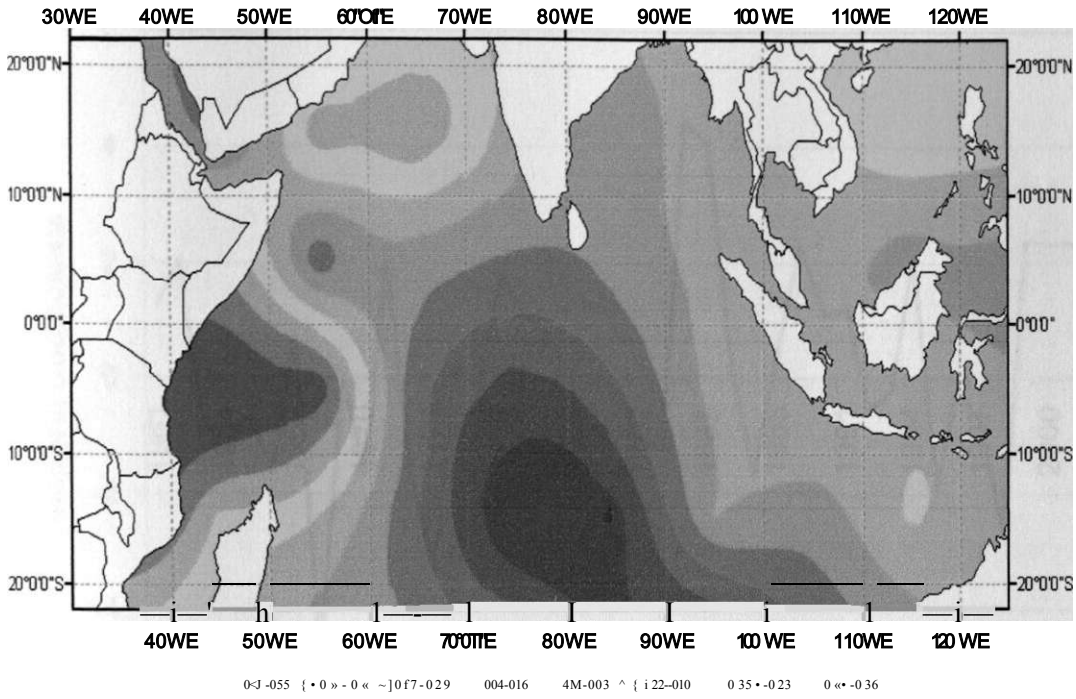

Figure 12: The spatial patterns of the loadings of the third principal component analysis mode of June-August sea surface temperatures for the Indian Ocean

Figure 13 gives the graphical plots of the time coefficients associated with the third mode. This mode had large positive coefficients in 1961, 1962, 1967, 1971, 1976-1978, 1984, 1985, 1988, 1989, 1990, 1991, 1994, 1999-2002 and 2004. The large negative time coefficients were observed in the years 1963-1966, 1968, 1970, 1972, 1973, 1980-1983, 1987, 1992, 1995-1998 and 2003. It can be observed that in most of the years when the coefficients were large positive/negative the region experienced dry/wet conditions in phase with the association observed with the mode representing the IOD. Some positive trend is also discernible. These results are in agreement with the findings of Behera et al. (2005).

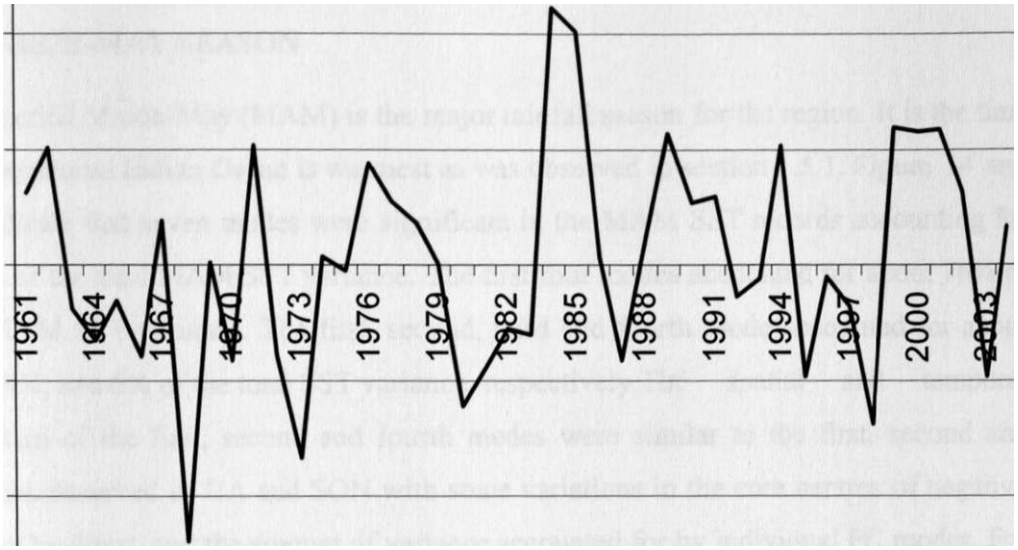

Figure 13: The graphical plot of the time coefficients of the third principal component analysis mode of June-August sea surface temperatures for the Indian Ocean

The spatial and temporal characteristics of the JJA PCA SST modes in the Indian Ocean continue to indicate the significant linkages amongst Indian Ocean SST modes of variability and the systems affecting the climate of the region. Indian Ocean is the key moisture source for inland rainfall processes. The recent major dry and wet conditions are also quite discernible from the interannual patterns of the major JJA and SON SST modes. The associations between rainfall and the SST modes were clear for both JJA and SON SSTs variability patterns. In the next section, the results from PCA of March-May (MAM) SST are discussed.

4.2.1.3 MARCH-MAY SEASON

The period March-May (MAM) is the major rainfall season for the region. It is the time when the equatorial Indian Ocean is warmest as was observed in section 1.5.1. Figure 14 and Table 6 indicate that seven modes were significant in the MAM SST records accounting for about 90% of the total MAM SST variance. The first four modes accounted for about 76% of the total MAM SST variance. The first, second, third and fourth mode accounted for about 55%, 9%, 6%, and 6% of the total SST variance, respectively.The spatial and temporal characteristics of the first, second and fourth modes were similar to the first, second and fourth modes observed in JJA and SON with some variations in the core centres of negative and positive loadings, and the amount of variance accounted for by individual PC modes. For example, the first PC mode in MAM accounted for about 55% of the SST variance compared to about 44% and 41% in JJA and SON, respectively. Only the spatial and temporal characteristics of the third mode that was unique for this season are presented in this section. Figure 15 gives the spatial patterns of the loadings of the third mode observed with MAM SST that was unique for the season. A similar mode, independent of ENSO, has been observed in the studies using AGCMs to simulate the climate of the Indian Ocean and has been associated with anomalous southeast trade winds (Huang and Shukla 2007) and the wind currents associated with Mascarine subtropical high-pressure system (Chiodi and Harrison 2007). This mode may be associated with the differences in the SST patterns linked to the Mascarene high pressure system, which is expected to warm/cool the ocean over the western/eastern parts of the anticyclone due to advection (Seagar et al. 2003).

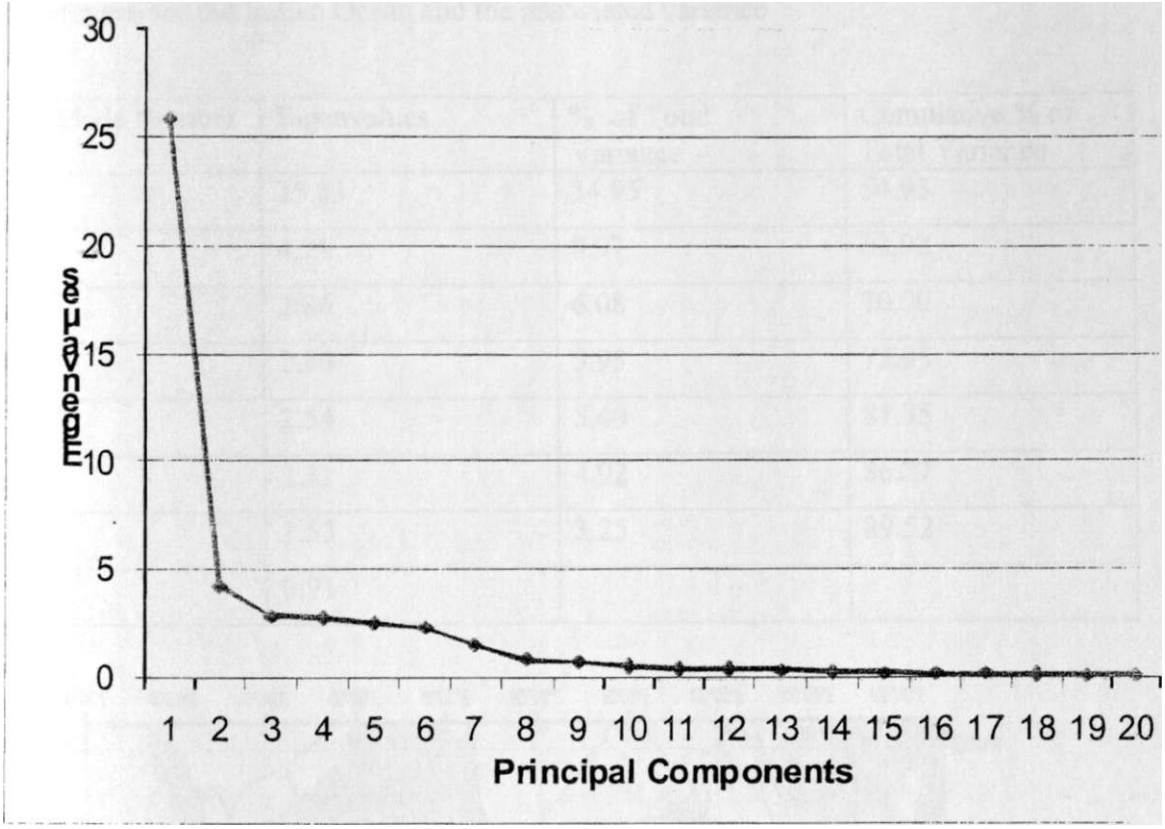

Figure 14: Results of scree test for principal component analysis of March-May sea surface temperatures for the Indian Ocean

Figure 16 gives the graphical plot of the time coefficients of the third mode observed with MAM SST. This mode had large positive time coefficients in 1962, 1963, 1965, 1967, 1971, 1972, 1974-1976, 1978, 1983-1985, 1988, 1989, 1994-1997, 1999, 2000, 2002 and 2004. This mode had large negative time coefficients in the years 1961, 1964, 1966, 1968, 1970, 1973, 1977, 1979-1982, 1986, 1987, 1990, 1991, 1993, 1998, 2001 and 2003. It can be observed that most of the wet/dry years correspond to the years when the time coefficients were large negative/positive.

Table 6: The significant principal component analysis modes of March-May sea surface temperatures for the Indian Ocean and the associated variance

PCA Mode Number	Eigenvalues	% of Total Variance	Cumulative % of Total Variance
1	25.83	54.95	54.95
2	4.21	8.97	63.92
3	2.86	6.08	70.00
4	2.80	5.95	75.95
5	2.54	5.40	81.35
6	2.31	4.92	86.27
7	1.53	3.25	89.52
8	0.91		

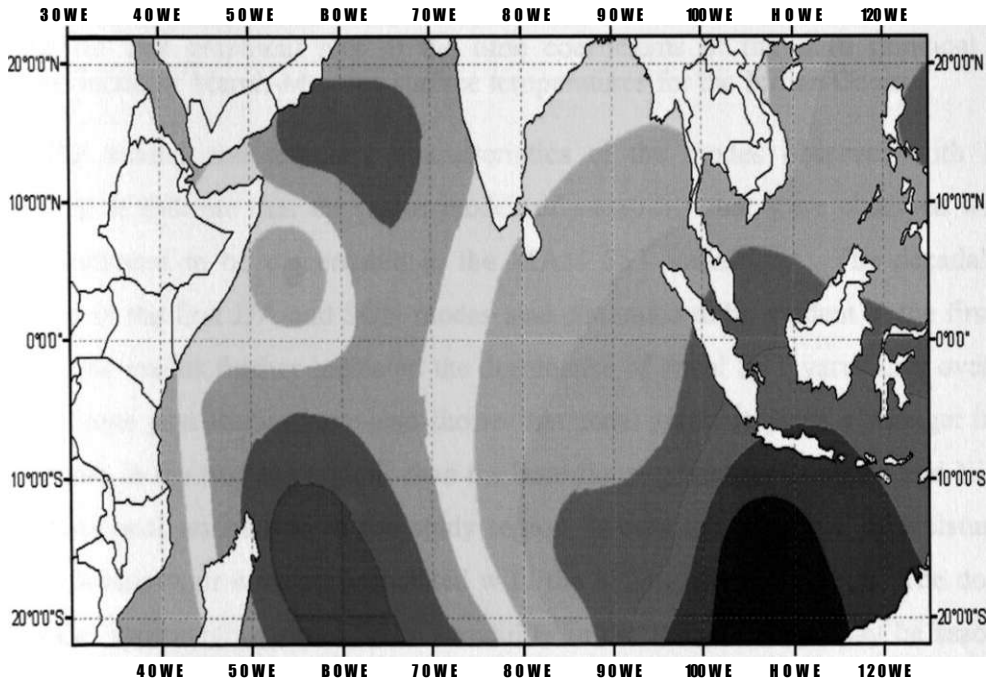

B 038 • 048 LJ 028 • 038] 018 • Q17 I bg017 Q -004 0 06 -014 -106^1 -025 • -0« rj -035 • -0 26 H -048 -026 ^ -057 • -042

Figure 15: The spatial patterns of the loadings of the third principal component analysis mode of March-May sea surface temperatures for the Indian Ocean

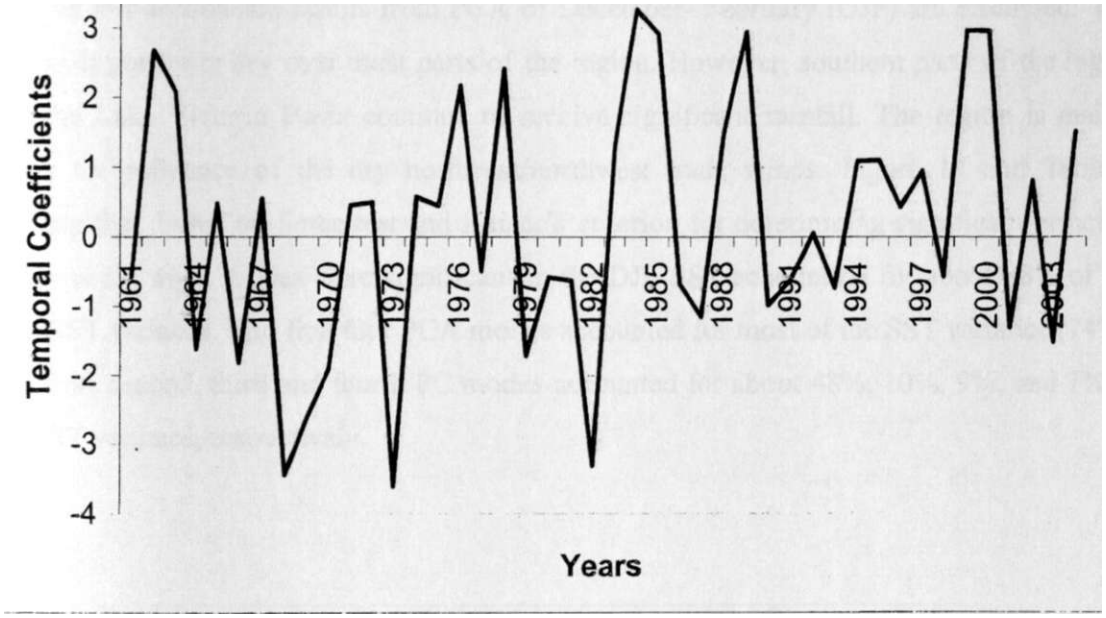

Figure 16: The graphical plot of the time coefficients of the third principal component analysis mode of March-May sea surface temperatures for the Indian Ocean

The spatial and temporal characteristics of the modes observed with MAM SST continued to indicate that the major modes of variability that were observed with JJA and SON continued to be discernable in the MAM SST variability. The decadal variability observed in the first JJA and SON modes also continued to be evident in the first MAM PC mode. The results further indicated the dominance of zonal SST variability over the Indian Ocean. Some past studies have also shown that zonal gradients have a stronger influence on the climate in the tropical regions than the meridional gradients (Lindzen and Nigam 1987). The meridional orientation of the study region favours the incursion of moisture from the easterly/westerly air currents associated with the Indian/Atlantic Oceans. The dominance of the modes representing zonal SSTs variability in the Indian Ocean may be associated with the strong influence of this ocean on the climate of the region as has been observed by many authors including Goddard and Graham (1999); Mutai et al. (1998); Mutai (2003); Okoola (1996); Omondi (2005); and Owiti (2005) among other authors. In the next section the results from the PCA of December- February (DJF) SST are discussed.

4.2.1.4 DECEMBER- FEBRUARY SEASON

In this section the results from PCA of December- February (DJF) are discussed. This season is generally dry over most parts of the region. However, southern parts of the region and the Lake Victoria Basin continue to receive significant rainfall. The region is mainly under the influence of the dry northeast/northwest trade winds. Figure 17 and Table 7 indicate that, based on Scree test and Kaiser's criterion for determining significant principal components, eight modes were significant in the DJF SST accounting for about 88% of the total SST variance. The first four PCA modes accounted for most of the SST variance (74%). The first, second, third and fourth PC modes accounted for about 48%, 10%, 9%, and 7% of the SST variance, respectively.

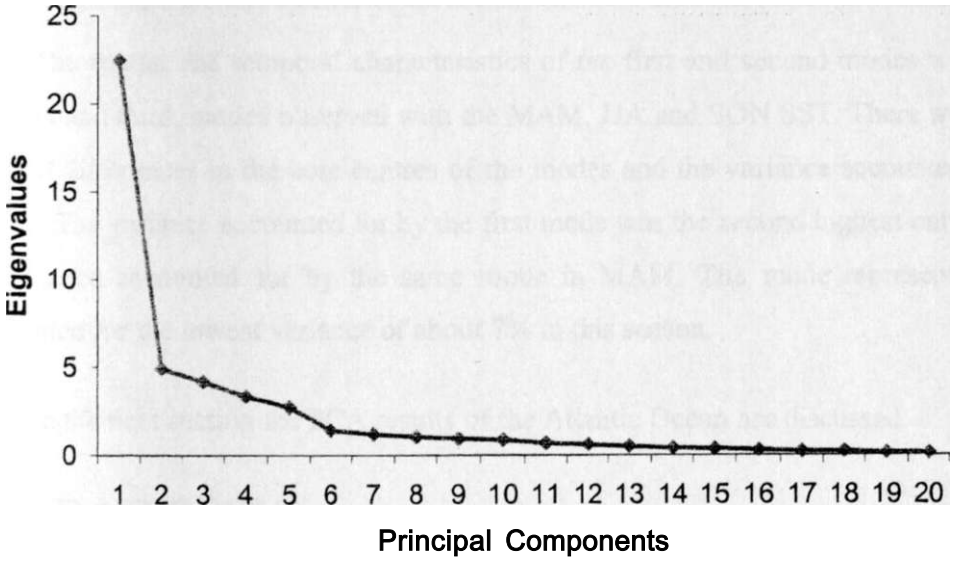

Figure 17: Results of scree test for principal component analysis of December-February sea surface temperatures for the Indian Ocean

Table 7: The significant principal component analysis modes of December-February sea surface temperatures for the Indian Ocean and the associated variance

PCA Mode Number	Eigenvalues	% Of Total Variance	Cumulative % of Total Variance
I	22.47	47.80	47.80
2	4.91	10.45	58.25
3	4.19	8.91	67.16
4	3.35	7.13	74.29
! 5	2.73	5.80	80.09
6	1.41	3.00	83.09
7	1.20	2.55	85.64
8	1.05	2.24	87.88
9	0.94		

The spatial and temporal characteristics of the first and second modes were similar to the first and third, modes observed with the MAM, JJA and SON SST. There were, however, marked differences in the core centres of the modes and the variance accounted for by each mode. The variance accounted for by the first mode was the second highest only comparable to variance accounted for by the same mode in MAM. The mode representing the IOD accounted for the lowest variance of about 7% in this season.

In the next section the PCA results of the Atlantic Ocean are discussed.

4.2.2 ATLANTIC OCEAN

In this section the results from principal component analysis (PCA) of seasonal SST for the Atlantic Ocean are discussed for the DJF, MAM, JJA and SON seasons. The SST variability in the Atlantic Ocean reaches its maximum in the period January to May (Wu et al. 2007). The next section discusses the results from PCA of the DJF SST.

.2.2.1 DECEMBER-JANUARY-FEBRUARY SEASON

The period December- February (DJF) is often used to predict the MAM rainfall season, which is a major rainfall season for the region. It is, therefore, important to understand the variability of SST over the Atlantic, which are often used as predictors of rainfall over the region. Only the spatial and temporal characteristics of the first three modes that accounted for most of the seasonal total SST variance are discussed.

Figure 18 and Table 8 indicate that a total of ten PCA modes accounting for about 90% of the total DJF SST variance were significant in this season. The first four modes accounted for a total of 66%. The first, second, third and fourth PCA mode accounted for about 34%, 15%, 11% and 7% of the variance, respectively. Figure 19 gives the spatial patterns of the loadings of the first three PCA modes observed with the DJF SST. Figure 19a indicates that the first mode had high loadings of a similar sign over most of the ocean basin, which represent mean SST characteristics over the basin.

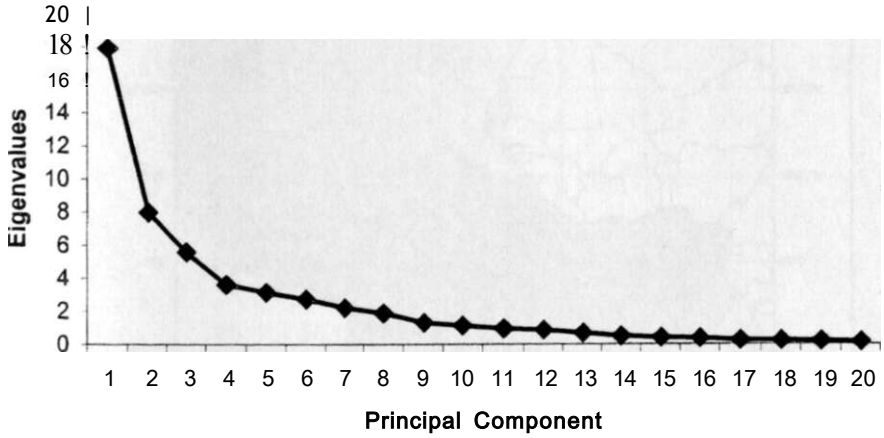

Figure 18: Results of scree test for principal component analysis of December-February sea surface temperatures for the Atlantic Ocean

Table 8: The significant principal component analysis modes of December-February sea surface temperatures for the Atlantic Ocean and the associated variance

PCA Mode Number	Eigenvalues	% of Total Variance	Cumulative % of Total variance
1	17.9	33.77	33.77
2	7.98	15.06	48.83
3	5.59	10.55	59.38
4	3.62	6.84	66.22
5	3.15	5.94	72.16
6	2.74	5.16	77.32
7	2.22	4.18	81.50
8	1.88	3.55	85.05
9	1.31	2.47	87.52
10	1.15	2.16	89.68
11	0.96		
12	0.88		

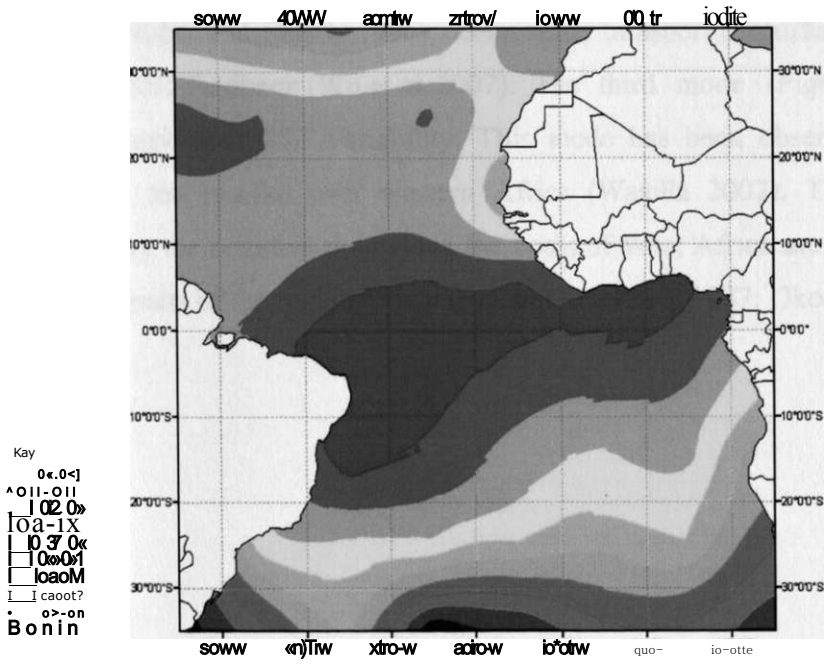

Figure 19a: The spatial patterns of the loadings of the first principal component analysis mode of December-February sea surface temperatures for the Atlantic Ocean

Figure 19b indicates that the second mode represents an inter-hemispheric dipole with the negative pole in the southern (0°S-30°S, 30°W-10°E) and the positive pole in the northern (0°N-30°N, 60°W-15°W) tropical Atlantic Ocean. This mode has been observed in the variability of SST over the Atlantic by many authors including Chang et al.(2007); Li et al. (2007); Moura and Shukla (1981); Nobre and Shukla (1996); Parker et al. (1988); Repelli and Nobre (2004); Weare(1977); and Wu et al. (2007) among many other authors. This mode has been associated with the development of ENSO (Li et al. 2007; Wu et al. 2007) and to have linkage with the North Atlantic Oscillation (NAO) (Wu et al. 2007). It has a strong influence on the climate of the regions neighbouring the Atlantic Ocean and beyond (Chang et al. 2007; Hastenrath and Heller 1977; Hu and Huang 2006; Moura and Shukla 1981; Parker et al. 198.8; Sutton and Hodson 2007). The inclusion of the gradient associated with this mode as a predictor of rainfall over northeast Brazil led to marked improvements in the skills of the forecasts (Moura and Shukla 1981). A similar pattern has been observed in the relationships between rainfall over parts of Brazil and SST over the Atlantic Ocean (Ward and Folland 1991). Its development has been associated with anomalous atmospheric circulation (Nobre and Shukla 1996), ocean water transport (Stouffer et al. 2007), and wind-evaporation-SST feedback (Wu et al. 2007). The third mode (Figure 19c) displays both zonal and meridional SST variability. This mode has been observed to have significant influence on the rainfall over western Africa (Wasilla 2007). The SSTs over the area represented by the negative pole along the coast of West Africa are negatively correlated to rainfall over parts of the region (Nicholson and Entekhabi 1987; Okoola 1996).

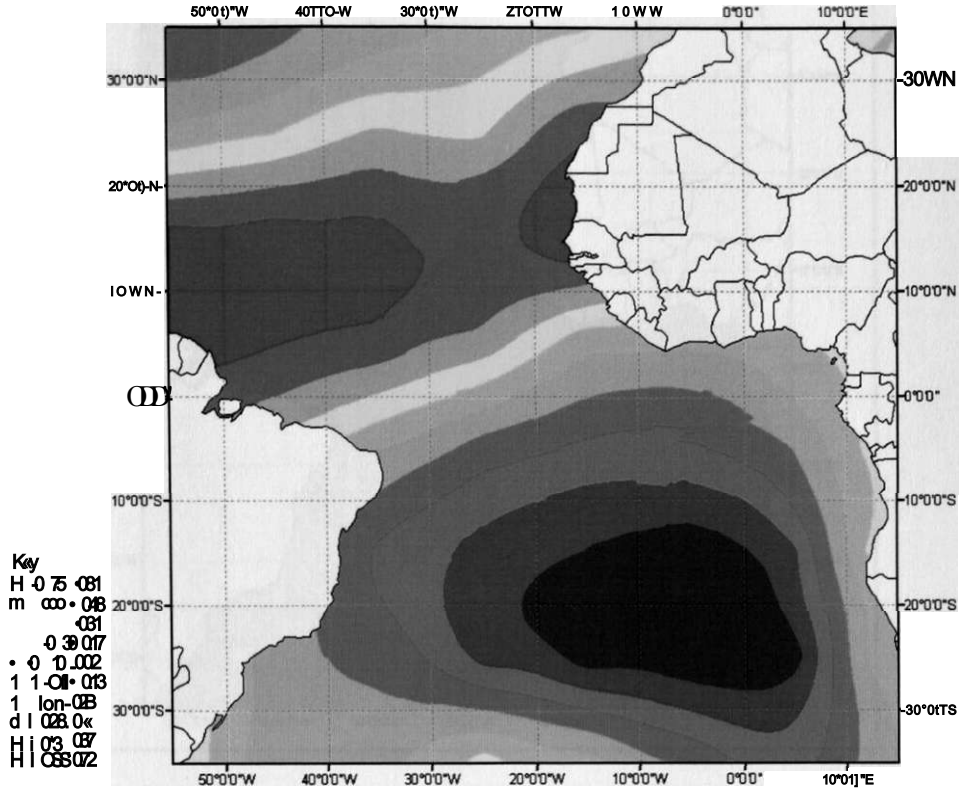

Figure 19b: The spatial patterns of the loadings of the second principal component analysis mode of December-February sea surface temperatures for the Atlantic Ocean

The temporal characteristics of the modes observed with the DJF SST (Figure 20) indicate that the modes represented interdecadal and decadal variability. Decadal and multidecadal variability associated with the variation of thermohaline circulation have been observed in the Atlantic Ocean (Latif et al. 2006). The first mode represented a trend similar to what was observed with the first DJF mode for the Indian Ocean. The years of large positive and negative values of the time coefficients correspond to some of the major wet and dry years over parts of central, eastern and western Africa associated with ENSO and interhemispheric SST gradient in the Atlantic (Nicholson and Entekhabi 1987; Nicholson Kim 1997; Schreck and Semazzi 2004; Wu et. al. 2007).

Temporal Coefficients
-8
-6
-4
-2
0
2
4
6
8
10
12
Years
1961
1964
1967
1970
1973
1976
1979
1982
1985
1988
1991
1994
1997
2000
2003

• • • • • • • • • I

SSSBsfiSfigfi

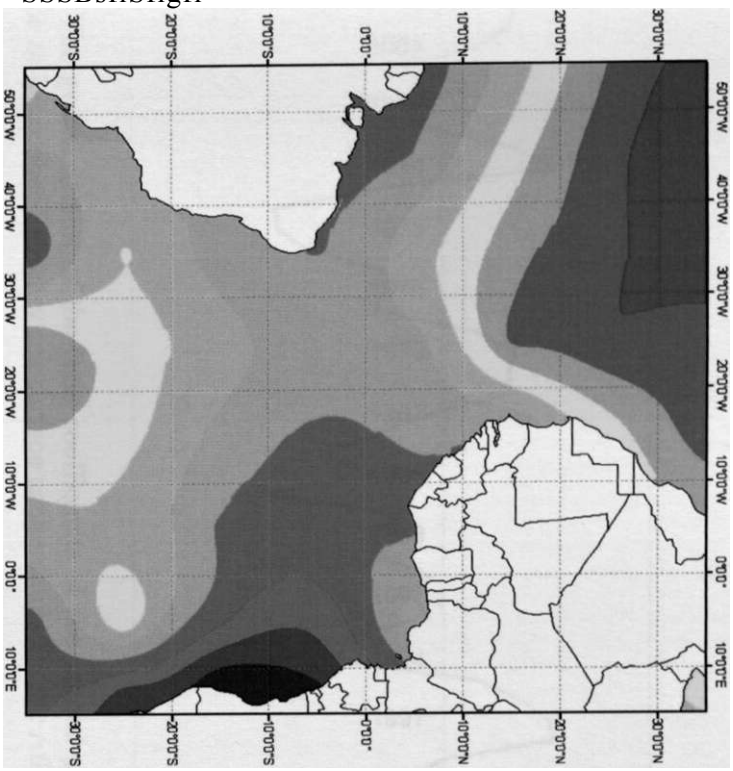

yO

o

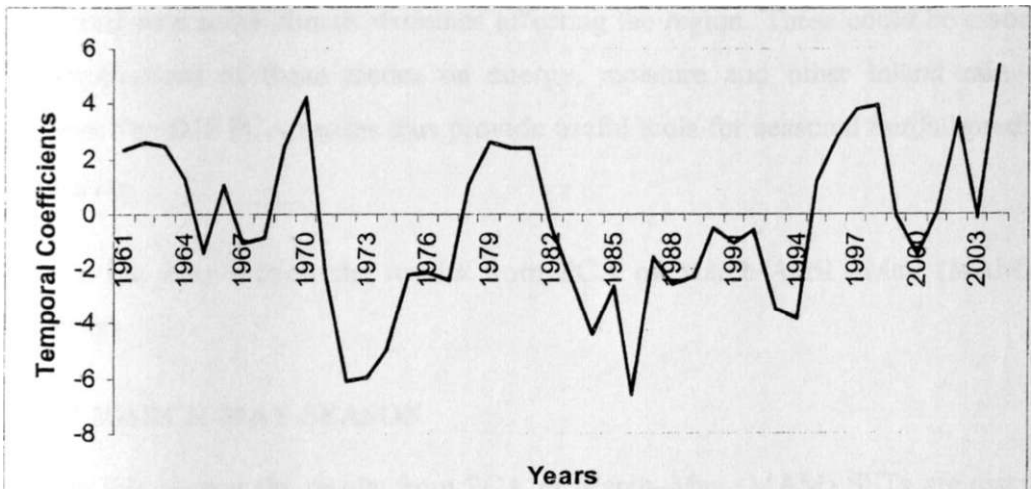

Figure 20b: The graphical plot of the time coefficients of the second principal component analysis mode of December-February sea surface temperatures for the Atlantic Ocean

r

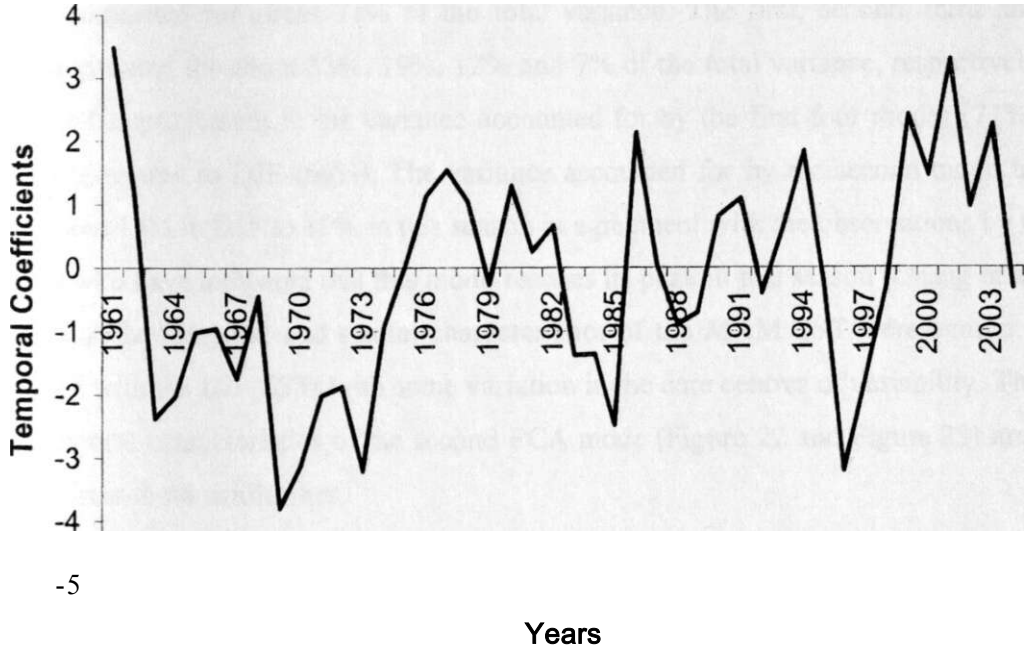

Figure 20c: The graphical plot of the time coefficients of the third principal component analysis mode of December-February sea surface temperatures for the Atlantic Ocean

These results indicate that the Atlantic Ocean PCA modes have significant influence on seasonal rainfall over eastern Africa. The characteristics of the PCA modes were closely

associated with some climate extremes affecting the region. These could be associated with the implications of these modes on energy, moisture and other inland rain generating systems. The DJF PCA modes thus provide useful tools for seasonal rainfall prediction over the region.

In the next section the results from PCA of March-April -May (MAM) SST are discussed.

4.2.2.2 MARCH-MAY SEASON

In this section the results from PCA of March-May (MAM) SSTs are discussed. The period MAM is useful for the Atlantic Ocean since it is the time when some of the modes reach their maximum peaks as is observed with the mode associated with the inter-hemispheric dipole (Chang et al. 2007). Figure 21 and Table 9 indicate that eleven PC modes accounting for about 92% of the variance were significant in MAM SSTs. The first four modes accounted for about 71% of the total variance. The first, second, third and fourth mode accounted for about 33%, 19%, 12% and 7% of the total variance, respectively. There is marked improvement in the variance accounted for by the first four modes (71%) in this season compared to DJF (66%). The variance accounted for by the second mode improved from about 15% in DJF to 19% in this season in agreement with the observations by the other authors who have indicated that this mode reaches its peak in this season (Chang et al. 2007). In general the temporal and spatial characteristics of the MAM SST were similar to those observed with the DJF SSTs with some variation in the core centres of variability. The spatial and temporal characteristics of the second PCA mode (Figure 22 and Figure 23) are used to demonstrate these similarities.

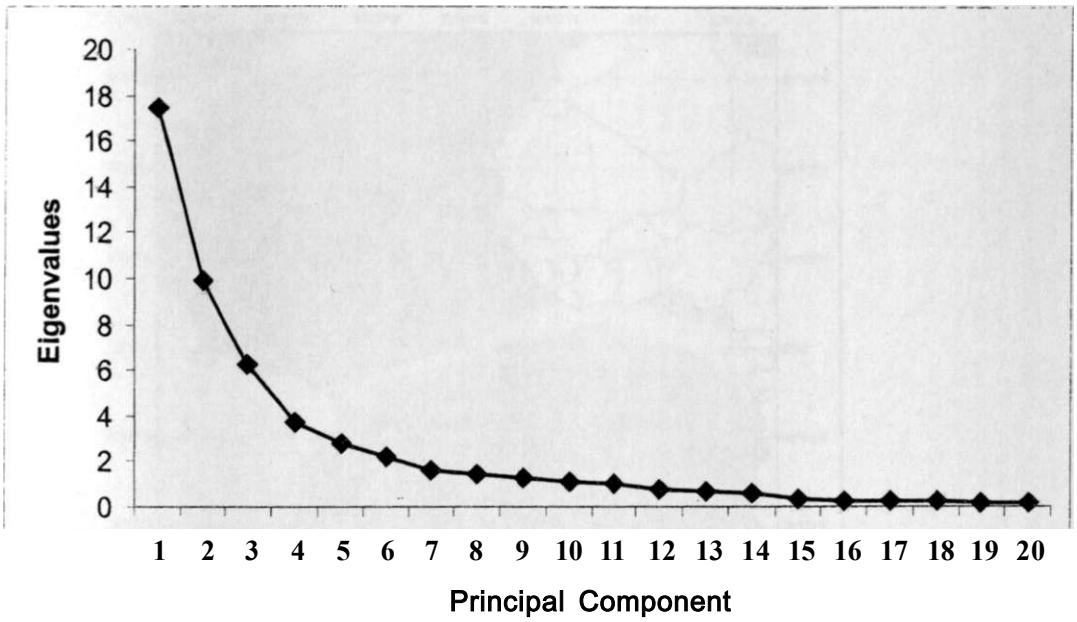

i

Figure 21: Results of scree test for principal component analysis of March-May sea surface temperatures for the Atlantic Ocean

Table 9: The significant principal component analysis modes of March-May sea surface temperatures for the Atlantic Ocean and the associated variance

PCA mode Number	Eigenvalues	% of Total Variance	Cumulative % of Total Variance
1	17.5	33.01	33.01
2	9.93	18.74	51.75
3	6.29	11.87	63.62
4	3.70	6.98	70.60
5	2.76	5.20	75.8
6	2.17	4.08	79.88
7	1.60	3.01	82.89
8	1.43	2.71	85.60
9	1.31	2.47	88.07
10	1.12	2.11	90.18
11	1.01	1.90	92.08
12	0.92		

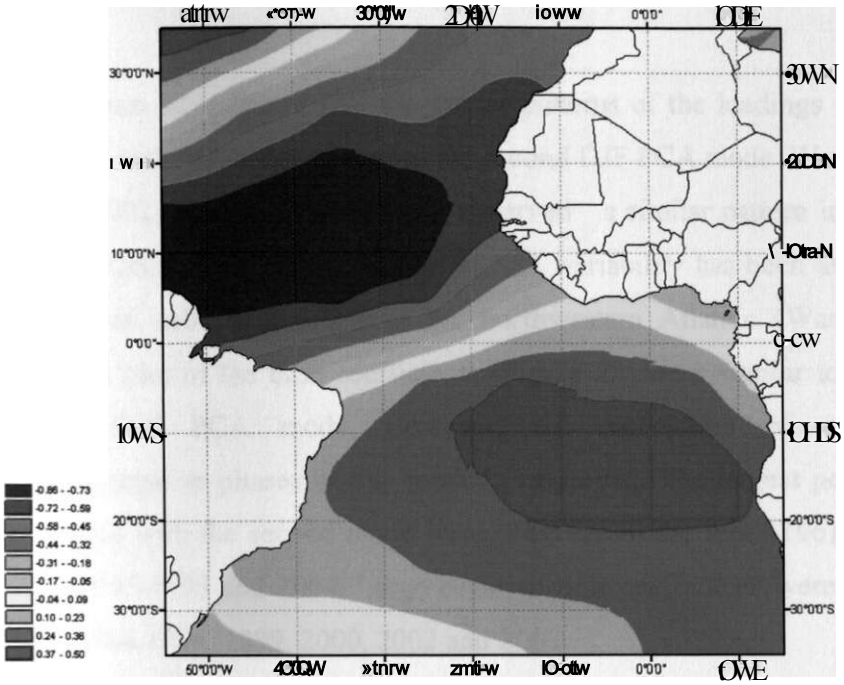

Figure 22: The spatial patterns of the loadings of the second principal component analysis mode of March-May sea surface temperatures for the Atlantic Ocean

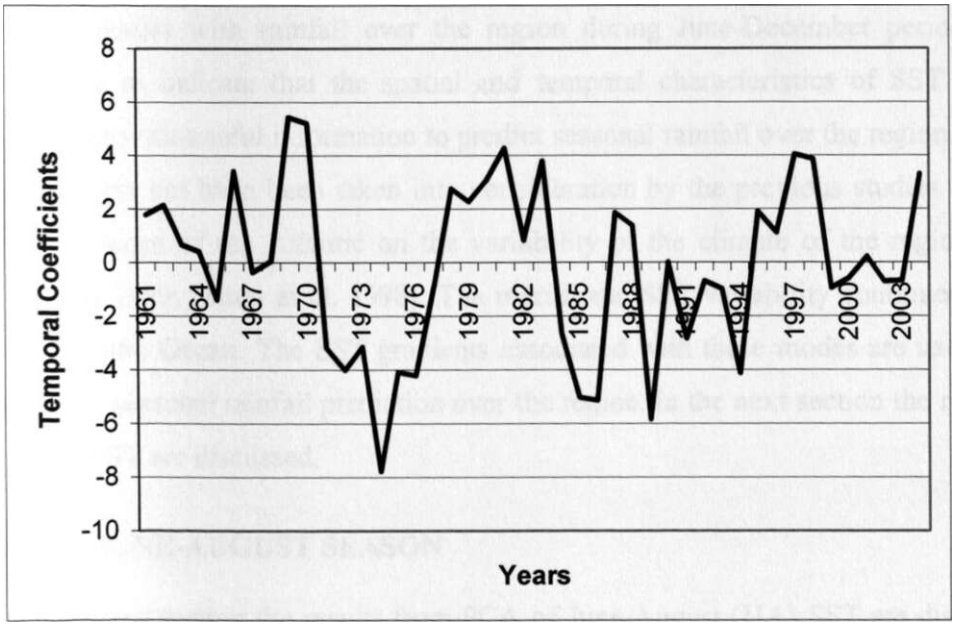

Figure 23: The graphical plot of the time coefficients of the second first principal component analysis mode of March-May sea surface temperatures for the Atlantic Ocean

Figure 22 indicates that the spatial patterns of the loadings of the second PCA mode observed with MAM are similar to the second DJF PCA mode. Ward and Folland (1991) and Wang (2002), among other authors, observed a similar pattern in SST variability over the Atlantic Ocean. This spatial pattern of SST variability has been associated with the Hadley and Ferrell cells observed over the northwestern Atlantic (Wang 2002). Similarly the graphical plot of the time coefficients (Figure 23) were similar to those observed with the second DJF PCA mode. However, the association of wet/dry conditions with positive/negative phases of this mode is improved. The largest positive time coefficients associated with the second mode were observed in the years 1961-1966, 1969-1983, 1987, 1988, 1995-1998 and 2004. Large negative time coefficients were observed in 1965, 1971-1977, 1984-1994, 1999, 2000, 2002 and 2003.

The spatial and temporal characteristics of the three modes associated with MAM SST continue to indicate that the climate extremes affecting the region correspond to some extreme phases of SST variability in the Atlantic Ocean. The MAM SST modes had lead-time linkages with rainfall over the region during June-December period. These results continue to indicate that the spatial and temporal characteristics of SST for the Atlantic Ocean provide useful information to predict seasonal rainfall over the region. This long lead-time might not have been taken into consideration by the previous studies that downplayed the influence of the Atlantic on the variability of the climate of the region (Goddard and Graham 1999; Mutai et al. 1998). The meridional SST variability continued to dominate in the Atlantic Ocean. The SST gradients associated with these modes are used in attempts to improve seasonal rainfall prediction over the region. In the next section the results from PCA of JJA SST are discussed.

4.2.2.3 JUNE-AUGUST SEASON

In this section the results from PCA of June-August (JJA) SST are discussed. The JJA marks the beginning of the decline in the intensity of the gradient associated with the inter-hemispheric dipole in the Atlantic. Figure 24 and Table 10 indicate that eleven PC modes were significant in the SST of this season. The eleven modes accounted for about 92% of the

total JJA SST variance for this season. The first four modes observed with JJA SST accounted for about 71% of the total JJA SST variance. The first, second, third and fourth mode accounted for about 33%, 19%, 12% and 7% of the total JJA variance, respectively. The spatial and temporal characteristics of the first three modes observed with JJA SST were similar to the first three modes observed in DJF and MAM. Such properties may be useful for long-range climate prediction. In the next section the results from PCA of September-October-November (SON) SST are discussed.

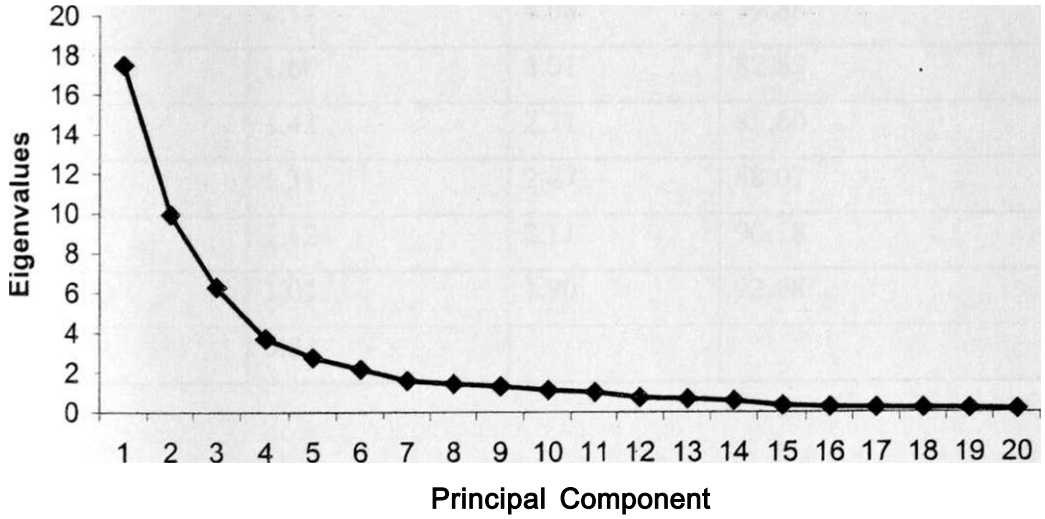

Figure 24: Results of scree test for principal component analysis of June-August sea surface temperatures for the Atlantic Ocean

Table 10: The significant principal component analysis modes of June-August sea surface temperatures for the Atlantic Ocean and the associated variance

, PCA Mode Number	Eigenvalues	% of Total Variance	Cumulative % of Total Variance
1	17.50	33.01	33.01
2	9.93	18.74	51.75
3	6.29	11.87	63.62
4	3.70	6.98	70.60
5	2.76	5.20	75.80
6	2.17	4.08	79.88
7	1.60	3.01	82.89
8	1.43	2.71	85.60
9	1.31	2.47	88.07
10	1.12	2.11	90.18
11	1.01	1.90	92.08
12	0.91		

4.2.2.4 SEPTEMBER-OCTOBER-NOVEMBER SEASON

In this section the results from PCA of SST for September- November (SON) are discussed. Unlike the Indian Ocean where major modes of variability reach a peak within the period June to September, the intensity of the modes weakens in this season (Wang 2002). Figure 25 and Table 11 indicate that eleven PC modes were significant in the SON SST. The eleven modes accounted for about 92% of the total SON SST variance for this season.

The spatial and temporal characteristics of the first three modes observed with the SON SST were similar to those observed with DJF, MAM and JJA SST. The four modes accounted for about 71% of the total SON SST variance. The first, second, third and fourth modes accounted for about 33%, 19%, 12% and 7% of the total SST variance, respectively.

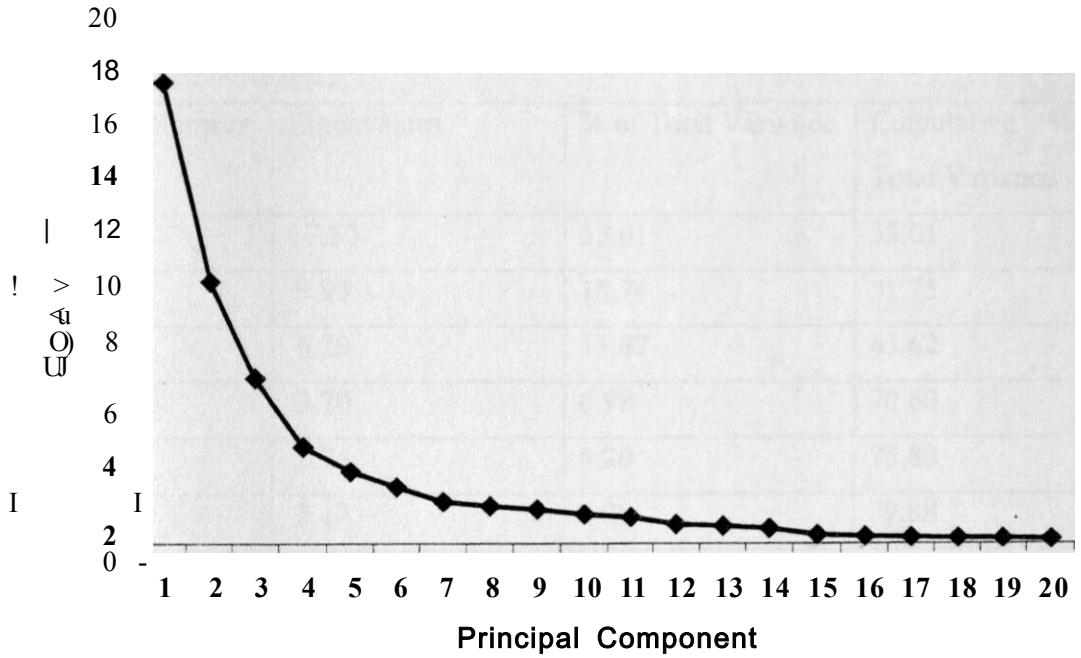

Figure 25: Results of scree test for principal component analysis of September-November sea surface temperatures for the Atlantic Ocean

The PCA modes from SON SST continue to demonstrate the important influence of Atlantic Ocean SST variability on rainfall over parts of eastern Africa. The major striking characteristic for the Atlantic Ocean SST PCA modes is the seasonal persistence of the patterns of the second mode within the seasons as can be observed from Figure 26. Figure 26 demonstrates that the negative and positive phases of the second PCA mode seem to persist over more than one season during the years of large SST anomalies in the Atlantic. The persistence of SST patterns over a long period of time can provide important tools for long-range climate prediction. These will form foundations for some of the seasonal rainfall prediction potential analyses in the later sections of the study.

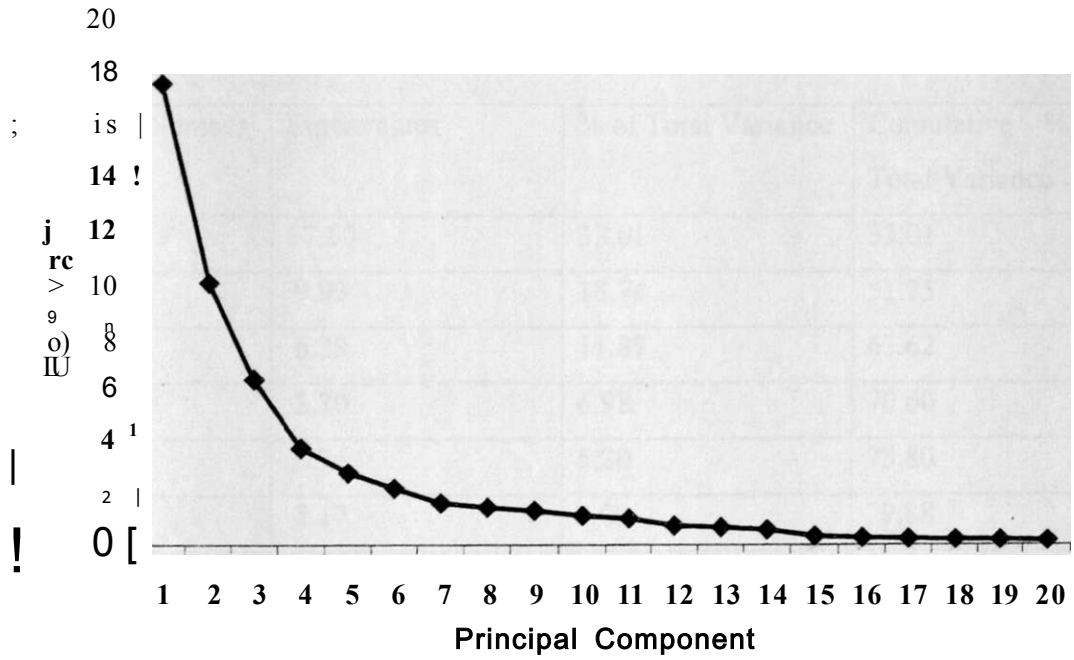

Figure 25: Results of scree test for principal component analysis of September-November sea surface temperatures for the Atlantic Ocean

The PCA modes from SON SST continue to demonstrate the important influence of Atlantic Ocean SST variability on rainfall over parts of eastern Africa. The major striking characteristic for the Atlantic Ocean SST PCA modes is the seasonal persistence of the patterns of the second mode within the seasons as can be observed from Figure 26. Figure 26 demonstrates that the negative and positive phases of the second PCA mode seem to persist over more than one season during the years of large SST anomalies in the Atlantic. The persistence of SST patterns over a long period of time can provide important tools for long-range climate prediction. These will form foundations for some of the seasonal rainfall prediction potential analyses in the later sections of the study.

Table 11: The significant principal component analysis modes of September-November sea surface temperatures for the Atlantic Ocean and the associated variance

PCA Mode Number	Eigenvalues	% of Total Variance	Cumulative % of Total Variance
1	17.50	33.01	33.01
i 2	9.93	18.74	51.75
3	6.29	11.87	63.62
4	3.70	6.98	70.60
5	2.76	5.20	75.80
6	2.17	4.08	79.88
7	1.60	3.01	82.89
8	1.43	2.71	85.60
9	1.31	2.47	88.07
10	1.118	2.11	90.18
11	1.008	1.9	92.08
12	0.93		

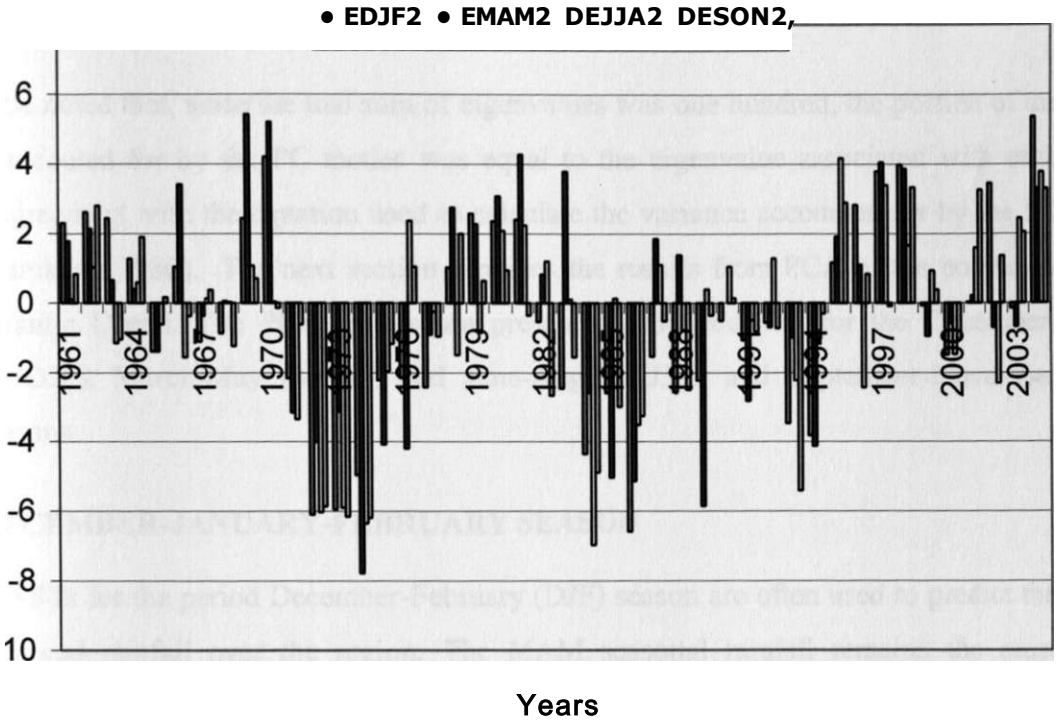

Figure 26: The graphical plot of the time coefficients of the second (2) December-February (EDJF2), March-May (EMAM2), June-August (EJJA2) and September-November (ESON2) sea surface temperatures principal component analysis modes for the Atlantic Ocean.

In the next section the results of PCA from the combined Indian-Atlantic Ocean are discussed.

4.2.3 THE COMBINED INDIAN AND ATLANTIC OCEANS

The results from PCA discussed in the previous sections addressed the Indian and Atlantic Oceans as separate fields. However, the oceans do not influence the regional climate independently but in some integrated manner through the interactions associated with the oceanic and atmospheric circulations (Wolter 1987). The ENSO and Walker circulation (Chervin and Druyan 1984; Julian and Chevrin 1978), and the Great Ocean Conveyor (Gross 1972; Saenko et al. 2002) are some examples of the atmospheric and oceanic processes that may be associated with the combined influence of the global oceans on global climate. Such processes may not be revealed adequately by PCA for individual oceans. A total of one hundred 10° x 10° latidute/longitude SST grid points were used to represent the two oceans.

It should be noted that, since the toal sum of eigenvalues was one hundred, the portion of the variance accouted for by the PC modes was equal to the eigenvalue associated with each mode in agreement with the equation used to calculate the variance accounted for by the PC modes(Murakami 1980). The next section provides the results from PCA of the combined Indian-Atlantic Ocean. The PCA results are presented independently for the December-February (DJF), iMarch-May (MAM) and June-August (JJA) and September-November (SON) seasons.

4.2.3.1 DECEMBER-JANUARY-FEBRUARY SEASON

The SSTs for the period December-February (DJF) season are often used to predict the MAM seasonal rainfall over the region. The MAM seasonal rainfall remains the most difficult to predict. The understanding of the modes that dominate SST variability when the oceans operate as a single field would help reduce the number of predictors. Figure 27 and Table 12 indicate that sixteen PC modes, accounting for about 93% of the total DJF SST variance, were significant. The first four modes accounted for about 61% of the total SST variance. The first, second, third and fourth mode accounted for about 36%, 10%, 8% and 7% of the total SST variance, respectively. The large number of significant PCA modes and the low variance that they explain may be a reflection of the complexity of the shared Indian and Altlatic oceans SST variances. Each of the oceans have their own ciculations systems, but some persistence in anomaly patterns are common during some periods and seasons, especially during major ENSO years (Chambers et al. 1999; Colberg and Reason 2004; Terray and Dominiak 2005). Only the spatial and temporal characteristics of the first three modes are discussed.

The first mode of the DJF SST for the combined Indian-Atlantic Ocean represented the first PCA modes observed with the SST for the individual oceans, which represented basinwide warming/cooling associated with ENSO. The second PCA mode of the DJF SST for the combined Indian-Atlantic Ocean represented the second PCA mode observed with the Atlantic Ocean, which was associated with interhemispheric SST variability over the Atlantic Ocean. The third mode was similar to the third mode observed with the Atlantic Ocean. The major anomalies in the time coefficients for the individual oceans were still

discernible from the PCA modes representing the combined SST variability of the two oceans. These could be reflecting persistence of SST variability modes over the two oceans in some years like during the major ENSO events.

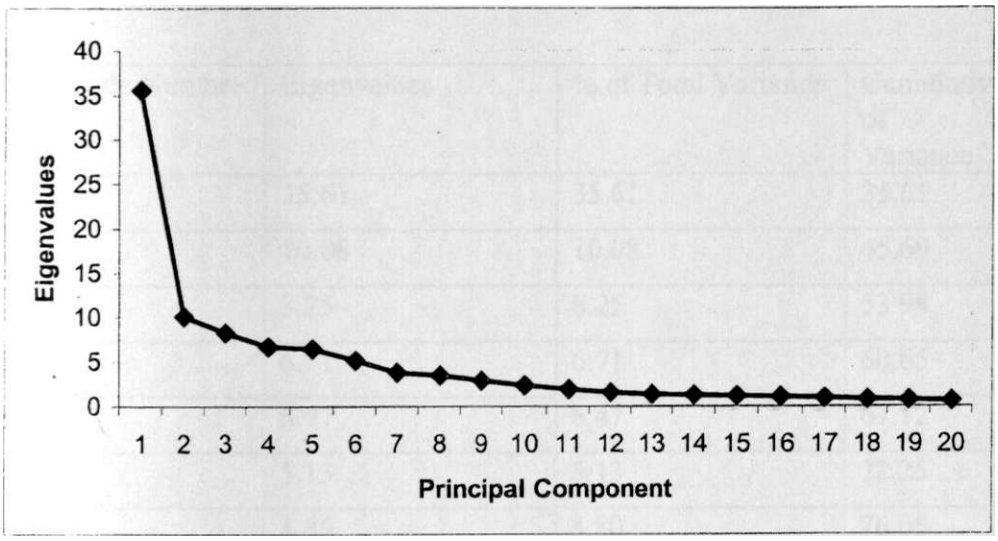

Figure 27: Results of scree test for principal component analysis of December-February sea surface temperatures for the combined Indian-Atlantic Ocean

Table 12: The significant principal component analysis modes of December-February sea surface temperatures for the combined Indian-Atlantic Ocean and the associated variance

PCA Mode Number	Eigenvalues	% of Total Variance	Cumulative % of Total Variance
1	35.61	35.61	35.61
2	10.08	10.08	45.69
3	8.25	8.25	53.94
4	6.71	6.71	60.65
5	6.47	6.47	67.12
6	5.13	5.13	72.25
7	3.80	3.80	76.05
8	3.47	3.47	79.52
9	2.88	2.88	82.40
10	2.33	2.33	84.73
11	1.90	1.90	86.63
12	1.56	1.56	88.19
13	1.36	1.36	89.55
14	1.27	1.27	90.82
15	1.16	1.16	91.98
16	1.10	1.10	93.08
17	0.96		

In the next section the results of PCA for the MAM SST are discussed.

4.2.3.2 MARCH-MAY SEASON

In this section the result from PCA of March-May (MAM) SST for the combined Indian-Atlatintic Ocean are discussed. Figure 28 and Table 13 indicate that 16 PCA modes, accounting for about 94% of the total SST variance, were significant. The first four modes

accounted for 68% of the total SST variance compared to 61% for DJF. The first, second, third and fourth mode accounted for about 39%, 13%, 10% and 6% of the total SST variance, respectively.

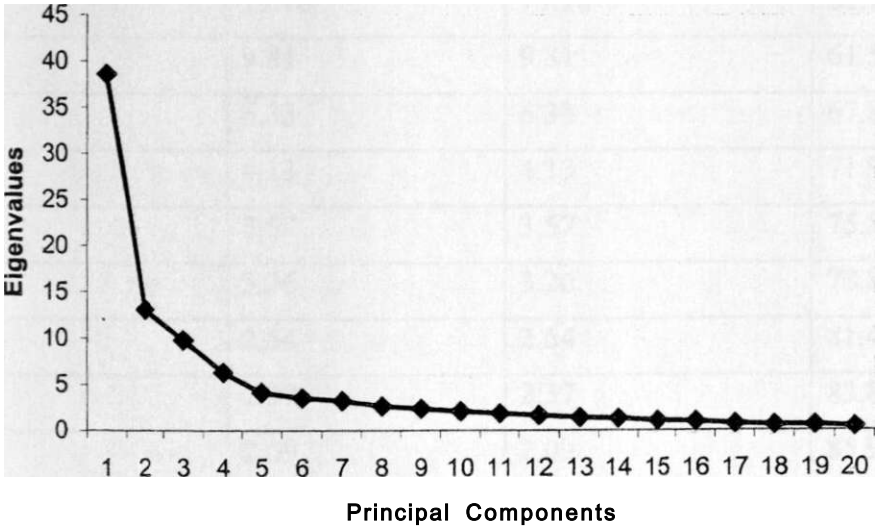

Figure 28: Results of scree test for principal component analysis of Marrch-May sea surface temperatures for the combined Indian-Atlantic Ocean

The spatial and temporal characteristics of the first three PCA modes were similar to those observed with the DJF SST, which represented the PCA modes obseved with the Indiviual oceans a part from the levels of the explained variences and areas dominated by specifc modes.

Table 13: The significant principal component analysis modes of March-May sea surface temperatures for the combined-Atlantic Ocean and the associated variance

PC	Eigenvalues	% Of Total Variance	Cumulative % of Total Variance
; i	38.62	38.62	38.62
2	13.10	13.10	51.72
3	9.81	9.81	61.53
4	6.33	6.33	67.86
5	4.13	4.13	71.99
6	3.57	3.57	75.56
7	3.26	3.26	78.82
8	2.64	2.64	81.46
9	2.37	2.37	83.83
10	2.09	2.09	85.92
U	1.88	1.88	87.8
12	1.64	1.64	89.44
13	1.43	1.43	90.87
14	1.32	1.32	92.19
15	1.08	1.08	93.27
16	1.01	1.01	94.28
17	0.75		

In the next section the results from PCA of June-July-August (JJA) are discussed.

4.2.3.3 JUNE-AUGUST SEASON

In this section the results from PCA of June- August (JJA) SST for the combined Indian-Atlantic Ocean are discussed. The period JJA is often used to predict the October-December (OND) seasonal rainfall over the region. The OND rainfall season is the most studied due to high potential of its predictability (Behera et al. 2005; Black et al. 2003; Omondi 2005; Owiti 2005). Figure 29 and Table 14 indicate that fifteen PCA modes, accounting for about 93% of the total JJA SST variance, were significant. The first four modes in this season accounted for about 64% of the total JJA SST variance. The first,

second, third and fourth mode accounted for about 37%, 13%, 8% and 6% of the total JJA SST variance, respectively.The spatial and temporal characteristics of the first and third PCA modes were similar to those observed with DJF and MAM SST, and represented SST variability in the individual Oceans. The second mode was, however, unique for the season. The spatial patterns of the second mode, which was unique for this season, are presented in Figure 30. This mode represent a dipole with a positive pole in the western Indian Ocean located in the region (20°N-20°S, 40°E-90°E) and a negative pole over the eastern Atlantic Ocean located in the region (10°N-10°S, 40°W-20°E). This dipole, which shall be referred to as Atlantic-Indian Ocean Dipole (AIOD), may be associated with the atmospheric and oceanic circulations linking the two oceans resulting from the Great Ocean Conveyor and the Walker cell across Africa linking the Western Indian Ocean and the Congo Basin (Hastenrath and Polzin 2004; Wang 2002). The opposite phases in the cooling/warming of the Atlantic/Indian Oceans have been associated with wet conditions over the region (Okoola 1996), The extreme wet conditions over the region have been associated with the convergence of moist air masses from the Congo basin and Indian Ocean over the region (Indeje 2000). Figure 30 indicates further a less prominent negative pole over the eastern Indian Ocean located in the region (0°-20°S, 100°E-130°E), which is often used to represent the eastern pole of the Indian Ocean Dipole mode (Behera et al. 2005; Saji et al. 1999). The less prominence of the eastern pole over the Indian Ocean in this season may imply that when the two oceans interact, the dipole linking the Atlantic and Indian Ocean is stronger than IOD in this season. The AIOD may be associated with the Walker cell linking the Congo Basin and Western Indian Ocean (Tanaka et al. 2004). El Nino/La Nina have been associated with the cooling /warming off of the western coast of South Africa and in the Gulf of Guinea during the period February -July (Frankignoul and Kestenare 2005) and warming/cooling in the western Indian Ocean (Chambers et al. 1999; Kug and Kang 2006; Jtug et al. 2007).

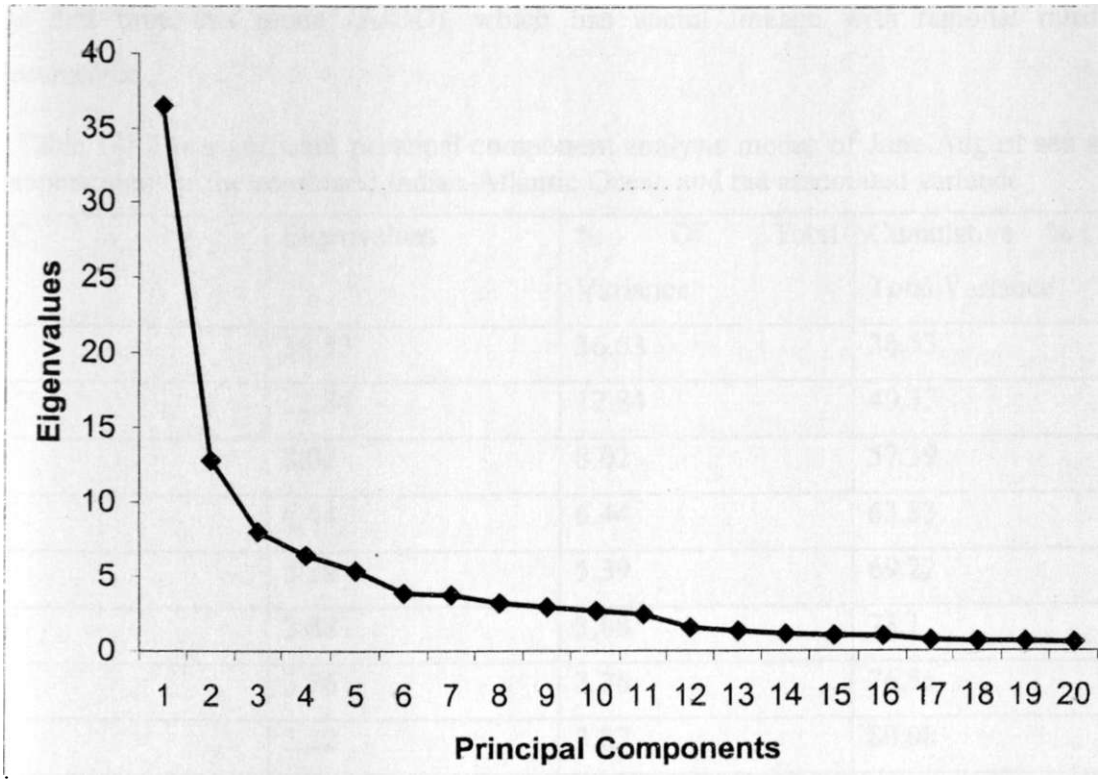

Figure 29: Results of scree test for principal component analysis of June-August sea surface temperatures for the combined Indian-Atlantic Ocean

Figure 31 gives graphical plot of the time coefficients associated with the unique second PCA mode observed with the JJA SST for the combined Indian-Atlantic oceans. Figure 3 I indicates that the large positive time coefficients were observed in the years 1962-1966, 1968, 1971-1975, 1984-1986, 1988, 1989, 1996 and 1998-2000. The large negative coefficients were observed in the years 1961, 1967, 1970, 1972, 1976-1983, 1987, 1990-1992, 1994, 1997, 2002 and 2003. Some of these years have been associated with ENSO and IOD events as defined by Behera et al.(2005); Owiti (2005); and Saji et al. (1999) among many other authors. It can be observed that most of the extreme wet/dry conditions over the region associated with El Nino/La Nina and positive/negative IOD correspond to negative/positive coefficients of this mode. The capability of this mode to separate the dry and wet years by JJA season makes it a more powerful tool than the classical IOD that has a maximum influence in SON as was observed for the PCA of the Individual oceans. This is

the first time this mode (AIOD), which has useful linkage with regional rainfall, is documented.

Table 14: The significant principal component analysis modes of June-August sea surface temperatures for the combined Indian-Atlantic Ocean and the associated variance

PC	Eigenvalues	% Of Total Variance	Cumulative % of Total Variance
I	36.53	36.53	36.53
2	12.84	12.84	49.37
3	8.02	8.02	57.39
4	6.44	6.44	63.83
5	5.39	5.39	69.22
6	3.88	3.88	73.1
7	3.76	3.76	76.86
8	3.22	3.22	80.08
9	2.93	2.93	83.01
10	2.69	2.69	85.7
11	2.45	2.45	88.15
12	1.55	1.55	89.7
13	1.31	1.31	91.01
14	1.12	1.12	92.13
15	1.04	1.04	93.17
16	0.91		

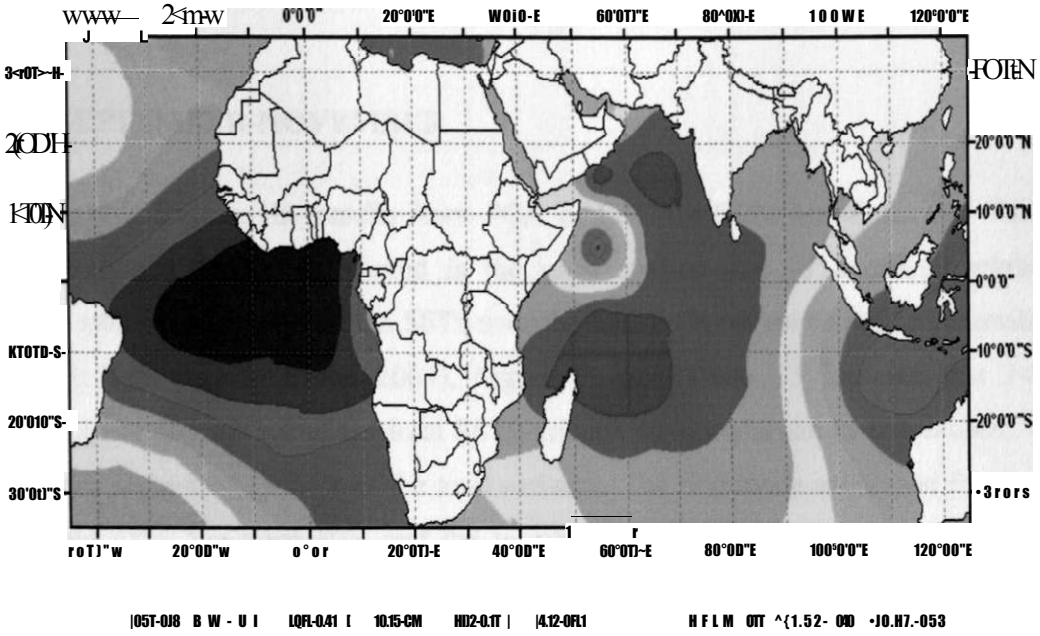

Figure 30: The spatial patterns of the loadings of the second principal component analysis mode of June-August sea surface temperatures for the combined Indian-Atlantic Oceans representing Atlantic-Indian Ocean Dipole

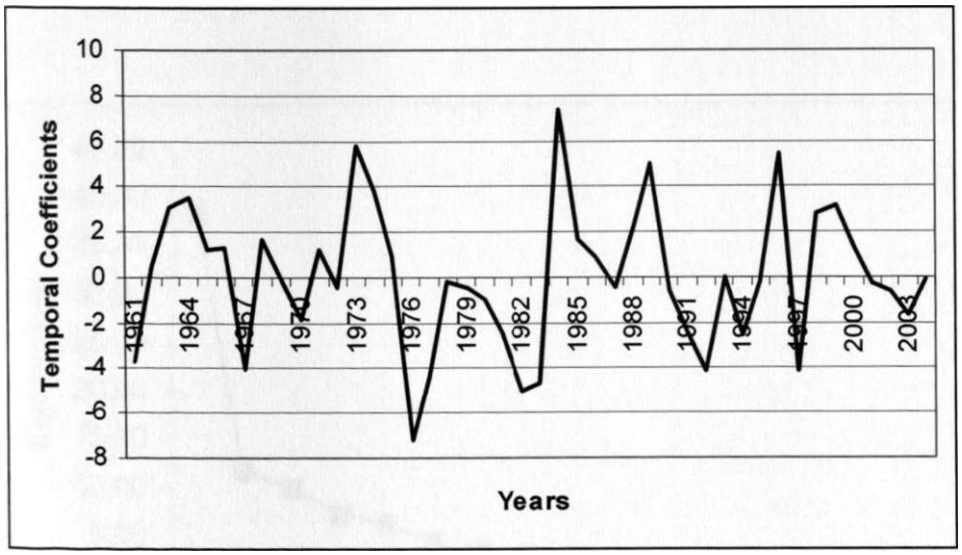

Figure 31: The graphical plot of the time coefficients of the second principal component analysis mode of June-August sea surface temperatures for the combined Indian-Atlantic Oceans associated with the Atlantic-Indian Ocean Dipole

In the next section the results from PCA of SST for the SON season are discussed.

4.2.3.4 SEPTEMBER-NOVEMBER

In this section, the results from PCA of SST for SON are discussed. The rainfall season coinciding with this period is the most studied due to improved relationships. Previous studies indicated that the SSTs over the Indian Ocean reach peak relationships with rainfall in this period (Mutai 2003). Figure 32 and Table 15 indicate that 14 modes accounting for about 93% of the total SST variance were dominant in this season. The first four modes accounted for 66% of the total variance. The first mode accounted for about 38%, the second 12%, the third 10% and the fourth about 7% of the variance. The spatial and temporal characteristics of the first, second, third and fourth modes were similar to those observed with the individual oceans. The second mode represented IOD as observed with SST for the Indian Ocean in this season indicating that the influence of the Indian Ocean improves by this season.

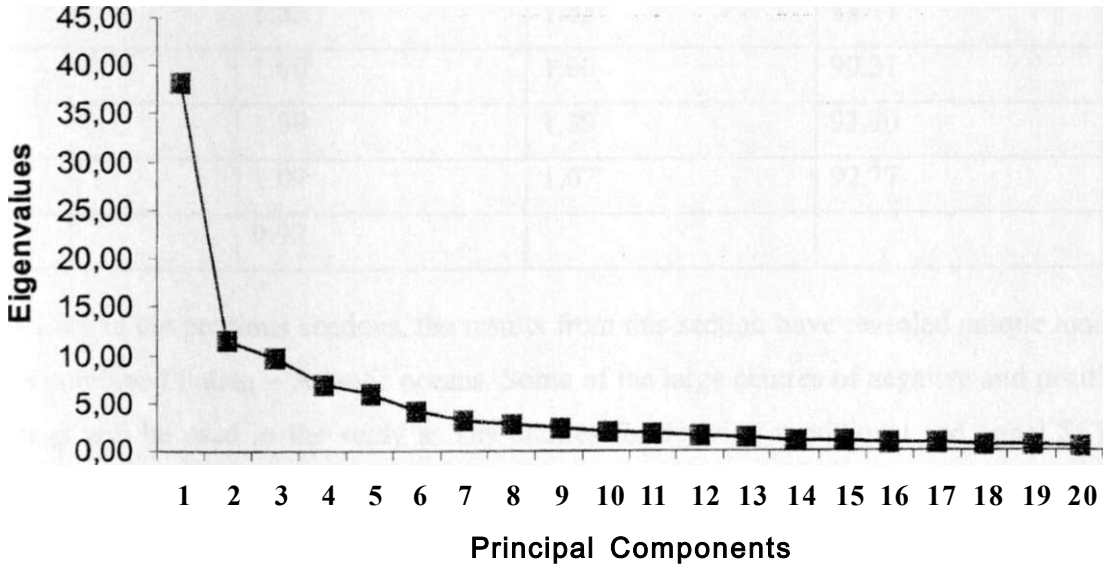

I

Figure 32: Results of scree test for principal component analysis of September-November sea surface temperatures for the combined Indian-Atlantic Ocean

Table 15: The significant principal component analysis modes of September-November sea surface temperatures for the combined-Atlantic Ocean and the associated variance

PC	Eigenvalues	% Of Total Variance	Cumulative % of Total Variance
1	38.27	38.27	38.27
2	11.53	11.53	49.80
3	9.71	9.71	59.51
4	6.93	6.93	66.44
5	5.85	5.85	72.29
6	4.21	4.21	76.50
7	3.27	3.27	79.77
8	2.72	2.72	82.49
9	2.46	2.46	84.95
10	1.93	1.93	86.88
11	1.83	1.83	88.71
12	1.60	1.60	90.31
13	1.39	1.39	91.70
14	1.07	1.07	92.77
15	0.92		

Like in the previous sections, the results from this section have revealed unique modes in the combined Indian - Atlantic oceans. Some of the large centres of negative and positive loadings will be used in the study as key centres for deriving meridional and zonal SSTG modes that will be related to seasonal rainfall and develop models to predict seasonal rainfall.

The major conclusions from the results from Principal component Analysis of sea surface temperatures are that both the Atlantic and Indian Oceans have significant influence on regional rainfall. The first four modes of variability that formed major sources of sea surface temperature influence on regional rainfall represented ocean wide warming, and zonal and meridional sea surface temperature variability associated with El Nino/Southern Oscillation, Indian Ocean Dipole, Antlantic-Indian Ocean Dipole and Interhemispheric

Dipole in the Atlantic Ocean. The extreme phases of the Principal Component Analysis modes are associated with some climate extremes affecting the region linked to El Nino/Southern Oscillation, Indian Ocean Dipole and Atlantic-Indian Ocean Dipole. There are unique seasonal modes that compliment the major modes of variability for the individual seasons. These major modes of sea surface temperature variability for the individual and combined Indian and Atlantic Ocean were used to develop SSTG modes for the oceans. The sea surface temperature gradient modes for the Pacific Ocean was based on previous studies (Chevrin and Druyan 1984; Colberg and Reason 2004; Mutemi 2003;Rao et al. 2007; Omondi 2005).

In the next section the results from correlation analysis are discussed.

4.3 **CORRELATION ANALYSIS**

In this section the results from correlation analysis are discussed. The correlation analysis is used to quantify the relationships between seasonal rainfall and sea surface temperatures (SST). The SSTs are represented by the dominant PCA and SST gradient modes. Details of the methods used to derive these modes were presented in the previous sections 3.3.2 and 3.3.3 under methodology. The time coefficients of the PCA modes represent the large-scale weighted areal averages. The significant correlation between the PCA modes and rainfall are a good representation of the responses of regional seasonal rainfall to SST variability over large parts of the oceans. In order to establish lead-time relationships, the MAM and SOND rainfall records are related to PCA modes observed with seasons preceding each rainfall season.

A part from the use of some coefficients of the dominant PCA modes to represent regional average rainfall, the stations representing homogenous rainfall zones are used to represent the respective zones based on the station within each region with the highest communality. The rainfall records were correlated with time lagged SST records. Details of the correlation analysis are discussed under methodology in section 3.3.4. Results from t-test showed that all values of correlation > 0.25 were declared significant at 95% confidence level. Details of the t-test were discussed in section 3.3.4.

In the next section the results from correlation analysis of March-May (MAM) and September - December (SOND) seasonal rainfall, and PCA modes are independently discussed.

4.3.1 SEPTEMBER-DECEMBER RAINFALL AND PRINCIPAL COMPONENT ANALYSIS MODES

In this section, the results from correlation analysis of September-December (SOND) rainfall and the dominant PCA modes observed with seasonal SST for the Indian and Atlantic Ocean are discussed. The SOND rainfall has been observed to have high potential of prediction (Black et al. 2003; Mutai 2003; Mwale and Gan 2005; Omondi 2005; Owiti 2005). The next subsection discusses the results from correlation analysis of SOND rainfall and the lagged PCA modes for the Atlantic Ocean.

4.3.1.1 SEPTEMBER-DECEMBER RAINFALL AND PRINCIPAL COMPONENT ANALYSIS MODES FOR THE ATLANTIC OCEAN

In this section the results from correlation analysis of SOND rainfall and the PCA modes for the Atlantic Ocean are discussed. The PCA modes associated with the Atlantic Ocean that had the highest relationships with SOND rainfall are the first, third and fourth MAM SST PCA modes. The spatial pattern of the values of correlation observed with the time coefficients of the third and fourth MAM SST PCA modes were similar. Both modes were positively correlated to SOND rainfall over the region.

Figure 33 gives an example of the the spatial patterns of the values of correlation observed between SOND rainfall and the time coefficients of the PCA modes associated with the Atlantic Ocean as represented by the fourth MAM PCA SST mode, which had the highest relationships with SOND rainfall. The largest value of correlation observed with the fourth PCA mode was 0.66 indicating that this mode accounted for about 43.56% of SOND rainfall variance. The highest relationships were observed with rainfall over most parts of Kenya, northern Uganda and Lake Victoria basin. The fourth MAM PCA mode for the Atlantic Ocean was centred over the southwestern Atlantic Ocean, which is associated with the west wind drift linked to the Banguela Current (EMS 1984). The largest value of correlation observed with the third mode was 0.36 indicating that this mode accounted for about 12.96% of SOND rainfall variance.

The JJA SST PCA modes associated with the Atlantic Ocean that had the highest relationships with the SOND rainfall were the first and fourth modes. Figure 34a indicates that the first JJA PCA mode for the Atlantic Ocean, centred over the tropical northern Atlantic Ocean, was negatively correlated to rainfall over the northern and eastern parts of the region indicating that the ocean-wide cooling/warming over the tropical northern Atlantic Ocean favour enhanced/deficient rainfall over parts of the region in agreement with the findings of Okoola (1996) among other authors. The largest value of correlation observed with this mode was 0.44 indicating that it accounted for about 19.36% of SOND rainfall variance. Similar relationships were observed with the first MAM PCA mode for the Atlantic Ocean.

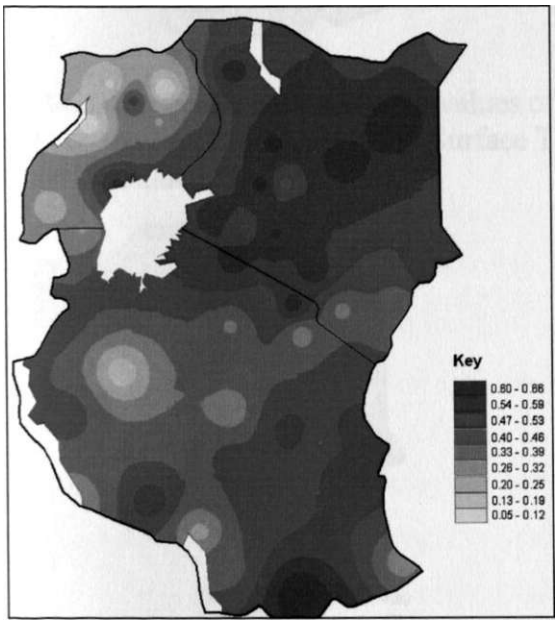

Figure 33: The spatial patterns of the values of correlation between September-December rainfall and the fourth March-May Principal Component Analysis mode for the Atlantic Ocean.

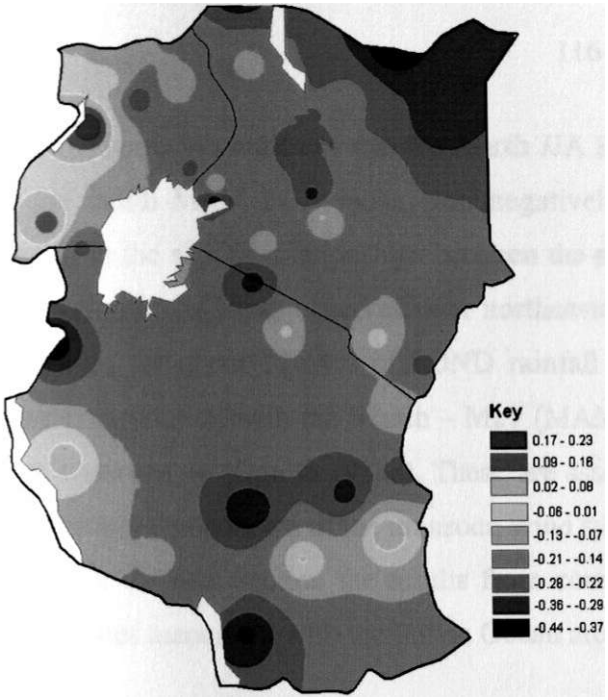

Figure 34a: The spatial patterns of the values of correlation between September-December rainfall and the first June-August Sea Surface Temperature Principal Component Analysis mode for the Atlantic Ocean.

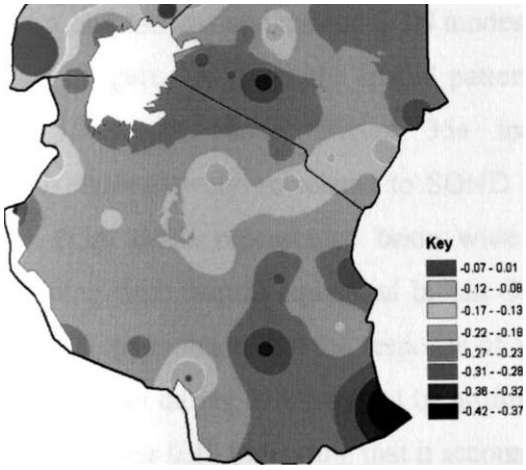

Figure 34b: The spatial patterns of the values of correlation between September-December rainfall and the fourth June-August Principal Component Analysis mode for the Atlantic Ocean.

Figure 34b indicates that the fourth JJA PCA mode, which had similar characteristics as the fourth MAM PCA mode, was negatively correlated to SOND rainfall indicating a change in the sign of relationships between the periods MAM and JJA. The largest value of correlation of 0.42 was observed over northeastern parts of Kenya indicating that this mode accounted for about 17.64% of SOND rainfall variance. Changes in the signs of SOND rainfall correlation with the March - May (MAM) and June - August (JJA) SSTs have also been observed by (Ogallo 1988a). These are associated with the strengthening or cooling of the westerly components of the monsoon wind systems from Atlantic Ocean into the region.

In the next section the results from correlation analysis of SOND rainfall and SST PCA modes associated with the Indian Ocean are discussed.

4.3.1.2 SEPTEMBER-DECEMBER RAINFALL AND SEA SURFACE TEMPERATURE PRINCIPAL COMPONENT ANALYSIS MODES FOR THE INDIAN OCEAN

In this section the results from correlation analysis of SOND rainfall and the PCA modes for the Indian Ocean are discussed. The SST PCA modes associated with the Indian Ocean that had the highest relationships with SOND rainfall are the first and second JJA modes and the first and second SON modes, which have similar characteristics.

Figure 35a gives the spatial patterns of the values of correlation observed with the first JJA PCA mode. Figure 35a indicates that the first JJA PCA mode was positively/negatively correlated to SOND rainfall over western/eastern parts of the region. This PCA mode represented basin wide warming or cooling with the largest loadings extending from central equatorial Indian Ocean to the northeastern parts of the ocean. These relationships indicate that the response of SOND rainfall to the warming or cooling over the Indian Ocean during JJA may not be uniform. The largest value of correlation observed with this mode was 0.45 indicating that it accounted for about 20.25% of SOND rainfall variance.

Figure 35b gives the spatial patterns of the values of correlation observed with the second JJA PCA mode, which represents the IOD and dominates SST variability in the Indian Ocean during JJA and SON. Figure 35b indicates that the second JJA PCA mode had significant negative relationships with SOND rainfall over all parts of the region. The largest value of correlations of 0.61, indicating that the highest amount of SOND rainfall variance accounted for by this mode was 37.21%, were observed over the northern and southwestern

parts of Kenya.The first SON PCA mode, which is similar to the first JJA SST PCA mode, was positively correlated to SOND rainfall over most parts of the region, unlike the first JJA mode that had positive and negative relationships with rainfall over parts of the region. The largest value of correlation was 0.37 indicating that this mode accounted for about 13.69% of SOND rainfall variance in this season.

The spatial patterns of the values of correlations observed with the second SON PCA mode, which was similar to the second JJA PCA mode representing IOD, continued to indicate negative and marked improvements in relationships with rainfall over most parts of the region. The largest value of correlation observed with this mode was 0.74 compared to 0.61 observed with the similar second JJA PCA mode. These results indicate that this mode accounted for the highest amount of SOND rainfall variance of about 54.76%.

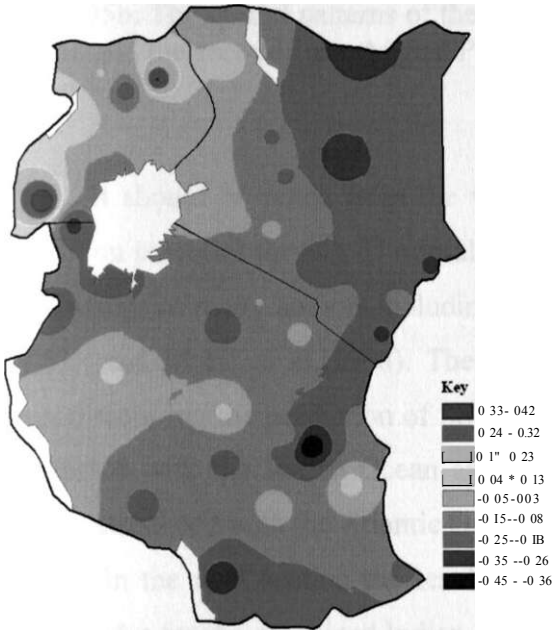

Figure 35a: The spatial patterns of the values of correlation between September-December rainfall and the first June-August Principal Component Analysis mode for the Indian Ocean.

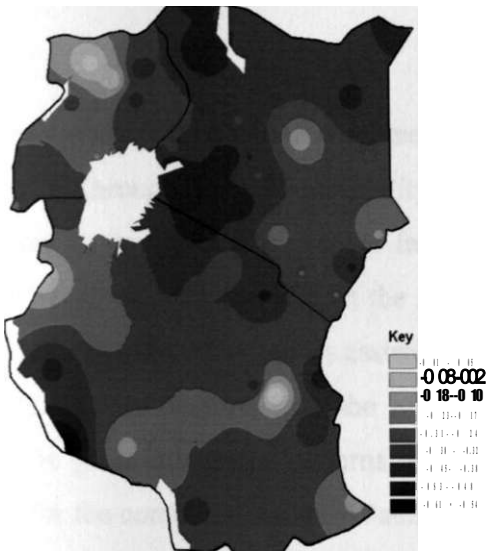

Figure 35b: The spatial patterns of the values of correlation between September-December rainfall and the second June-August Principal Component Analysis mode for the Indian Ocean.

It should be noted from the values of correlation that the Indian Ocean has higher prediction potential for SOND rainfall season compared to Atlantic Ocean in agreement with the findings of many authors including Goddard and Graham (1999); Ogallo (1988a); Mutai (2003); and Mutai et al.(1998). The peak relationships are, however, achieved within the season requiring the prediction of SST. The relationships observed with the JJA PCA modes associated with the Indian Ocean are comparable to those observed with the MAM PCA modes associated with the Atlantic Ocean.

In the next section the results from correlation analysis of SOND rainfall and the PCA modes for the combined Indian-Atlantic Ocean are discussed.

4.3.1.3 SEPTEMBER-DECEMBER RAINFALL AND PRINCIPAL COMPONENT ANALYSIS MODES FOR THE COMBINED INDIAN-ATLANTIC OCEAN.

In the previous sections the relationships were established for the modes associated with the oceans operating singly. The global oceans, through the influence of ocean and wind currents, and the associated transport of water with varying salinity, act as a single field in influencing the SST and global climate (Shukla 1991; Stouffer et al 2007; Wunsch and Heimbach 2006). The relationships with the combined Indian-Atlantic Ocean PCA modes

may be representative of the combined influence of the two ocean basins on the climate of the region through the SST variability as affects the associated wind currents and moisture transport. In this section the results from correlation analysis of SOND rainfall and the PCA modes observed with the SST of the Indian and Atlantic Ocean treated as a single field are discussed. The JJA PCA modes associated with the combined Indian-Atlantic Ocean that had the highest relationships with the SOND rainfall were the first and second PCA modes. Figure 36 gives the spatial patterns of the values of correlation observed with the JJA PCA modes for the combined Indian-Atlantic Ocean.

Figure 36a indicates that the first JJA PCA mode for combined Indian-Atlantic Ocean, which represented basin wide warming or cooling over the tropical northern Atlantic and Indian Ocean, had significant negative correlation with SOND rainfall over the eastern parts of the region and positive correlation over the southwestern parts of Uganda. The largest value of correlation of 0.44, indicating that this mode accounted for about 19.36% of SOND rainfall variance, was observed over the northeastern parts of Kenya.

The second JJA PCA mode for the combined Indian-Atlantic Ocean, which represents a seesaw zonal SST variability between the equatorial eastern Atlantic and western Indian Ocean, had significant negative correlation with rainfall over most parts of the region (Figure 36b). The largest value of correlation of 0.41, indicating that this mode accounted for about 16.81% of SOND rainfall variance, was observed over the northern parts of Kenya and Uganda. These results indicate that the JJA PCA modes associated with the joint Indian-Atlantic Ocean had significant relationships with SOND rainfall comparable to those observed with PCA for the individual oceans. The second mode associated with the Indian Ocean had the highest relationships with the SOND rainfall that reached a peak in SON.

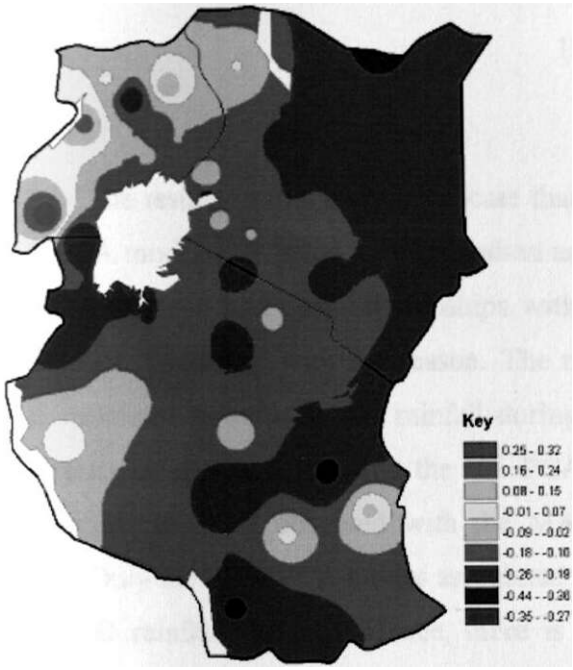

Figure 36a: The spatial patterns of the values of correlation between September-December rainfall and the first June-August Principal Component Analysis mode for the combined Indian-Atlantic Ocean.

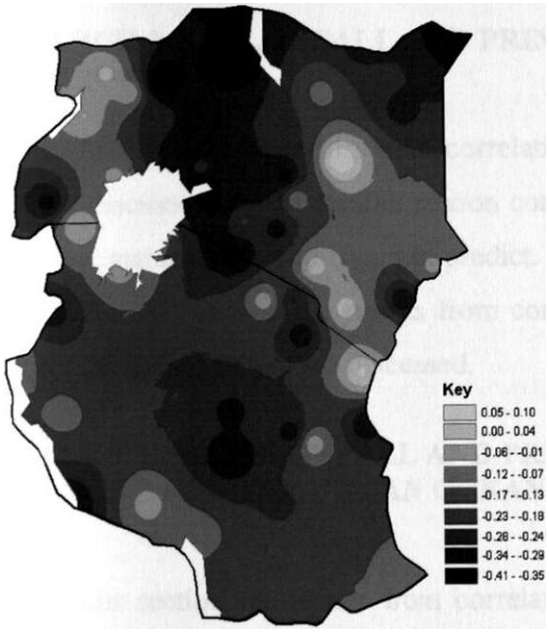

Figure 36b: The spatial patterns of the values of correlation between September-December rainfall and the second June-August Principal Component Analysis mode for the combined Indian-Atlantic Ocean.

The results in this section indicate that SOND rainfall was significantly correlated to SST PCA modes associated with the Indian and Atlantic Oceans. The modes associated with the Indian Ocean had peak relationships with SOND rainfall during the period September-November coinciding with the season. The modes associated with the Atlantic Ocean had peak relationships with SOND rainfall during the period March-May preceding the season. The relationships observed with the JJA PCA modes associated with the Indian Ocean are comparable to those observed with the MAM PCA modes associated with the Atlantic Ocean. Only the SON PCA modes associated with the Indian Ocean accounted for over 50% of SOND rainfall variance. Hence, there is a need to identify other predictors that may account for more rainfall variance.

In the next section the results from correlation analysis of MAM rainfall and the PCA modes are discussed.

4.3.2 MARCH-MAY RAINFALL AND PRINCIPAL COMPONENT ANALYSIS MODES

In this section the results from correlation analysis of MAM rainfall and the PCA modes are discussed. MAM rainfall season contributes to most of the annual rainfall in the region but remains the most difficult to predict.

In the next section the results from correlation analysis of MAM rainfall and PCA modes for the Indian Ocean are discussed.

4.3.2.1 MARCH-MAY RAINFALL AND PRINCIPAL COMPONENT ANALYSIS MODES FOR THE INDIAN OCEAN

In this section the results from correlation analysis of March-May (MAM) rainfall and the Principal Component Analysis (PCA) modes for the Indian Ocean are discussed. The DJF PCA mode associated with the Indian Ocean that had the highest relationships with MAM rainfall was the third mode.

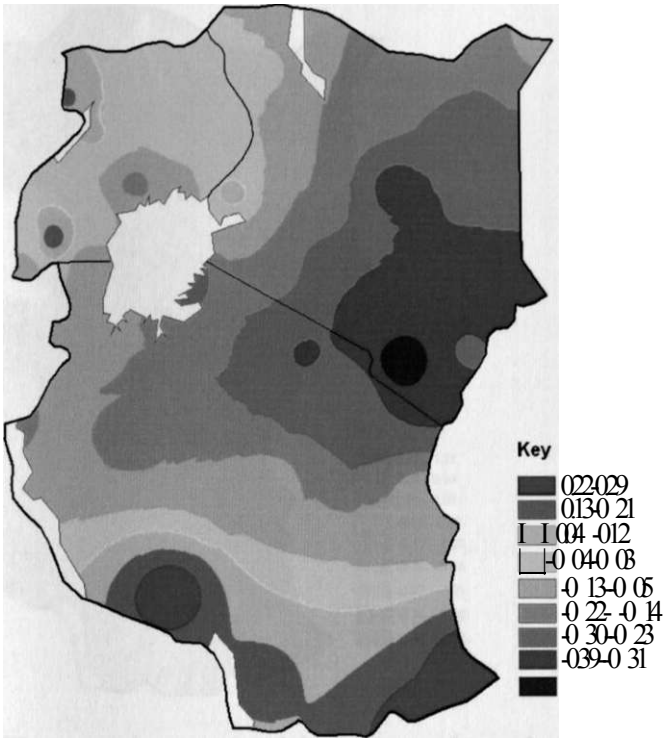

Figure 37: The spatial patterns of the values of correlation between March-May rainfall and the third December-February Principal Component Analysis mode for the Indian Ocean.

Figure 37 indicates that this mode had significant negative relationships with MAM rainfall over eastern parts of Kenya and northern Tanzania. The largest value of correlation of 0.49 was observed over eastern parts of Kenya indicating that this mode accounted for about 24.01% of MAM rainfall variance.

In the next section, the results from correlation analysis of MAM rainfall and the lagged PCA mode for the joint Indian- Atlantic Ocean are discussed.

4.3.2.2 MARCH-MAY RAINFALL AND PRINCIPAL COMPONENT ANALYSIS MODES FOR THE JOINT INDIAN-ATLANTIC OCEAN

In this section the results from correlation analysis of March-May (MAM) rainfall and PCA modes for the joint Indian-Atlantic Ocean are discussed. The PCA mode associated with the combined Indian-Atlantic Ocean that had the highest relationship with MAM rainfall was the second DJF mode, which represented interhemispheric SST variability in the Atlantic Ocean.

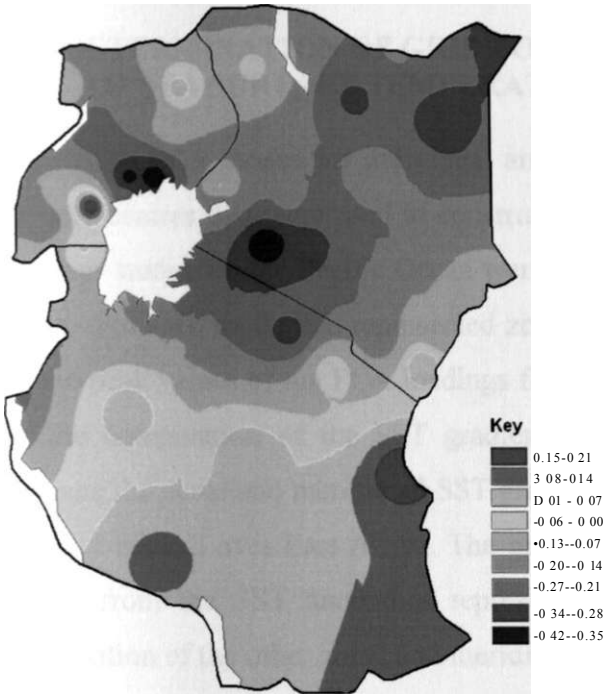

Figure 38: The spatial patterns of the values of correlation between March-May rainfall and the second December-February Principal Component Analysis mode for the combined Atlantic-Indian Ocean.

Figure 38, presenting the spatial patterns of the values of correlation between the second DJF PCA mode and MAM rainfall, indicates that this mode was negatively correlated to MAM rainfall over most parts of Kenya, and parts of central and eastern Uganda. The largest value of correlation of 0.42, indicating that this mode accounted for about 16.64% of MAM rainfall variance, was observed over parts of eastern and southern Kenya, and Lake Victoria basin in Uganda. The low values of correlation observed between MAM and PCA modes indicate that rainfall in the season was weakly correlated to the PCA modes. Some modes had only small pockets of high relationships with MAM rainfall. The highest rainfall variance accounted for by the PCA modes was 24.01%. These weak relationships create a need to identify other predictors that may improve the forecasts of MAM seasonal rainfall.In the next section the centres for developing SST gradient modes that could improve the prediction of seasonal rainfall over the region are discussed.

4.3.3 DETERMINATION OF GRID POINT CENTRES FOR THE DEVELOPMENT OF SEA SURFACE TEMPERATURE GRADIENT MODES

The PCA modes for individual and combined Indian-Atlantic were used to identify the core centres that were used to construct SST gradient modes as defined in section 3.3.3. Previous studies on the Pacific Ocean were used to derive the equatorial zonal mode over the ocean. For each mode that represented zonal or meridional SST variability, the central grids for the peak values of the PCA loadings for the opposite poles were used as reference points for the computation of the SST gradient modes. Figure 39 gives the locations used to compute the zonal and meridional SST gradient modes that had the highest relationships with seasonal rainfall over East Africa. The gradient modes are computed in the direction of the arrows from the SST anomalies representing the grids as indicated in Table 16a. The computation of the other zonal and meridional modes was done in a similar manner using the grid points indicated in Table 16b.

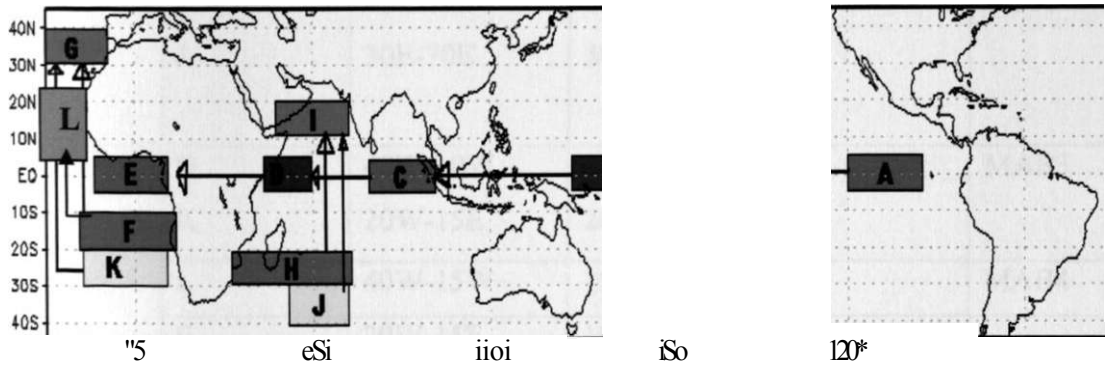

Figure 39: The locations used to compute the Sea Surface Temperature gradient modes that had the highiest relationships with seasonal rainfall over East Africa

Table 16a: Computation of meridional and zonal sea surface temperature gradient modes that had the highest relationships with seasonal rainfall over East Africa.

Ocean	Region	Longitude	Latitude	Gradient Computation	Gradient Name
Pacific	A B	120W-90W 150E-180E	5N-5S 5N-5S	B-A	ZPAC
Indian	C D	80E-100E 40E-60E	5N-5S 5N-5S	D-C	ZIND
	I H	50E-75E 35E-70E	20N-10N 20S-30S	I-H	MIB1
	I J	50E-75E 30E-70E	20N-10N 30S-40S	I-J	MIB3
Atlantic	G K	40 W-10W 20W-15E	40-3 ON 20-30S	G-K	MAB3
	L	40W-15W	10N-20N	L-F	MAB4
	F G	20W-15E 40 W-10W	10-20S 40-30N	G-F	MAB6
Atlantic and Indian	D E	40E-60E 10W-10E	5N-5S 5N-5S	E-D	ZAF

Table 16b: The computation of the other sea surface temperature modes that had significant relationships with seasonal rainfall over East Africa

Ocean	Region	Longitude	Latitude	Gradient Computation	Gradient Name
INDIAN OCEAN	INB2 INB4	40-70E 50-75E	10-20S 20-ION	INB4 - INB2	MIB2
	SIN3 SIN 9	50E-60E 110E-20E	0-10S 0-1 OS	SIN3-SIN9	GSI39
	14 I2AB	40E-50E 90E-130E	10N-30S 0-20S	14-12 AB	I42AB
	I7A I7B	40E-60E 70E-90E	0-1 OS 10S-20S	I7A-I7B	17 AB
Atlantic Ocean	ATB1 ATB2 ATB3 ATB4 ATB5	20W-15E 20W-15E 40-15W 40-10W 40-10W	10-20S 20-30S 20-10N 30-20N 40-30N	ATB3 - ATB2 ATB4- ATB2 ATB5- ATB2 ATB4-ATB1 ATB5-ATB1 ATB5-ATB3	MAB1 MAB2 MAB5 MAB6 MAB7

These SST gradient modes are used to further study the relationships between seasonal rainfall and SSTs based predictors. In the next section the results from correlation analysis of seasonal rainfall and SST gradient modes are discussed.

Table 16b: The computation of the other sea surface temperature modes that had significant relationships with seasonal rainfall over East Africa

Ocean	**Region**	**Longitude**	**Latitude**	**Gradient Computation**	**Gradient Name**
INDIAN OCEAN	INB2 INB4	40-70E 50-75E	10-20S 20-ION	INB4 - INB2	MIB2
	SIN3 SIN9	50E-60E 110E-20E	0-10S 0-1 OS	SIN3-SIN9	GSI39
	l4 I2AB	40E-50E 90E-130E	10N-30S 0-20S	I4-I2AB	I42AB
	I7A I7B	40E-60E 70E-90E	0-1 OS 10S-20S	I7A-I7B	I7AB
Atlantic **Ocean**	ATBl ATB2 ATB3 ATB4 ATB5	20W-15E 20W-15E 40-15W 40-10W 40-10W	10-20S 20-30S 20-10N 30-20N 40-30N	ATB3 - ATB2 ATB4- ATB2 ATB5- ATB2 ATB4-ATBl ATB5-ATBl ATB5-ATB3	MAB1 MAB2 MAB5 MAB6 MAB7

These SST gradient modes are used to further study the relationships between seasonal rainfall and SSTs based predictors. In the next section the results from correlation analysis of seasonal rainfall and SST gradient modes are discussed.

4.3.4 SEASONAL RAINFALL AND SEA SURFACE TEMPERATURE GRADIENT MODES

In this section the results from correlations analysis of seasonal rainfall and SST Gradient Modes described in Figure 39 and Table 16a, are discussed starting with SOND rainfall.

4.3.4.1 SEPTEMBER-DECEMBER RAINFALL AND SEA SURFACE TEMPERATURE GRADIENT MODES

The September-December (SOND) rainfall season has been observed to have high potential of prediction (Black et al. 2003; Mutai 2003; Mwale and Gan 2005; Ogallo 1988a; Omondi 2005; Owiti 2005). The results of t-test indicated that any correlation value >0.25 was statistically significant at the 95% level. The SST gradient modes that had correlation value >0.25 with SOND rainfall include the zonal and meridional SST gradient modes associated with the Indian Ocean, zonal SST gradient mode associated with the Pacific Ocean, zonal SST gradient mode associated with the equatorial eastern Atlantic and western Indian Ocean, and meridional SST gradient modes associated with the Atlantic and Indian Ocean. The relationships observed with the zonal and meridional SST gradient modes represent the influence of the respective modes on the zonal and meridional components of the general circulation that affect regional rainfall. The zonal SST gradient modes associated with the Indian Ocean that had the highest relationships with SOND rainfall were presented in Table 16a, while Figure 39 presented locations used to derive them. The zonal SST gradient (SSTG) mode associated with the equatorial Indian Ocean (ZIND) had the strongest relationships with the SOND rainfall. This Indian Ocean mode was derived from grids C and D as presented in Figure 39 and indicated in Table 16a. These locations are associated with the centers of the Indian Ocean Dipole (IOD)(Owiti 2005). Figure 40 gives the spatial patterns of the values of correlations between SOND rainfall and the October ZIND SST gradient mode together with the associated SST centres.

The spatial patterns of the values of correlations observed with the individual SST centres(C and D) and the associated gradient mode are shown in Figures 40a-40c. Figure 40a indicates that the zero-lagged SST anomalies centered to the eastern Indian Ocean (centre C)

was negatively correlated to SOND rainfall with maximum values of correlation of about 0.70 indicating that the October SST associated with centre C accounted for about 49% of SOND variance.. Figure 40b indicates that the October SST anomalies associated with the centre D over the western Indian Ocean were positively correlated to SOND rainfall with the largest value of 0.65 indicating that the SST associated with this centre accounted for about 42.25% of SOND rainfall variance. The negative/positive values of correlation observed between SOND rainfall and SST over the eastern/western Indian Ocean (C/D) reflect opposite responses of rainfall to SST representing the opposite poles associated with the IOD.

The most striking results, as can be seen in Figures 40a-40c, is the higher correlation values obtained when the ZIND SST zonal gradient mode was used as reflected in Figure 40c. The highest value of correlations was 0.85 indicating that the October ZIND SST zonal gradient mode accounted for about 72.25% of SOND rainfall variance. The positive relationships between SOND and ZIND SST gradient mode continue to indicate that the warming/cooling over the western/eastern equatorial Indian Ocean favour enhanced SOND rainfall over most parts of the region in agreement with the observations from many authors including Behera et al (2005); Mutai et al. (1998); Ogallo (1988a); Okoola (1996); Owiti (2005); and Schreck and Semazzi (2004) among other authors.

The improvement in relationships when the gradient mode is used is indicative of the advantages that SST gradient mode could have in the prediction of seasonal rainfall over the grid point SSTs. Similar results were observed with the other zonal gradient modes for the Indian Ocean including IOD, which has been studied extensively by many authors including Behera et al.(2005); Black et al. (2003); Clark et al. (2003); Meyers et al. (2007) and Owiti (2005) among other authors. However, ZIND SST gradient mode, developed on similar principles as IOD but centred along the equator, had stronger relationships with SOND rainfall than the classical IOD. Since the month of October falls in the rainfall season, the use of this gradient in regression models to predict SOND rainfall requires accurate prediction of October SSTs. Some attempts have been made to predict SST, as well as ENSO, to help predict rainfall (Frederiksen et al. 2001; Luo et al. 2008a; Schott 2003)..

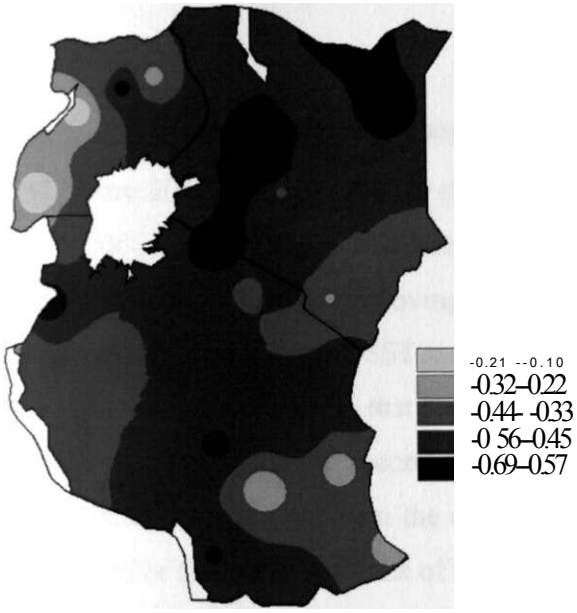

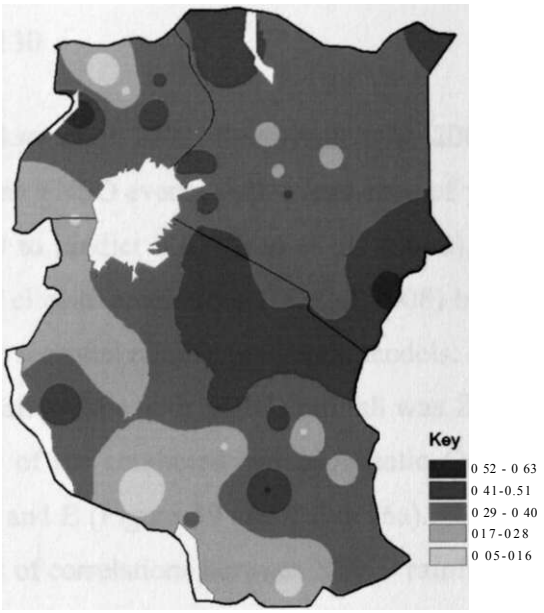

Figure 40a Figure 40b

Figure 40: The spatial patterns of correlation between September-December rainfall and the October sea surface temperatures for the centre (a) C over the eastern (b) D over the western equatorial Indian Ocean

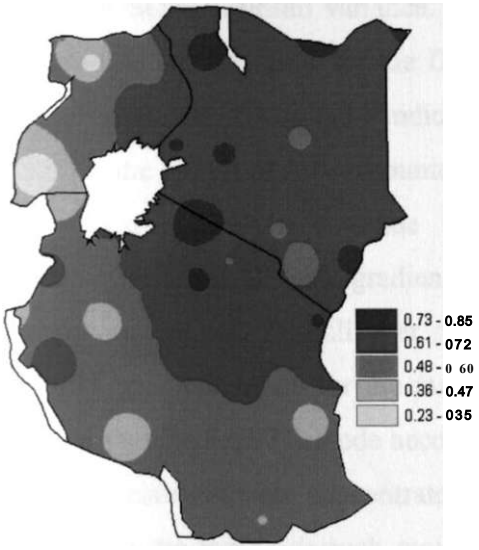

Figure 40c: The spatial patterns of correlation between September-December rainfall and the October zonal sea surface temperature gradient mode for the equatorial Indian Ocean (D-C).

The International Research Institute for Climate and Society (IRI), United States of America, has been predicting global SSTs since 1997, which are available on their website. SST anomalies over parts of Pacific, Atlantic and Indian Ocean can be predicted with skill

(Alexander et al. 2008; Carson 1998; Frederiksen et al. 2001; Keenlyside et al. 2008; Repelli and Nobre 2004). It is possible to predict some ENSO events with a lead-time of years (Luo et al. 2008a). There have also been attempt to predict IOD (Luo et al. 2008b). The SST predictions would help in improving seasonal climate predictions (Li et al. 2008) by enabling the inclusion of zero-lagged SST modes in the seasonal rainfall prediction models.

Another zonal mode that had high relationships with SOND rainfall was ZAP SSTG mode associated with the second JJA mode of the combined Indian-Atlantic Ocean. This SSTG mode was derived from the centres D and E (Figure 39 and Table 16a). Figures 41a and 41b give the spatial patterns of the values of correlations between SOND rainfall and the July SST representing the centres D and E. Figure 41a indicates that SOND rainfall over the northern parts of the region was negatively correlated to the July SST over the eastern equatorial Atlantic Ocean (centre E). The largest value of correlation was 0.39 indicating that the July SST over the eastern equatorial Atlantic Ocean (centre E) accounted for about 15.21% of SOND rainfall variance. Figure 41b indicates that SOND rainfall was positively correlated to the July SST for the D over the equatorial western Indian Ocean. The largest value of correlation was 0.54 indicating that the SST over the western equatorial Indian Ocean for the month of July accounted for about 29.16% of SOND rainfall variance.

Figures 41a-4lc continue to indicate marked improvements in the values of correlation when ZAF SST gradient mode is used as reflected in Figure 41c. Figure 41c indicates that SOND rainfall over most parts of the region was significantly correlated to ZAF SST gradient mode for the month of July. The highest value of correlation of 0.63 indicated that ZAF SSTG mode accounted for about 39.69% of SOND rainfall variance. The lowest correlations were concentrated in the coastal region. The Atlantic Ocean influences rainfall over the region through moisture incursions by the westerly wind currents over the western parts of the region (Indeje 2000; Indeje and Semazzi 2000; Okoola 1996).

The improvement in relationships when the gradient mode are used as indicated in Figures 41a- 41c continue to indicate the advantages of the SST gradient modes could have in the prediction of seasonal rainfall over the grid point SSTs.

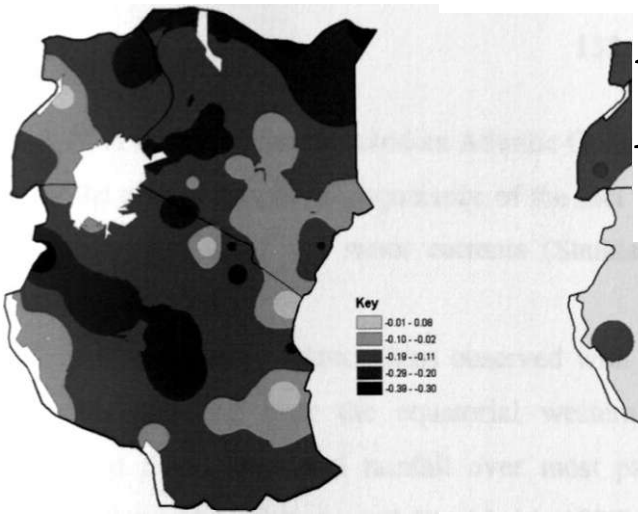

Figure 41a Figure 41b

Figure 41a: The spatial patterns of correlation between September-December rainfall and the July sea surface temperatures for the centre (a) E in the equatorial eastern Atlantic Ocean (b) D in the equatorial western Indian Ocean associated with the Atlantic-Indian Ocean Dipole.

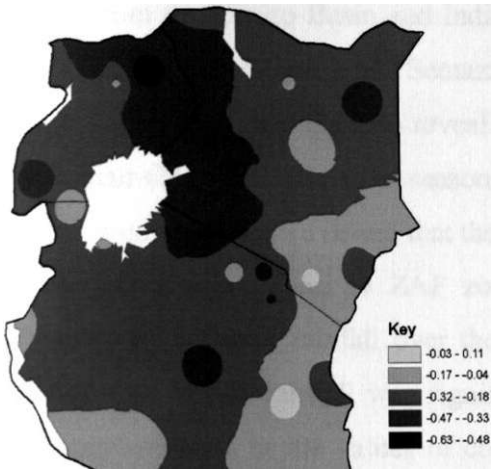

Figure 41c: The spatial patterns of correlation between September-DEcember rainfall and the July zonal sea surface temperature gradient mode associated with the equatorial eastern Atlantic and western Indian Ocean mode (E-D) associated with the Atlantic-Indian ocean Dipole.

The negative/positive correlation observed with the SST over the equatorial eastern Atlantic (centre E)/ western Indian Ocean (D) is indicative of a dipole as was observed in the second

JJA PCA mode for the Joint Indian Atlantic Ocean. The influence of this mode on the rainfall over the region may be in cognizance of the fact that the oceans act as a single field through the associated wind and water currents (Shukla 1991; Stouffer et al 2007; Wunsch and Heimbach 2006).

The negative relationships observed with ZAF SST gradient mode indicate that the warming /cooling over the equatorial western Indian /eastern Atlantic Ocean favour enhanced SOND seasonal rainfall over most parts of the region in agreement with the observations of Nicholson and Entekhabi (1987); and Okoola (1996). This pattern of SST variations is likely to influence the Walker circulation cell linking the western Indian Ocean and the Congo Basin. The negative ZAF could be associated with the warm equatorial western Indian Ocean and a relatively cold equatorial eastern Atlantic Ocean that would imply the reverse of the Walker circulation favouring enhanced influx of moisture into the region from the Congo Basin and Indian Ocean as has been observed for wet years (Indeje and Semazzi 2000, Schreck and Semazzi 2004).

These relationships also reveal the importance of the combined role of the Atlantic and Indian Ocean as influences seasonal rainfall over the region. The spatial patterns of the values of correlation also reveal that the responses of SOND rainfall over western parts of the region and Kenyan coast to ZAF zonal SST gradient mode are in agreement with the responses of seasonal rainfall over the respective regions to SST variablity. These results indicate that SOND rainfall was significantly correlated to the zonal SST gradient modes. The improvements in the values of correlation beyween rainfall and SST based predictors when SSTG modes are used indicate that the use of the zonal SST gradient modes improves the relationships between SOND rainfall and SST based predictors compared to grid point SSTs.

The meridional SST gradient modes that had the highest relationships with SOND rainfall were MAB6 and MIB1 defined in figure 39 and Table 16.

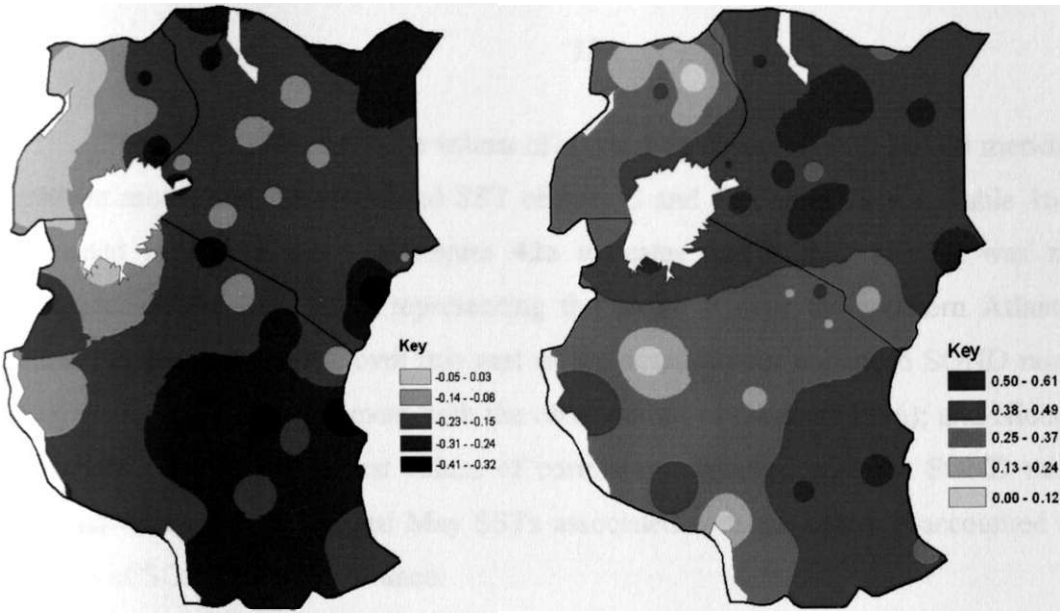

Figure 42a Figure 42b

Figure 42a: The spatial patterns of correlation between September-December rainfall and the May sea surface temperatures for the centre (a) F over the southern (b) G over the northen Atlantic Ocean associated with a meridional sea surface gradient mode.

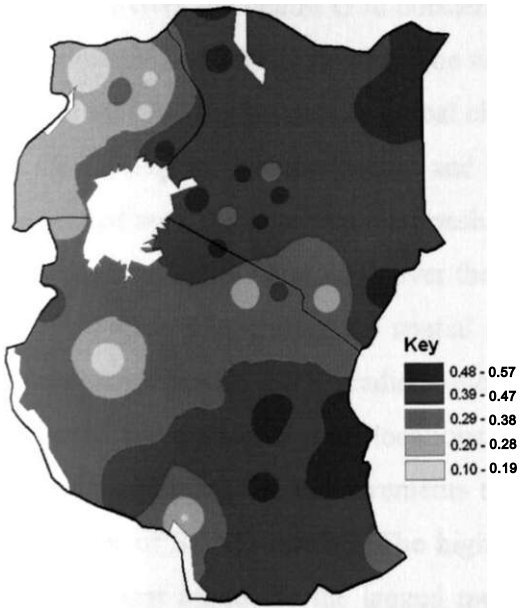

Figure 42c: The spatial patterns of correlation between September-December rainfall and a meridional sea surface temperature gradient mode associated with the Atlantic Ocean (G-F) for the month of May.

The spatial patterns of the values of correlation observed with MAB6 meridional SST gradient mode, and the associated SST centres G and F (Figure 39 and Table 16a), are as presented in Figure 42a-42c. Figure 42a indicates that SOND rainfall was negatively correlated to the May SSTs representing the centre F over the southern Atlantic Ocean indicating that the cooling over this part of the ocean favour enhanced SOND rainfall over parts of the region in agreement with the observations of Okoola (1996); and Nicholson and Entekhabi (1987). The largest values of correlation observed with the SOND rainfall was 0.42 indicating that the lagged May SSTs associated with the centre F accounted for about 17.64% of SOND rainfall variance.

Figure 42b indicates that May SSTs associated with the centre G over northern Atlantic were positively correlated to SOND rainfall- implying that the warming over the northern Atlantic Ocean favour enhanced SOND rainfall.

The largest values of correlation observed with the SOND rainfall was 0.65 indicating that SSTs over the centre G in northern Atlantic Ocean for the month of May accounted for about 42.25% of SOND rainfall. The warming and cooling of the North Atlantic Ocean in the period March-May influences global climate and the evolution of ENSO in the Pacific Ocean in the subsequent months (Sutton and Hodson 2007; Wu et al. 2007). Such linkages may be associated with the observed relationships with SOND rainfall over the region that is strongly influenced by ENSO and SSTs over the neighbouring oceans.

Figure 42c, giving the spatial patterns of the values of correlation between SOND rainfall and MAB6 SST gradient mode, indicates marked improvement in the observed values of correlation at most locations compared to those presented in Figures 42a and 42b further reaffirming the improvements that the use of SST gradient modes could have on the prediction of SOND rainfall. The highest value of correlation was 0.57 indicating that this SST gradient mode for the lagged month of May accounted for about 32.49% of SOND rainfall variance, which was slightly lower than the value observed with the SST for the centre G over the northern Atlantic Ocean, but much higher than the values observed with SST for the centre F over the southern Atlantic Ocean. The second PCA mode representing interhemispheric SST variability in the Atlantic Ocean, on which the development of this gradient is based, is strongest in the period March-May and has linkages with the North Atlantic Oscillation (NAO) and ENSO (Wu et al. 2007). Similar results were observed with

the other meridional SST gradient modes associated with the Atlantic Ocean as defined in Table 16a and 16b.

It should be noted that the values of correlation observed with the centre F were relatively small compared to those observed with the centre G, making it difficult to use correlation and simple SST derived modes within the Atlantic Ocean. The use of SST gradient mode, however, produced better prediction signals than the SST associated with the centres G and F. These results indicate that the warming/ cooling over the northern/southern Atlantic Ocean during the month of May preceding SOND rainfall favour enhanced SOND rainfall over parts of the region. This lead-time would be useful for improving the lead-time in the prediction of SOND seasonal rainfall. These results indicate further that the use of the SST predictors from the Atlantic Ocean may require the inclusion of the period March to May when the SOND has peak, which has shown strong relationships with the SOND rainfall.

The meridional gradient mode used to represent the influence of interhemispheric SST variability in the Indian Ocean on the climate of the region is MIB1, which is associated with the centres H and I (Figure 39), and derived as indicated in Table 16a. Figures 43a and 43b give the spatial patterns of the values of correlations between SOND rainfall and October SST for the centres H and I. Figure 43a indicates that October SSTs representing the centre H were positively/negatively correlated to SOND rainfall over the eastern parts of Kenya/western parts of Uganda implying that the warming over the southern Indian Ocean favour enhanced/deficient SOND rainfall over parts of eastern Kenya/western Uganda. The highest value of correlation was 0.52 indicating that October SST for the centre H accounted for about 27.04% of SOND rainfall variance.

Figure 43 b indicates that SSTs representing the centre I over the northern Indian Ocean were positively/negatively correlated to SOND rainfall over the eastern /western parts of the region. The largest value of correlation was 0.44 indicating that September SST for the centre H accounted for about 19.36% of SOND rainfall variance.

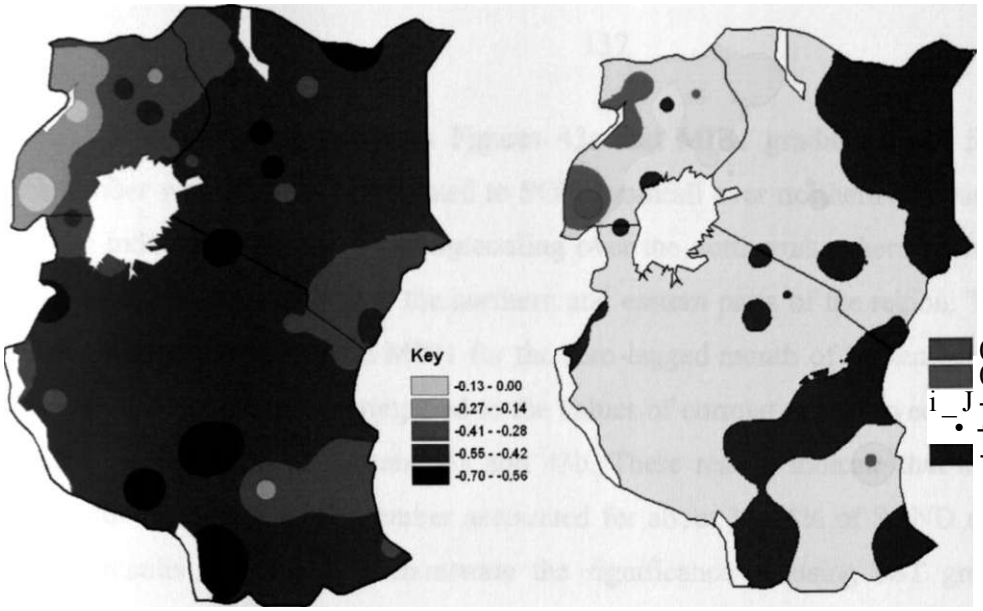

Figure 43a Figure 43b

Figure 43: The spatial patterns of correlation between September-December rainfall and September sea surface temperature for the centre (a) H in the southern (b) I in the northern Indian Ocean associated with a meridional gradient for the ocean.

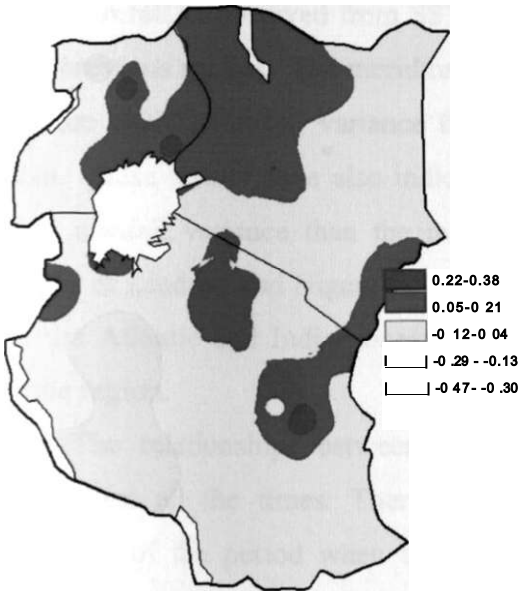

Figure 43c: The spatial patterns of correlation between September-December rainfall and September meridional sea surface temperature **gradient mode (I-H)** associated with the Indian Ocean.

It can be observed from Figures 43c that MIB1 gradient mode for the month of September was positively correlated to SOND rainfall over northern and eastern parts of the region indicating that the warming/cooling over the northern/southern Indian Ocean favour enhanced SOND rainfall over the northern and eastern parts of the region. The largest value of correlation observed with MIB1 for the zero-lagged month of September was 0.62 which is a marked improvement compared to the values of correlation observed with the individual centres as presented in Figures 43a and 43b. These results indicate that this SST gradient mode for the month of September accounted for about 38.44% of SOND rainfall variance. These results continue to demonstrate the significance of using SST gradient modes as predictors compared to the SST associated with the centre. Higher values of correlation were observed with the SST gradients modes compared to the SST associated with the centres H and I.

These results further indicated that the Atlantic Ocean has significant influence on the SOND rainfall as observed from SST gradients modes that might not have been established in the previous studies. The meridional SST gradient modes in the Atlantic Ocean accounted for more SOND rainfall variance than the meridional modes associated with the Indian Ocean. These results have also indicated that the zonal SST gradient modes accounted for higher rainfall variance than the meridional SST gradient modes in agreement with the findings of Lindzen and Nigam (1987). The strong/weak meridional SSTG modes associated with the Atlantic and Indian oceans would generally favour/inhibit inland moisture influx into the region.

The relationships between SOND rainfall and atmospheric systems may not be synchronous all the times. There might be some time lag between the variables. The knowledge of the period when the peak relationships could be achieved is important to ensure that the right predictors are included in the models. Figure 44 indicates that the correlation between ZIND and SOND rainfall peaks from very weak values early in the year to reach a maximum around October then declines. Hence, efficient use of this gradient mode would require the prediction of the conditions for the months of September and October when the peak relationships are achieved. Attempts to predict IOD, which has characteristics similar to this mode, have indicated that the major events can be predicted with skill

(Wajsowicz 2004). Similar results were observed with the zonal and meridional SST gradient modes associated with the Indian Ocean defined in Table 16b.

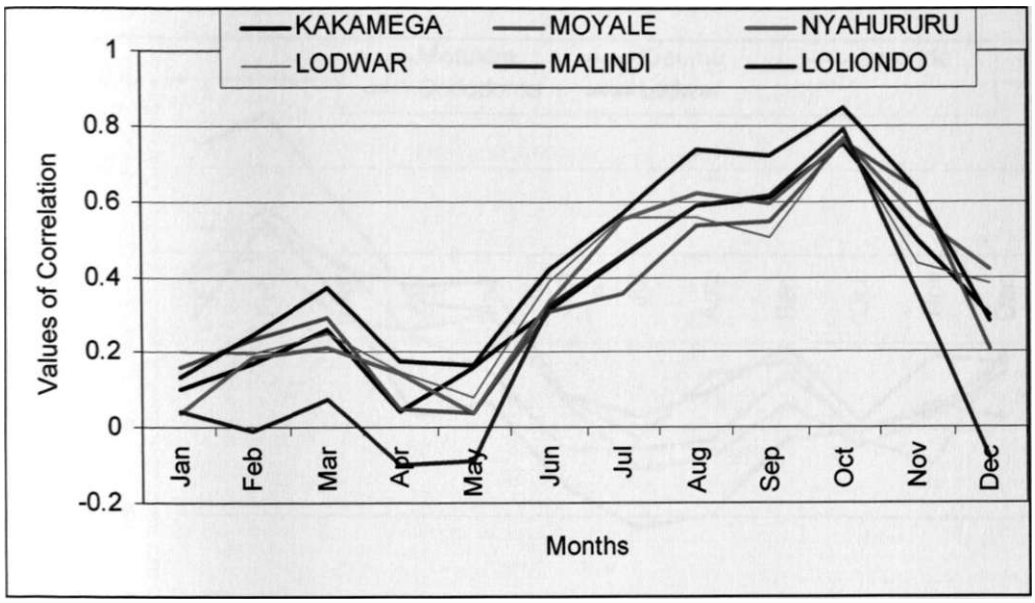

Figure 44: The temporal evolution of the correlation between September-December rainfall and sea surface temperatue gradient mode for the equatorial Indian Ocean (D-C)

This temporal evolution of the correlation between SOND rainfall and SSTA index representing ZIND SST gradient mode show that this mode has significant prediction potential from June to December.

Figure 45 indicates that the relationship between SOND rainfall and ZAF SST gradient mode improves gradually from around March to reach a peak around July-September then starts to decline. It should be noted from Figure 45 that although this mode has predictive potential for predicting SOND between June and November, it had significant potential to predict rainfall for the same season as early as the period March - May.

Figure 46 gives the evolution of correlation observed with MAB6 SST gradient mode, which is defined in Figure 39 and Table 16. Figure 46 indicates that the relationships between SOND rainfall and MAB6 meridional SST gradient mode reach their peak in the months of April and May preceeding the season when the interhemispheric mode associated with this gradient has the highest amplitude (Weare 1977). The values of correlation drop significantly towards the season with the lowest values observed in the months of July,

August and September, which are often used to predict SOND rainfall. Hence, the use of SST predictors associated with the months of June, July and August for all oceans may be leaving out potential predictors from the Atlantic Ocean.

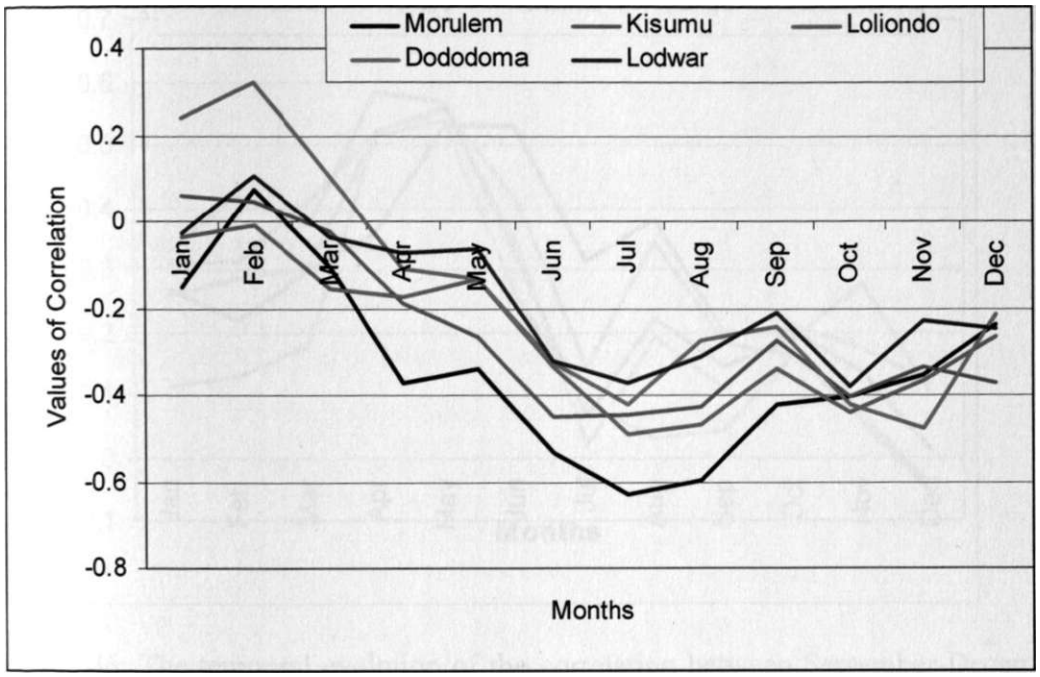

Figure 45: The temporal evolution of the correlation between September-December rainfall and zonal sea surface temperature gradient mode associated with the Atlantic-Indian Ocean Dipole (E-D).

Similar results were observed with the other meridional SST gradient modes associated with the Atlantic Ocean. The lead-time of the predictors from the Atlantic Ocean is interesting and could be suggesting a possibility of the processes in the Atlantic Ocean leading the Pacific and Indian oceans as has been observed by Sutton and Hodson (2007); and Wu et al. (2007) among other authors. The Great Ocean Conveyor, discussed in section 2.1.8, links all the global oceans and makes them to act as a single field.

The results discussed in this section indicate that SOND rainfall was significantly correlated to SST gradient modes. The results also indicate that the use of SST gradient modes as predictors have advantage over grid point SSTs, and the SST gradient modes have the potential to improve the relationships between SOND rainfall and SST based predictors. The zonal SST gradient modes accounted for higher rainfall variance than the meridional

SST gradient modes. The meridional SST gradient modes associated with the Atlantic Ocean accounted for more SOND rainfall variance than those associated with the Indian Ocean.

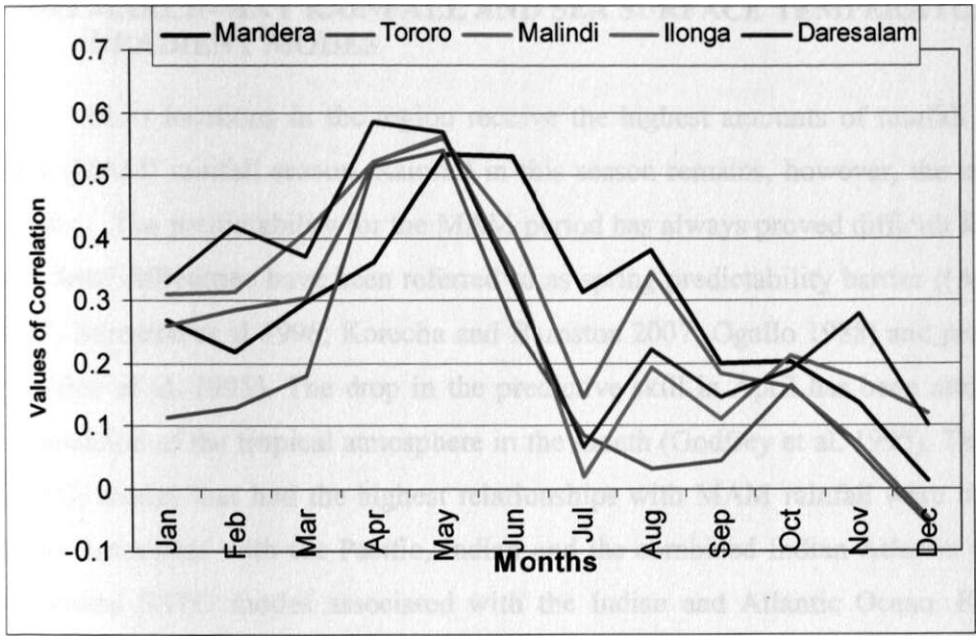

Figure 46: The temporal evolution of the correlation between September-December rainfall and a meridional sea surface temperature gradient mode for the Atlantic Ocean (G-F)

In the next section we provide more results for March-April -May (MAM) rainfall and SST gradient modes.

4.3.4.2 MARCH-MAY RAINFALL AND SEA SURFACE TEMPERATURE GRADIENT MODES

Most locations in the region receive the highest amounts of rainfall during March-May (MAM) rainfall season. Rainfall in this season remains, however, the most difficult to predict. The predictability for the MAM period has always proved difficult for most models and these difficulties have been referred to as spring predictability barrier ((Annamalai et al. 2007; Barnston et al 1996; Korecha and Barnston 2007; Ogallo 1988) and predictability gap (Godfrey et al. 1995). The drop in the predictive skill in April has been attributed to weak organization of the tropical atmosphere in the month (Godfrey et al. 1995). The SST gradient (SSTG) modes that had the highest relationships with MAM rainfall were the zonal SSTG modes associated with the Pacific, Indian and the combined Indian-Atlantic Ocean, and the meridional SSTG modes associated with the Indian and Atlantic Ocean. For each SSTG mode, starting with the zonal modes, the results of correlation from MAM rainfall and SST representing parts of the global oceans used to derive the gradient modes are discussed to determine any improvements in relationships associated with the use of gradient modes.

Figure 47a and 47b give the spatial patterns of the values of correlation observed between MAM rainfall and SST representing the centres D and E associated with ZAF SST gradient mode based on Atlantic-Indian Ocean Dipole (AIOD). Figure 47a indicates that MAM rainfall over parts of Lake Victoria Basin and northern coast was positively correlated to the March SST representing the centre D over the western Indian Ocean. However, rainfall over southern Tanzania was negatively correlated to SST representing the centre D. These results indicate that the response of MAM rainfall over parts of the region to SST over the equatorial western Indian Ocean was not uniform. The largest value of correlation observed with SST representing the centre D for the month of March was 0.51 indicating that they accounted for about 26.01% of the MAM rainfall variance.

Figure 47b indicates that MAM rainfall over parts of the region was negatively correlated to the March SST for the centre E over the equatorial eastern Atlantic Ocean. The negative relationships observed between SST over the equatorial eastern Atlantic Ocean and MAM rainfall is in agreement with findings of Nicholson and Entekhabi (1987); and Okoola (1996) among other authors.

4.3.4.2 MARCH-MAY RAINFALL AND SEA SURFACE TEMPERATURE GRADIENT MODES

Most locations in the region receive the highest amounts of rainfall during March-May (MAM) rainfall season. Rainfall in this season remains, however, the most difficult to predict. The predictability for the MAM period has always proved difficult for most models and these difficulties have been referred to as spring predictability barrier ((Annamalai et al. 2007; Barnston et al 1996; Korecha and Barnston 2007; Ogallo 1988) and predictability gap (Godfrey et al. 1995). The drop in the predictive skill in April has been attributed to weak organization of the tropical atmosphere in the month (Godfrey et al. 1995). The SST gradient (SSTG) modes that had the highest relationships with MAM rainfall were the zonal SSTG modes associated with the Pacific, Indian and the combined Indian-Atlantic Ocean, and the meridional SSTG modes associated with the Indian and Atlantic Ocean. For each SSTG mode, starting with the zonal modes, the results of correlation from MAM rainfall and SST representing parts of the global oceans used to derive the gradient modes are discussed to determine any improvements in relationships associated with the use of gradient modes.

Figure 47a and 47b give the spatial patterns of the values of correlation observed between MAM rainfall and SST representing the centres D and E associated with ZAF SST gradient mode based on Atlantic-Indian Ocean Dipole (AIOD). Figure 47a indicates that MAM rainfall over parts of Lake Victoria Basin and northern coast was positively correlated to the March SST representing the centre D over the western Indian Ocean. However, rainfall over southern Tanzania was negatively correlated to SST representing the centre D. These results indicate that the response of MAM rainfall over parts of the region to SST over the equatorial western Indian Ocean was not uniform. The largest value of correlation observed with SST representing the centre D for the month of March was 0.51 indicating that they accounted for about 26.01% of the MAM rainfall variance.

Figure 47b indicates that MAM rainfall over parts of the region was negatively correlated to the March SST for the centre E over the equatorial eastern Atlantic Ocean. The negative relationships observed between SST over the equatorial eastern Atlantic Ocean and MAM rainfall is in agreement with findings of Nicholson and Entekhabi (1987); and Okoola (1996) among other authors.

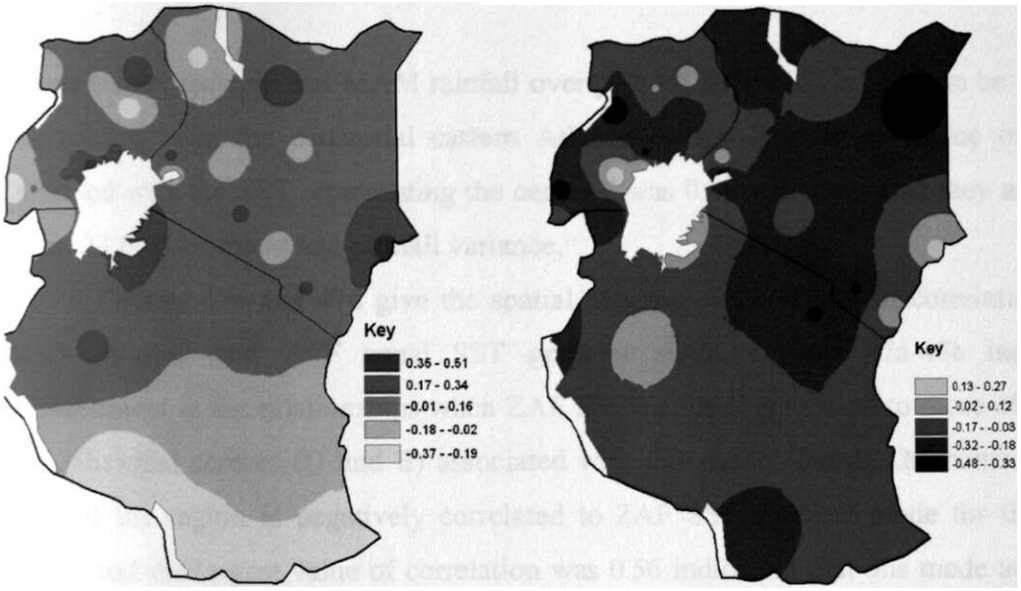

Figure 47a Figure 47b

Figure 47: The spatial patterns of the values of correlation between March-May rainfall and the March Sea surface temperaturw for the centre in the equarorial (a) D we western Indian (b) E eastern Atlantic Ocean associated with the Atlantic-Indian Ocean Dipole.

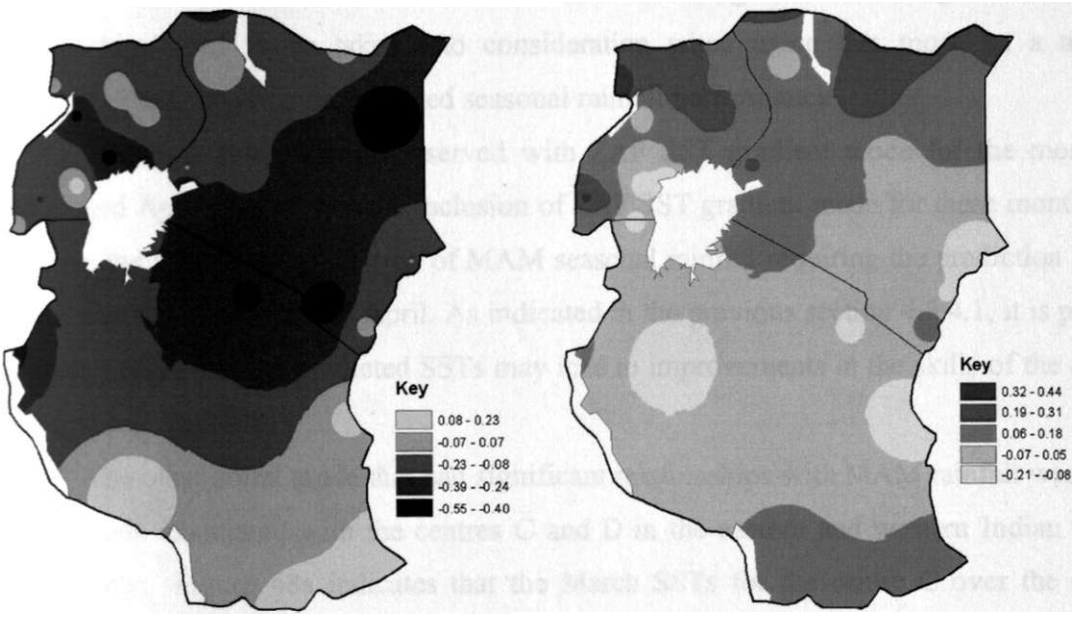

Figure 47c Figure 47d

Figure 47: The spatial patterns of correlation between March-May rainfall and the zonal sea surface temperature gradient mode (E-D) associated with the Atlantic-Indian Ocean Dipole for (c) March (d) January.

These results indicate that MAM rainfall over parts of the region is likely to be enhanced by the cooling over the equatorial eastern Atlantic Ocean. The largest value of correlation observed with the SST representing the centre E was 0.48 indicating that they accounted for about 23.04% of the MAM rainfall variance.

Figures 47c and 47d give the spatial patterns of the values of correlations between MAM rainfall and ZAF zonal SST gradient mode. Figures 47a-47c indicate some improvement in the relationships when ZAF SSTG is used compared to those observed with the individual centres (D and E) associated with this mode. The MAM rainfall over most parts of the region is negatively correlated to ZAF SST gradient mode for the month of March and the largest value of correlation was 0.56 indicating that this mode accounted for about 31.26% of MAM rainfall variance. Similar relationships were observed with the ZAF SST gradient mode for the months of February, April and May. However, Figure 47d indicates a change in the relationships in the month of January when this mode was positively correlated to MAM rainfall over parts of the region. Such changes in the sign of relationships need to be taken into consideration when using this mode as a tool for monitoring and advising on expected seasonal rainfall performance.

The peak relationships observed with ZAF SST gradient mode for the months of March and April suggest that the inclusion of ZAF SST gradient mode for these months may improve the skill in the prediction of MAM seasonal rainfall requiring the prediction of SST for the months of March and April. As indicated in the previous section 4.3.4.1, it is possible to predict SSTs and the predicted SSTs may lead to improvements in the skills of the models (Mauget and Ko 2008).

The other zonal mode that had significant relationships with MAM rainfall was ZIND SSTG mode associated with the centres C and D in the eastern and western Indian Ocean, respectively. Figure 48a indicates that the March SSTs for the centre C over the eastern Indian Ocean were negatively correlated to MAM rainfall over southern Tanzania and parts of Uganda. The largest values of correlation observed with the MAM rainfall was 0.55 indicating that the March SSTs for the centre C accounted for about 30.25% of MAM rainfall variance. The spatial patterns of the values of correlation observed with the other centre D used to derive ZIND SST gradient mode are as presented in Figure 47a above.

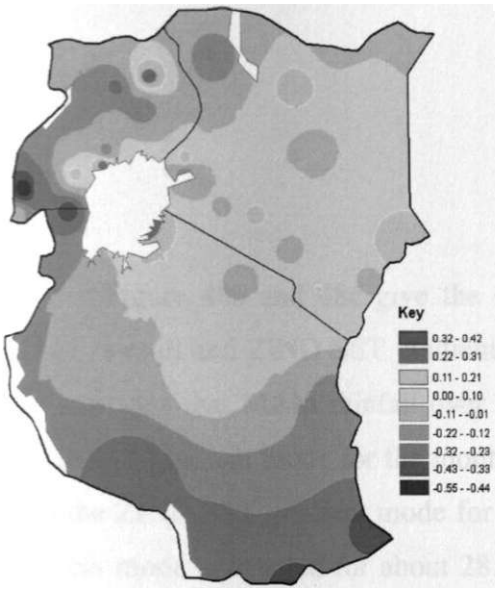

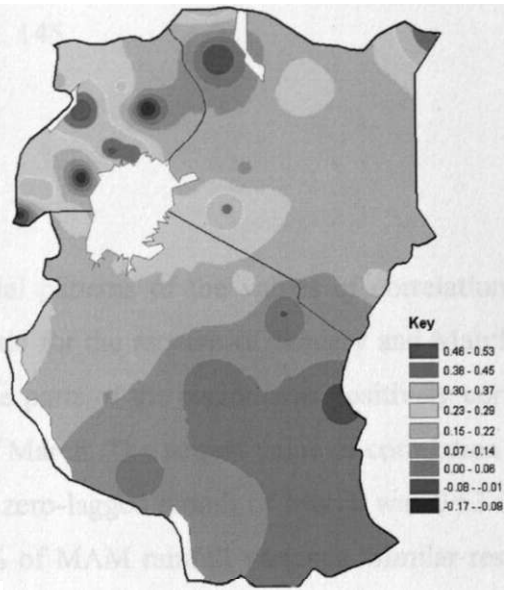

Figure 48a Figure 48b

Figure 48: The spatial patterns of correlation between March-May rainfall and (a) March sea surface temperatures for the centre (a) C in the equatorial eastern Indian Ocean (b) the zonal sea surface gradient mode for the equatorial Indian Ocean associated with the Indian Ocean Dipole (D-C)

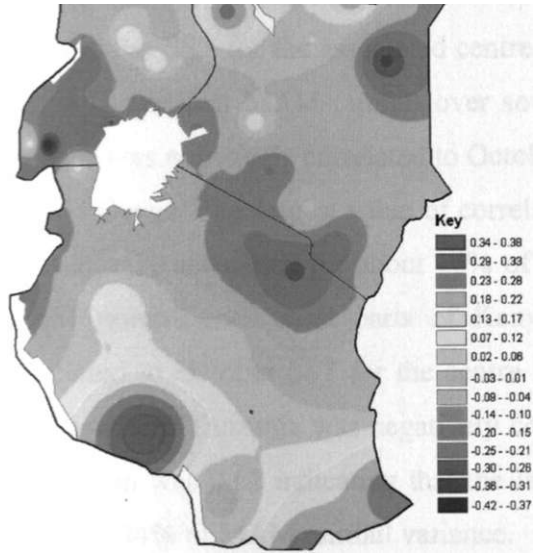

Figure 48c: The spatial patterns of the values of correlation between March-May rainfall and the zonal sea surface temperature gradient mode for the equatorial Indian Ocean associated with the Indian Ocean Dipole (D-C) for the month of January.

Figure 48b and 48c give the spatial patterns of the values of correlation between MAM rainfall and ZIND SST gradient mode for the months of January and March. Figure 48b indicates that MAM rainfall over some parts of the region was positively correlated to ZIND SST gradient mode for the month of March. The largest value of correlation observed with the ZIND SST gradient mode for the zero-lagged month of March was 0.53 indicating that this mode accounted for about 28.08% of MAM rainfall variance. Similar results were observed with ZIND for the months of February and April.

Figure 48c, however, indicates a change in the sign of relationships with the ZAF SSTG for the month of January whent MAM rainfall over some parts of the region was negatively correlated to the ZIND SST gradient mode. A similar changes in relationships between MAM rainfall and SSTG modes for the month of January has also been observed with the other SSTG modes.

The spatial patterns of correlation observed with the zonal mode in the Pacific Ocean together the SST for the associated centres A and B are presented in Figure 49a-49d. Figure 49a indicates that MAM rainfall over southern Tanzania, northeastern Kenya and parts of Uganda was negatively correlated to October SST for the centre A over the equatorial eastern Pacific Ocean. The largest value of correlation was 0.40 indicating that the October SST for the centre A accounted for about 16% of MAM rainfall variance. Figure 49b indicates that MAM rainfall over most parts of Kenya, parts of Lake Victoria Basin was positively correlated to October SST for the centre B over western Pacific Ocean. The MAM rainfall over southern Tanzania was negatively correlated to SST for centre B. The largest value of correlation was 0.62 indicating that the lagged October SST for the centre B accounted for about 38.44% of MAM rainfall variance.

Figure 49c indicates that MAM rainfall over parts of the region was positively correlated to ZPAC SST gradient mode associated with the centres A and B for the month of October indicating that the cooling/warming of SST over centres A/B favour enhanced MAM rainfall over parts of the region.

Figure 49a

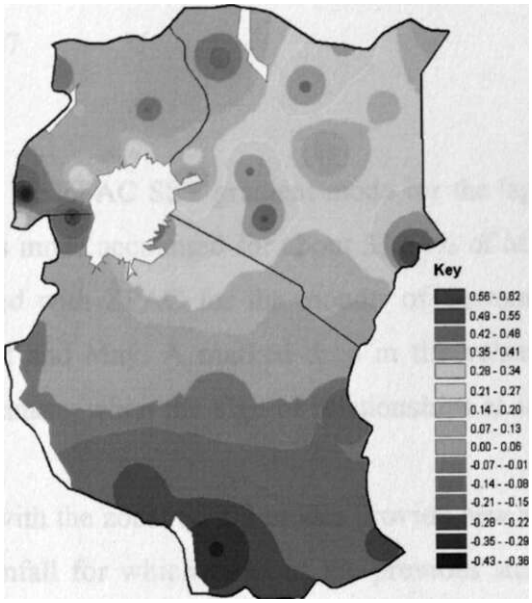

Figure 49b

Figure 49: The spatial patterns of the values of correlation between March-May rainfall and the October sea surface temperatures **for the centre (a)** A **in the eastern (b) B** in the western **Pacific Ocean associated with the zonal gradient mode for the ocean.**

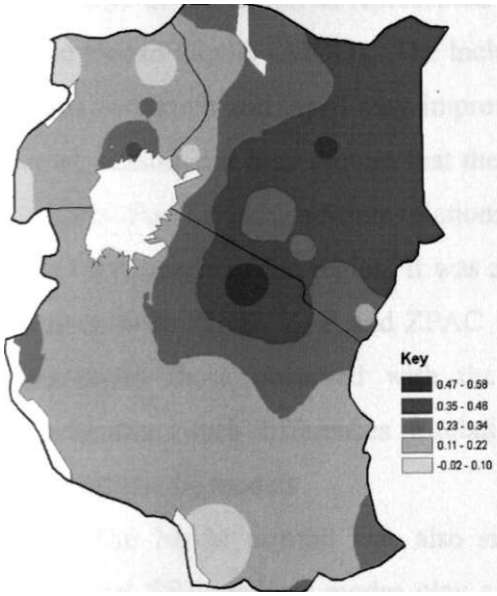

Figure 49c

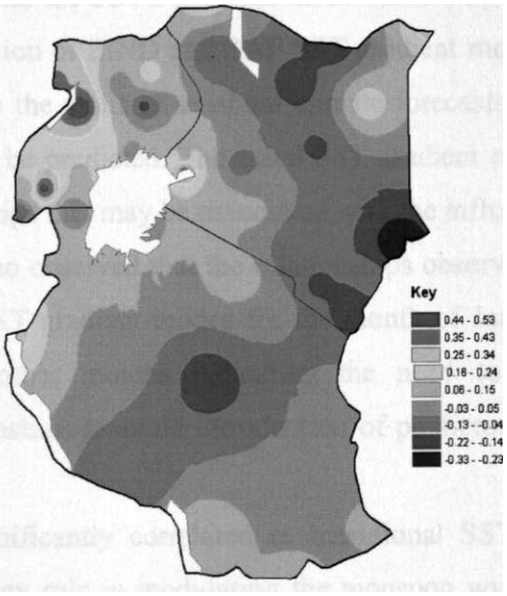

Figure 49d

Figure 49: The spatial patterns of the values of correlation between March-May rainfall and zonal sea surface temperatures gradient mode for the equatorial Pacific Ocean (B-A) for the month of (c) October (d) January.

The largest value of correlation observed with the ZPAC SST gradient mode for the lagged month of October was 0.58 indicating that this mode accounted for about 33.64% of MAM rainfall variance. Similar results were observed with ZPAC for the months of September, November, December, February, March, April and May. A marked drop in the values of correlation was observed with the month of January when the sign of relationships at some locations changed (Figure 49c).

The significant relationships observed with the zonal SSTG modes provide new tools for the prediction of March-May seasonal rainfall for which most of the previous studies have been unable to detect strong predictability signals from SST variables (Annamalai et al. 2007; Korecha and Barnston 2007). These results continue to indicate significant improvements in the predictability signals in the region through the use of SST gradient modes for the two major rainfall seasons of MAM and SOND. The results also continue to reaffirm the importance of a combined role of the Indian and Atlantic Ocean in influencing the climate of the region as represented with the SSTG gradient mode based on the Atlantic-Indian Ocean Dipole (AIOD). The inclusion of ZIND and ZAF SST gradient modes for the months of March and April may improve the skills of seasonal climate forecasts for MAM rainfall season, but may require that they be predicted. The zonal SST gradient mode in the equatorial Pacific had lead-time relationships that may be associated with the influence of the ENSO on climate of the region. It was also observed that the relationships observed at some locations with ZIND, ZAF and ZPAC SST gradient modes for the month of January were opposite to those observed with the other months indicating the need to take into considerations such differences in relationships to avoid introduction of predictors that may only confuse the models.

The MAM rainfall was also significantly correlated to meridional SSTG modes. Meridional SST gradient modes play a key role in modulating the monsoon wind currents affecting the region. The spatial patterns of the values of correlation observed between MAM rainfall and MAB6 meridional SST gradient mode associated with the centres F and G over the Atlantic Ocean are presented in Figure 50.

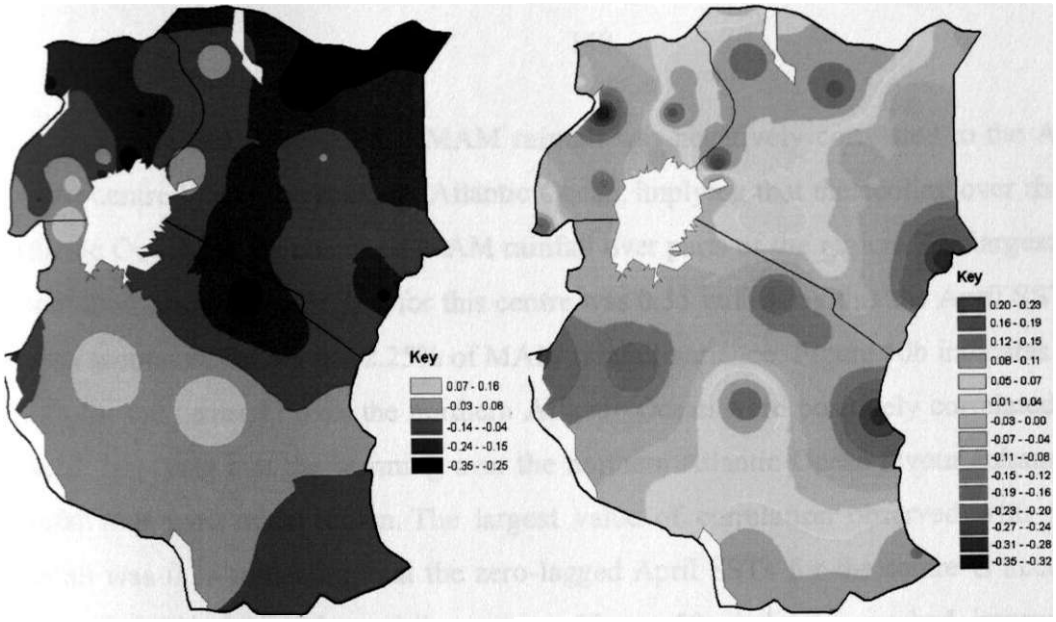

Figure 50a Figure 50b

Figure 50: The spatial patterns of correlation between March-May rainfall and April sea surface temperatures for the centre (a) F in the southern (b) G in the northern Atlantic Ocean.

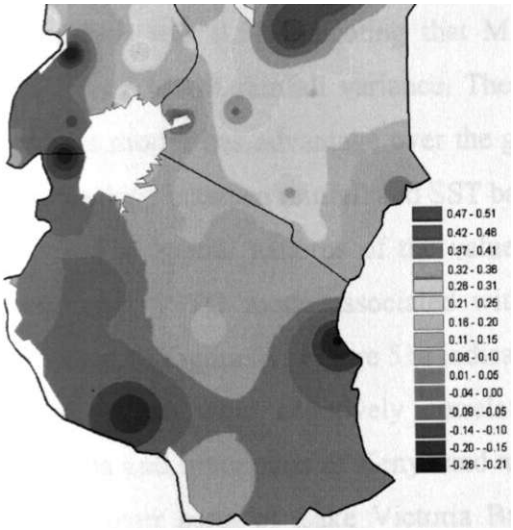

Figure 50c: The spatial patterns of correlation between March-May rainfall and the meridional sea surface temperatures gradient mode (G-F) representing Atlantic Ocean for the month of April.

Figure 50a indicates that MAM rainfall was negatively correlated to the April SSTs for the centre F over the southern Atlantic Ocean, implying that the cooling over the southern Atlantic Ocean favour enhanced MAM rainfall over parts of the region. The largest values of correlation observed with SST for this centre was 0.35 indicating that the April SSTs for this centre accounted for about 12.25% of MAM rainfall variance. Figure 50b indicates that April SSTs for the centre G over the northern Atlantic Ocean were positively correlated to MAM rainfall implying that the warming over the northern Atlantic Ocean favour enhanced MAM rainfall over parts of the region. The largest value of correlation observed with the MAM rainfall was 0.35 indicating that the zero-lagged April SSTs for the centre G accounted for about 12.25% of MAM rainfall variance. Figure 50c indicates marked improvement in relationships with MAB6 SST mode compared to the associated SST centres (Figures 50 and 50b) and the SSTG mode was positively correlated to MAM rainfall over northeastern parts of the region reaffirming that the warming/cooling of the northern/southern Atlantic Ocean favour enhanced MAM rainfall over northeastern parts of the region. The largest value of con-elation was 0.51 indicating that MAB6 for the month of April accounted for about 26.01% of MAM rainfall variance. These results continue to indicate that the use of SST gradient modes has advantage over the grid point SST, and may lead to improvement in the relationships between rainfall and SST based predictors.

The spatial patterns of the values of correlation between MAM rainfall and MIB3 meridional SSTG mode associated with the centres I and J over the Indian Ocean are presented in Figure 51. Figure 51a indicates that April SSTs for the centre I over the northern Indian Ocean were negatively correlated to MAM rainfall over the southern parts of Tanzania and some parts of Kenya and northern Tanzania, and positively correlated to MAM rainfall over parts of Lake Victoria Basin and Uganda. The largest value of correlation observed with the MAM rainfall was 0.49 indicating that the April SSTs for the centre I accounted for about 24.01% of MAM rainfall variance.

Figure 51b indicates that MAM rainfall over most parts of the region was not significantly correlated to the April SSTs representing centre J over the southern Indian Ocean.

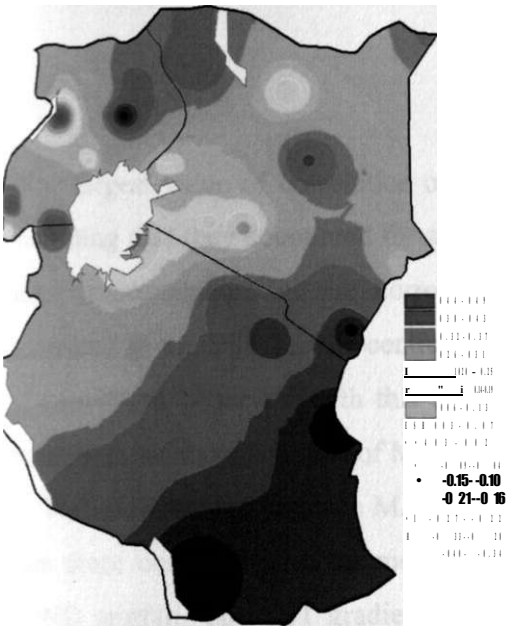

Figure 51a

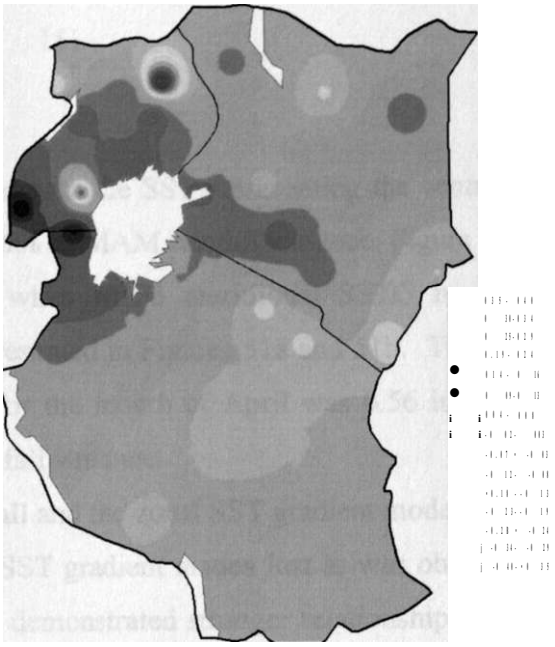

Figure 51b

Figure 51: The spatial patterns of the values of correlation between March-May rainfall and the sea surface temperatures for the centre (a) I in northern (b) J in the southern Indian Ocean for the moth of April.

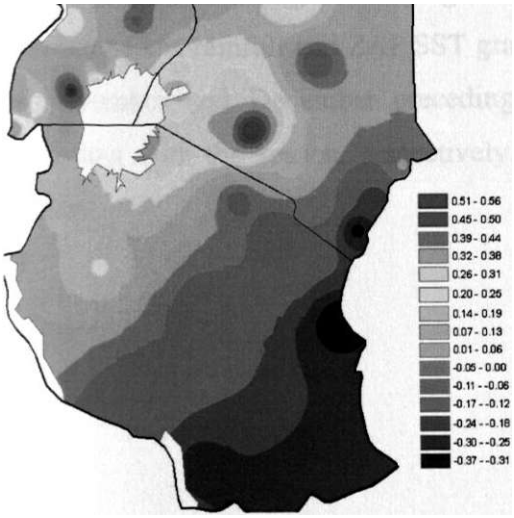

Figure 51c: The spatial patterns of the values of correlation between March-May rainfall and the April meridional sea surface temperature gradient mode (I-J) for the Indian Ocean.

The largest value of correlation observed with the SST representing the centre J was 0.40 indicating that they accounted for about 16% of MAM rainfall variance. Figure 51c indicates some improvements in the correlation when MIB3 meridional SSTG mode was used compared to the SST for the centres as presented in Figures 51a and 51b. The largest value of correlation observed with this mode for the month of April was 0.56 indicating that it accounted for about 31.36% of MAM rainfall variance.

The relationships between MAM rainfall and the zonal SST gradient modes were stronger than those observed with the meridional SST gradient modes just as was observed with the SOND rainfall. The SST gradient modes demonstrated stronger relationships with seasonal rainfall than were observed with the associated SST for most of the centres associated with the SSTG modes. These results continue to indicate that the SST gradient modes have a potential to improve relationships between seasonal rainfall and SST based predictors.

The relationships between the SST gradient modes and MAM rainfall may not be the same for all the months of the year. It is important to identity the few months when the relationships are strongest. Figure 52 gives the temporal evolution of the correlation between MAM rainfall and ZAF zonal SST gradient mode. Figure 52 indicates that the relationships between MAM rainfall and ZAF SST gradient mode have two peaks observed in the months of November and December preceding the season and the months of March to April coinciding with the season, respectively. The relationships were weakest in the month of January.

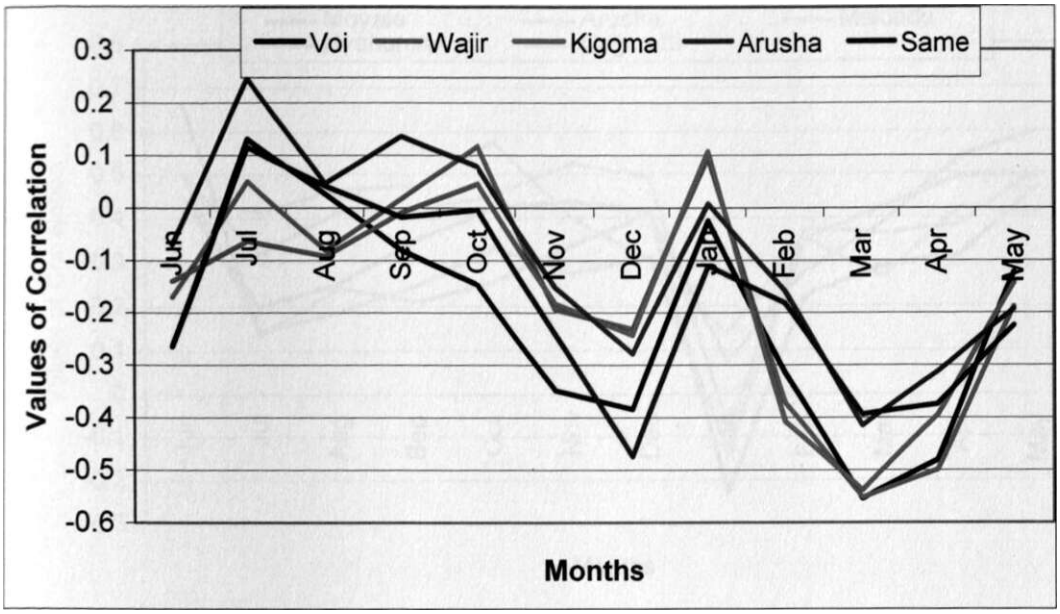

Figure 52: The temporal evolution of the correlation between March-May rainfall and the zonal sea surface temperature gradient mode (E-D) associated with the Atlantic-Indian Ocean Dipole.

Figure 53 gives the temporal evolution of the correlation between MAM rainfall and ZPAC SSTG mode for the lagged months of June-February and the zero-lagged months of March-May. Figure 53 indicates that the values of correlation observed with ZPAC SST gradient mode are generally large for the months of June- February preceding the season and March-May coinciding with the season. The values of correlation were very low in January and even changing the sign at some locations continuing to reaffirm the weaknesses in the use of January in the models predicting MAM rainfall season.

Figure 54 indicates that MAM rainfall has the strongest relationships with MAB3 meridional SST gradient mode for the months of July to September preceding the season. The values of correlation reduce as the season approaches. Similar results were observed with the other meridional SST gradients modes associated with the Atlantic Ocean defined in Table 16b.

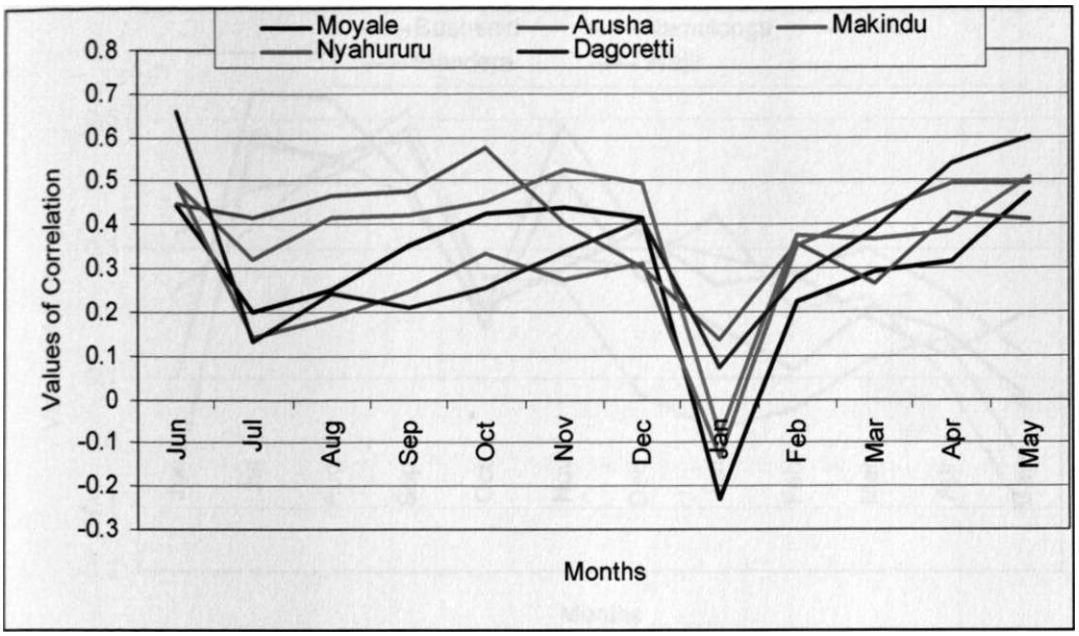

Figure 53: The temporal evolution of correlation between March-May rainfall and zonal sea surface temperature gradient mode (B-A) for the Pacific Ocean.

The values of correlation observed with MIB3, which is associated with the Indian Ocean, increase towards the season reaching the peak in April coinciding with the season (Figure 55). Similar results were observed with zonal SST gradient modes associated with the Indian Ocean. There is significant reduction in the values of correlation observed with this mode in the months of January and February, which are often used to predict MAM seasonal rainfall. These results indicate that the use of predictors from the Atlantic and Pacific Ocean needs to consider the inclusion of the months of July to September preceding the season.

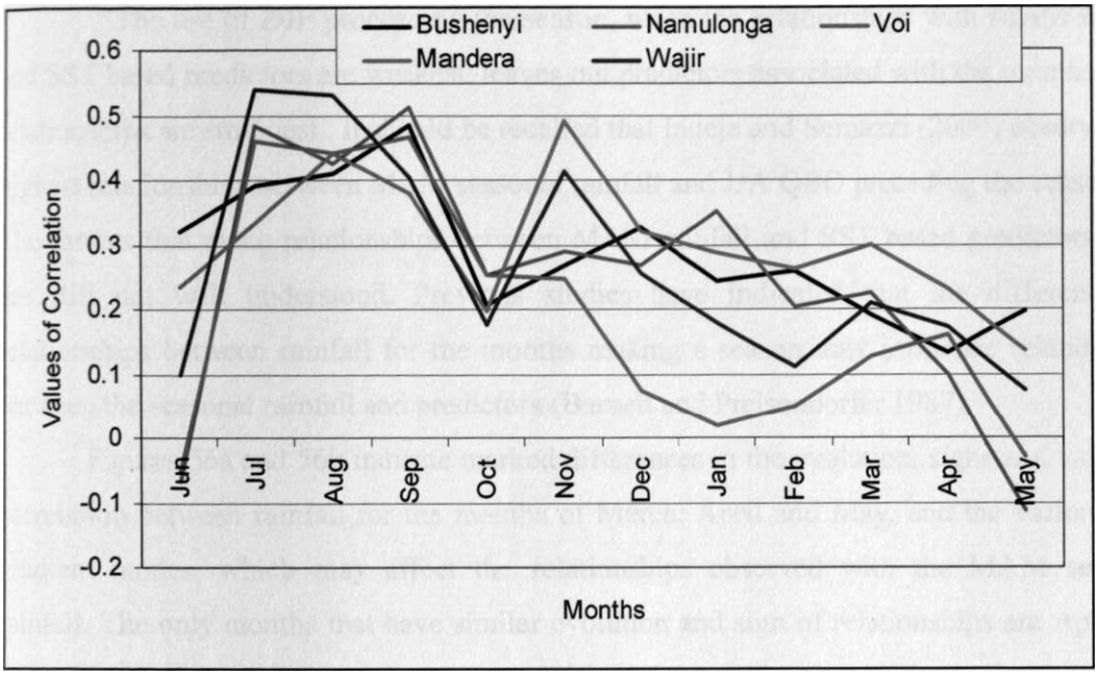

Figure 54: The temporal evolution of the values of correlation between March-May rainfall and meridional sea surface temperature gradient mode (G-K) for the Atlantic Ocean.

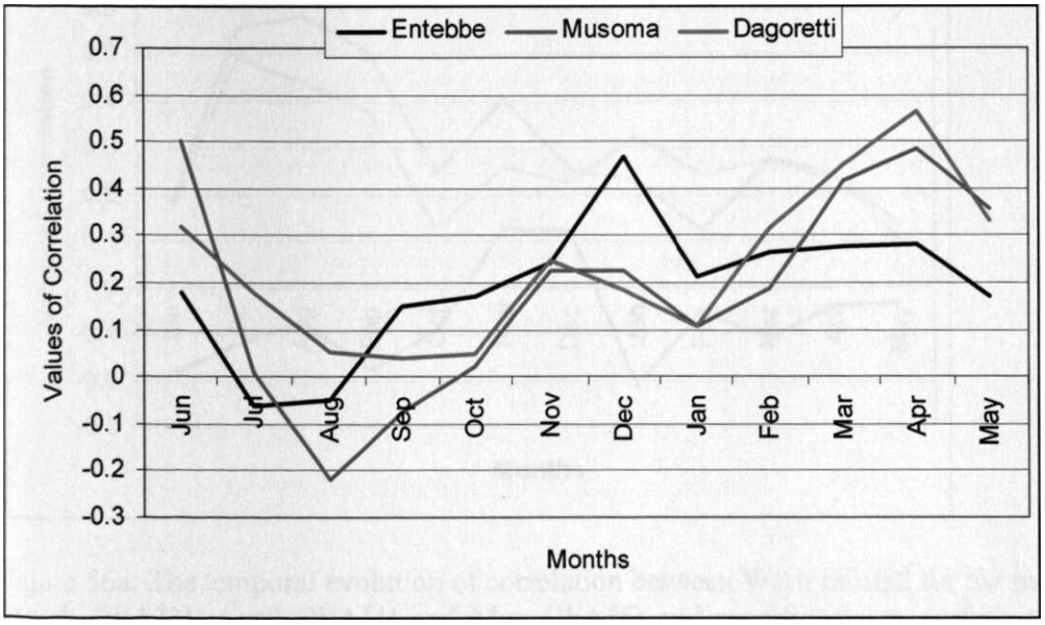

Figure 55: The temporal evolution of the correlation between March-May rainfall for Entebbe (EBBE), Musoma (MUS MAM), and Dagoretti, and meridional sea surface temperature gradient mode (I-J) for the Indian Ocean

The use of DJF proceeding the season, when the relationships with MAM rainfall and SST based predictors are weakest, leaves out predictors associated with the months when relationships are strongest. It should be recalled that Indeje and Semazzi (2000) observed the highest relationships between MAM seasonal rainfall and JJA QBO preceding the season. The factors that make relationships between MAM rainfall and SST based predictors weak are still not well understood. Previous studies have indicated that the differences in relationships between rainfall for the months making a season may influence relationships between the seasonal rainfall and predictors (Barnett and Preisendorfer 1987).

Figures 56a and 56b indicate marked differences in the evolution, signs and values of correlation between rainfall for the months of March, April and May, and the various SST gradient modes, which may affect the relationships observed with the MAM seasonal rainfall. The only months that have similar evolution and sign of relationships are April and May. More work need to be done to establish if these differences are associated with the weak prediction signals observed with this season.

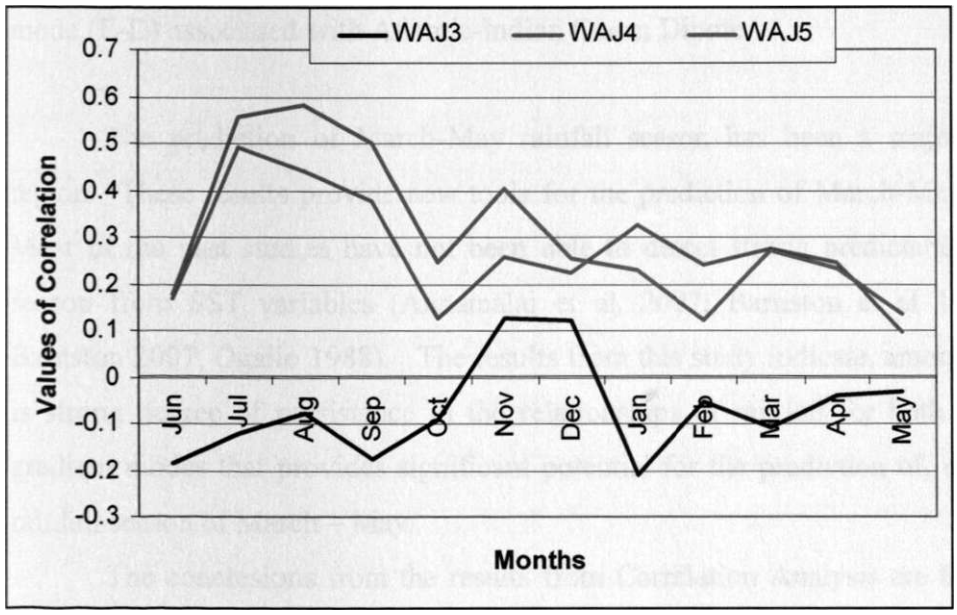

Figure 56a: The temporal evolution of correlation between Wajir rainfall for the months of March (WAJ3), April (WAJ4) and May (WAJ5) and meridional sea surface temperature gradient mode (G-K) for the Atlantic Ocean.

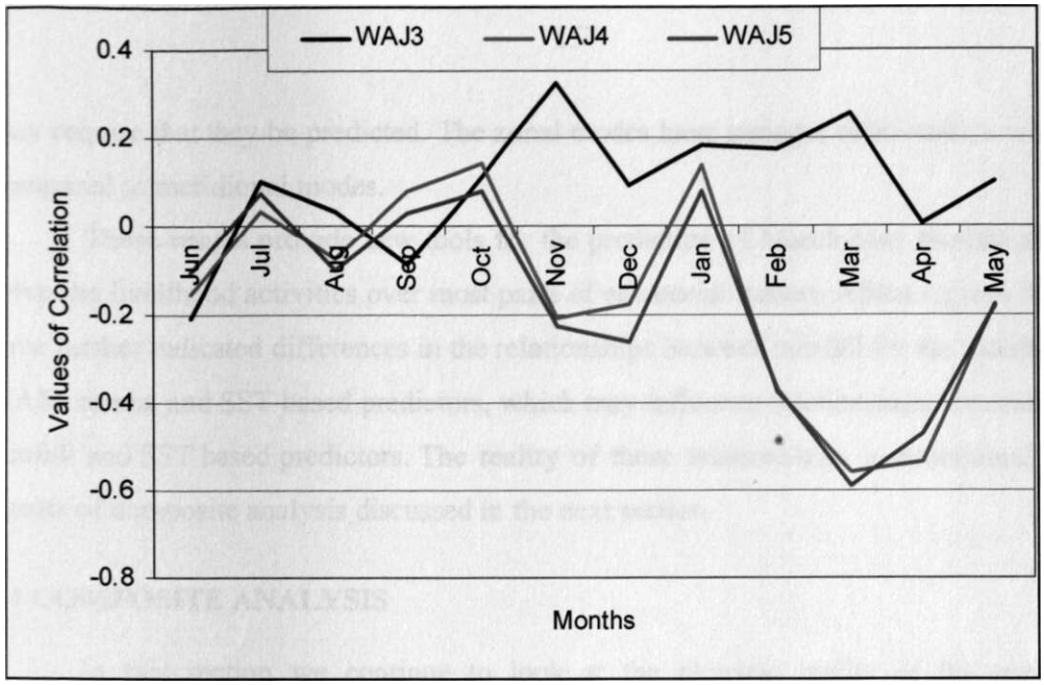

Figure 56b: The temporal evolution of correlation between Wajir rainfall for the months of March (WAJ3), April (WAJ4) and May (WAJ5), and zonal sea surface temperature gradient mode (E-D) associated with Atlantic-Indian Ocean Dipole.

The prediction of March-May rainfall season has been a major challenge in the region. These results provide new tools for the prediction of March-May seasonal rainfall. Most of the past studies have not been able to detect strong predictability signals for the season from SST variables (Annamalai et al. 2007; Barnston et al 1996; Korecha and Barnston 2007; Ogallo 1988). The results from this study indicate, among others, that there is strong degree of persistence in the relationships of rainfall for both seasons with SST gradient modes that provides significant potential for the prediction of, especially the main rainfall season of March - May.

The conclusions from the results from Correlation Analysis are that the use of SST gradient modes as predictors has advantage over grid point sea surface temperatures and Principal Component Analysis modes, and has the potential to improve seasonal rainfall forecasts especially for the March-May season. The September-December rainfall continues to have higher potential of predictability than March-May. The predictors from the Atlantic and Pacific Oceans have longer lead-time than those associated with the Indian Ocean, which achieve peak relationships within the seasons. The use of predictors from the Indian Ocean

may require that they be predicted. The zonal modes have stronger relationships with rainfall compared to meridional modes.

These results provide new tools for the prediction of March-May rainfall season that drive the livelihood activities over most parts of equatorial eastern Africa region. The results have further indicated differences in the relationships between rainfall for the months making MAM season and SST based predictors, which may influence relationships between seasonal rainfall and SST based predictors. The reality of these relationships is established from the results of composite analysis discussed in the next section.

4.4 COMPOSITE ANALYSIS

In this section we continue to look at the physical reality of the results from correlation analysis using composite analysis. Details of Composite analysis were presented in section 3.3.7. The composite analysis involves the choice of a basis for developing composites and selection of cases that meet specific categories of the decided base. The selected cases are then averaged to set a mean pattern of the element in response to the phases of the selected base (Drbohlav et al. 2007; Kayano et al. 2007; Krishnamurthy and Shukla 2007; Nobre and Shukla 1996). The basis of composite analysis in this study was mapping mean rainfall, wind and OLR anomalies for years of similar sea surface temperature gradients (SSTG) values for specific seasons. The categories for composite analysis are the extreme negative (EN) referring to values of SSTG <-a/2, moderate negative (MN) referring to values -a/2< SSTG<0, moderate positive (MP) referring to 0< SSTG < a/2 and extreme positive (EP) referring to SSTG >cr/2. In the next section the results from composite analysis of SOND rainfall and SSTG modes are discussed.

4.4.1 SEPTEMBER-DECEMBER RAINFALL AND SEA SURFACE TEMPERATURES GRADIENT MODES

The years with similar gradient categories on which the composite analysis of SOND was based are given in Tables 17a and 17b.

Figures 57 - 59 gives the spatial patterns of the values of the composites of SOND rainfall anomalies associated with the various categories of the gradient modes. The clear shifts in the signs of the rainfall anomalies map patterns for extremely positive and negative

values of the gradient modes are quite evident. For example, Figures 57a and 57b indicates that the SOND rainfall composite anomalies associated with the positive/negative phases of ZAF SST gradient mode were negative/posistive. This spatial pattern of SOND rainfall composite anomalies indicates that the positive/negative phases of ZAF SST gradient mode favour deficient/enhanced SOND rainfall over most parts of the region. This is in agreement with the negative correlation observed between ZAF SST gradient mode and SOND rainfall.

Table 17a: The years during the period 1961 to 2006 associated with the various categories of the phases of the zonal sea surface temperature gradient modes.

GRADIENT	EXN	EXP
	SSTG A<cr/2	SSTG>a/2
ZAF (July)	1961, 1962,1967, 1972, 1975, 1976, 1983, 1982, 1992, 1997,	1963, 1964, 1966, 1973, 1979, 1984, 1985, 1986, 1987, 1988, 1991, 1995, 1996 1998, 1999,,
! ZIND (September.)	1964, 1969, 1975, 1976, 1979, 1981, 1984, 1988, 1993, 1996, 1998, 1999,	1961,1962, 1963, 1965, 1966, 1967, 1972, 1978, 1982, 1994, 1997,

KEY: EXN-Extreme Negative, EXP- Extreme Positive

Table 17b: The years during the period 1961 to 2006 associated with the various categories of the phases of the meridional sea surface temperatures gradient modes.

! GRADIENT	EXN	EXP
	SSTG A<g/2	SSTG>a/2
MAB3(March)	1964, 1969, 1970, 1971, 1972, 1973, 1975, 1984, 1986, 1988, 1990, 1993, 1996,	1961, 1966, 1967, 1968, 1977, 1980, 1981, 1982, 1983, 1985, 1992, 1995,1997, 1998, 1999,
MAB3(April)	969, 1972,1973, 1974, 1979 1986, 1990, ,1 , 1991,	1961, 1967,1968, 1978, 1981, 1982, 1983, 1992, 1995, 1998, 1997,1999,
MAB6(May)	1962,1963, 1969, 1971, 1972, 1973, 1974, 1984, 1988, 1991,1993, 1994, 1996,	1961, 1964,1965, 1967,1968, 1970, 1977, 1978, 1980, 1982, 1983,, 1992, 1995, 1997, 1999,

KEY: EXN-Extreme Negative, EXP- Extreme Positive

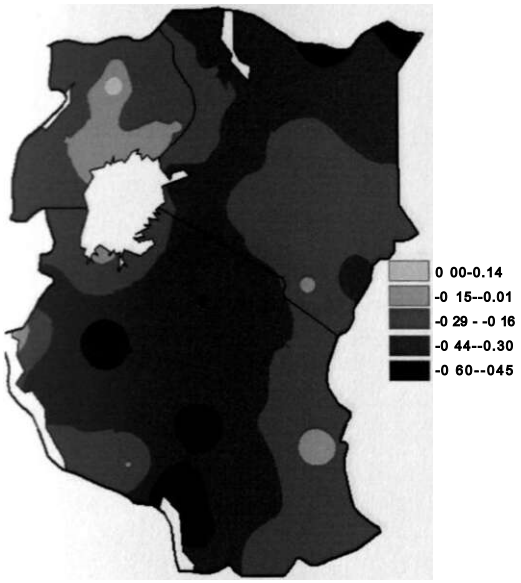

Figure 57a

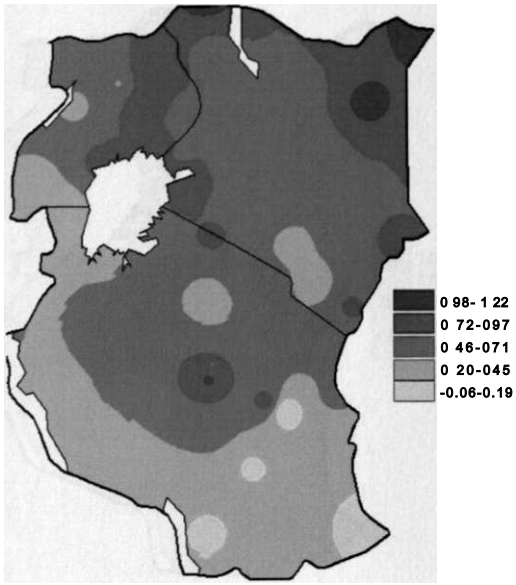

Figure 57b

Figure 57: The spatial patterns of the values of composite of September-December rainfall anomalies associated with extreme (a) negative (b) positive categories of zonal sea surface temperature gradient mode based on Atlantic-Indian Ocean Dipole for the month of July.

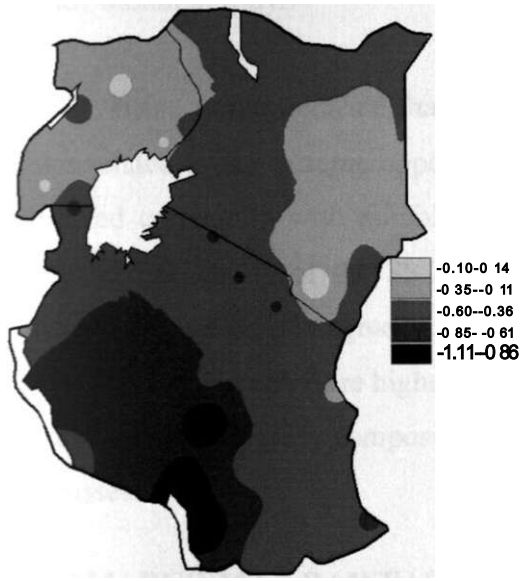

Figure 58a

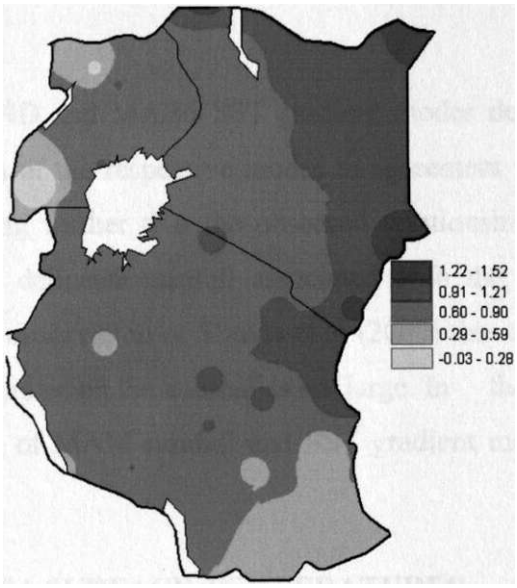

Figure 58b

Figure 58: The spatial patterns of the values of the composite of September-December rainfall anomalies associated with extreme (a) negative (b) positive categories of the zonal sea surface temperature gradient mode based on Indian Ocean Dipole for the month of September.

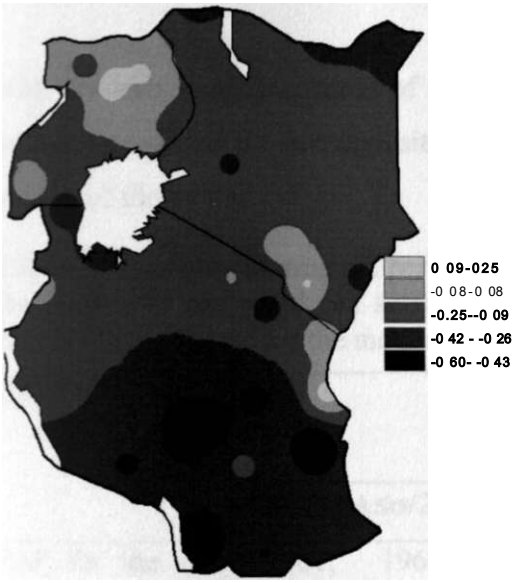

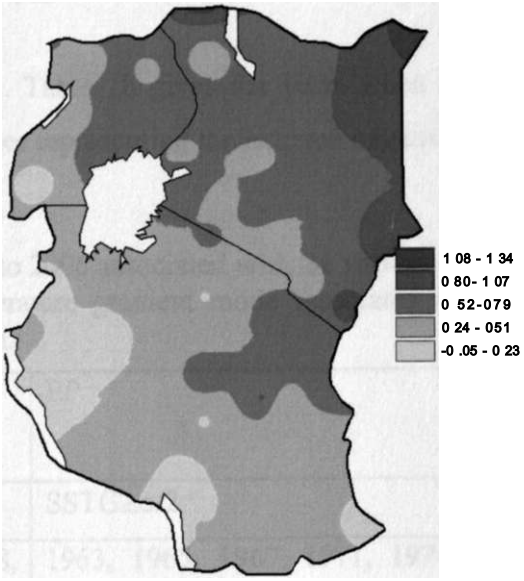

Figure 59a Figure 59b

Figure 59: The spatial patterns of the values of the composite of September-December rainfall anomalies associated with extreme (a) negative (b) positive categories of meridional sea surface temperature gradient mode based on interhemispheric dipole in the Atlantic ocean for the month of May.

These results indicate that ZAF, ZIND and MAB6 SST gradient modes delineated cases related to the extreme opposite phases of the respective modes in agreement with the observed correlation with rainfall confirming further that the observed relationships were realistic. The ability of the SST modes to delineate rainfall associated with the extreme opposite categories is in agreement with the observation of Shukla et al (2000) that the skills of models based on SST are higher in the years when the anomalies are large. In the next section the results from composite analysis of MAM rainfall and SST gradient modes are discussed.

4.4.2 MARCH-MAY RAINFALL AND SEA SURFACE TEMPERATURES GRADIENT MODES

The only mode that had significant relationships with MAM rainfall at most locations was ZAF SSTG. The composite analysis is used to confirm the reality of correlations by examining the capability of this SST gradient mode to delineate rainfall variability associated

with the two opposite phases of the mode. Table 18 gives the years when the ZAF SST gradient mode had the two opposite categories representing the extreme negative and positive phases of the mode.

Table 18: The years during the period 1961 to 2006 associated with the various categories of the phases of the zonal sea surface temperature gradient mode associated with Atlantic-Indian Ocean Dipole for the month of March.

! GRADIENT	EN	EP
	SSTG A<a/2	SSTG>a/2
ZAF for the zero-lagged month of March	1961, 1962, 1968, 1970, 1972, 1978, 1981, 1990, 2001	1963, 1965, 1967, 1971, 1974, 1975, 1982, 1984, 1988, 1989, 1991, 1993, 1994, 1995, 1996, 1999, 2000, 2003, 2004, 2005,

Figure 60 gives the spatial patterns of the values of composites of MAM rainfall anomalies associated with the extreme negative and positive categories of ZAF SST gradient mode for the zero-lagged month of March. Figure 60a indicates that the MAM rainfall composites associated with the extreme negative values of the zero-lagged ZAF SST gradient mode for the month of March were positive over most parts of the region indicating that the extreme negative phase of this mode favour enhanced MAM rainfall over most parts of the region.

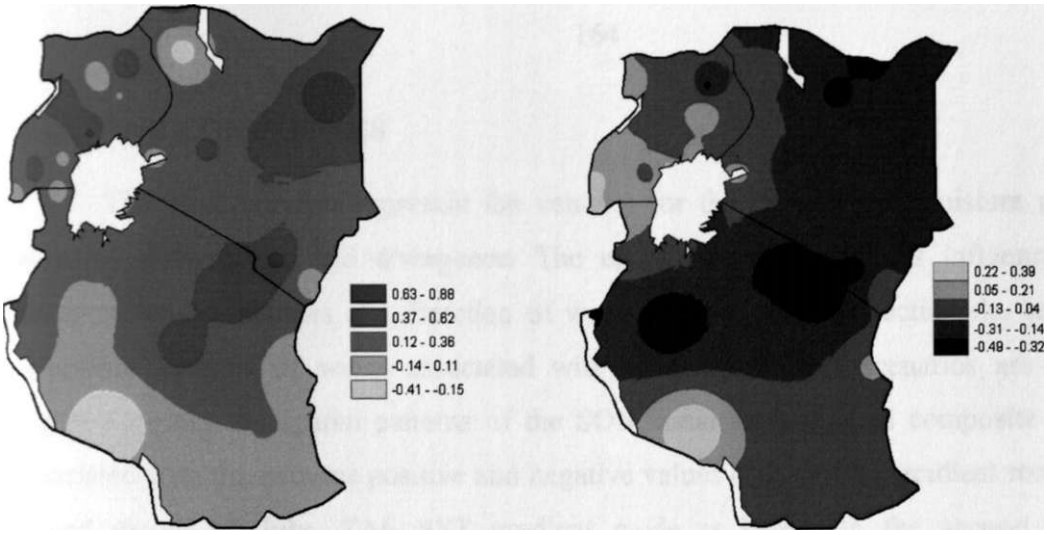

Figure 60a Figure 60b

Figure 60: The spatial patterns of the values of the composite of March-May rainfall anomalies associated with extreme (a) negative (b) positivecategories of zonal sea surface temperature gradient mode associated with the Atlantic-Indian Ocean Dipole for the month of March.

Figures 60b indicate that MAM rainfall associated with the extreme positive values of the zero-lagged ZAF SST gradient mode for the month of March were negative over most parts of the region indicating that the extreme positive phase of this mode favour deficient MAM rainfall over most parts of the region. These results from composite analysis of MAM rainfall and ZAF SST gradient mode for the zero-lagged month of March indicates further that the correlations observed between MAM rainfall and ZAF SST gradient mode were realistic since the mode was able to delineate cases associated with each phase. These results also indicate that ZAF SST gradient mode could be useful in the monitoring and prediction of MAM seasonal rainfall. However, since the peak relationship is achieved in the season, the use of this gradient requires that it be predicted.

The results of composite analysis of seasonal rainfall and SST gradient modes have continued to indicate significant linkages omongst some of the extreme phases SSTG modes and rainfall PCA modes over the region and confirmed that the observed relationships between the seasonal rainfall and SST gradient modes were realistic. The modes provide useful tools for seasonal climate prediction. In the next section, the results of composite analysis of wind and SST gradient modes are discussed.

4.4.3 WIND COMPOSITES

The wind currents represent the vehicles for the transport of moisture and dictate areas of convergence and divergence. The climate of the region is influenced by the strengths, tracks, sources and direction of wind currents. In this section the results from composite analysis of winds associated with various gradients scenarios are discussed. Figure 61 gives the spatial patterns of the SON zonal surface wind composite anomalies associated with the extreme positive and negative values of ZAF SST gradient mode, for the lagged month of July. ZAF SST gradient mode is based on the second JJA PCA mode,representing Atlantic-Indian Ocean Dipole with opposite poles in equatorial eastern Atlantic and western Indian Ocean.

Figure 61a indicates that the extreme negative values of ZAF SST gradient mode are associated with westerly wind anomaly over the region 40°N-35°S, 20W-HOE and easterly wind anomaly in equatorial central Indian Ocean. This pattern may favour enhanced rainfall over the region through the influence of the penetration of the Congo air-mass that interacts with the dominant easterly wind current from the Indian Ocean. The largest values of the westerly and easterly anomaly were 0.6 and -1.4, respectively.

Figure 61b indicates that SON wind composite anomalies associated with the extreme positive values of ZAF SST gradient mode for the lagged month of July were dominated with easterly wind anomalies, which would be associated with the acceleration of surface wind speeds and divergence. In the equatorial Indian Ocean, the easterly anomalies are replaced by westerly anomalies, which would be associated with the deceleration of the easterlies over the ocean and reduced moisture incursion into the region. The highest westerly anomaly was 1.2 and easterly anomaly was -0.8.

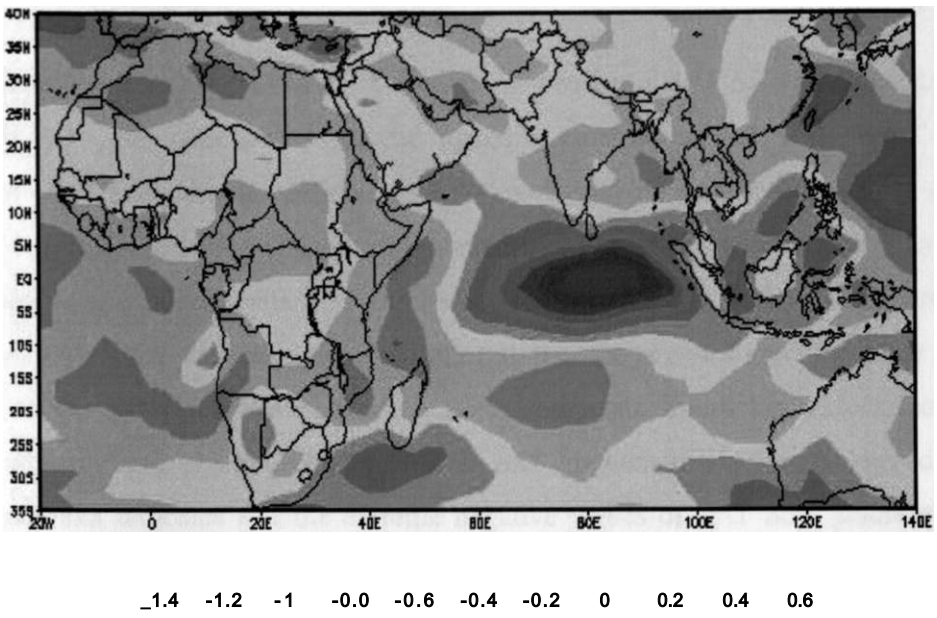

Figure 61a: The spatial patterns of surface zonal wind composites anomalies for the years when the zonal sea surface temperature gradient mode associated with the Atlantic-Indian Ocean Dipole for the month of July was extremely negative.

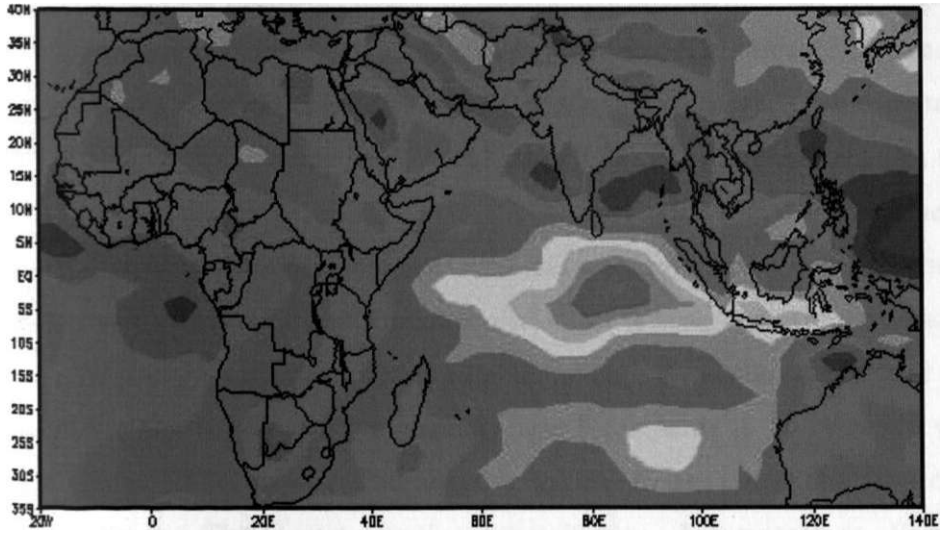

Figure 61b: The spatial patterns of surface zonal wind composites for the years when the zonal sea surface temperature gradient mode associated with the Atlantic-Indian Ocean Dipole for the month of July was extremely positive

These results indicate that the two extreme phases of ZAF SST gradient mode for the month of July are associated with the opposite patterns of the SON wind composite anomalies confirming that the influence of the mode may be associated with the changes in the wind currents, moisture transport and convergence. These results continue to confirm that the relationships observed with SST modes are realistic and the SSTG would provide new and realistic tools for predicting seasonal rainfall over the region.Figure 62 gives the spatial patterns of the SON meridional surface wind composite anomalies associated with the extreme negative and positive phases of ZAF SST gradient mode for the lagged month of July. Figure 62a indicates that the extreme negative values of ZAF SST gradient mode are associated with enhanced SON southerly surface winds over the southern and western Indian Ocean, and southeastern Atlantic Ocean. These are the major sources of moisture for the region. The enhanced meridional component in these areas would lead to improvements in the moisture incursion. The largest positive anomaly was 10. A negative anomaly was observed over the northern Atlantic. The negative anomaly would imply enhanced northerly flow associated with the Azores high-pressure system. The largest negative anomaly was -8.

Figure 62b indicates that the SON meridional surface wind composite anomalies associated with the extreme positive values of ZAF SST gradient mode for the lagged month of July were generally weaker than those associated with the extreme negative phase especially over the western Indian Ocean and were positive over the southern Indian Ocean and southern Atlantic Ocean. A marked difference is observed over the western Indian Ocean where the positive anomalies observed with the negative phase are replaced with the negative anomalies. The largest positive anomaly was 7 compared to 10 observed with the negative phase of the SSTG mode. The negative anomalies were still observed over the northern Atlantic Ocean. The largest negative anomaly was -4 compared to -8 observed with the negative phase.

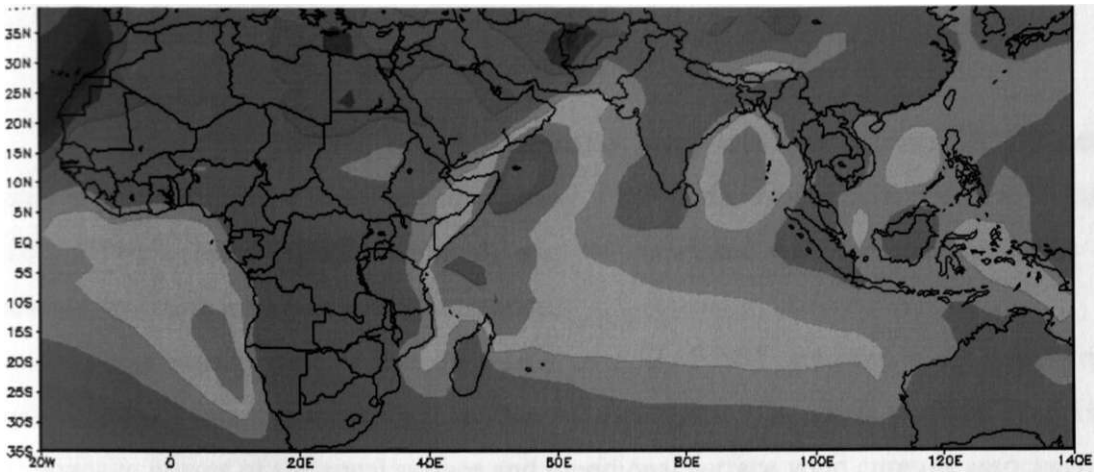

Figure 62a: The spatial patterns of surface meridional wind composites for the years when the zonal sea surface temperature gradient mode associated with the Atlantic-Indian Ocean Dipole mode for the month of July was extremely negative.

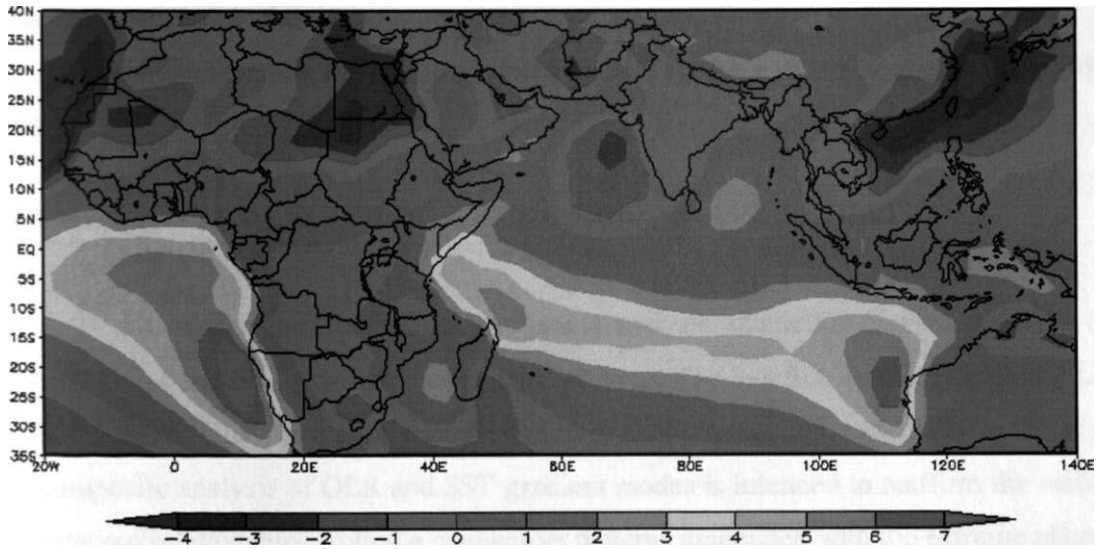

Figure 62b: The spatial patterns of surface meridional wind composites for the years when zonal sea surface gradient mode associated with Atlantic-Indian Ocean Dipole for the month of July was extremely positive.

It should be observed that the anomalies were relatively weaker for the extreme positive phase compared to the negative phase of the mode, these results continue to indicate that the influence of AIOD on rainfall may be associated with the changes in the wind currents, moisture transport and convergence.

These results indicate that the influence of ZAF SST gradient mode is discernable from both the zonal and meridional surface wind currents. The mode was able to delineate the opposite phases of the zonal surface and meridional surface wind currents associated with opposite phases of the mode. The results confirm further that the observed correlations between SOND rainfall and SST gradient modes are realistic and may be associated with the influence of the SSTG modes on atmospheric circulation, moisture transport and convergence. These results indicate further that the SSTG mode based on AIOD together with the other SSTG modes provide new and realistic tools for improving the prediction of seasonal rainfall over the region.

In the next section the results from composite analysis of SSTG modes and OLR are discussed.

4.4.4 SATELLITE DERIVED OUTGOING LONG-WAVE RADIATION COMPOSITES

In this section the results from composite analysis of satellite derived outgoing long-wave radiation and SST gradient modes are discussed. The Satellite Derived Outgoing Long-wave Radiation (OLR) is a good representation of deep convection, especially in the tropics. The composite analysis of OLR and SST gradient modes is intended to reaffirm the reality of the observed relationships from the convective patterns associated with the extreme phases of the modes.

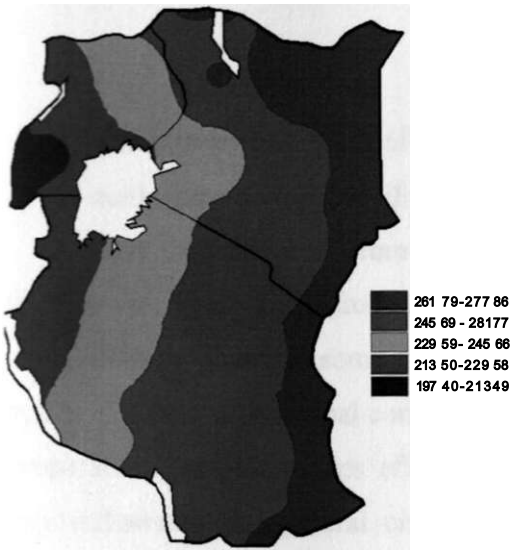

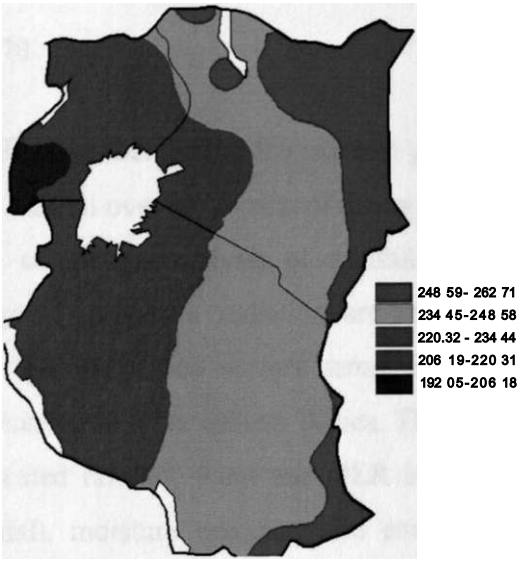

Figure 63 a Figure 63b

Figure 63: The spatial patterns of the composites of OLR for SOND season representing the years when zonal sea surface temperature gradient mode associated with the Indian Ocean Dipole was extremely (a) negative (b) positive.

The composite analysis of SOND rainfall and ZIND SST gradient mode for the zero-lagged month of September is used to demonstrate the influence of the SST gradient modes on the rainfall. It is important to note that ZIND SST gradient mode is developed on the same basis as IOD but centred along the equator. Figure 63 gives the spatial patterns of the values of SOND OLR composites associated with the extreme negative and positive values of ZIND SST gradient mode. It should be noted that OLR values <240 $WM"^{2}$ are associated with deep convection (Motell and Weare 1987). However, shallow layer clouds with OLR as high as 250 WM^{-2} could still give rainfall (Motell and Weare 1987). Figure 63a indicates that the OLR associated with the extreme negative values of ZIND SST gradient mode for the zero-lagged month of September (Table 10a) were >248WM^{-2} over most of eastern parts of the region that receive most of its rainfall from the shallow layer clouds and is dominated by relatively high values of OLR throughout the year (Nyakwada et al. 1992; WMO 1953). Most of the western parts of the region that receive most the rainfall from deep convective clouds have OLR<248 $WM"^{2}$. Figure 63b, indicates that the values of SOND OLR composites associated with the extreme positive values of ZIND SST gradient mode were

<248 WM ^{2} over most parts of the region indicating that during the extreme positive phase of this mode deep convective clouds dominate rainfall over most parts of the region.

The conclusions from results from composite analysis of rainfall, sea surface temperature, wind and satellite derived outgoing longwave radiation are that significant linkages exist amongst some of the extreme phases of sea surface temperature gradient modes and rainfall Principal component Analysis modes over eastern Africa. The sea surface temperature gradient modes effectively delineated rainfall, wind and OLR indicating that they influenced the general circulation, rainfall, moisture transport and convection, and confirming that the observed relationships were realistic. The sea surface temperature gradient mode associated with the equatorial western Indian and eastern Atlantic Oceans had the highest capability to delineate March-May rainfall while September-December rainfall could be delineated effectively by the zonal modes associated with both oceans and the Indian Ocean Dipole. These results continue to indicate that SSTG modes provide new tools to improve the predictability of seasonal ranfall especially the MAM season.

In the next section the results from regression analysis are discussed.

4.5 REGRESSION ANALYSIS

In this section the results from regression analysis of seasonal rainfall and SST gradient modes are discussed. The details of the regression analysis methods were presented in section 3.3.5 and the details of the SST gradient modes that were significantly correlated with rainfall over various parts of the region were presented in section 3.3.3. It should be noted that in all cases, the data for the period 1961-1990 was used for fitting and training the regression models, while the data for the period 1991-2006 was used to test the skill of regression models. The results for the individual seasons are presented separately in the following sections.

4.5.1 SEPTEMBER - DECEMBER RAINFALL AND SEA SURFACE TEMPERATURE GRADIENT MODES

In this section the results from regression analysis of September - December (SOND) rainfall and SST gradient (SSTG) modes are discussed. Only SSTG modes that had significant correlation with SOND rainfall were included in stepwise regression analyses. The regression models presented in this section include only cases where the various SSTG

modes accounted for over 50% of SOND rainfall variance. Regression results for the various regions as represented by individual stations based on principal component analysis (PCA) homogenous groupings are given in Table 19. It can be observed from Table 19 that, although there were significant variations of the skill of the models from region to region, as represented by the values of Heidke Skill Score (HSS), the HSS values were >0.20 at all locations indicating the models could provide forecasts with useful skills.

Figures 64a-64e give examples of time series plots of observed and model estimates of the SOND rainfall for stations representing some of the rainfall homogeneous zones. It is evident from Figures 64a- 64e that in general better model fits were observed during the training period of 1961-90 compared to the skill-testing period of 1991-2006. The results from the study also indicated that although the general direction of the extreme rainfall anomalies were discernible from the model forecast, the models generally over /under estimated rainfall anomalies at most locations. This requires some corrections to be made on the forecast before such regression forecasts can be used in the tercile type of forecast presentations that are commonly used in the National Meteorological/Hydrological Services (NMHSs) and regional climate centres for the presentation of seasonal rainfall outlooks. Mean standard errors were used to adjust the forecasts in this study by subtracting/adding to the overestimated/underestimated forecasts.

Table 19: Assessment of the skill of the September-December regression models

Zone	Station	HSS
1	Gulu	0.20
4	Lodwar	0.37
	Narok	0.41
5	Dagoretti	0.43
	Tororo	0.34
11	Mandera	0.43
12	Wajir	0.41
15	DIA	0.32
	Malindi	0.61

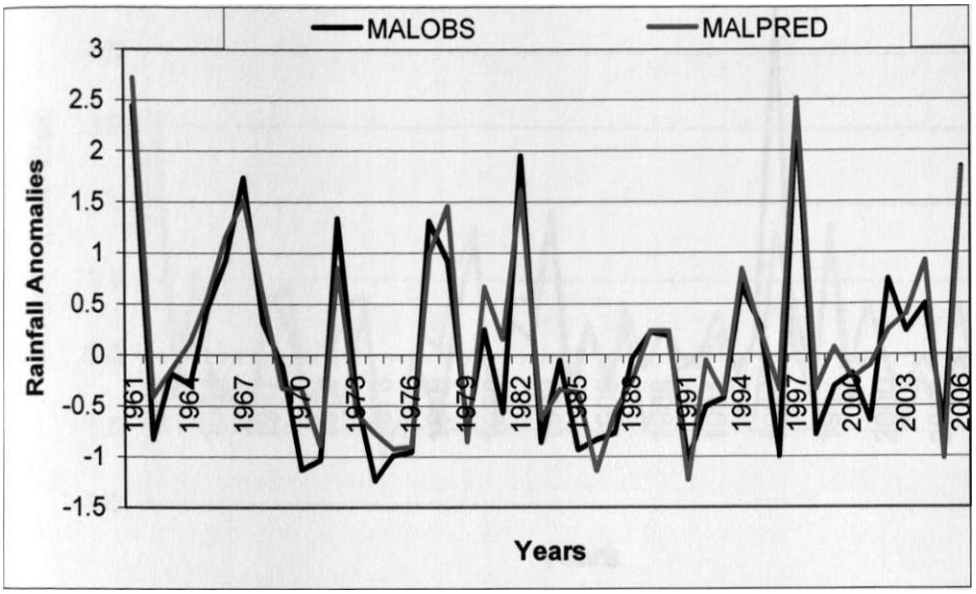

Figure 64a: The time series plot of the observed (MALOBS) and model estimates (MALPRED) of the Malindi September-December rainfall representing zone 17

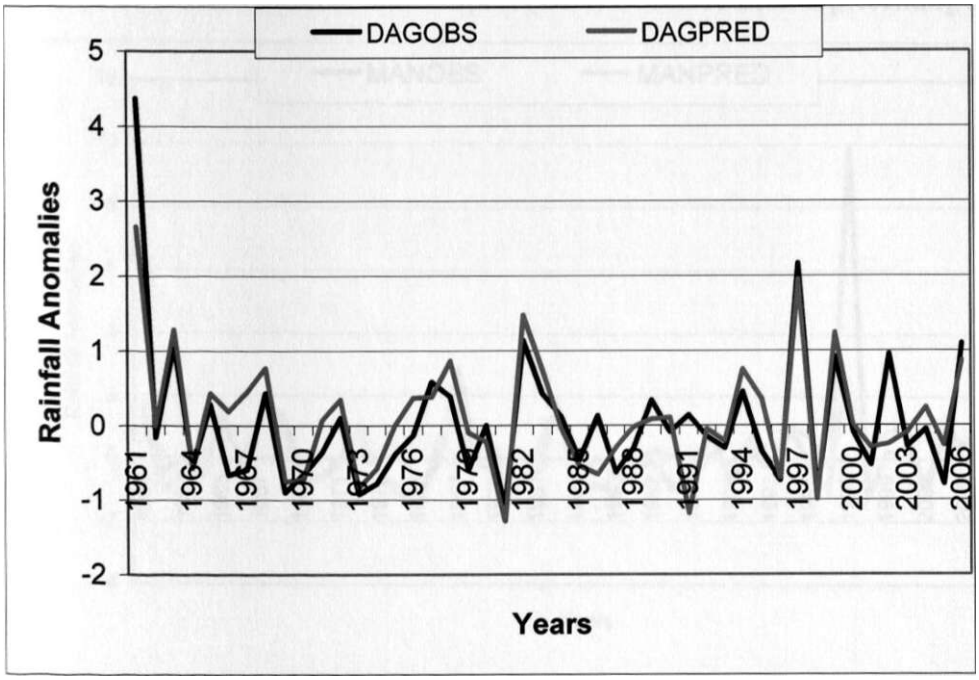

Figure 64b: The time series plot of the observed (DAGOBS) and model estimates (DAGPRED) of the Dagoretti September-December rainfall representing zone 5.

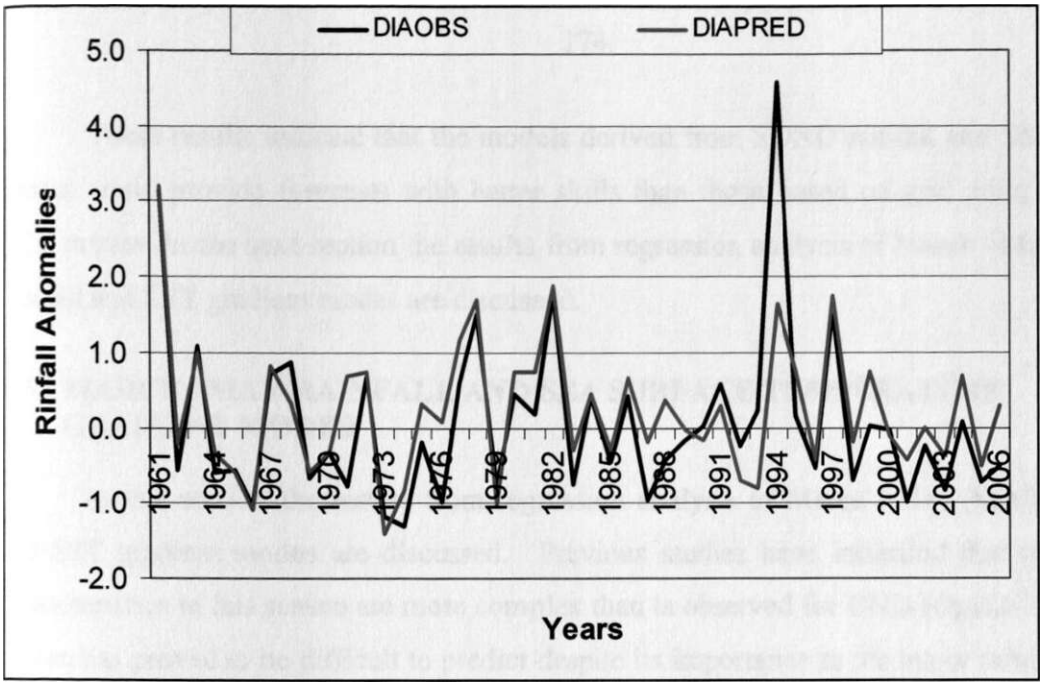

Figure 64c: The time series plot of the observed (DIAOBS) and model estimates (DIAPRED) of the Dar es Salaam International Airport (DIA) SOND rainfall representing zone 15.

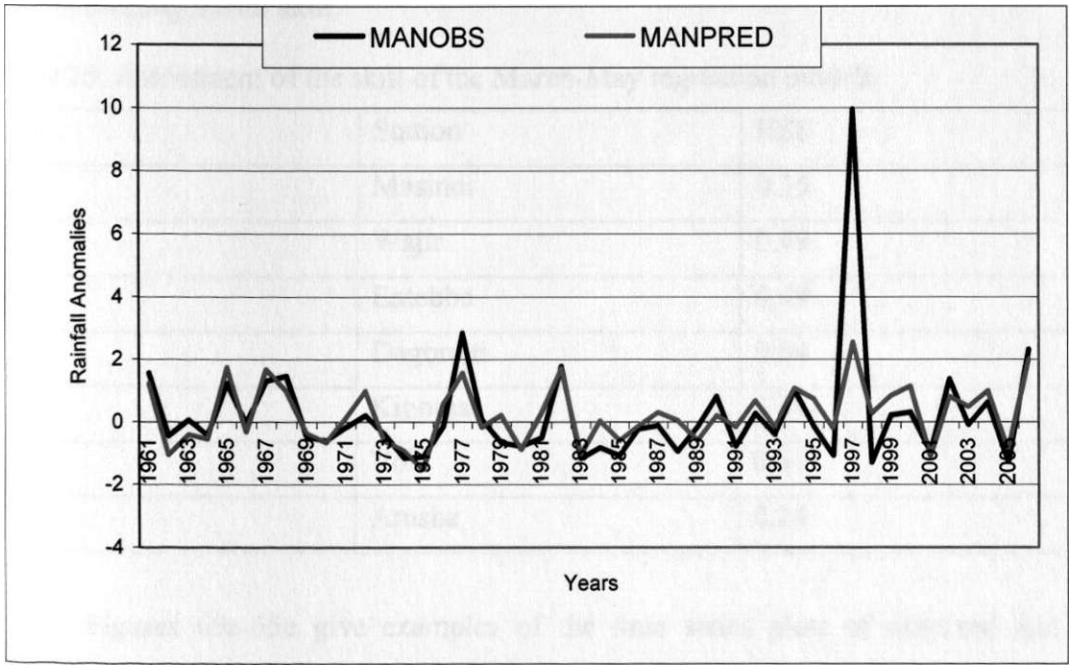

Figure 64d: The time series plot of the observed (MANOBS) and model estimates (MANPRED) of the Mandera September-December rainfall representing zone 11.

These results indicate that the models derived from SOND rainfall and SST gradient modes could provide forecasts with better skills than those based on grid point SSTs and PCA modes. In the next section the results from regression analysis of March -May (MAM) rainfall and SST gradient modes are discussed.

4.5.2 MARCH -MAY RAINFALL AND SEA SURFACE TEMPERATURE GRADIENT MODES

In this section the results from regression analysis of March -May (MAM) rainfall and SST gradient modes are discussed. Previous studies have indicated that the rainfall characteristics in this season are more complex than is observed for OND (Ogallo 1989). The season has proved to be difficult to predict despite its importance as the major rainfall season for the countries of the region. Table 20 gives the skills of some of the models observed with SST gradient modes. It can be observed that the HSS values for the models were >0.24indicating useful skill.

Table 20: Assessment of the skill of the March-May regression models

Zone	Station	HSS
3	Masindi	0.35
7	Wajir	0.49
11	Entebbe	0.49
14	Dagoretti	0.64
17	Kigoma	0.41
19	Voi	0.51
19	Arusha	0.24

Figures 65a-65e give examples of the time series plots of observed and model estimates of the MAM rainfall for the stations representing some of the rainfall homogeneous zones. As was the case for SOND rainfall, discussed in the previous section, the model fitting in the training period of 1961-90 was better than for the skill-testing period of 1991-2005.

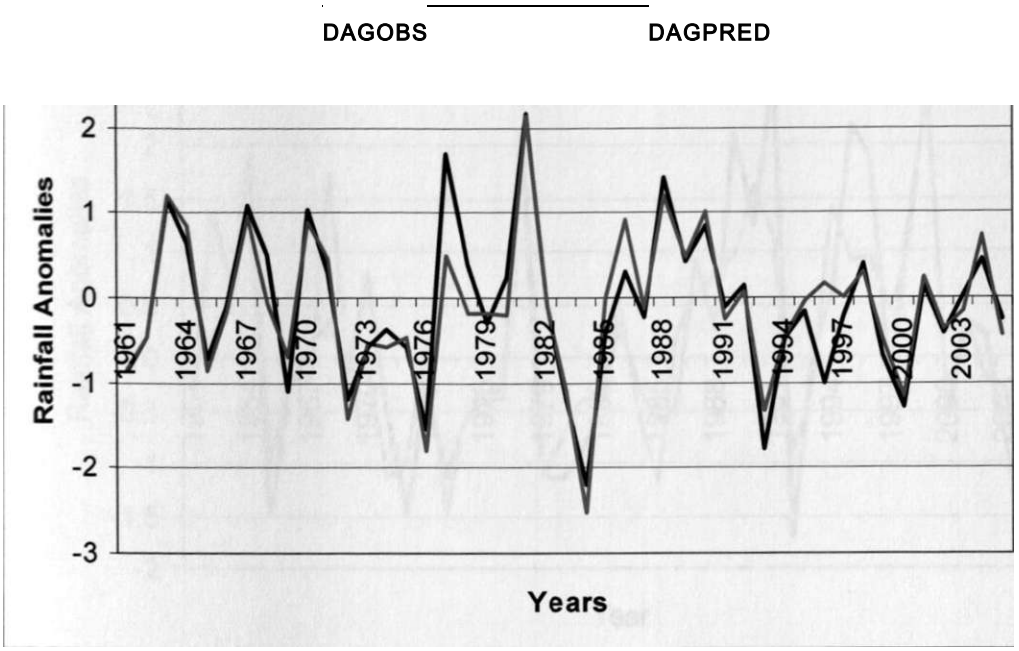

Figure 65a: The time series plot of the observed (DAGOBS) and model estimates (DAGPRED) of the Dagoretti March -May rainfall representing zone 14

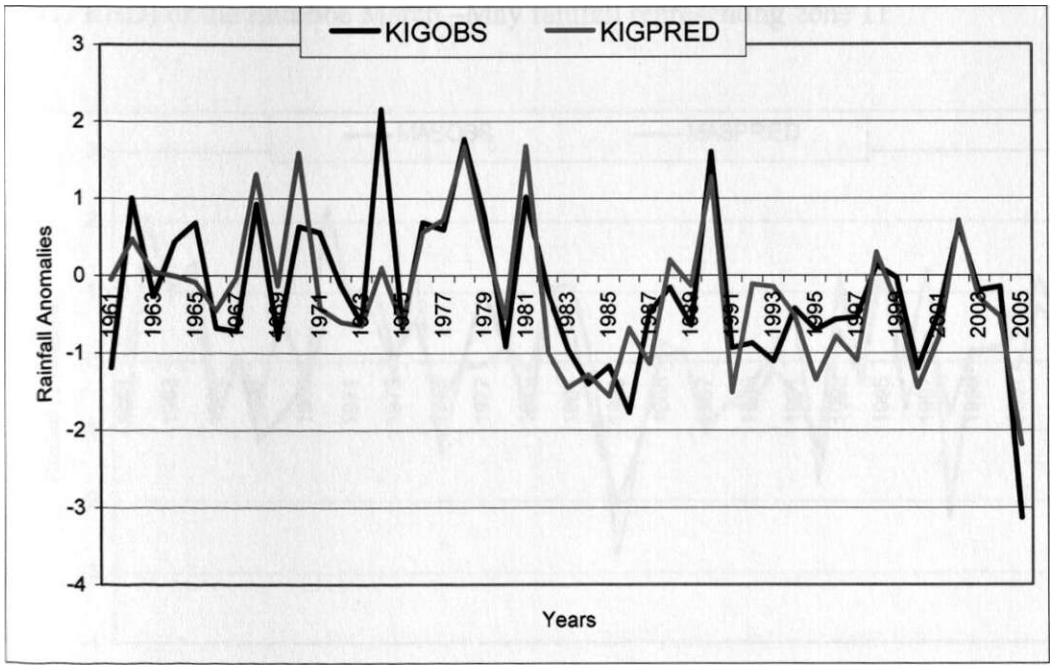

Figure 65b: The time series plot of the observed (KIGOBS) and model estimates (KIGPRED) of the Kigoma March -May rainfall representing zone 17.

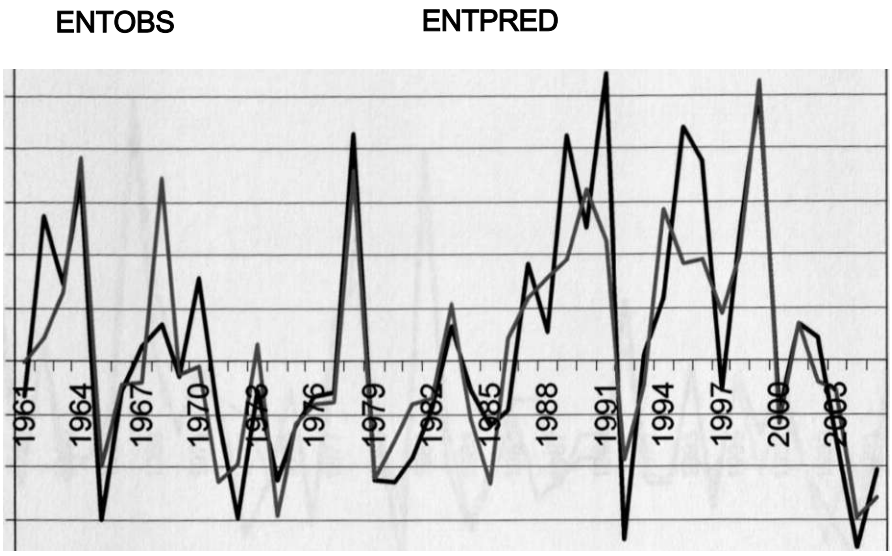

Figure 65c: The time series plot of the observed (ENTOBS) and model estimates (ENTPRED) of the Entebbe March -May rainfall representing zone 11

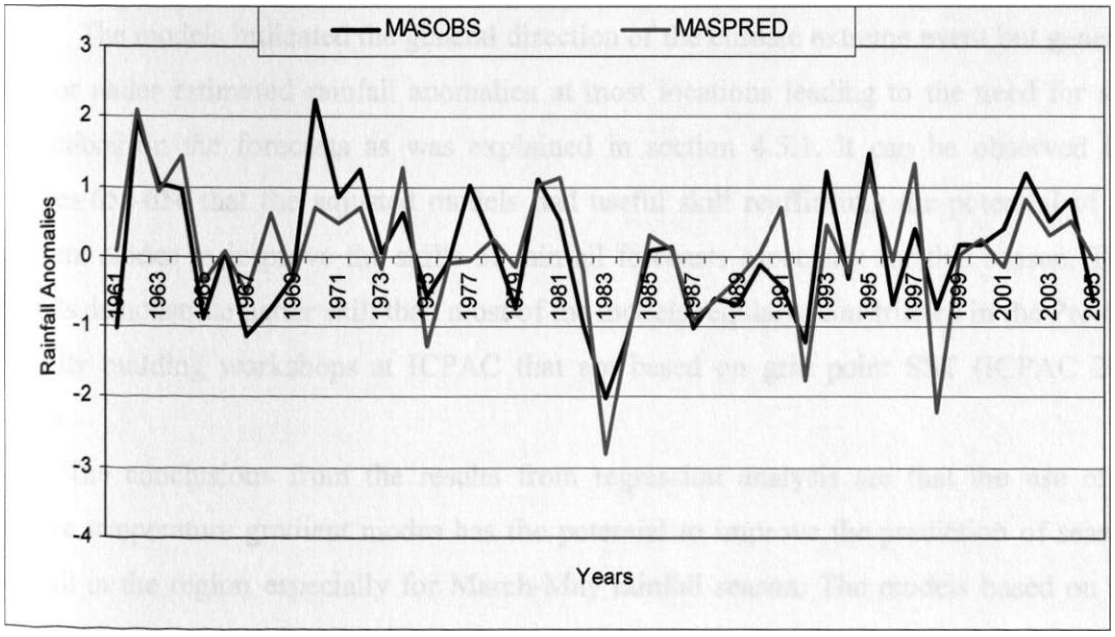

Figure 65d: The time series plot of the observed (MASOBS) and model estimates (MASPRED) of the Masindi March -May rainfall representing zone 3

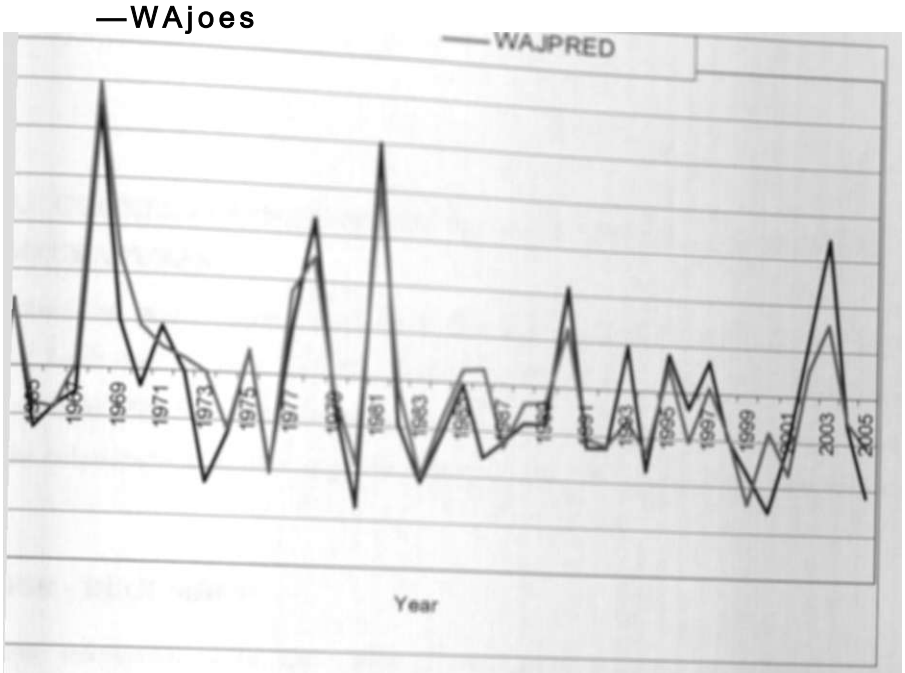

e time series plot of the observed (WAJOBS) and model estimates
he Wajir March –May rainfall representing zone 7

:!s indicated the general direction of the climate extreme event but generally itimated rainfall anomalies at most locations leading to the need for some he forecasts as was **explained in section 4 5.1 It can be observed from that the adjusted models had useful skill reaffirming the potential of SST to improve the skills of rainfall forecasts especially for this season. These ate better skill than most of the models regularly constructed in the Prc-COF g workshops at ICPAC that are based on grid point SST (ICPAC 2006;**

usions from the results from regression analysis arc that the use of sea ure gradient modes has the potential to improve the prediction of seasonal gion especially for March-May rainfall season. The models based on SST showed marked improvements both in the training and model skill-testing improvements were also observed for the SOND rainfall season. In the next ts from canonical correlation analysis are discussed

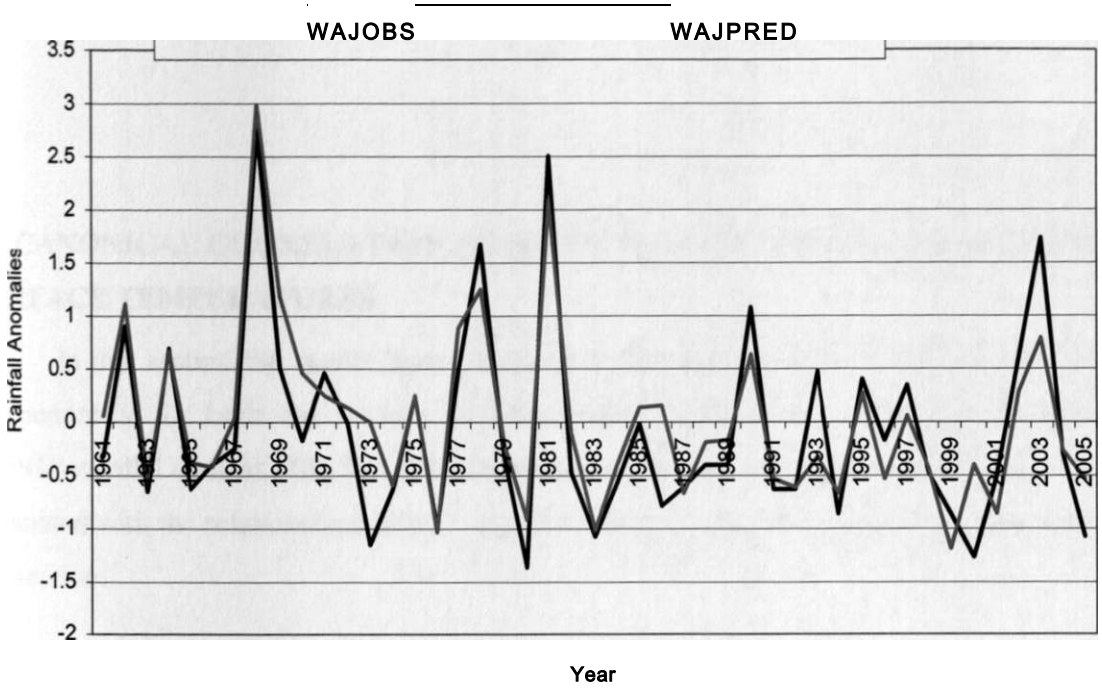

Figure 65e: The time series plot of the observed (WAJOBS) and model estimates (WAJPRED) of the Wajir March - May rainfall representing zone 7

The models indicated the general direction of the climate extreme event but generally over or under estimated rainfall anomalies at most locations leading to the need for some corrections on the forecasts as was explained in section 4.5.1. It can be observed from Figures 65a-65e that the adjusted models had useful skill reaffirming the potential of SST gradient modes to improve the skills of rainfall forecasts especially for this season. These models demonstrate better skill than most of the models regularly constructed in the Pre-COF capacity building workshops at ICPAC that are based on grid point SST (ICPAC 2006; 2008).

The conclusions from the results from regression analysis are that the use of sea surface temperature gradient modes has the potential to improve the prediction of seasonal rainfall in the region especially for March-May rainfall season. The models based on SST gradient modes showed marked improvements both in the training and model skill-testing periods. Marked improvements were also observed for the SOND rainfall season. In the next section, the results from canonical correlation analysis are discussed.

4.6 CANONICAL CORRELATION ANALYSIS SEASONAL RAINFALL AND SEA SURFACE TEMPERATURES

In this section the results from Canonical Correlation Analysis (CCA) are discussed independently for both the seasons of March-May (MAM) and September -December (SOND) rainfall seasons. The first few canonical patterns always extract most of the variance associated with the relationships. Hence only the first two canonical patterns are presented in this section.

4.6.1 SEPTEMBER - DECEMBER

The results associated with the pairs of canonical patterns representing the relationships between September-December (SOND) rainfall and SSTs for the June-August (JJA) and September-November (SON) are presented in this section. The first two canonical patterns associated with the influence of JJA SST on SOND rainfall are presented in Figures 66a and 66b. The first canonical pattern of SOND rainfall had negative loadings over the whole region as presented in Figure 66a and represented the influence of second JJA SST PCA modes for both oceans associated with the IOD and interhemispheric dipole in the Atlantic Ocean discussed in section 4.2. This canonical pattern, which had a canonical correlation of 0.86 with the first JJA SST canonical pattern (Figure 66b), was associated with negative loadings over the western Indian Ocean and northern-southern tropical Atlantic Ocean together with positive loadings over the eastern Indian Ocean and the northern and farther southern Atlantic Ocean.

This canonical pattern indicated that the warming over the western Indian Ocean and northern-southern Atlantic Ocean together with the cooling over eastern Indian Ocean, and northern and the farther southern Atlantic Ocean is associated with enhanced rainfall over most parts of the region in agreement with the influence of IOD, which has been documented by many authors including Behera et al.(2005); Clark et al(2003); Owiti (2005); Saji et al.(1999); Singhrattna et al (2005); Webster et al.(1999); and Yu and Riennecker(2000) among others. The positive phase of IOD has been associated with enhanced rainfall over most parts of the region (Black et al. 2003; Hastenrath and Polzin 2004; Owiti 2005). The

association between SOND rainfall and the SST over the Atlantic Ocean has not been well documented with some authors indicating the ocean to have minimal influence on the regional seasonal rainfall (Goddard and Graham 1999). The influence from the Atlantic Ocean may be associated with the Interhemispheric dipole which has been observed to influence rainfall in the neighbouring regions and beyond (Clark et al 2003; Firth et al 2005; Hu and Huang 2006; Kushnir et al. 2006; Moura and Shukla 1981; Nagura and Konda 2007; Ogallo 1988a; Okoola 1996; Omondi 2005; Owiti 2005; Rasmusson and Carpenter 1982; Sutton and Hodson 2007). The warming over the northern southern Atlantic and the cooling to the north and farther southern Atlantic Ocean is suitable for the strengthening of trade winds in both hemispheres which may improve the incursions of westerly wind currents into the region which has been associated with enhanced SOND rainfall during IOD and ENSO events (Indeje 2000; Schreck and Semazzi 2004).

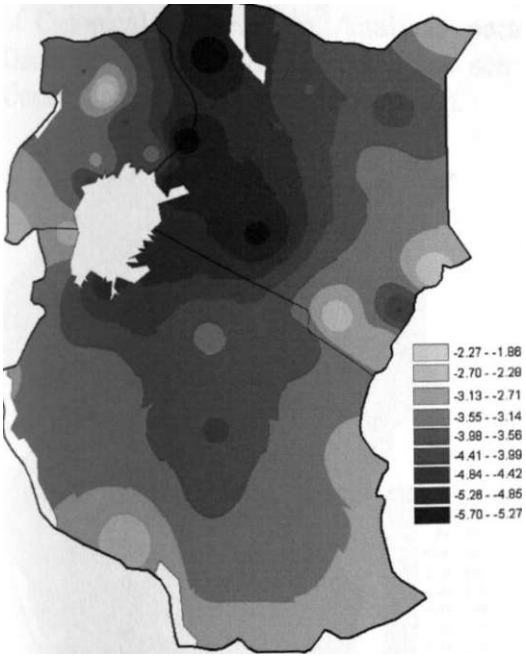

Figure 66a: The first canonical pattern of September-December rainfall representing association with the second June-August sea surface temperature canonical pattern for the joint Indian-Atlantic Ocean.

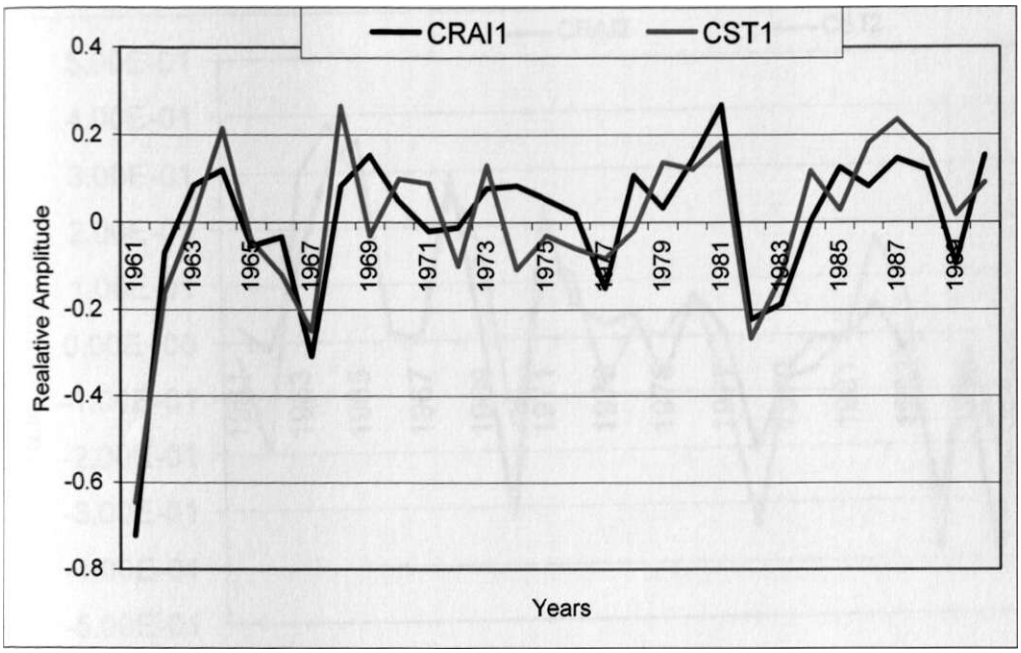

Figure 66b: The graphical plot of the normalized temporal functions (u and v) of the first pair of Canonical Correlation Analysis patterns representing association between September-December rainfall and June-August sea surface temperature for the joint Indian-Atlantic Ocean (Canonical correlation= 0.86).

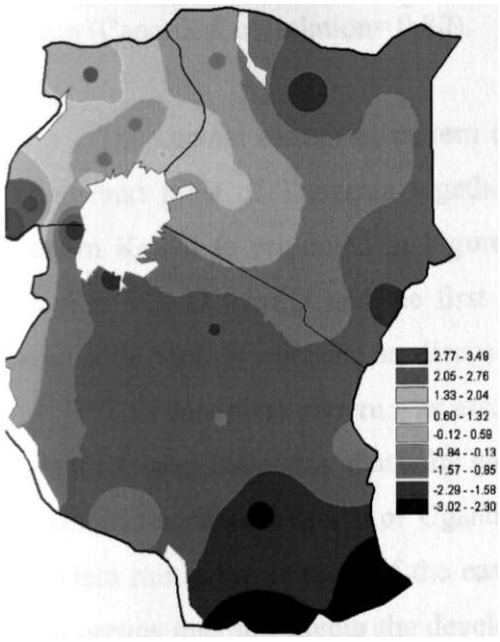

Figure 67a: The second canonical pattern of September-December rainfall representing association with the second June-August sea surface temperature canonical pattern for the joint Indian-Atlantic Ocean.

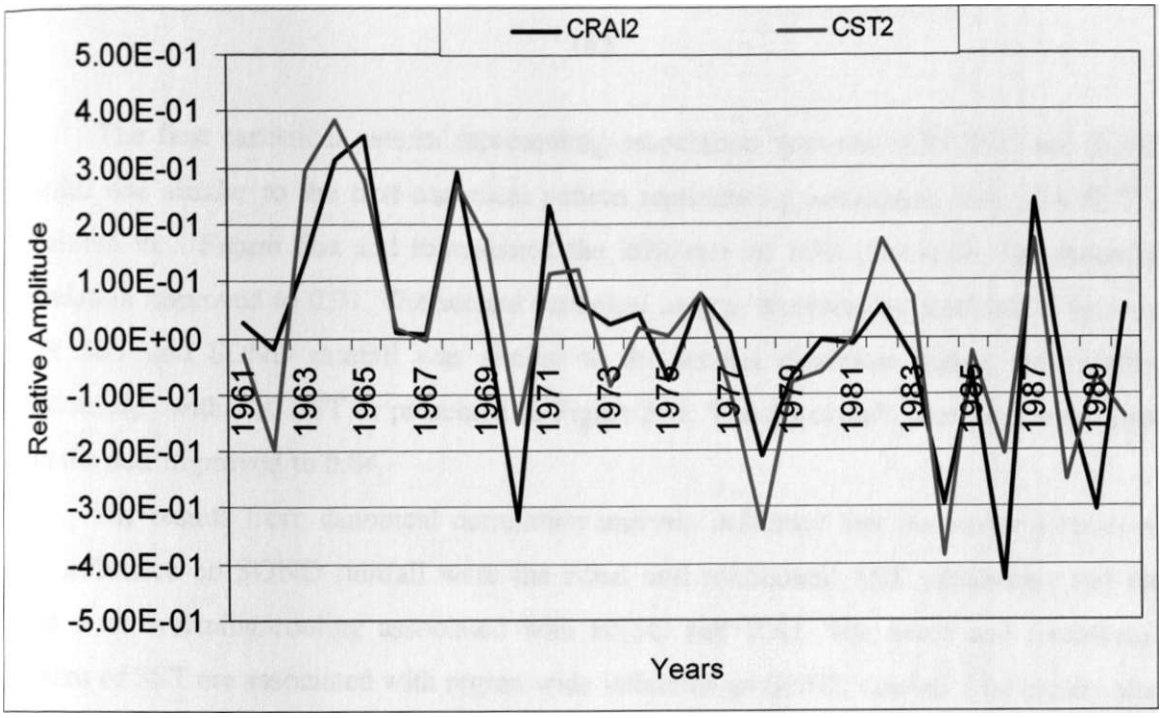

Figure 67b: The graphical plot of the normalized temporal functions (u and v) of the second pair of Canonical Correlation Analysis patterns representing association between September-Decemberrainfall and June-August sea surface temperaturefor the joint Indian-Atlantic Ocean (Canonical correlation= 0.80).

The second canonical pattern of SOND rainfall had negative loadings over eastern Kenya and most of Tanzania together with positive loadings over most of Uganda and western Kenya as presented in Figure 66a. This canonical pattern represented association between SOND rainfall and the first JJA PCA modes for both oceans, which represented basin wide cooling/warming as, discussed in section 4.3.

This canonical pattern was associated with positive loadings over both the Indian and Atlantic Ocean indicating that the basin wide warming over both oceans is associated with enhanced rainfall over most of Uganda, western Kenya and extreme western Tanzania, and deficient rainfall over most of the eastern Kenya and most of Tanzania. The warming over both oceans may not favour the development of monsoon over the Indian Ocean that have a strong signature on the rainfall over the eastern parts of the region. The canonical correlation associated with this pair of canonical pattern was 0.80 indicating strong relationship (Figure 67b)..

The first canonical pattern representing association between SON SST and SOND rainfall was similar to the first canonical pattern representing association with JJA SST as presented in Figure 66a and represented the influence of IOD. However, the canonical correlation improved to 0.91. The second canonical pattern representing association between SON SST and SOND rainfall was similar to the second canonical pattern representing relationships with JJA SST as presented in Figure 66b. The canonical correlation associated with the pair improved to 0.84.

The results from canonical correlation analysis indicated that the major sources of SST influence on SOND rainfall were the zonal and meridional SST variability, and the basin wide warming/cooling associated with ENSO and IOD. The zonal and meridional patterns of SST are associated with region wide influence on SOND rainfall. The results also indicated strong associations between SST and SOND rainfall. The SST variability in the Atlantic and Indian Ocean are vital for the prediction of seasonal rainfall in the region. In the next section the results from canonical correlation of March-May (MAM) rainfall and SST are discussed.

4.6.2 MARCH-MAY

The results associated with the pairs of canonical patterns representing the relationships between March-May (MAM) rainfall and SSTs for December-February (DJF) and March-May (MAM) are discussed.The first two canonical patterns of MAM rainfall associated with the influence of the DJF SST are presented in Figures 68 and 69. The first canonical pattern of MAM rainfall had negative loadings over the northern parts of the region and positive loadings over the southern parts of Tanzania as presented in Figure 68a. This canonical pattern, which was associated with large negative loadings over most of the Indian and Atlantic Ocean together with weak positive loadings over the southeastern Indian Ocean, represented the influence of the first DJF SST PCA modes for individual oceans and the combined Indian-Atlantic Ocean discussed in section 4.3, that represented basin wide warming/cooling associated with ENSO events. The association represented by this canonical pattern indicates that the basin wide cooling/warming over the Atlantic and Indian Ocean is associated with deficient/enhanced rainfall over the northern parts of the region and enhanced/deficient rainfall over southern Tanzania.

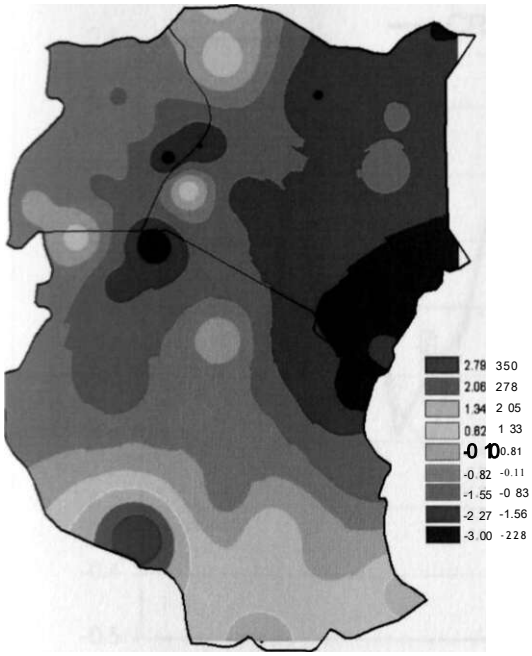

Figure 68a: The first canonical pattern of March-May rainfall representing association with the first December-February Sea Surface Temperature canonical pattern for the joint Indian-Atlantic Ocean.

This pattern of rainfall is often observed in MAM season following La Nina/El Nino ENSO event that sustain cool/warm conditions over both oceans beyond December. The canonical correlation associated with the pair was 0.85 (Figure 68b).

The second canonical pattern of MAM rainfall had positive loadings over most parts of the region together with negative loadings over the southeastern Tanzania as presented in Figure 69a and was associated with positive loadings over the northwestern Indian and northern Atlantic Oceans, and negative loadings over the northeastern Indian and southern Atlantic oceans. The influence from the the Atlantic Ocean is associated with second DJF SST PCA mode representing interhemispheric dipole while the influence from the Indian Ocean is associated with a zonal dipole similar to IOD with northward displacement. The influence of IOD and ENSO are often sustained beyond December and influence the following MAM rainfall season. The inter-hemispheric dipole over the Atlantic Ocean is well documented (Moura and Shukla 1981; Nobre and Shukla 1996).

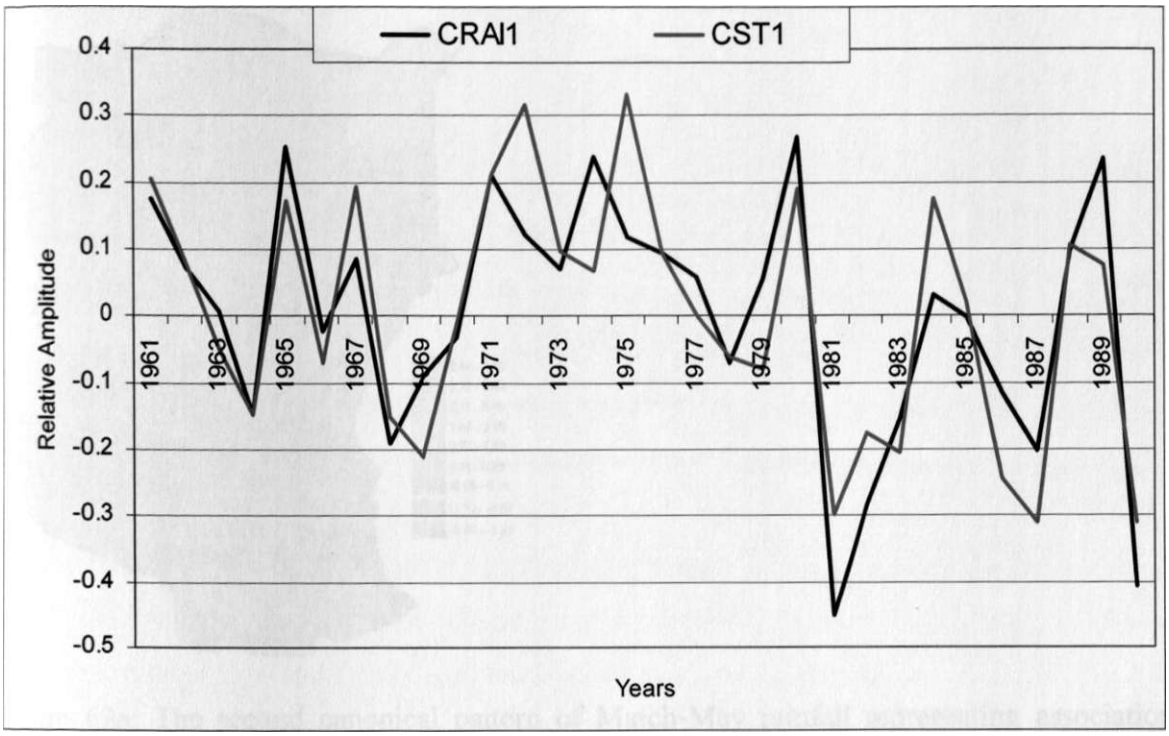

Figure 68b: The graphical plot of the normalized temporal functions (u and v) of the first pair of Canonical Correlation Analysis patterns representing association between March-May rainfall and December-February Sea Surface Temperature for the joint Indian-Atlantic Ocean (Canonical correlation = 0.85).

The association represented by the second canonical pattern representing association between MAM rainfall and DJF SST indicates that the warming over northwestern Indian Ocean and northern Atlantic together with the cooling over the northeastern Indian Ocean and southern Atlantic Ocean is associated with enhanced rainfall over the northern parts of the region and deficient rainfall over the southern parts of the region. This rainfall pattern is often associated with ENSO and IOD. The opposite phases of ENSO and IOD have opposite influences. The canonical correlation observed with this pair was 0.70 (Figure 69b).

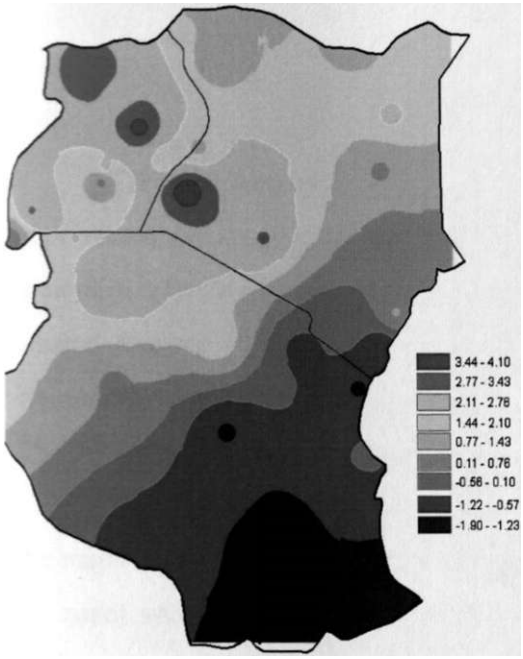

Figure 69a: The second canonical pattern of March-May rainfall representing association with the second December-February Sea Surface Temperature canonical pattern for the joint Indian-Atlantic Ocean.

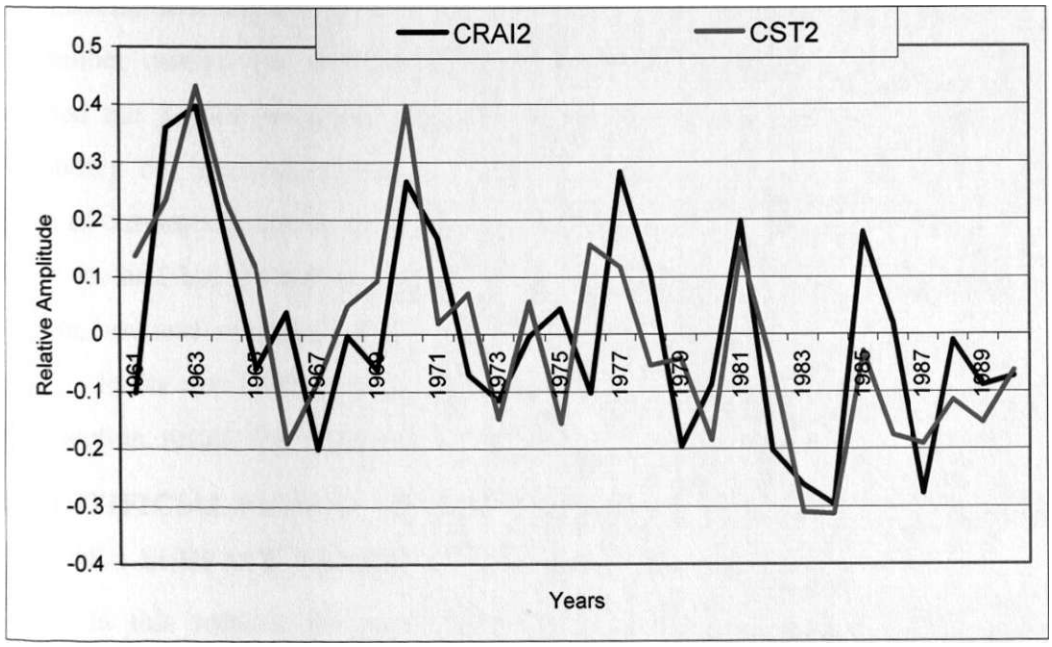

Figure 69b: The graphical plot of the normalized temporal functions (u and v) of the first pair of Canonical Correlation Analysis patterns representing association between March-May rainfall and December-February Sea Surface Temperature for the joint Indian-Atlantic Ocean (Canonical correlation = 0.70)

The first canonical pattern of association between MAM rainfall and MAM SST represented similar relationships to the first canonical pattern associated with DJF SST. The canonical correlation associated with the pair was 0.82 indicating strong associations. The second canonical pattern representing association between MAM rainfall and MAM SST represented similar relationships to the second canonical pattern associated with DJF SST. The canonical correlation associated with the pair was 0.72 indicating strong associations.

The conclusions from Canonical Correlation Analysis is the continued indication that the major sources of influence of sea surface temperature on regional seasonal rainfall were the zonal and meridional sea surface temperature variability, and the basin wide warming/ cooling associated with El Nino Southern Oscillation and Indian Ocean Dipole. There are marked differences in the major sources of influence of SST on seasonal rainfall over the region. The zonal surface temperature variability in the Indian Ocean together with the Interhemispheric Dipole in the Atlantic Ocean provided the highest influence on September-December rainfall but was secondary for March-May. The ocean-wide warming/cooling formed the highest source of sea surface temperature influence on March-May but was secondary for September-December. The high canonical correlations associated with the pairs of canonical patterns observed with MAM rainfall and seasonal SSTs indicate that the CCA method has the ability to improve the skill of MAM rainfall predictions. The SOND season, however, continued to show high potential of prediction.

In the next section, results from artificial neural network method are discussed. In the next section, results from artificial neural network method are discussed.

4.7 ARTIFICIAL NEURAL NETWORKS ANALYSIS OF SEASONAL RAINFALL AND SEA SURFACE TEMPERATURE GRADIENT MODES

In this section, the results from Artificial Neural Networks (ANN) analysis are discussed. The results from regression and canonical correlation analyses discussed in sections 4.5 and 4.6 represent mainly linear relationships. The relationships between seasonal rainfall and sea surface temperature gradient (SSTG) modes may not necessarily be linear. The ANN method, discussed in section 3.3.7, has the ability to represent complex and non-linear relationships. In the next subsection the results from ANN analysis of September-December (SOND) rainfall and SSTG modes are discussed.

4.7.1 SEPTEMBER-DECEMBER

In this section, the results from Artificial Neural Network (ANN) analysis of September-December (SOND) rainfall and SSTG modes are discussed. Like was the case for regression analysis and canonical correlation analysis (CCA), the period 1961-90 was used to train the models and the period 1991-2006 used to establish the skill of the models. The skill of the models was assessed using time series analysis and the analysis of the variance (ANOVA) methods.Figure 70 gives an example of the level of fitting achieved by ANN method from SOND and SSTG modes.

Figure 70 indicates that the ANN had high skill in fitting the SOND rainfall and SSTG modes in the training period. The model efficiently simulated both phases of variability of SOND rainfall in the training period. The Heidke Skill Score (HSS) was >0.90 in the training period of all the models developed using the ANN method reaffirming the high capability of the ANN method to simulate complex and non-linear relationships, and abilty to improve the seasonal rainfall forecasts for both seasons especially MAM. Table 21 indicates that the Hiedke Skill Score (HSS) associated with the models was >0.24. There were marked improvements for the model performance as was observed with Tabora for which no skillful model was achieved with regression method but the ANN method had a skill with the HSS value of 0.69.

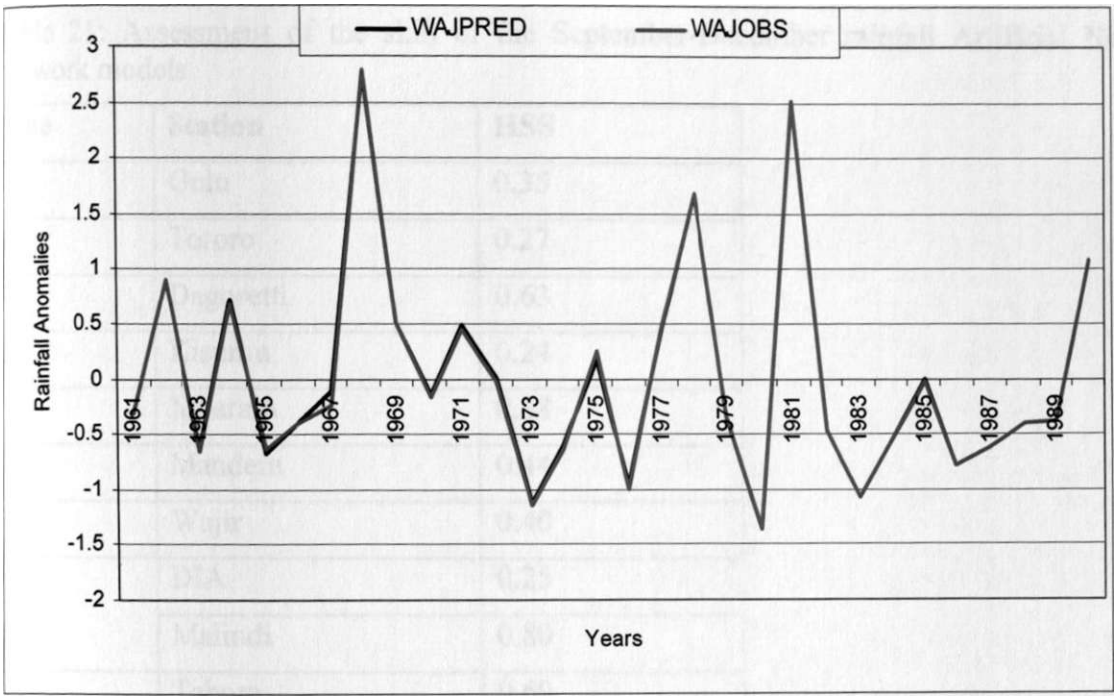

Figure 70: The time series plot of the Artificial Neural Networks predicted and observed March-May rainfall for Wajir for the training period 1961-1990 with the the two line plots overlapping due to high fitting skill associated with the method.

The time series plots of some examples of the models achieved with the ANN methods, as presented in Figures 71a-71c, indicate that the ANN method efficiently simulated both phases of rainfall variability.

Table 21: Assessment of the skill of the September-December rainfall Artificial Neural Network models

Zone	Station	HSS
1	Gulu	0.35
4	Tororo	0.27
5	Dagoretti	0.63
8	Kisumu	0.24
9	Mbarara	0.38
11	Mandera	0.44
12	Wajir	0.40
15	DIA	0.25
	Malindi	0.80
17	Tabora	0.69

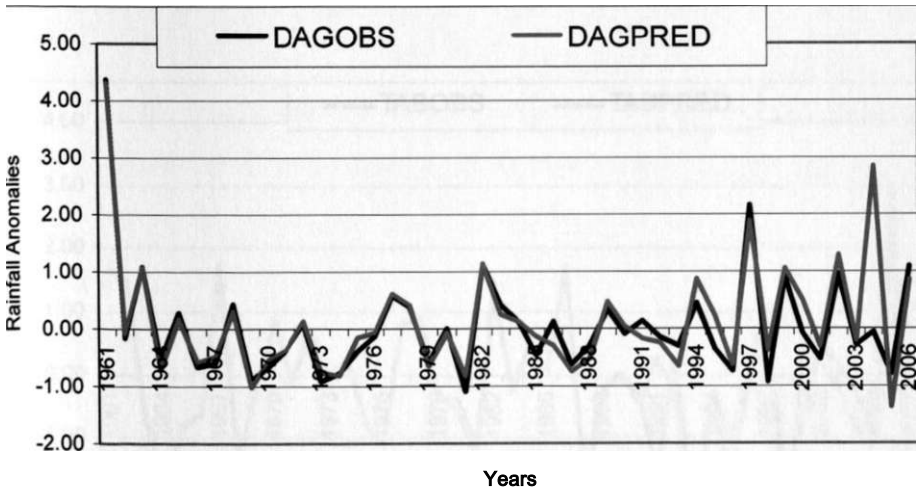

Figure 71a: The time series plot of the artificial neural network predicted (DAGPRED) and observed (DAGOBS) September-December rainfall for Dagoretti for the period 1961-2006 representing zone 5.

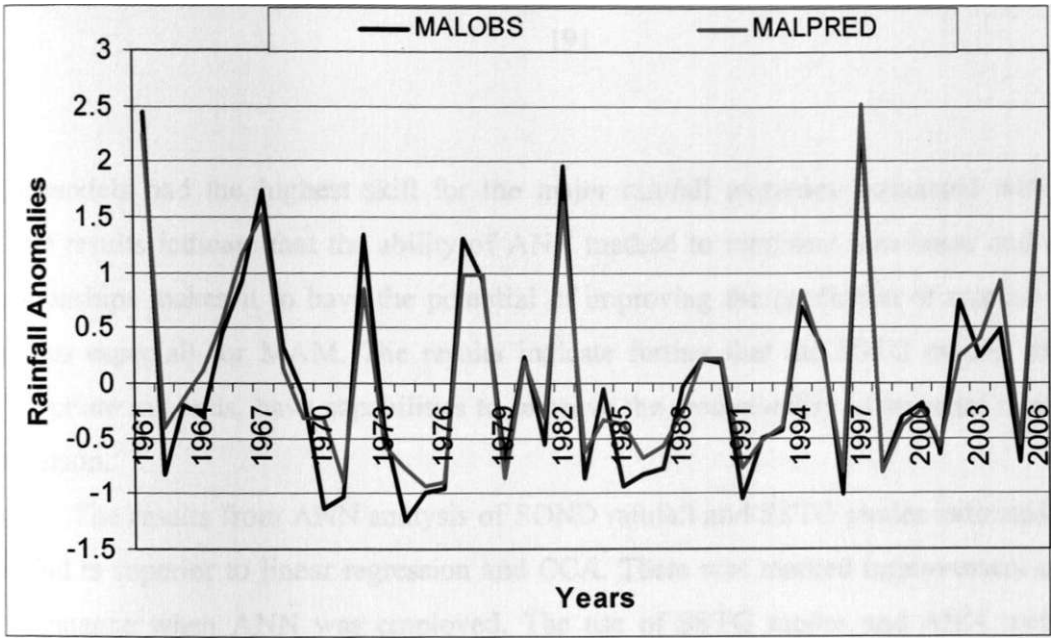

Figure 71b: The time series plot of the artificial neural network predicted (MALPRED) and observed (MALOBS) September-December rainfall for Malindi for the period 1961-2006 representing zone 15.

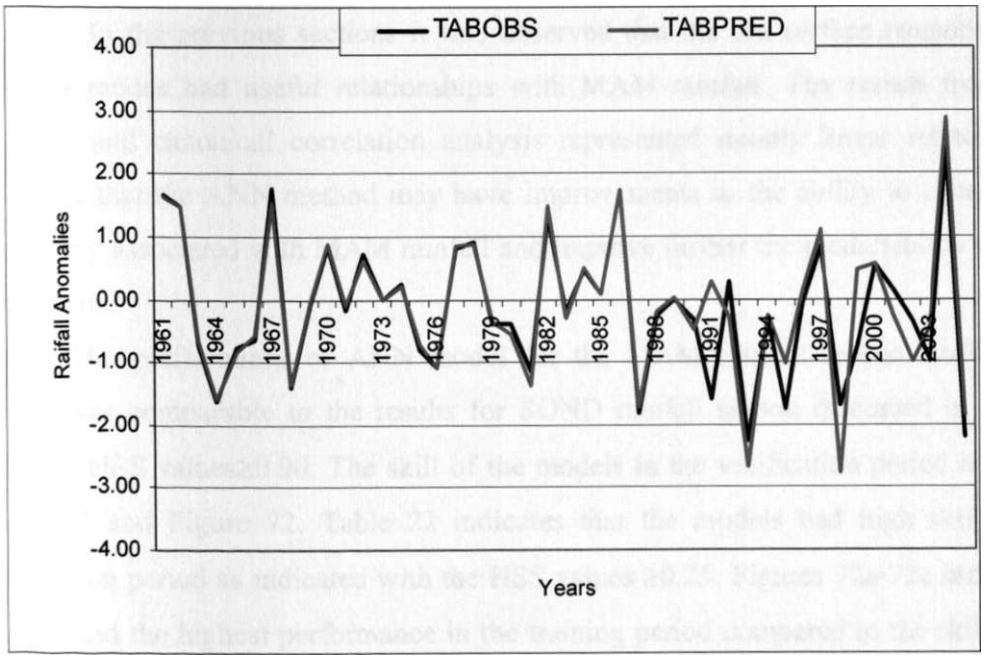

Figure 71c: The time series plot of the artificial neural network predicted (TABPRED) and observed (TABOBS) September-December rainfall for Tabora for the period 1961-2005 representing zone 17.

The models had the highest skill for the major rainfall extremes associated with ENSO. These results indicate that the ability of ANN method to represent non-linear and complex relationships makes it to have the potential of improving the prediction of rainfall for both seasons especiall for MAM. The results indicate further that the SSTG modes, used with appropriate methods, have capabilities to improve the predictability of seasonal rainfall over the region.

The results from ANN analysis of SOND rainfall and SSTG modes indicated that the method is superior to linear regression and CCA. There was marked improvement in model performance when ANN was employed. The use of SSTG modes and ANN method has potential to improve the predictability of SOND rainfall. In the next subsection the results from ANN analysis of MAM rainfall and SSTG modes are discussed.

4.7.2 MARCH-MAY

. In the previous sections it was observed that the sea surface temperature gradient (SSTG) modes had useful relationships with MAM rainfall. The results from regression analysis and canonical correlation analysis represented mainly linear relationships. It is expected that the ANN method may have improvements in the ability to simulate complex variability associated with MAM rainfall and improve further the predictability of rainfall for this season.

The performance of ANN model for the MAM rainfall season during the fitting period was comparable to the results for SOND rainfall season discussed in section 4.7.1 with the HSS values>0.90. The skill of the models in the verification period is presented in Table 22 and Figure 72. Table 22 indicates that the models had high skills during the verification period as indicated with the HSS values >0.25. Figures 72a-72c indicate that the models had the highest performance in the training period compared to the skill verification period. The models, however, represent an improvement in performance compared to regression and canonical correlation analyses. It should, however, be noted that the skill of ANN is highly dependent on the representation of the various cases in the data for the training period to feed the memory. Hence, the model under or over predicted some cases

and such results were corrected using a similar approach as indicated in the previous section 4.5.

Table 22: Assessment of the skill of the March-May Artificial Neural Network models

Zone	Station	HSS
4	Soroti	0.60
7	Wajir	0.48
12	Bukoba	25
14	Dagoretti	0.25
17	Kigoma	0.55
21	Malindi	0.32
22	Lamu	0.25
24	Songea	0.34

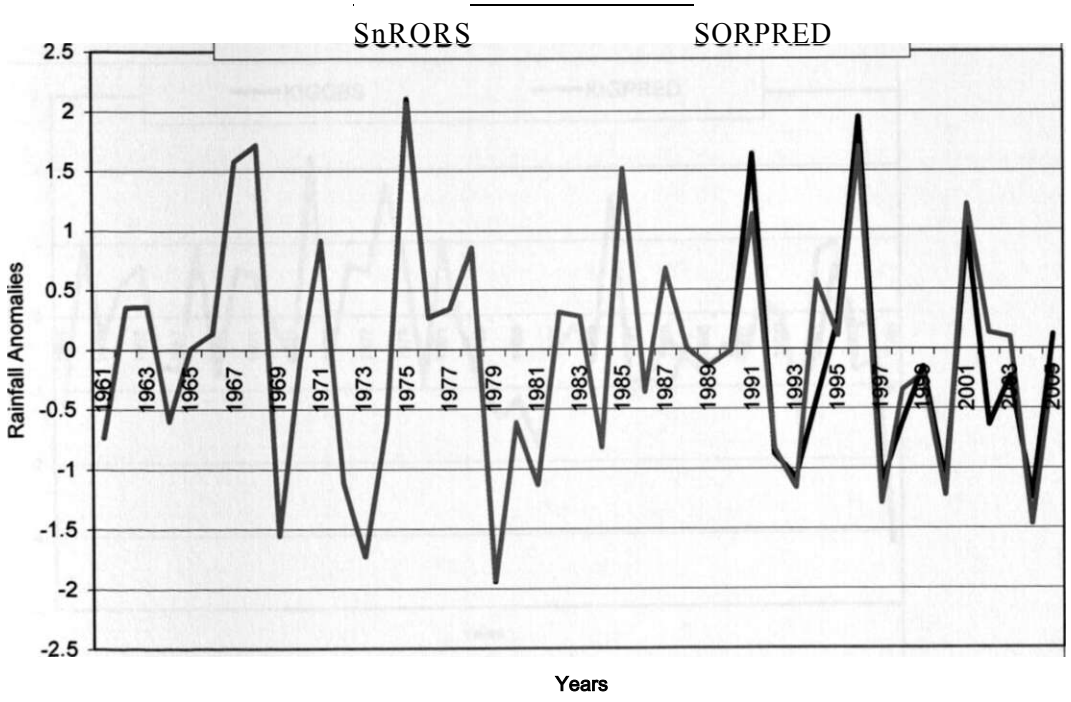

Figure 72a: The time series plot of the artificial neural network predicted (SORPRED) and observed (SOROBS) March-May rainfall for Soroti representing zone 4.

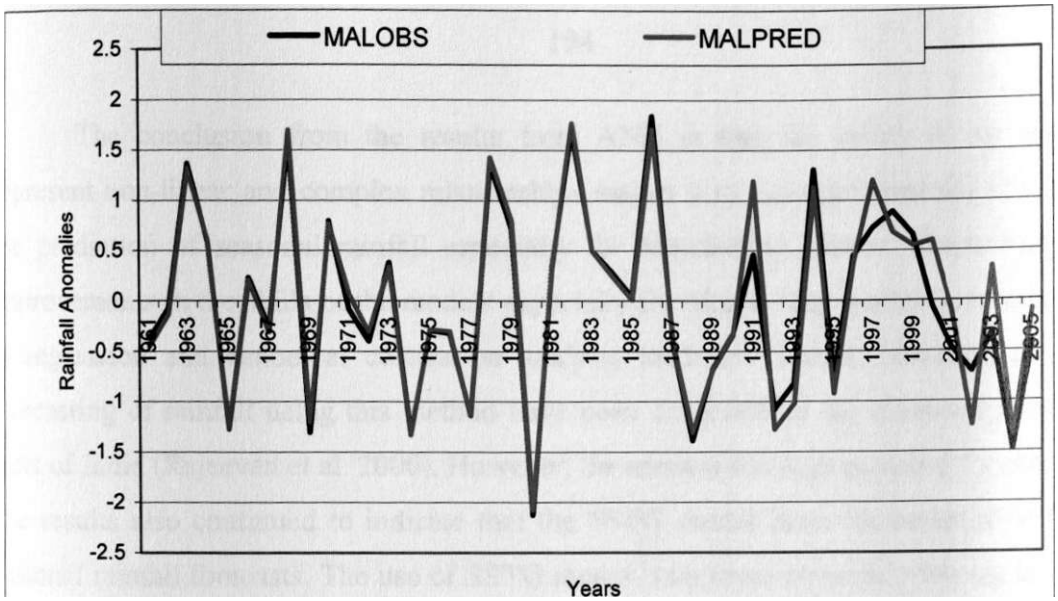

Figure 72b: The time series plot of the artificial neural network predicted (MALPRED) and observed (MALOBS) March-May rainfall for Malindi representing zone 21.

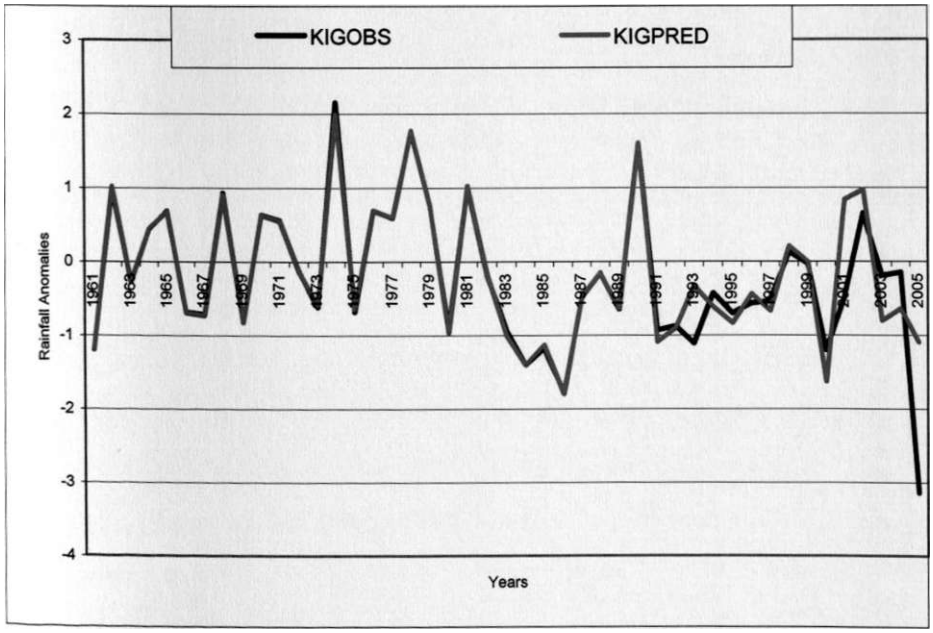

Figure 72c: The time series plot of the artificial neural network predicted (KIGPRED) and observed (KIGOBS) March-May rainfall for Mandera representing zone 17.

The conclusion from the results from ANN is that the ability of the method to represent non-linear and complex relationships makes it to have the potential of improving the prediction of seasonal rainfall especially for March-May season. There was marked improvements in the skills of the models especially for March-May rainfall season compared to regression and canonical correlation analysis methods. Similar improvements in the forecasting of rainfall using this method have been observed for the monsoon rainfall over parts of India (Rajeevan et al. 2000). However, the method has high potential for over fitting. The results also continued to indicate that the SSTG modes have the potential to improve seasonal rainfall forecasts. The use of SSTG modes with more powerful tools such as ANN, has high potential to improve the predictability of seasonal rainfall.

In the next section the summary, conclusions and recommendations from this study are presented.

CHAPTER FIVE

5. SUMMARY, CONCLUSIONS AND RECOMMENDATIONS

5.1 SUMMARY

This thesis is composed of six chapters. In the first chapter, the problem addressed by this study was introduced. The chapter also gave assumptions, hypothesis and limitations of this study study. A review of the literature relevant to this study, which includes systems influencing the climate of the region and the previous efforts to predict seasonal rainfall, is presented in chapter two.

It is recognized that seasonal rainfall extreme events influence the social and economic activities, and are associated with the majority of disasters affecting the region. Seasonal rainfall forecasts could help society, economic institutions and governments to minimize the negative impacts and take advantage of the positive aspects of extreme rainfall events. Seasonal rainfall forecasts are important inputs for climate early warnings and the improvements in the skills of the forecasts could contribute to the improvement of early warnings of climate extremes. Such forecasts would contribute to disaster risk reduction including enhanced economic development, food production and water resource management among other climate related activities.

Most of the previous studies have used grid-point sea surface temperature data in the diagnostic studies of regional climate, especially in attempts to enhance the understanding of regional climate processes and improve the prediction of seasonal rainfall. Such sea surface temperature (SST) based efforts are still having several limitations as is revealed by the weakness in predicting the major rainfall season of March-May (MAM). The grid-point SST based methods have shown high skill mainly during OND and when SST anomalies are very high like in the cases of strong El-Nino/ Southern Oscillation (ENSO) and Indian Ocean Dipole (IOD) that have significant influence on regional atmospheric circulations.

The overall objective of this study is to improve the skills of seasonal rainfall prediction in the region through the use of sea surface temperature gradient modes. This study recognizes that temperature gradients have a strong influence on atmospheric and ocean circulations associated with the distribution of heat energy and moisture that could

provide better prediction indices than those that have been derived from simple grid-point sea surface temperature predictors. Several specific objectives were developed to enable the accomplishment of this overall objective. The first specific objective involved the use of Principal Component Analysis (PCA) to delineate the key spatial sea surface temperature modes for all seasons of the year namely December-February (DJF), March-May (MAM), June-August (JJA) and September-November (SON). The grids associated with the maximum loadings of the dominant Principal Component Analysis modes were then used to derive sea surface temperature gradient modes for specific seasons by obtaining differences between SST of pairs of grid boxes for the individual PCA modes of each of the season.

The sea surface temperature gradient modes were derived for the Indian, Atlantic and Pacific oceans separately, and for the Indian and Atlantic oceans combined. The study assumed that the combined Indian and Atlantic Ocean SST gradient modes could provide other unique predictors that cannot be picked by the Principal Component Analysis modes of the individual oceans. Since the best SST predictor is that associated with the variability that leads seasonal rainfall, the SST predictors were searched from all seasons of the year namely DJF, MAM, JJA and SON. Rainfall prediction studies were, however, restricted to the main rainfall seasons of the region that are concentrated within MAM and September-December (SOND) months.

The second specific objective involved the use of time series, correlation and composite analysis methods to establish the space-time characteristics and inter-linkages between SSTG modes and seasonal rainfall extremes. The third specific objective involved the use of composite and canonical correlation analysis methods to examine the global/regional climate systems that may be associated with the relationships observed between seasonal rainfall, and SST gradient modes. The results from the first to third specific objectives were then used to develop relationships that could improve seasonal rainfall prediction and early warning tools for the region. In addition to regression and Canonical Correlation Analysis (CCA) methods, Artificial Neural Networks (ANN) was included for to determine its potential in improving the skills of seasonal rainfall forecasts.

The data and methods used in the study are presented in chapter three. The data used included rainfall, sea surface temperature (SST), outgoing long-wave radiation (OLR) and reanalyzed wind data. The study used rainfall data for the period 1960-2006 available at the

provide better prediction indices than those that have been derived from simple grid-point sea surface temperature predictors. Several specific objectives were developed to enable the accomplishment of this overall objective. The first specific objective involved the use of Principal Component Analysis (PCA) to delineate the key spatial sea surface temperature modes for all seasons of the year namely December-February (DJF), March-May (MAM), June-August (JJA) and September-November (SON). The grids associated with the maximum loadings of the dominant Principal Component Analysis modes were then used to derive sea surface temperature gradient modes for specific seasons by obtaining differences between SST of pairs of grid boxes for the individual PCA modes of each of the season.

The sea surface temperature gradient modes were derived for the Indian, Atlantic and Pacific oceans separately, and for the Indian and Atlantic oceans combined. The study assumed that the combined Indian and Atlantic Ocean SST gradient modes could provide other unique predictors that cannot be picked by the Principal Component Analysis modes of the individual oceans. Since the best SST predictor is that associated with the variability that leads seasonal rainfall, the SST predictors were searched from all seasons of the year namely DJF, MAM, JJA and SON. Rainfall prediction studies were, however, restricted to the main rainfall seasons of the region that are concentrated within MAM and September-December (SOND) months.

The second specific objective involved the use of time series, correlation and composite analysis methods to establish the space-time characteristics and inter-linkages between SSTG modes and seasonal rainfall extremes. The third specific objective involved the use of composite and canonical correlation analysis methods to examine the global/regional climate systems that may be associated with the relationships observed between seasonal rainfall, and SST gradient modes. The results from the first to third specific objectives were then used to develop relationships that could improve seasonal rainfall prediction and early warning tools for the region. In addition to regression and Canonical Correlation Analysis (CCA) methods, Artificial Neural Networks (ANN) was included for to determine its potential in improving the skills of seasonal rainfall forecasts.

The data and methods used in the study are presented in chapter three. The data used included rainfall, sea surface temperature (SST), outgoing long-wave radiation (OLR) and reanalyzed wind data. The study used rainfall data for the period 1960-2006 available at the

IGAD Climate Prediction and Application Centre (ICPAC) formerly known as the Drought Monitoring Centre (DMC), Nairobi obtained from the Kenya Meteorological Department (KMD), Tanzania Meteorological Agency (TMA) and Uganda Meteorological Department (UMD). The homogeneous climate zones developed through previous studies and operationally used at ICPAC (ICPAC 1999) were employed in this study. The SST data used was for the period 1960 to 2006 for 10°x10° latitude/longitude boxes located over Indian Atlantic and Pacific Oceans mainly to the north of 30°S since the quality of SST further south may not be good (Weare 1977).

The wind data used was for the period 1960-2006. This data have been used in various climate studies (Malony and Shaman 2008, Owiti 2005, Indeje 2000). Both wind and SST data were obtained from NCEP/NCAR database. The OLR data was available for the period 1974-2004.The data were quality controlled and normalized using standard methods before they were used in the study.

The normalized grid point and areal records were subjected to several analyses including Principal Component Analysis, Correlation Analysis, Composite Analysis, Regression Analysis, Canonical Correlation Analysis and Artificial Neural Networks to establish functional relationships between sea surface temperature gradient modes and rainfall. The results obtained from the various methods are presented in chapter four. The results from quality control analyses indicated that most of the data used in the study were of acceptable qualities.

The time series analyses of the standardized data indicated inter annual recurrences of large positive and negative values of anomalies in all records. The large sea surface temperature anomalies are evident during the El-Nino/Southern Oscillation and Indian Ocean Dipole years. The extreme positive and negative rainfall values, on the other hand, reflected the major flood and drought years.

The results from Principal Component Analysis of SST over the Indian Ocean indicated that the sea surface temperature variability for DJF and SON was represented by eight modes accounting for 87.9% and 89.5% of SST variance, respectively. The sea surface temperature variability for MAM and JJA was dominated by seven modes accounting for 81.4% and 92.8% of SST variance respectively. The first mode in seasonal SST generally represented basin wide warming/cooling associated with El-Nino/Southern Oscillation

events. The first mode also indicated some decadal variability signals, increasing trend and a climate regime shift during the period 1976-77 that has been observed by many authors (An and Wang 2000; Wang and An 2001; Harrison and Carson 2007).

The periods of the recurrence of the largest positive/negative time coefficients corresponds to El Nino/La Nina in agreement with the expected warming/cooling of the Indian Ocean in response to El Nino/La Nina events (Behera et al. 2005; Kug et al. 2006). The second Indian Ocean PCA mode represented IOD, especially during MAM, JJA and SON. The modes observed with SON and JJA SST were discernable in MAM. The modes representing zonal SST variability dominated SST variability in the Indian Ocean and may be linked to the strong influence of this ocean on the rainfall of the region (Goddard and Graham 1999, Mutai et al. 1998; Mutai 2003; Okoola 1996); Omondi 2005, and Owiti 2005) in agreement with the observations of Lindzen and Nigam (1987). The Principal Component Analysis of SST for the Atlantic Ocean indicated that the sea surface temperature variability for DJF was dominated by ten modes accounting for 89.9%. The SST variability in MAM, JJA and SON was dominated by eleven modes that accounted for about 92% of sea surface temperature variance in each season. Like in the case of Indian Ocean, the first mode represented basin wide warming/ cooling associated with ENSO. The second mode, representing interhemispheric sea surface temperature variability, was the second most dominant in all seasons as has been observed by many authors (Chang et al. 2007; Li et al. 2007; Moura and Shukla 1981; Nobre and Shukla 1996; Parker et al. 1988; Repelli and Nobre 2004; Weare 1977; and Wu et al. 2007). The modes observed in DJF were discernable in MAM, JJA and SON.

The locations associated with the modes that represented the zonal and meridional SST variability were used in deriving SST gradient modes associated with the Atlantic and Indian Oceans.

The temporal characteristics of the modes represented inter-decadal and decadal variability. The years with large positive and negative values of the time coefficients of the modes correspond to some of the major wet and dry years over parts of the region in agreement with the observations of Nicholson and Entekhabi (1987) indicating significant influence of the oceans on the rainfall of the region. The locations associated with the modes representing the interhemispheric SST variability in the Atlantic Ocean were used to derive

meridional SST gradient modes associated with the ocean. The results from PCA of SST for the combined Atlantic-Indian Ocean indicate that the sea surface temperatures variability for DJF and MAM was dominated by 16 modes accounting for 93% and 94%, respectively. The SST variability in JJA and SON was dominated by fifteen modes that accounted for about 93% of sea surface temperature variance in each season.

The modes observed with the individual oceans dominated SST variability for the combined oceans. The second PCA mode in JJA was unique and represented three poles with the strongest poles located over the equatorial western Indian and eastern Atlantic Ocean associated with the Atlantic-Indian Ocean Dipole. A relatively weaker pole was located over the eastern Indian Ocean. The locations in the equatorial eastern Atlantic and western Indian Ocean associated with this mode were used to derive the SST gradient mode associated with the combined influence of the two oceans.

The results from correlation analysis indicated that both March-May and September-December seasonal rainfall had significant relationships with Principal Component Analysis (PCA) modes and the associated sea surface temperature gradient modes. The largest value of correlation between September-December rainfall and sea surface temperature gradient modes was 0.85 indicating that the sea surface temperature gradient modes accounted for about 72.25% of September-December rainfall variance. The sea surface temperature gradient mode that had the largest correlation with the September-December rainfall was linked to the Indian Ocean Dipole. The largest value of correlation observed between March-May rainfall and sea surface temperature gradient modes was 0.56 indicating that sea surface temperature modes accounted for about 31.56% of March-May rainfall variance.

The sea surface temperature gradient mode that had the strongest relationships with March-May rainfall was associated with Atlantic-Indian Ocean Dipole linking the equatorial western Indian and eastern Atlantic Ocean. The higher variance of September-December rainfall explained by sea surface temperature gradient modes (above 72%) compared to March-May (about 32%) indicates that, although some prediction skill can be obtained for March-May rainfall using sea surface temperature gradient based predictors, the prediction skill for the September-December rainfall is still relatively higher.

Many previous studies have obtained relatively low prediction skills for March-May rainfall season. It was observed from the study that seasonal rainfall relationships were

stronger with the zonal sea surface temperature gradient modes than with the meridional sea surface temperature gradient modes. The sea surface temperature gradient modes in the Atlantic and Pacific Oceans, in general, had longer lead-time compared to those associated with the Indian Ocean.

The peak relationships with the sea surface temperature gradient modes associated with the Indian Ocean were achieved within the respective seasons. This requires skilful sea surface temperature prediction if sea surface temperature gradient based results from the study are to be used for seasonal rainfall prediction. For example, the relationships between March-May rainfall and sea surface temperature gradient modes are highest during the months of March, April and May. The relationships observed with the months making MAM season showed marked differences that may contribute to the diffticuties to predict the season.

Sea surface temperature gradient modes based predictors for September-December season extend as early as January months. These could be linked to common peaking of sea surface temperatures during the last quarter of the years during the major El- Nino/Southern Oscillation and Indian Ocean Dipole years. Such sea surface temperature anomalies persist for several months and sometimes extend beyond one year.

Results from composite analysis of rainfall, wind and satellite derived outgoing long wave radiation confirmed significant linkages amongst some of the extreme phases of sea surface temperature gradient modes and rainfall Principal Component Analysis modes over the region. The sea surface temperature gradient mode associated with the the Atlantic-Indian Ocean Dipole had the highest capability to delineate March-May rainfall while September-December rainfall could be delineated effectively by both the zonal gradients associated with the Atlantic-Indian Ocean Dipole and the Indian Ocean Dipole.

The results from composite analysis also indicated that the major sources of SST influence on seasonal rainfall were the zonal and meridional SST variability associated with the individual oceans and the interactions of the two oceans especially as regards the MAM rainfall season, which was better delineated with the mode representing the combined influence of the Atlantic and Indian Ocean. The results further indicated that extreme phases of the SSTG modes were associated with the distinct patterns of wind circulation and convection as reflected in the composites of wind and OLR.

The extreme positive and negative phases of the SST modes influenced both the zonal and meridional wind circulation. For example the extremely negative phase of the SSTG mode based on the Atlantic-Indian Ocean Dipole was associated with mainly westerly anomaly with an easterly anomaly over the eastern Indian Ocean together with a southerly anomaly in the Indian and Southern Atlantic Ocean. On the other hand, the extremely positive phase of the same mode was associated with mainly easterly anomaly with a westerly anomaly over the eastern and central Indian Ocean together with a relatively weaker southerly anomaly over the Indian and southern Atlantic Ocean.

The results from regression analysis indicated that the use of sea surface temperature gradient modes would improve the prediction of seasonal rainfall in the region especially March-May rainfall season. The Heidke Skill Score associated with the models based on sea surface temperature gradient modes was >0.20 indicating the models had useful skills. Canonical Correlation Analysis results indicated high prediction skill of September-December rainfall from June-August sea surface temperatures. The first canonical pair, with a canonical correlation of 0.86, indicated that the warming over the western Indian Ocean and northern southern Atlantic Ocean together with the cooling over the eastern Indian Ocean, and northern and the further southern Atlantic Ocean favour enhanced rainfall over most parts of the region. Such sea surface temperature and rainfall patterns are associated with El-Nino/ Southern Oscillation, Indian Ocean Dipole and Atlantic Ocean interhemispheric dipole events as represented by the second SST PCA modes of individual oceans.

The results from CCA also indicated marked improvements in the association between SOND rainfall and SST within the season when the canonical correlation improved to 0.91. The first pair of canonical patterns observed with December-February sea surface temperatures and March-May rainfall, which had a canonical correlation of 0.85, indicated that the basin wide cooling/warming over the Atlantic and Indian Ocean is associated with deficient/enhanced rainfall over the northern parts of the region and enhanced/deficient rainfall over southern Tanzania. The results from Canonical Correlation Analysis also indicated that the associations between March-May rainfall and SST were more complex compared to those observed with September-December rainfall. The results further indicated •that Canonical Correlation Analysis had higher capability than regression methods in the

prediction of seasonal rainfall as indicated by the high values of canonical correlations. The association at zero-time lag did not have much improvement for MAM as observed with SOND.

The results from Artificial Neural Networks indicated marked improvements in the skills of the models especially for March-May rainfall season. The Heidke Skill Score in the training period for both seasons was >0.90 indicating high capability in fitting the models and high potential for over fitting which is a major weakness of the method. Some regions that did not have any linear model with good skill had skilful models from ANN. The Heidke Skill Score for the March-May and September-December models were >0.24 indicating high potential of Artificial Neural Networks methods in improving the predictability of rainfall especially for March-May season. The other major weakness of this method is limitations to predict cases not represented in the training period since it relies on the memory in the data records.

This study has for the first time developed new prediction tools based on sea surface temperature gradient modes for seasonal rainfall prediction, especially for the March-May rainfall season that many previous studies have found to be extremely difficult to predict. Other new tools that were developed in the study are associated with more advanced Canonical Correlation Analysis and Artificial Neural Networks methods that improved the skill of seasonal rainfall forecasts for both March-May and September-December seasons. This study has also documented for the first time the Atlantic-Indian Ocean Dipole that has significant influence on the rainfall of the region.

The results of the study can be used to improve seasonal rainfall forecasts especially for the major rainfall season of March-May. The skillful seasonal forecasts would be useful in reducing and managing the risks associated with seasonal rainfall extremes. They would provide useful inputs to the improvement of early warnings of extreme rainfall events and contribute to disaster risk reduction in the region. Such results would not only provide new climate risk management tools for coping with past and current climate extremes, but also experiences and lessons that can be extended to addressing climate change adaptation challenges.

The next section presents the major conclusions from the study.

5.2 CONCLUSIONS

The finding of this study is that sea surface temperature gradient modes have potential to improve the skill of seasonal rainfall forecasts especially for the major rainfall season of March-May. However, their use may require that SSTs be predicted since some of the peak relationships coincide with the seasons. The September-December rainfall season continues to have higher potential of predictability than March-May. The Atlantic-Indian Ocean Dipole(AIOD), which is documented for the first time, has significant influence on regional rainfall for both seasons.

The major sources of influence of SST on seasonal rainfall over the region are the ocean wide warming/cooling, and zonal and meridional SST variability associated with the ENSO, IOD, AIOD and interhemispheric dipole in the Atlantic Ocean. There are, however, marked differences in the sources of influence of SST on MAM and SOND rainfall. While the IOD and interhemispheric dipole in the Atlantic Ocean are the major sources of influence of SST on SOND rainfall, the ocean wide warming in the Atlantic and Indian Oceans are the major sources of SST influence on MAM rainfall.

The PCA modes for both oceans represent inter-decadal and decadal variability. The first modes for both oceans represented an increasing trend. The SST variability in the Indian/Atlantic Ocean is dominated with zonal/meridional SST variability. The extreme phases of the modes are associated with some climate extremes affecting the region linked to ENSO, AIOD and IOD.

The zonal SST gradient modes have a stronger influence on seasonal rainfall than the meridional modes. The SSTG modes effectively delineated rainfall, wind and OLR indicating that the observed relationships were realistic and may be associated with the influence of SSTG modes on the general circulation, moisture transport and convection. The zonal SST gradient mode associated with the Atlantic-Indian Ocean Dipole had the highest capability to delineate March-May rainfall.

The SOND rainfall could be delineated with the zonal SST modes associated with the Indian Ocean Dipole and the one associated with the Atlantic-Indian Ocean Dipole. The extreme negative and positive values of SST gradient modes coincided with some wet and dry conditions associated with ENSO, AIOD and IOD.

The SST gradient modes associated with the Atlantic Ocean have peak relationships with rainfall several months before the season. However, the SST gradient modes associated with the Indian Ocean have peak relationships with rainfall within the season.

The results from CCA continued to indicate that the major sources of influence of sea surface temperature on seasonal rainfall were the zonal and meridional sea surface temperature variability, and the basin wide warming/ cooling associated with El Nino Southern Oscillation, Indian Ocean Dipole and interhemispheric dipole in the Atlantic Ocean. The zonal surface temperature variability in the Indian Ocean together with the Interhemispheric Dipole in the Atlantic Ocean provided the highest influence on September-December rainfall but was secondary for March-May. The ocean-wide warming/cooling formed the highest source of sea surface temperature influence on March-May but was secondary for September-December.

The canonical correlation analysis method had better performance than regression anslaysis method. The ability of artificial neural networking to represent non-linear and complex relationships makes it to have the potential to improve the prediction of seasonal rainfall espcially for MAM season. The artificial neural networks showed marked improvements in the prediction of seasonal rainfall especially for the major rainfall season of March-May.

In conclusion, this study has, for the first time, developed new prediction tools that have improved the skill of seasonal rainfall forecasts for both seasons, especially for MAM. The new tools were derived from SST gradient modes, as well as the inclusion of more powerful artificial neural networks (ANN) and canonical correlation analysis (CCA) methods. The skilful forecasts would significantly contribute to disaster risk reduction and improve the resilience of communities in the region to adapt to climate variability and change. The study has also documented for the first time Atlantic-Indian Ocean Dipole that has siginificant influence on seasonal rainfall over the region.

The recommendations associated with this study are presented in the next section.

5.3 RECOMMENDATIONS

The recommendations from this study address issues related to the generation of climate outlooks by the national and regional meteorological services, their applications and necessary further studies. The national meteorological services, users and research scientists

in the countries covered in this study, and ICPAC may wish to take into consideration the recommendations provided in the next subsections.

5.3.1 RECOMMENDATIONS TO NATIONAL METEOROLOGICAL SERVICES, TRAINING INSTITUTIONS AND IGAD CLIMATE PREDICTION AND APLICATION CENTRE

The National Meteorological Services (NMSs) in Kenya, Uganda and Tanzania provide meteorological services to meet the needs of the governments, public and various sectors in the respective countries. To be able to provide such services, the NMSs have to gather, archive and process data. The NMSs have also to disseminate the climate outlooks to the users. Data and observations form the foundation of any meteorological service. The skills of forecasts are highly dependent on data quality, and the distribution of data in space and time. No country is self reliant in the provision of meteorological services since the data to provide services is needed beyond the territorial boundaries. Hence systems must be in place to facilitate efficient exchange of data.

The spatial distribution of stations in the region is not adequate especially over arid/semi arid areas and water bodies. Also most of the stations were opened recently and have very short records that make it difficult to calibrate models. In addition to data, skilful human resource is an important element in the management and processing of data including providing forecasts. The WMO Regional Training Centre(RTC)/Institute for Meteorological Training and Research (IMTR), Nairobi and the Department of Meteorology at the University of Nairobi, have helped develop capacities of NMSs in the region. ICPAC has helped a great deal in developing capacities of the NMSs in the region in seasonal forecasting especially using empirical methods. ICPAC has also conducted training aimed at improving capacities in the use of dynamical methods in forecasting seasonal rainfall. Most of the NMSs have capacity to use empirical methods to predict rainfall.

More training in the generation and application of climate information is needed. Hence, the following recommendations are aimed at addressing the gaps highlighted above.

i. NMSs should consider partnerships with users of meteorological services to open and operate more stations.
ii. NMSs should consider incentives for volunteer observers to make the programme sustainable and avoid frequent closure of stations operated by the volunteers.

iii. NMSs should assess the distribution of stations to ensure that the critical and regional climate representative stations are sustained.

iv. NMSs should automate the databases to facilitate research.

v. NMHs should work with the government and interested institutions to improve the data networks over the Indian Ocean, inland lakes and arid lands.

vi. NMSs should consider the possibilities of making arrangements with other institutions to manage backups of their databases as a fall back position incase of incidences that may lead to loss of data at the main office.

vii. NMSs and ICPAC should promote partnerships with academia and research institutions to conduct research aimed at improving the services.

viii. NMSs should consider using the SST gradient modes developed in this study to monitor and predict seasonal climate for the respective countries.

ix. WMO/RTC -Nairobi and ICPAC should consider forming partnerships to have a training programme on seasonal climate prediction and applications that the students attending courses at the RTC and communities in the region could benefit from.

5.3.2 RECOMMENDATIONS FOR FURTHER RESEARCH

Research remains a pillar for the development of any nation. Improvements in understanding and prediction of our climate would enable the communities in the region take advantage of the positive aspects of climate extreme and minimize the related negative risks. Several efforts have been made by individual institutions and scientists to study our climate. Research would have more value if the results were implemented to serve humanity. This work has shown that SST gradient modes would improve the prediction of seasonal rainfall forecasts. More work would be needed to establish if SST gradient modes could help in the prediction of other factors that influence the welfare of our society and our economy such as crop yields, stream flow, diseases such as malaria and air temperature including human comfort indices which influence tourism.

It should also be noted that climate change would influence predictors. The following recommendations are aimed at addressing the highlighted needs.

i. More studies should be conducted to establish improvements in the ability of ANN through the use of various transfer functions.

More studies should be conducted to establish the physical and dynamical factors associated with the linkages between SST gradient modes and seasonal rainfall.

More studies should be conducted to establish potential of seasonal rainfall prediction when SST gradient modes are used with other predictors especially for the major rainfall season of MAM.

ICPAC should develop some tools for prediction of monthly SSTs over the Indian Ocean since they are required for improving the forecast of MAM seasonal rainfall.

Joint studies involving climate scientists and scientist from the user sectors such as agriculture, health, energy, tourism and wildlife and economists should be encouraged to develop user targeted products based on SST gradient modes and other predictors.

More studies should be conducted to improve our understanding of the impacts of the trends observed in the SST modes associated with the Indian and Atlantic Oceans on the regional climate.

This study used regression, CCA and ANN methods to develop models to predict rainfall. It was observed that these methods have varying capabilities both in the fitting of the models and skill. More studies need to be conducted using longer records to verify further the ability of these methods.

The wind data used in the composite analysis may not be representative of the local factors affecting our rainfall. More studies should be conducted using high-resolution regional models to establish the responses of regional atmospheric circulation patterns to extreme phases of SST gradient modes.

More studies should be conducted to establish if the SST gradient modes developed in the study could have the potential to predict rainfall beyond the area of current study.

More studies should be conducted to improve our understanding of the role of the Atlantic Ocean in influencing the rainfall over the region.

5.3.3 RECOMMENDATIONS TO USERS OF CLIMATE PREDICTION/ OUTLOOKS

This study has shown that SST gradient modes have the potential to improve seasonal climate outlooks especially for MAM season. Climate outlooks are only useful if they trigger an action. For climate outlooks to trigger action, they need to be integrated into decisions for operating institutions in climate dependent sectors. Climate outlook fora have demonstrated that efficient generation and application of climate outlooks require partnerships among the providers and users of climate information. The following recommendations are aimed at actions that could improve application of climate information for the benefit of our society and economy.

i. NMSs consider promoting partnerships with the users in the generation and application of climate information in a model similar to climate outlook fora.
ii. NMSs should promote feedbacks from the users and keep the users updated of any changes in the prediction.
iii. Users should be encouraged to give feedbacks and make any enquiries on climate predictions as affects their respective activities.
iv. Users should be encouraged to conduct joint research with climate scientists to help improve services for their respective sectors including developing sector targeted forecasts.
v. Users should be encouraged to diversify the use of climate information in various activities relevant to their sectors.
vi. Users should be encouraged to train in application of climate information in a model similar to the aviation and marine transport where captains are trained on meteorology to enable them interpret and apply meteorological information.

6 REFERENCES

Agumba, F. 0., 1985: Fluctuations of long rains in Kenya in relation too large scale circulation, *IMTR Res. Report No.* **1/85,** 27 pp.

Ajayamohan, R.S., and S. A. Rao, 2008: Indian Ocean Dipole Modulates the Number of Extreme Rainfall Events over India in a Warming Environment, *J. Meteorol. Society Japan,* **86, No. 1,** .245-252

Alexander, M.A., L. Matrosova, C. Penland, J. D. Scott, P. Chang, 2008: Forecasting Pacific SSTs: Linear Inverse Model Predictions of the PDO, *J.Climate,* 21, No. 2, 385-402

Alusa, A. L., 2003: Early warning, prevention-preparedness and response continnum in the management of hydrometeorological disasters, *Proc. Kenya Meteor. Soc. Workshop on meteorological research, applications and services,* Mombasa, Kenya, 29 Sept. to 3 Oct. 2003, pp 23-26

An, S. I and B Wang, 2000: Inter decadal change of the structure of the ENSO mode and its impact on ENSO frequency. *J Climate,* 13, 2044-2055

An, S-I., **J**-S. Kug, A. Timmermann, I.-S. Kang, and O. Timm, 2007: The influence of ENSO on the generation of decadal variability in the north Parcific. *J. Climate***, 20, No.4,** 667-680

Anderson, J., H. Van den Dool, A Barnstorn, W. Chen, W. Stern, and J. Ploshay, 1999: Present-day capabilities of numerical and statistical models for atmospheric extra tropical seasonal simulation and prediction. *Bull. Amer. Meteor. Soc.* 80, 1349-1361.

Annamalai, H., K. Hamilton, and K. R. Sperber, 2007: The South Asian Summer Monsoon and Its Relationship with ENSO in the IPCC AR4 Simulations. *J. Climate,* **20,** No.6, 1071-1092.

Anyah, R. O., and F.H.M. Semazzi, 2006: Climate variability over the greater horn of East Africa based on NCAR AGCM ensemble. *Theor. Appl. Climatol.,* 86, 39-62.

Anyah, R. O., F.H.M. Semazzi, and L. Xie, 2006: Simulated physical mechanisms associated with climate variability over Lake Victoria Basin in East Africa. *Mon. Wea. Rev.,* **134,** 3588-3609

Anyamba, E. K., 1983: On the monthly mean lower tropospheric circulation and anomalous circulation during the 1961/62 floods in East Africa. *MSc. Thesis, Department of Meteorology, University of Nairobi,* Kenya

Anyamba, E K, 1984: Some aspects of the origin of rainfall deficiency in East Africa. *Proc. Of the WMO regional scientific conf On GATE, WAMEX and Tropical Meteorology,* Dakar, Senegal, pp 110-112

Anyamba, E.K., 1993: Short term climate variability in East Africa. Proc. *First International Conference of African Meteor. Soc.,* Nairobi Kenya, 8-12 February 1993, PP224-235

Asnani, G. C., and Kinuthia J.H., 1979: Diurnal variation of precipitation in East Africa., *KMD, Res. Rept.* **8/79**

Asnani, G.C., 1982: The climate of Africa including feasibility study of climate alert system -Africa. Proc. *Techn. Conf. onclimate - Africa, 25-30 Jan 1982, Arusha, United Republic of Tanzania* pp. 107-129

Asnani, .C., 1993: *Tropical meteorology.* Published By Prof. .C. Asnani Pune India.

Baines, P. G, and C. K. Folland, 2007: Evidence for a Rapid Global Climate Shift across the Late 1960s. *J Climate,* **20 No.12,** 2721-2744

Barnett, T.P, 1981: Statistical Prediction of North America air temperatures from Pacific predictions. *Mon. Wea. Rev.,* **109,** 1021 - 1041.

Barnett, T.P and R. Preisendorfer, 1987: Origins and levels of monthly and seasonal forecasts skill for United States surface air temperatures determined by Canonical Correlation Analysis. *Mon. Wea. Rev.,* **115,** 1825 - 1850

Barnston, A.G., and R.E. Livezy, 1987: Classification, seasonality and persistence of low frequency circulation patterns. *Mon. Wea. Rev.,* 115, 1083-1126

Barnston, A. G., H. M. van den Dool, D. R. Rodenhuis, C. R. Ropelewski, V. E. Kousky, E. A. O'Lenic, R. E. Livezey, S. E. Zebiak, Mark A. Cane, T.P. Barnett, N. E. Graham, M. Ji, and A. Leetmaa, 1994: Long-lead seasonal forecasts—Where do we stand? *Bull. Amer. Meteor. Soc.,* 75, 2097-2114

Barnston, A.G. and T.M. Smith, 1996: Specification and Prediction of global surface temperature and precipitation from Global SST using CCA. *J. Climate,* **9, No.l 1**,2660-2697

Barnston, A.G., W Thiao, and V Kumar, 1996: long-lead forecasting of seasonal precipitation in Africa using CCA. *Weather and Forecasting,* 11, 506-520

Barnston, A. G., Y. He. and D. A. Unger, 2000: A forecast product that maximizes utility for state of art seasonal climate prediction, *Bull. Amer. Meterol. Soc;* 81, *No.* 6, 1271-1279

Barnston, A. G., S. J. Mason, L. Goddard, D. G. Dewitt, and S. E.Zebiak, 2003: Multimodel ensembling In seasonal climate Forecasting at IRI. *Bull. Amer. Meteor. Soc.,* 84, 1783-1796

Barring, L., 1987: Spatial patterns of daily rainfall in Central Kenya. Application of pincipal component analysis, common factor analysis and spatial correlations. *Intern. J. Climatol*, 7, 267-289

Barry, R.G., and R. J. Chorley, 1968: Atmosphere, Weather and Climate, 4-h Edition, Methuen, London and New York, 407pp

Basalirwa, C.P.K, 1979: Estimation of areal rainfall in some catchments of upper Tana River*, MSc. Thesis, Dept. of Meteorology, University of Nairobi,* Kenya

Basalirwa, C.P.K., 1999: Delineation of Uganda into climatological rainfall zones using the method of principal component analysis. *Int. J. Climatol.* 15, 1161-1177.

Basalirwa ,C.P.K, J. O. Odiyo, R. J. Mngodo, and J. Mpeta, 1999: The climatological regions of Tanzania based on rainfall characteristics. *Int. J. Climatolog.,* **19,** 69-80.

Battacharyaa, G.K. and A.J. Johnson, 1977: *Statistical Concepts and Methods.* John Willey & Sons, New York

Behera, S. K, J-J. Luo, S. Masson, P. Delecluse, S. Gualdi and A. Navarra, 2005: Paramount Impact of the Indian Ocean Dipole on the East African short Rains: ACGCM study. J. *Climate*, 18,41-54

Beltrando, G., and D L Cadet, 1990: Relationship between the short rain season in Africa and the atmospheric circulation over Africa and Indian Ocean. *Proc. 2nd Techn. Conf on weather forecasting in East and southern Africa, Nairobi, Kenya* 3-7 September 1990. pp 64-66.

Bhalme, H.N, Rahalla, S.S, and Skiddev, A.B., 1987: Tropical Quasi-biennial oscillation of the lOmb wind and Indian Ocean Monsoon rainfall implications of forecasting. *Int. J. Climatology*, 7, 345-353

Bjerkness, J., 1969: Atmospheric teleconnections from the equatorial Pacific. Mon Wea Rev 97, 163-172

Black, E, J. Slingo and K. R. Sperber, 2003: An observational study of the relationship between excessively strong short rains in the coastal East Africa and Indian Ocean SST., *Mon Wea. Rev.* **131,** 74-94.

BrainCom, 2007: Software for Predictive Modeling and Forecasting. http://www.freedownloadscenter.com/Utilities/Misc_Utilities/BrainCom.html.

Brankovic, C, T. N. Palmer and L Ferranti, 1994: Predictability of seasonal atmospheric variations. *J Climate,* 7, 217-237.

Brewer, A.W., 1949: Evidence for a world circulation provided by measurement of helium and water vapour distribution in the stratosphere, *Quart. J. Roy. Meteor. Soc.,* **75**,351-363

Briceno, S., 2004: Global challenges in disaster reduction. *The Australian J. Emergency Management***, 19 No.l,** 3-5.

Burhanuddin, S.2004: International Nusantara STratification and Transport, INSTANT, *Presented at 1st IOP Meeting, Pune,* 18-20 February 2004.

Burroughs ,W. J. ,1999: The climate revealed ., *Mitchell Beazley, An Imprint of Octopus Publishing Group Ltd, 2-4 Heron Quays,* London; 129pp.

Burt, C., 1952: Tests of significance in factor analysis. *Br. J. Phychol,* 5, 109 - 133.

Byers H. R., 1959: General Meteorology, *McGraw-Hill Book Company Incooperated,* New York, Toronto, London.

Cadet, D., and P Olory-Togbe, 1977: The propagation of tropical disturbances over the Indian Ocean during the summer monsoon. *Mon. Wea. Rev,* **105**,700-708

Cai, W., and T. Cowan, 2007: Trends in the southern Hemisphere circulation in IPCC AR4 models over 1950-99: Ozone depletion versus greenhouse forcing. *J. Climate,* **20, No.4,** 681-693.

Camberlin, P, 1997: Rainfall anomalies in the source of the Nile and their connection with the Indian summer monsoon. *J Climate,* **10,** 1380- 1392.

Carson, D.J., 1998: Seasonal forecasting. *Q.J.R. Meteorological Society,* 124, 1 - 26.

Catell, R.B., 1966: The scree test for the number of factors.A/w/f/vtfr *Behav. Res.,* 1, 245-276.

Challinor, A.J., J.M. Stingo, T.R. Wheeler and P.Q. Cranfurd, D.I.F.Grimes, 2003: Towards a Combined Seasonal Weather and Crop Productivity Forecasting System: Determination of the working spatial scale. *J. Appl. Meteorology,* **42,** 175-192.

Chambers, D. P., B.D. Tapley and R. H. Stewart, 1999: Anomalous warming in the Indian Ocean coincident with El Nino. *J. Geophys. Res.,* **104,** 3035-3047.

Chang, P., 1998: The Unusual tropical Atlantic Ocean temperatures Cause climate swings in Brazil and West Africa. *Quarterdeck***, 2, No.2,** summer, 1998, http://www-ocean.tamu.edu/ Quarterdeck/ QD6.2/chang.html#modeI

Chang, C.-Y., J. A. Carton, S. A. Grodsky, and S. Nigam, 2007: Seasonal Climate of the Tropical Atlantic Sector in the NCAR Community Climate System Model 3: Error Structure and Probable Causes of Errors. *J. Climate,* **20,**1053-1070

Chervin, R. M., and M. Druyan, 1984: The influence of ocean surface temperature gradient and continentality on the Walker circulation. Part I: Prescribed tropic changes. *Mon Wea Rev*, 112, 1510-1523.

Child, D, 1990: Essentials of Factor Analysis, *2nd Ed. Cassell Educational Ltd.* pp 119.

Chiodi, A. M, and D. E. Harrison, 2007: Mechanisms of summertime subtropical southern Indian Ocean sea surface temperature variability: on the importance of humidity anomalies and the meridional advection of water vapour, *J. Climate,* **20, No. 19,** 4835-4852.

Chow, V.T., 1964: Handbook of applied hydrology. *Mc Graw-Hill Book Company,* New York

Chu, P. C., 1989: Relationship between thermally forced surface wind and sea surface temperature gradient. *J. Pure and Applied Geophysics,* 130, No. 1,31-45.

Clark, C. O., P. J. Webster and J. E. Cole, 2003: Interdecadal variability of the relationship between the Indian Ocean Zonal Mode and East African coastal rainfall anomalies. J. *Climate*, 16, 548-554.

Claud, C, and P. Terry, 2007: Revisiting the possible links between Quasi-biennial oscillation and Indian summer monsoon using NCEP R-2 and CMAP. J. climate, 20 No. 5, 773-787

Colberg, F., and C.J.C. Reason, 2004: South Atlantic response to El-Nino-Southern Oscillation induced climate variability in an ocean general circulation model. *J. Geophys. Res.,* **109,** C12015, 14pp.

Collimore, C., D.W. Martin, M.H. Hitchman, A. Huesmann, and D.E. Waliser, 2003: On the relationship between the QBO and Tropical Deep Convection. *J. Climate, 16,* 2552-2558.

Craddock, J.M., and C.R. Flood, 1969: Eigenvectors representing the 500 mb geopontential surface over the northern hemisphere. *Quart. Jounr. Roy. Met. Soc.,* **95,** 576-593.

Craddock J.M., and Flintoff, 1970: Eigenvector representation of Northern hemisphere fields. *Quart. J. Roy. Met. Soc.,* 96, 124-129.

De, U.S. and R.K. Mukhopadhyay, 1999: The effect of ENSO/Anti-ENSO on northeast monsoon rainfall. *Mausam,* 50, No. 4, 343 - 354.

Delsole, T., **J.** Shukla, 2002: Linear Prediction of Indian Monsoon Rainfall. *J. Climate,* **15,** 3645-3658

Dong , S., and K. A. Kelly ,2004: Heat budget in the Gulf Stream Region: The importance of heat storage and advection. *J. Phys. Oceanogr.,* **34 No. 5,** 1214-1231

Drbohlav, H. K. L., S. Gualdi, A. Navarra: 2007: A Diagnostic Study of the Indian Ocean Dipole Mode in El Nino and Non-El Nino Years. *J. Climate,* **20,** 2961-2977

Druyan, L.M, M. Fulakeza, P. Lonergan, 2002: Dynamic Downscaling of seasonal Climate Predictions over Brazil. *J. Climate,* **15,** 3411-3426

Dyer, T.G.J., 1975: The assignment of rainfall stations intohomogeneous groups. An application of Principal Component analysis. *Quart. J. Roy. Meteor. Soc.,* **101,** 1005-1013.

EAMD, 1962: The climate seasons of East Africa. *E.A.M.D. pamphlet,* **No. 8,** Nairobi, Kenya, 1962.

Eldaw, A.K., J.D. Salas, and L.A. Garcia, 2003: Long-range Forecasting of the Nile River Flows Using Climatic Forcing. *J. Appl. Meteor.,* **42,** 890-904.

EMS, 1984: *World Map,* lppElsner, J.B, 2003: Tracking Hurricanes. *Bull. Amer. Meteor. Soc.,* **84,** 353-356.

England, M. H., and F. Huang, 2005: On the interannual variability of the Indonesian through flow and its linkage with ENSO., *J Climate,* 18,1435-1444.

Fabbian, D., R. de Dear, and S. Lellyett, 2007: Application of Artificial Neural Network Forecasts to Predict Fog at Canberra International Airport. *Weather and Forecasting, 12* **No.2,** 372-381

Fedorove, A.V., S.L. Harper, S.G. Philander, B. Winter and A Wittenber, 2003: How predictable is El-Nino. *Bulletin Amer. Meteo. Soc.,* 84, 911-919.

Findlater, J., 1969a: A major low-level air current near the Indian Ocean during the northern summer. *Quart. J. Roy. Meteor. Soc*., 95, 362-380

Findlater, J., 1969b: Interhemispheric transport of air in the lower troposphere over the western Indian. *Quart. J. Roy. Meteor. Soc.,* 95, 400-403

Findlater, J., 1971: Mean monthly airflow at low levels over the western Indian Ocean. *Geophys. Mem.,* **No.** 115, HMSO London, UK

Findlater, J., 1974: The low-level cross equatorial air current of western Indian Ocean during Northern Summer. *Mon. Wea. Rev.,* 29, 411-416

Firth, L., M.L. Hazelton, and E.P. Campbell, 2005: Predicting the onset of Australian winter rainfall by non-linear classification. J. *Climate,* 18, 772-781.

Fisher, Sir R.A, 1958: Statistical methods for research workers. *13th Edition, Oliver and Boyd, Edinburgh: Tweedale Court, London:* 39A Welbeck Street, W.I., 351 pp.

Folland, C., T. Palmer, and D. Parker, 1986: Sahel rainfall and worldwide sea surface temperatures. *Nature,* **320,** 602-606.

Folland, C.K, J. Owen, .M. N. Ward and A Colman, 1991: Prediction of seasonal rainfall in the Sahel region using empirical and dynamic methods. *J. Forecasting***, 10,** 21-56

Folland, C.K., A.W. Colman, D.P. Rowell and M.K. Davey, 2001: Predictability of Northeast Brazil Rainfall and Real Time Forecast Skill, 1987-98. *J. Climate,* **14,** 1937-1958

Franchito, S. H., V. B. Rao, P. R. B. Barbieri, C. M. E. Santo, 2008: Rainy-Season Duration Estimated from OLR versus Rain Gauge Data and the 2001 Drought in Southeast Brazil, J. *Appl. Meteor, and Climatol.,* **47,** 1493-1499

[r]rankel, D.S., J.S. Draper, J.E. Peak, and J.C. Mcleod; 1995: Artificial Intelligence needs workshop 4-5 November 1993, Boston, Massachusetts. *Bull. Amer. Meteor. Soc.,* **76,** 728 - 738.

Frankignoul, C., and E. Kestenare, 2005: Observed Atlantic SST Anomaly Impact on the NAO: An Update. *J. Climate*, 18, 4089-4094

Frankignoul, C.,and N. Sennechael, 2007: Observed influence of North Pacific SST anomalies on the Atmospheric Circulation. *J. Climate,* **20, No. 3,** 592-606

Franchito, S. H., V. B. Rao, P. R. B. Barbieri , and C. M. E. Santo, 2008: Rainy-Season Duration Estimated from OLR versus Rain Gauge Data and the 2001 Drought in Southeast Brazil, J. *Appl. Meteorol. and Climatol,* **47,** 1493-1499

Fratantoni, D. M., W. E. Johns, T. W.Townsend and H. E. Hurlburt, 2000: Low-latitude circulation and mass transport pathways in a model of tropical Atlantic Ocean. *J. Phys. Oceanog.,* 30, 1944-1966.

Frederiksen, C. S., H Zhang, R C. Balgovind, N. Nicholls, W.Drosdowsky, and L Chambers, 2001: Dynamical Seasonal Forecasts During the 1997/98 ENSO Using Persisted SST Anomalies. *J Climate***, 14,** 2675-2695

Fremming, D., 1970: Notes on easterly disturbances affecting East Africa 5-7 Sept 1967, *EAMD, Techn. Memo.,* No. 13, 13 pp.

French, N.N., W.F. Krajewski, and R.R. Cuy Kendal, 1992: Rainfall forecasting in space and time using neural network. *J. Hydrology*, 137, 1-31.

Fu, X., B. Wang, and T. Li, 2002: Impacts of air sea coupling on the simulation of mean Asian Summer Monsoon in the ECHAM 4 Model. *Mon. Wea. Rev.,* **130,** No. **12,** 2889-2904

Fu, X., B. Wang, D. E. Waliser, and L. Tao, 2007: Impact of atmosphere-ocean coupling on the predictability of monsoon intraseasonal oscillation. *J. Atmos. Sci***., 64, No**.l, 157-174.

Georgakakos, K. P., and N. E. Graham, 2008: Potential Benefits of Seasonal Inflow Prediction Uncertainty for Reservoir Release Decisions,./. *Appl. Meteor, and Climatol.* ,47, 1297-1321

Gichuiya, S.N., 1970: Easterly disturbances in the southeast monsoon. *Proc. Symp. On tropical Met, Honolulu,* Hawai

Gill, A. E, 1980: Some simple solutions for heat induced tropical circulation. *Q J R Meteo Soc,* **106,** 447 - 462

Glahn, H, 1963: Canonical correlation and its relationship to discriminate analysis and multiple regressions. *J. Atmos Sci,* **25,** 23-31.

Goddard, L., and N.E. Graham, 1999: Importance of the Indian Ocean for simulating rainfall anomalies over eastern and southern Africa. *J. Geophysical Research,* **104, No. D16,** 19099-19116.

Goddard, L., S. J. Mason, S. E. Zebiak, C. F. Ropelewski, R. Basher and M. A. Cane, 2000: Current Approaches to Seasonal to Interannual Climate Predictions. 62pp. http://www.ogp.noaa.gov/mpe/csi/econhd/fy99/lach99.htm

Godfrey J.S., A. Alexiou, A.G. llahude, M.E.Luther, J.P.McCreary, Jr., G.A. Meyers, K. Mizumo, R. R. Rao, S.R. Shetye, J. H. Toole, S. Wacongne, 1995: The role of the Indian Ocean in the global climate system: Recommendations regarding the global ocean observing system., *OOSDP Background Report*, No. 6, 89pp

Gorawiker, V., V. Thapliyal, R. P. Sarker,G. S. Mandal, and D.R. Sikka,1989: Parametric and power regression models: New approach to long range forcasting of monsoon rainfall in India. *Mausam,* 40,115-122

Greenfield, R.S., and M. Fisher, 2003: Improving Responses to Climate Predictions: An introduction. *Bull. Amer. Meteor. Soc.,* **84,** 1685-1685.

Gregory, S., 1975: On the delimitation of recent climatic situations. *Weather*, 30, 276-287.

Greischar, L. and S. Hasternrath, 2000: The rainy season for the 1990s in northeast Brazil: Real-time Forecasts and Verification. *J. Climate,* **13,** 3821-3826

Griffith, J.F., 1958: Climatic zones of East Africa. *East African Agricult. J.,* **23,** 179-185.

Grimmer, M., 1963: The space filtering of monthly surface temperature anomaly data in terms of patterns using the emperical orthogonal functions. *Quart. Journ. Roy. Meteor Soc.,* **89,** 395-408.

Grodsky, S. A., and J. A. Carton, 2003: The Intertropical Convergence Zone in the South Atlantic and the Equatorial Cold Tongue. *J. Climate,* 16, 723-733

Gross, M.G., 1972: Oceanography-A view of the Earth, *Prentice-Hall, Inc., Eaglewood Cliffs, New Jersey,* 58 lpp

Hall, J. D, A.J. Matthews, and D.J. Karoly, 2001: The modulation of tropical cyclone activity in the Australian region by the Madden - Julian Oscillation, MJO). *Mon. Wea. Rev.,* **129, No. 12,** 2970 - 2982

Harman, H.H., 1967: Modern Factor Analysis. Chicago Univ. Press, pp 469

Harrison, D. E., and M. Carson, 2007: Is the world ocean warming? Upper ocean temperature trends: 1950-2000. *J. Phys. Oceanogr.,* **37, No. 2,** 174-187.

Hashizume, H., S-R Xie, N. Fujwana, M. Shiotani, T. Watanabe, Y. Tanimoto, W.T. Liu, and K. Takeuchi, 2003: Direct Observations of Atmospheric Boundary layer response to SST variations associated with tropical Instability waves over the eastern EquatorialPacific. *J. Climate*, 15, 3379 - 3393

Hastenrath, S., and L. Heller, 1977: Dynamics of Climate Hazards in the Northeast Brazil. *Quart, J. Roy. Meteor. Soc.,* **103,** 77-92

Hastenrath, S., 1986: On climate prediction in the tropics. *Bull. Amer. Meteor. Soc.,* 67, 696-702

Hastenrath, S., 1990: Recent advances in tropical climate prediction. *J Climate*, 8, 1519 - 1532

Hastenrath, S..1995: Recent advances in tropical climate prediction. *J. Climate,* 8,. 1519-1532

Hastenrath, S., A. Nicklis and L. Greishar, 1993: Atmospheric-hydrospheric mechanisms of climate anomalies over the western equatorial Indian Ocean. *J. Geophys. Res,* **98,** 20 219-20 235.

Hasternrath, S. and D. Polzin, 2004: Dynamics of the surface wind field over the equatorial Indian Ocean, *Q.J.R. Meteor. Soc,.* 130, 503-517

Hendon, H.H., M. C. Wheeler and C. Zhang, 2007: Seaonal dependence of the MJO-ENSO relationships. *J. Climate,* **20,** NO.3, 531-543

Hickey, H. and A.J. Weaver, 2004: The southern Ocean as a source region for tropical Atlantic variability. *J. Climate*, 17, 3960-3972

Hsieh, W. W., 2004: Nonlinear multivariate and time series analysis by neural network methods. *Rev. Geophysics***, 42, RG1003/2004,** 25pp

Hsu, K.-L., X. Gao, S. Sorooshian and H. V. Gupta, 1997: Precipitation estimation from remotely sensed information using artificial neural networks. *J. Applied Meteorology*, 36, 1176 - 1190.

Hu, Z.-Z., and B. Huang, 2006: Physical Processes Associated with the Tropical Atlantic SST Meridional Gradient. *J. Climate*, 19, 5500-5518

Huang, B., P. S. Schopf, and Z. Pan, 2002: The ENSO effect on the tropical Atlantic variability: A regionally coupled model study. *Geophys. Res. Lett.,* **29,** 2039, doi: 10.1029/2002GL014872.

Huang, B., and J. Shukla, 2007: Mechanisms for the Interannual Variability in the Tropical Indian Ocean. Part I: The Role of Remote Forcing from the Tropical Pacific, *J. Climate***, 20,** 2917-2936

Hwang, S.-O., J-K. E. Schemm, A. G. Barnston and W-T. Kwon, 2001: Long-lead seasonal forecast skill in far eastern Asia using canonical correlation analysis. *J. Climate,* **14,** 3005-3016.

ICPAC, 2006:Seasonal Prediction For September- December 2006 Rainfall Using Empirical Statistical Models, *Capacity Building Training Workshop for The Great Horn Of Africa (GHA) Regions, IGAD Climate Prediction and Application Centre,* Nairobi-Kenya 14-30 August 2006

ICPAC, 2008: Seasonal Prediction for March- May 2008 Rainfall Using Empirical Statistical Models, *Pre-Forum Capacity Building Training Workshop for Burundi, Djibouti, Eritrea, Ethiopia, Kenya, Rwanda, Somalia, Sudan, Tanzania And Uganda, Nairobi, Kenya*, 10-26 February 2008.

Ihara, C., Yochanan Kushnir, and Mark A. Cane, 2008: Warming Trend of the Indian Ocean SST and Indian Ocean Dipole from 1880 to 2004, *J. Climate***, 21.,** 2035-2046

Indeje, M., 2000: Prediction and numerical simulation of regional climate of equatorial eastern Africa. *PhD Thesis, North Carolina State University,* U.S.A. pp 327

Indeje, M., Semazzi, F.H.M., Ogallo L. J., 2000: ENSO signals in East African rainfall seasons. *Int. J. Climatology***, 20,** 19-46.

Indeje, M. and Semazzi, F.H.M, 2000: Relationships between QBO in the lower equatorial stratospheric zonal winds and East African seasonal rainfall, *Meteorol. Atmos. Phys.,* 73, 227-244

Ininda, J., 1998: Numerical simulation of the influence of the sea surface temperature anomalies on March-May rainfall over East Africa. *Proc. 4th Kenya Meteor. Soc. Workshop on Meteor. Res., Appl. and Services,* Mombasa-Kenya 7-11 September 1998 pp 192-197.

IPCC, 2007: Climate Change 2007: Synthesis Report, 73pp

ISDR, 2005: *World Conference on Disaster Reduction, 18 to 22 January 2005, Kobe,* Hyogo Prefecture, Japan.

ISDR, 2006: People affected by natural disasters in the period 1971-2000 *http://w\vw. unisdr. ore/*

Janowiak, J.E., 1988: An investigation of interannual rainfall variability in Africa, J. Climate, 1, 240-255.

Janowiak, J., 1992: Tropical Rainfall: A comparison of satellite-derived rainfall estimates with model precipitation forecasts, climatologies and observations; *Mon. Wea. Rev.,* **120,** 448-426

Jochum, M., C. Deser, and A Phillips, 2007: Tropical Atmospheric Variability forced by ocean internal variability. *J. Climate***, 20,** 765-771

Jolliffe, I. T., 2002: *Principal Component Analysis*, 2nd Ed. Springer, 487pp.

Julian, P. R. and R. M. Chevrin, 1978: A study of the southern oscillation and Walker phenomenon, *Mon. Wea. Rev.,* **106,** 1433-1451

Jury, M. R., B. Pathack and B. Parker, 1999: Climatic determinants and statistical prediction of tropical cyclone days in the Southwest Indian Ocean. *J Climate, 12,* 1738-1746.

Kaiser, H.F., 1959: Computer programme for varimax rotation in factor analysis. *Educ. Psychol. Meas.,* **19**,413-420.

Kaiser, H.F., 1960: The application of electronic computers to factor analysis. *Educ. and Psycol. Meas.,* **20,** 141-151.

Kalnay, E, M Kanamistu, R. Kistler, W. Collins, d Deavan, L. Gandiu, M. Iredell, S. Sana, G. White, J. Woolen, Y. Zhu, M. Chelliah, W. Ebusaki, W. Higgins, J. Janowiak, K. C. Mo, C. Ropelewski, J. Wang, A. Leetmaa, R. Reynolds, R. Jenne, and Denniss J., 1996: The NCEP/NCAR 40-YEAR Reanalysis Project. *Bull Amer Meteor. Soc.,* 77, NO 3, 437-471

Kanamitsu, M., W. Ebisuki, J. Wollen, S. K Yang, J. J. Hnilo, M. Fiorino and G. L. Potter ,2002: NCEP -DOE AMIP - II reanalysis ,R-2, *Bull. Amer. Meteor. Soc*,, 83, No. 11, 1631-1643

Kane, R P ,1998: El-Nino, Southern Oscillation, equatorial eastern Pacific sea surface temperatures and summer monsoon rainfall in India., *Mausam,* 49, 103 - 114.

Kanemba, A. D., 1993: The use of ocean-space observations to forecast rainfall at the coast of East Africa (Kenya and Tanzania) during the dry-cool season: June-August. *Proc. 3rd Technical conference on meteorological Research in eastern and southern Africa*, Arusha, Tanzania, 22-26 February 1993. pp53-56.

Karl, T.R, A.S. Koscielny and H.F. Diaz, 1982: Potential errors in the application of principal component (eigenvectors) Analysis to gyophysical data. *Journ. Appl Meteor.,* 21, 1183-1186.

Kate, E.J., 1997: Waves along the equator in the Atrlantic. *J. Physcal Oceanogr*., 27 No 12, 2536 - 2544

Katz, E .J., 1997: Waves along the equator in the Atlantic. *J. Physc. Oceanogr.* 27, 2536-2544.

Kayano, M. T. and R. V. Andreoli, 2007: Volume Relations of South American summer rainfall interannual variations with the Pacific Decadal Oscillation. *Int. J. Climatol*.**, 27, No. 4** , 531 - 540

Keenlyside, N. S., M. Latif, J. Jungclaus, L. Kornblueh and E. Roeckner, 2008: Advancing decadal-scale climate prediction in the North Atlantic sector, *Nature* **, 453,** 84-88

Keller, K., C. Deutssch; M. G. Hall; And D. F. Bradford, 2007: Early detection of changes in the north Atlantic meridional overturning circulation: Implications for the design of ocean observation systems. *J. Climate***, 20 No. 2,** 145-157

Kettleborough, J. A., B. B. B. Booth, P.A. Stott, and M. R. Allen, 2007: Estimates of uncertainty in predictions of global mean surface temperature. *J. Climate***, 20, No.5,** 843-855

Kinuthia, J. H, S. S. B. Otengi, M W Macodras, J. O. Odak, S. M. Gachara and P. D. Munah ,1988: Towards the forecasting of seasonal rains in Kenya. *Kenya Met Dept IMTR Res Report,* No 1/88, 18pp.

Kirtman, B. P., J. Shukla, B. Huang, Z. Zhu, and E. K. Schneider, 1997: Multiseasonal Predictions with a Coupled Tropical Ocean-Global Atmosphere System. *Mori. Wea. Rev.,* **125,** 789-808

Kleemam, R., 2007: Information flow in ensemble weather prediction. *J. Atrnos. Sci.,* 64, No.3, 1005-1016.

Kohler, M. A., 1949: On the use of double mass analysis for testing the consistency of, Meteorological records and for making required adjustment. *Bull. Amer. Met. Soc*., 30, 188-189.

Komutunga, E. T, 2006: Optimum cropping calendars derived for rain-fed agriculture of Uganda. *PhD Thesis, Department of Meteor. University of Nairobi,* Kenya.93pp

Korecha, **D., and A. N.** Barnston, 2007: Predictability of June-September rainfall in Ethiopia. *Mon. Wea. Rev.* **135, No.2,** 628-650.

Koster, R. D., M. J. Suarez and M. Heiser, 2000: Variance and Predictability of precipitation at seasonal-to-interannual time scales. *Journ. Hydrometeorolog)>,* 1 No.l, 26-46

Krishnamurthy, V., and B. P. Kirtman, 2003: Variability of the Indian Ocean: Relation to monsoon and ENSO. Quart. *J. Roy. Meteor. Soc.,* **129,** 1623-1646.

Krishnamurthy, V., and J. Shukla, 2007: Intraseasonal and Seasonally Persisting Patterns of Indian Monsoon Rainfall. *J. Climate***, 20, No.l,** 3-20.

Kug, J-S., S.-I. An, F-F. Jin, and I-S. Kang, 2005: Preconditions for El Nino and La Nina onsets and their relation to the Indian Ocean. *Geophys. Res. Lett.,* 32, L05706.

Kug, J-S, B. P. Kirtman, and I-S. Kang, 2006: Interactive Feedback between ENSO and the Indian Ocean in an Interactive Ensemble Coupled Model. *J. Climate,* **19,** 6371-6381

Kug, J-S., and I-S. Kang, 2006: Interactive feedback between the Indian Ocean and ENSO. *J. Climate,* **19,** 1784-1801.

Kug, J. -S., J.-Y. Lee, and I.-S. Kang, 2007: Global Sea Surface Temperature Prediction Using a Multi-model Ensemble. *Mon. Wea. Rev.* **135,** 3239-3247

Kuligowsk; R.S. and A.P. Brros, 1998: Experiments in short-term precipitation forecasting using artificial neural networks. *Monthly weather Review, 126,* 470 - 482

Kuleshov, Y, L. Qi, R. Fawcett, D. Jones, 2008:0n tropical cyclone activity in the Southern Hemisphere: Trends and the ENSO connection, *Geophysical Research Letters,* **35,** L14S08, doi:10.1029/2007GL032983

Kumar, A and M. P. Hoerling, 2000: Analysis of a conceptual model of seasonal climate variability and implications for seasonal prediction, *Bull. Amer. Meteorol. Soc, 81, No 2,* 255-264

Kushnir, Y., W. A. Robinson, P. Chang, and A. W. Robertson, 2006: The physical basis for predicting Atlantic sector seasonal-to-interannual climate variability. *J. Climate,* **19,** 5949-5970.

Kutzbach, J.E., 1967: Empirical eigenvectors of sea level pressure, surface temperature, and precipitation complexes over North America. *Jourrt. Appl. Meteor*., 6, 791-802.

Lamb. P. J., 1978: Case studies of Tropical Atlantic Surface Circulation patterns during recent sub-Saharan weather anomalies: 1967 and 1968, *Mon Wea. Rev,* **106,** 482-491.

Latif, M., M. Collins, H. Pohlmann, and N. Keenlyside, 2006:A Review of Predictability Studies of Atlantic Sector Climate on Decadal Time Scales. *J. Climate,* **19,** 5971-5987

Lau, N C, 1985: Modeling the seasonal dependence of the atmospheric response to observed **El-**Nino in 1962-1976. *Mon Wea Rev,* **113,** 1970- 1996

Lau, N.-C., 1997: Interactions between Global SST anomalies and the mid latitude Atmospheric circulating, *Bull. Amer. Metero. Soc,* **78,** No 1, 21-33.Lau K M, H T Wu and S Bony, 1997: The role of large-scale atmospheric circulation in the relationship between tropical convection and sea surface temperature. J *Climate,* **10,No 3,** 381-392.

Lee, T. C. K., F. W. Zwiers, X. Zhang, and M. Tsao, 2006: Evidence of Decadal Climate Prediction Skill Resulting from Changes in Anthropogenic Forcing. *J. Climate***, 20, No.19,** 5305-5318.

Leetmaa, A, 2003: Seasonal Forecasting, *Bulletin Amer. Meteor. Soc.,* **84,** 1686-1691.

Li, S., W.A. Robinson, M.P. Hoerling and K. M. Weickmann, 2007: Dynamics of the extratropical response to a tropical Atlantic SST anomaly. *J. Climate,* **20, No.3,** 560-574.

Li, F., and Q. Zeng, 2008: Statistical Prediction of East Asian Summer Monsoon Rainfall Based on SST and Sea Ice Concentration, *J. Meteorol. Soc. Japan*, **86 , No. 1,** 237-243

Li, S., L. Goddard, and D. G. DeWitt, 2008: Predictive Skill of AGCM Seasonal Climate Forecasts Subject to Different SST Prediction Methodologies, *J. Climate*, 21, 2169-2186

Lindzen, R.S., and S. Nigam, 1987: On the role of sea surface temperature gradients in forcing low-level winds and convergence in the tropics. *J. Atmos. Sci*., 44, 2418-2436.

Liu, C., Edward J. Zipser, and S. W. Nesbitt, 2007:Global Distribution of Tropical Deep Convection: Different Perspectives from TRMM Infrared and Radar Data, *J. Climate,* **20 No.3,** 489-503

Livezy, R.E., M. Masutani, and M. Ji, 1996: SST-Forced seasonal simulation and prediction skill for versions of the NCEP/MRF Model, *Bull. Amer. Meteor. Soc.;*77, 507-517

Long, J. J. Jin, and Y. Cai, 2005: A short-term climate prediction model based on a modular fuzzy neural network. *Advances Atmospheric Sciences,* **22, No.3,** 428-435

Lorenz, E. N., 1963: Deterministic nonperiodic flow. *J. Atmos. Sciences.,* 20 : 130—141 Losada T, B. Rodrguez-Fonseca, C.R. Mechoso and H-Y. Ma, 2007: Impacts of SST anomalies on north Atlantic atmospheric circulation: a case study for the northern winter 1995/1996, *Climate Dynamics,* **20,** NO. **7-8,** 807-819.

Losada T, B. Rodrguez-Fonseca, C.R. Mechoso and H-Y. Ma, 2007: Impacts of SST anomalies on north Atlantic atmospheric circulation: a case study for the northern winter 1995/1996, *Climate Dynamics,* **20, NO. 7-8,** 807-819.

Loyah, J. M, 1986: Tropical Atlantic Sea Surface temperature and rainfall variations in sub-Saharan Africa. *Mon Wea. Rev.,* **114,** 561- 570

Lumb, F.E., 1966: Synoptic disturbances causing rainy periods along the East African Coast. *Met. Magazine,95,* 150-159

Luo, J.-J., S. Masson, S. K. Behera, T. Yamagata, 2008a:Extended ENSO predictions using a fully coupled ocean-atmosphere model, *J. Climate,* **21.No 1,** 84-93

Luo, J., S. Behera, Y. Masumoto, H. Sakuma, and T. Yamagata (2008), Successful prediction of the consecutive IOD in 2006 and 2007, *Geophys. Res. Lett.,* 35, L14S02, doi: 10.1029/2007GL032793 |

Madden, R. A., 1976: Estimates of natural variability of time-averaged sea level pressure. *Mon. Wea. Rev.,* 104, 942-952

Maloney, E. D.,and J. Shaman, 2008: Intraseasonal Variability of the West African Monsoon and Atlantic ITCZ,./. *Climate,* **21,** No **12,** 2898-2918

Marmorino, G. O., G. P. Smith, and G. J. Lindemann, 2004: Infrared imaging of ocean internal waves. *Geophys. Res. Letters,* **111309,** 4pp.

Martin, A., and F. Lott, 2007: Synoptic responses to mountain gravity waves encountering directional critical levels. *J. Atrnos. Sci.,* **64,** No.3, 828-848

Mason, S. J., L. Goddard, N. E. Graham, E. Yulaeva, L. Sun, and P. A. Arkin, 1999: The IRI seasonal climate prediction system and the 1997/98 El Nin~o event. *Bull. Amer. Meteor.* Soc., **80,** 1853-1874.

Matari, E., 1993; Predicting the seasonal rainfall from the onset, cessation and length of growing period. *Proc. 1st Intern. Conf. African Met. Soc.,* Nairobi, Kenya 8-12 February 1993, pp 508-524.

Matthews, A. J., 2008: Primary and successive events in the Madden-Julian Oscillation, *Quart. J. Royal Meteorol. Society,* **134 No. 631,** 439 - 453

Matthews, A.J. 2000: Propagation mechanism for the Madden-Julian oscillation. *Quart. J. Roy. Meteo. Soc.,* **126,** 26367 - 2651

Mauget, S. A. and J. Ko, 2008: A Two-Tier Statistical Forecast Method for Agricultural and Resource Management Simulations, *J. Appl. Meteorol. and ClimatoL,* 47, No 6, 1573-1589

May, P.T. and A. Ballinger, 2007: The statistical characteristics of Convective cells in a monsoon regime (Darwin, Northern Australia). *Mon. Wea. Rev.,* 135, **No.** 1, 82-92

McCann, D.W., 1992: A neural network short-term forecast of significant thunderstorms. *Weather forecasting,* 7, 525 - 534

McGregor, G. R., and Phillips I. D., 2004: Specifications and prediction of monthly and seasonal rainfall over the south-west peninsula of England. *Q.J.R. Meteorol. Soc*, **130,** 193-210.

McPhaden, M. J., M. J., A. J. Busalacchi, R. Cheney, J-R. Donguy, K. S. Gage, D. Halpern, M. Ji, P. Julian, G. Meyers, G. T. Mitchum, P. P. Niiler, J.l Picaut, R. W. Reynolds, N. Smith, and K. Takeuchi 1998: The tropical ocean global atmosphere (TOGA) observing system: A decade of progress. *J. Geophys. Res.,* **103,** 14169-14240.

Meyers, G., P. Mcintosh, L. Pigot, and M Pook, 2007: The Years of El Nino, La Nina, and Interactions with the Tropical Indian Ocean. *Journal of Climate,* **20,** 2872-2880

Meng, L., Y. He, J. Chen, and Y. Wu, 2007: Neural Network Retrieval of Ocean Surface Parameters from SSM/**I** Data. *Mon. Wea. Rev.,* **135,** No.2, 586-597

Meza, F. J., J. W. Hansen and D. Osgood, 2008: Economic Value of Seasonal Climate Forecasts for Agriculture: Review of Ex-Ante Assessments and Recommendations for Future Research, *J. Appl. Meteorol. and Climatol.,* 47, 1269-1286

Misra, V., and Y. Zhang, 2007: The fidelity of NCEP CFS seasonal hindcasts over Nordeste. *Mon. Wea. Rev.,* **135, No.2,** 618-627.

Misra, V., 2007: Addressing the Issue of Systematic Errors in a Regional Climate Model. *Journal of Climate,* **20, No.5,** 801-818

Mo, C.K, J.N. Paegle, and R.N. Higgins, 1997: Atmospheric processes associated with summer floods and droughts in Central United States, *J. Climate,* **10,** 3028 - 3046

Mo, R., and D. M. Straus, 2002: Statistical-Dynamical Seasonal Prediction Based on Principal Component Regression of GCM Ensemble Integrations. *Mon. Wea. Rev.,* **130**,2167-2187

Mokhov, 1.1., D . V. Khvorostyanov, and A.V. Elissen, 2004: Decadal and longer term changes in El Nino -Southern Oscillation characteristics. *Int. J.climatolog*., **24 No.4,** 401-414

Motell, C. E., and B. C. Weare, 1987: Estimating tropical Pacific rainfall using digital satellite data. *J. Appl. Meteor.,* 26, 1436-1446

Moura, A. D., and J. Shukla, 1981: On the dynamics of droughts in northeast Brasil: observations, theory, and numerical experiment with a general circulation model. *JAtmos. Sci,* **38,** 2653-2375.

Mukabana, J R, and R A Pielke, 1993: Three dimensional modeling of the large-scale flows and their interaction with the local meso-scale circulation over Kenya. *Proc. First Intern. Conf. OfSMA,* Nairobi, Kenya, 8-12 February 1993.

Mungai, D.N., 1984: Analysis of some seasonal rainfall characteristics in Lake Victoria region of Kenya. *M.A. Thesis, Department of Geography, University of Nairobi*, Kenya

Mungai, J. G. and Mukabana, J. R., 2003: The current status of NWP model application in forecasting at the Regional Meteorological Centre-Nairobi. *Proc. The sixth Kenya Meteor. Soc. Workshop on Meteor. Research, Applications and Services,* Mombasa, Kenya, 29September to 3 October 2003. pp 51-59

Murakami, T.,1980: Emperical orthogonal Function Analysis of satellite-observed outgoing longwave radiation during summer, *Mon Wea. Rev.,* 108, 205-222

Mutai, C. C., M. N. Ward, and A. W. Colman, 1998: Towards the prediction of the East African Short Rains based on sea-surface temperature - atmosphere coupling. *Int J Climatol,* 18, 975 -997

Mutai, C.C., and M.N. Ward, 2000: East African rainfall and the tropical circulation / convection on intraseasonal to interannual time scales. *J. Climate*, 13, 3915-3939.

Mutai ,C.C, 2003: The role of Indian Ocean SST on East African Short rains. *Proc. The sixth Kenya Meteor. Soc. Workshop on Meteor. Research, Applications and Services,* Mombasa, Kenya, 29 September to 3 October 2003. pp 55-59.

Mutemi, J. N., 2003: *Climate anomalies over East Africa,* PhD Thesis, Department of Meteorology, University of Nairobi. 191pp.

ICPAC, 1999: Homogeneous Climatological Zoning *DMC Lecture Notes, chapter 3,* 29 - 43

Murtugudde, R.G., J.P McCreary, and A.J. Busalacchi, 2000: Oceanic processes associated with anomalous events in the Indian Ocean with relevance to 1997-199, *J Geophys Res.,* **105,** 3295-3306.

Mwale, D., and T.Y. Gan, 2005: Wavelet Analysis of variability, tele-connection, and predictability of the September-November East African Rainfall. *J. Applied Met*, **44,** 256-269.

Nagura, M.and M. Konda, 2007: The Seasonal Development of an SST Anomaly in the Indian Ocean and Its Relationship to ENSO. Journal of Climate, **20, No.l,** 38-52.

Nagura, M, K. Ando, and K. Mizuno, 2008: Pausing of the ENSO Cycle: A Case Study from 1998 to 2002, *J. Climate*, **21, No.2,** 342-363

Namias, J., 1978: Multiple causes of the North American abnormal winter 1976-77. *Mon. Wea. Rev.,* **106,** 279-295.

Namias, J., 1985: Remarks on the long-range forecasting. *Bull. Amer. Meteor. Soc.,* 66 No. 2, 165-173.

Neetin, J.D, D.S. Battish, A.C. Hrist, F.F. Jin U. Wakata, T.Yamagata and S.F.Zebiak, 1998: ENSO theory. *J.Geophys. Res.,* **103,** 14,261 - 14,290..

Ngara, T., 1977: Some aspects of the East African Low Level Jet. *M.sc. Thesis, Dept. of Meteor.,* University ofNairobi. 240pp

Nicholson, S.E, 1986: The spatial coherence of African rainfall anomalies: Interhemispheric teleconnections. *J. Climate and Appl. Meteorol.,* **25,** 1365.

Nicholson S E and D Entekhabi, 1987: Rainfall variability in Equatorial and Southern Africa. Relationships with sea surface temperature along the south-western coast of Africa. *J. Climate Applied Meteor.,* 26, No 5, 561 - 578.

Nicholson, S. E. and J. Kim, 1997: The relationship of the El Nino-Southem Ooscillation to African rainfall. *Int. J. Climatol.,* 17,117.-135.

Nilson, J., 2000: Propagation, Diffusion and Decay of SST anomalies beneath an advective Atmosphere. *J. Phys. Oceanogr*., **30,** 1505 - 1513

Njau, L.N., 1982: Tropospheric wave disturbances in East Africa. *M.Sc Thesis, Department of Meteor. University of Nairobi,* Kenya.

Njau, L N, 1987: Seasonal variability of Kenya rainfall and its teleconnections. *Proceedings First Techn. Conf on Meteorological Res. in eastern and Southern Africa, Nairobi, Kenya, -9 January 1987,* PP 160-165

Njau, L. N., 2006: Diagnostics and predictability of East Africa rainfall with tropospheric circulation parameters. *PhD Dissertation, Department of Meteor.* University of Nairobi, 170pp

Nobre, P. and J. Shukla, 1996: Variations of sea surface temperature, wind stress, and rainfall over the Tropical Atlantic and South America. *J. Climate,* 9, 2464 - 2479.

North, G. R., 1984: Empirical Orthogonal functions and normal modes. *J. Atmos. Sci*., 41, 879-887

North, G.R., T.L. Bell and R.E. Cahalan, 1982: Sampling errors in the estimation of empirical orthogonal functions. *Mon. Wea. Rev.,* 110, 699-706.

Ntale, H.K, T.Y. Gan, and D. Mwale, 2003: Prediction of East African Seasonal Rainfall Using Complex Canonical Correlation Analysis. *J. Climate*, 16, 2105 - 2112.

Nyakwada, W., 1992: Relationships between satellite derived outgoing longwave radiation and some meteorological parameters. *M.Sc. Thesis,* Department of Meteorology, University of Nairobi

Nyakwada, W., L. J Ogallo, E K. Anyamba, 1995: Relationships between satellite derived outgoing longwave radiation and rainfall over East Africa, *J. African Mteoror. Soc*1, 19-27

Nyakwada, W., 2003: Climate risk and vulnerability in Kenya. *Proc. The sixth Kenya Meteor. Soc. Workshop on Meteor. Research, Applications and Services,* Mombasa, Kenya, 29September to 3 October 2003. pp 35-45

OFDA/CRED, 2006: Emergency Events Data Base, http://www.emdat.be/

Ogallo, L.J., 1980a: Time series analysis of rainfall in East Africa, *PhD Thesis Dept. Meteorology, University of Nairobi,* Kenya.

Ogallo, L. J., 1980b: Regional classification of the East African Rainfall stations into homogeneous groups using the method of Principal Component Analysis. *Stat. Climatol. Devel. Atmos. Sci.,* 13, 255 - 266

Ogallo, L J, 1981a: Reliability of rainfall in East Africa, *1MTR, Res Report,* No 5/81.

Ogallo, L.J., 198bI: The nature of homogeneity in rainfall records over East Africa. KMD *Res. Report No. 4/81*

Ogallo, L J, 1982: The persistence of monthly rainfall over East Africa. *IMTR, Res. Report,* **No 3/82,** 25pp.

Ogallo, L.J., 1986: Stochastic modelling of regional annual rainfall anomalies in East Africa. *J. Appl. Statistics***, 13,** 49-55.

Ogallo, L J, 1987a: Teleconnection between rainfall in East Africa and some global parameters. *Proc. First Technical Conference on meteorological Res. In Eastern and Southern Africa, Nairobi, Kenya*, 6-9 January 1987, pp 77-75

Ogallo, L.J., 1987b: Some weather systems associated with the rainfall anomalies over Eastern, Central, and Southern Africa. *Proc. First Tech. Conf Meteor. Research in Eastern and Southern Africa, Nairobi,* Kenya 6-9, January 1987, pp 129-132.

Ogallo, L J, 1988a: Relationships between seasonal rainfall in East Africa and Southern Oscillation. *Int. J. Climatology*, 8, 31-43.

Ogallo, L.J., 1988b: Climatology of rainfall of East Africa. WMO Tropical Meteorology Research Programme, *Rept. No. 28,* pp 136-142

Ogallo, L. J., 1989: The spatial and temporal patterns of the East African seasonal rainfall derived from Principal Component Analysis. *Intern. J. Climatol.* 9, 145-167.

Ogallo, L. J., 1993: Climate change signals over eastern and southern Africa. *Proc. 3rd Technical conference on meteorological Research in eastern and southern Africa,* Arusha, Tanzania, 22-26 February 1993. pp41-46

Ogallo, L. J., and K. A. Suleiman, 1987: Rainfall characteristics in East Africa during the El-Nino years. *Proc First Techn Conf on Meteorological Res. in Eastern and Southern Africa, Nairobi, Kenya, 6-9 January 1987,* pp 6-9 January 1987, pp 76-80.

Ogallo, L. J., J. E. Janowiak, and M S Halpert, 1988: Teleconnections between seasonal rainfall over East Africa and Global Sea Surface Temperature Anomalies. *J Meteorological Society, Japan,* 66, No6, PP 807 -821

Ogallo, L J, R E Okoola, and D.N. Wanjohi, 1994: Characteristics of Quasi-Biennial Oscillation over Kenya and their predictability potential for seasonal rainfall. *Mausam,* **45, No**.l, 57-62.

Ogallo, L. A., M. S. Boulahya and T Keane, 2000: Applications of seasonal to interannual climate prediction in agricultural planning and operations. *Intern. J. Agricultural and Forestry Meteorology,* 103, 159-166.

Okoola, RE A., 1996: Space-time Characteristics of the ITCZ over equatorial Eastern Africa during anomalous rainfall years. *PhD Thesis Department of Meteorology, University of Nairobi,* Kenya 25 lpp

Omeny, **P**.A, 2006: East African Rainfall Variability Associated with the Madden-Julian Oscillation. *MSc. Dissertation, Department of Meteorology, University of Nairobi,* Kenya 66pp

Omondi, P. A., 2005: Potential causes and predictability of the space- time patterns of the decadal rainfall variability modes over east Africa. *MSc Thesis, Department of Meteorology, University of Nairobi,* 150pp

Oort, A., and J.J. Yienger, 1996: Observed inter-annual variability in the Hadley circulation and its connection to ENSO, *J. Climate,* 9, No.l 1, 2751-2767.

OP, 2007 .*National Diaster Mangement Policy, Kenya*

Owiti, O. Z., 2005: Use of the Indian Ocean Dipole indices as predictor east African rainfall anomalies. *MSc Thesis, Department Of Meteorology, University of Nairobi,* 130pp

Oyaya, O. E., 1999: *Macmillan Secondary School Atlas,* Macmillan Education Ltd, 128pp

Palmer, T. N., 1986, Influence of the Atlantic, Pacific, and Indian oceans on Sahel Rainfall. *Nature,* **322,** 251 -253.

Parker, D. E., C. K. Folland, and M. N. Ward., 1988: Sea surface temperature anomaly patterns and prediction of seasonal rainfall in the Sahel region of Africa, *Nature,* **324,** 483-485.

Patricola, C. M., and K. H. Cook, 2007: Dynamics of the West African Monsoon under Mid-Holocene Precessional Forcing: Regional Climate Model Simulations. *J. Climate,* **20, No 4,** 694-716

Pauluis, O., 2004: Boundary layer dynamics and cross-equatorial Hadley circulation. *J. Atmos.Sci,* **61,** 1161-1173

Peng, P., and A. Kumar, 2005: A Large Ensemble Analysis of the Influence of Tropical SSTs on Seasonal Atmospheric Variability., *J. Climate,* **18,** 1068-1085

Phelps, M. W., A. Kumar, J. J. O'Brien, 2004: Potential Predictability in the NCEP CPC Dynamical Seaonal Forecast System, *J Climate,* **17,** 3775-3785.

Pire, C. A., and R.A. P. Perdigao, 2007: Winter monthly precipitation estimation from the NAO., *Mon Wea. Rev.,* **135,** 430-448

Poccard ,1., S. Janicot, and P. Camberlin, 2000: Comparison of rainfall structures between NCEP/NCAR reanalysis and observed data over over tropical Africa. Climate Dynamics, 16, 897-915.

Pothergill, A and L. A. Peek, 2004: Poverty and Disasters in the United States: A Review of Rescent Sociological Findings. *Natural Hazards,* 32, 89-110.

Qiao, F., Y. Yuan, Y. Yang, Q. Zheng, C. Xia, and J. Ma,2004:Wave-induced mixing in the upper ocean: Distribution and application to a global ocean circulation model. *Geophys. Res Letters,* **31,** LI 1303, pp4

Raghavan, S., and S. Rajesh, 2003: Trends in tropical cyclone impact: A study in Andhra Pradesh,, *India Bulletin Amer. Meteor. Soc.,* **84,** 635-644

Rajeevan, M., V. Thapliyal, S.R. Patil, and U.S. De, 1999: Canonical correlation analysis (CCA) model for long-range forecasts of sub-divisional monsoon rainfall over Indian. *Mausam,* **50,** No.2, 145 - 152.

Rajeevan, M., P. Guhathakurta, V. Thapliyal, 2000: New models for long range forecasts of summer monsoon rainfall over north west and peninsular India, *Meteor and Atmos. Physics,* **73, No.3-4,** 211-225

Ramirez, M. C. V., N. J. Ferreira, and H. F. de Campos Velho, 2007: Linear and non-linear statistical downscaling for rainfall forecasting over southern Brazil. *Weather and Forecasting,* **21, No.6,** 969-989

Rao, **P**.S, 2005: Arabian Sea Monsoon Experiment: An overview. *Mausam,* **56, No. 1,** 1-6.

Rao, V. V. M. J., A. N. Babu, S. V. B. Rao, and D. N. Rao, 2007: Anomalous wind circulation observed during 1997/98 El Nino using Indian MST Radar,./ *Appl. Meteor and Climatol.,* **46, No. 1, 112-119.**

Rasmusson, E M, and T H Carpenter, 1982: Variations in tropical sea surface temperature and surface with fields associated with the Southern Oscillation/El-Nino. *Mon. Wea Rev,* **110,** 354 - 384

Reason, C., 2004: Variability of the Atlantir n
DMC-Workshop on Numerical wZ^r n"^ ^
2004. CQl Weather *Prediction,* Nairobi. Krny.. Febmwy

Repelli, C. A., and P. Nobre, 2004- Statistic
tropical Atlantic. *Int. T a ^ o ^ T ^ s T ^* *OV* * *

Reynolds, R. W., N. A. Rayner, T. M. Smith, D. C. Stokes, and W Wan* 2002 An
improved m situ and satellite SST Analysis for C l i m a t ,

Richman, M.B., 1981: Obliquely rotated Principal Components and improved
Meteorological map typing technique. *J. Appl. Meteor.,* 20. 1145-1 H9

Richman, M.B., 1986: Rotation of Principal Components. *J Climatology*. 6 293-VIS

Richter, I , C. R. Mechoso, Los A. L. Angeles, A.W. Robertson, **2008: What Determines On-**
position and intensity of the South Atlantic Anticyclone in **Austral Winter''**
An AGCM Study, *J. Climate,* 21, No. 2, **214-229**

Rinne, J., and S. Jarvenoja, 1979: Truncation of EOF series representing 50Omh bright
Quart. Journ. Roy. Meteor. Soc., 105, 873-

Riviere, G., and I. Orlanski, 2007; Characteristics of the Atlantic Storm-track eddy ac tivity
and its relation with the north Atlantic oscillation., *J Atmos Sci 2A\ ?<><>*

Rodrigues, R. R,, L. M. Rothstein and M Wimbush, 2007: Seasonal **variability** of **the south**
equatorial current bifurcation in the Atlantic Ocean: **A** numerical **Study,**
Phys. Oceanography, 37, 16-30.

Ropelewski, C. F,, and M. S. Halpert, 1987: Global and r e g ™ a l s c a l e ^ t ^ . » o c i « « l
with El-Nino/Southern Oscillation. *Mon. Wea. Rev.*. 115. H.06- IfiJft

Ropelewski, C. F,, and S. M. Ha,pert, 1989: P r e c i p i t a t i o n " " "
index phase of the southern oscillat.on. ./. C ***hmate. 2.***

Al u* nH a 1987: *Tropical marine climatic alia*
Sadler, J. C. M.A. Lander, A. M.Hon, and M L K-W M „ . , „
Vol.1. Indian Ocean and Atlantic ucean.
Hawaii, 5lpp

. .. p h h v 2002: Distinguishing the Influcncc

SAE!KQ° ^ M w ^ m ^ X . -....

Climate. *J. Climate,* 15, 3686-3697.

Saji, N. H, B. M. Goswami, P. N. Vinayachandran, and T. Yamagata, 1999: A dipole mode in the tropical Indian Ocean. *Nature*, **401,** 360-363

Saji, H. N., and T. Yamagata, 2003: Structure of SST and surface wind variability in COADs observations during IOD years. *J. Climate,* 16, 2735-2751.

Salby, M. L, and P. F. Callaghan, 2005: Interaction between the Brewer-Dobson Circulation and the Hadley Circulation, *J. Climate,* 18, 4303-4316

Sansom, H. W., 1955: Prediction of the seasonal rains of Kenya by means of correlation. *Weather*, **10,** 81-86

Sansom, H. W., 1965: The structure and behaviour of the ITCZ. *WMO Tech. Note No.* 69, pp 91-108

Schreck, C. J and F. H. M. Semazzi, 2004: Variability of the recent climate of eastern Africa., *Int. J. Climatol.,* **24,** 681-701.

Scott, R. B., 2003: Predictability of SST in an idealized one dimensional,coupled atmosphere-ocean climate model with stochastic forcing and advection. *J. Climate*, **16,** 323-335.

Seagar, R., R. Murtugudde, N. Naik, A. Clement, N. Gordon and J. Miller ,2003. Air-Sea Interaction and the Seasonal Cycle of the subtropical anticyclone. *J. Climate,* **16,** 1948-1966.

Shabbar, A. and A G Barnston, 1996: Skill of seasonal climate forecasts in Canada using canonical correlation analysis. *Mon. Wea. Rev.* **124,** 2370-2385

Shaw, E.M., 1988: Hydrology in practice, *2nd edition, T.J. Press, Padstow Ltd. Padstow, Cornwall,* Britain

Shongwe, M. E.: 2005: Performance of recalibration Systems of GCM forecasts over Southern Africa. *MSc Thesis, Dept. of Geography, Geoinformatics and Agricultural Sciences, University of Pretoria,* South Africa. 77pp

Schreck, C. J and F. H. M. Semazzi, 2004: Variability of the recent climate of eastern Africa., *Int. J. Climatol.,* **24,** 681-701.

Shukla, J., 1981: Dynamical predictability of monthly means. *J. Atmos. Sci.,* 38, 2547-2572.

Shukla, **J.,** 1991 :Short term climate variability and predictions, *Proceedings Second World Climate Climate Conference,* 29 October-7 November 1990, Geneva, Switzerland, pp203-210

Shukla, J., 1998: Predictability in the Midst of Chaos: A Scientific Basis for Climate Forecasting. *Science,* **282,** 728-731.

Shukla, **J.** J. Anderson, D. Baumhefner, C. Brankoric, Y. Chang, E. Kalnay, L. Marx, T. Paler, D. Paolino, J. Ploshay, S. Schubert, D. Strans, M. Suarez, and J. Tribbia, 2000: Dynamical seasonal prediction. *Bull. Amer. Meteor. Soc.,* 81, 2593-2606.

Singhrattna, N., B Rajagopalan, M Clark, and K K Kumar,2005:Seasonal forecasting of Thailand summer monsoon rainfall, *Int. J. Climatol*., 25, 649-664.

Smith, T. M., and R. W. Reynolds, 2002: Bias corrections for historic sea surface temperatures based on marine air temperatures. *J. Climate,* 15, 73-87.

Smith, T. M. and R. W. Reynolds, 2004: Improved Extended Reconstruction of SST (1854-1997). J. *Climate,* 17, 2466-2477.

Smith, T. M. , R. W. Reynolds, T. C. Peterson, and J. Lawrimore, 2008improvements to NOAA's Historical Merged Land-Ocean Surface Temperature Analysis (1880-2006), ./. *Climate***, 21,** No **10,** 2283-2296

Song, Q., G. A. Vecchi, and A. J. Rosati, 2007: Indian Ocean Variability in the GFDL Coupled Climate Model. *J. Climate,* 20, 2895-2916

Statsoft, *2007-.Notes on neural networks:* http**://www**.statsofl.com/textbook/stneunet.html; http://en.wikipedia.Org/wiki/lmage:Artificial neural network.svg, http://www.sofl32.com/download 10063.html

Stewart, T. S., R. A. Pielke, Jr., and R. Nath, 2004: Understanding User Decision Making and the Value of Improved Precipitation Forecasts: Lessons from a Case Study, *Bull. Amer. Meteorol. Society,* 85, No. 2, 223-235.

Stone, H P and R M Chervin, 1984: The influence of ocean surface temperature gradient and continentality on Walker Circulation. Part II: Prescribed Global changes *Mon. Wea. Rev.,* 112, 1524-1534.

Stone, D. A, M. R. Allen, F. Selten, M. Kliphuis, and P. A. Stott,2007: The Detection and Attribution of Climate Change Using an Ensemble of Opportunity ,J. *Climate,* **20 No.3,** 504-516

von Storch , H. and F. W. Zweirs, 1999: Statistical Analysis in Climate Research. *Cambridge University Press,* 484pp

Stouffer, R. J., D. Seidov, and B. J. Haupt, 2007: Climate Response to External Sources of Freshwater: North Atlantic versus the Southern Ocean. *J. Climate,* **20,** No.3, 436-448

Stockdale, T. N., M. A. Balmaseda, and A. Vidard,2006:Tropical Atlantic SST Prediction with Coupled Ocean-Atmosphere GCMs. *J. Climate,* **19, No.23,** 6047-6061

Stuart, N. A. and R. H. Grumm,2007:using wind anomalies to forecast east coast winter storms. *Weather Forecasting,* **21,** No**.6,** 952-968

Sun, L., H. Li, M. N. Ward, and D. F. Moncunill, 2007:Climate variability and corn yields in semiarid Cear'a, Brazil. *J. Appl. Meteor, and Climatol.,* **46,** 226-240.

Sutton, R. T., and D. L. R. Hodson, 2007: Climate Response to Basin-Scale Warming and Cooling of the North Atlantic Ocean. *J. Climate,* **20,** No.5, 891-907

Swiers, F. W. and H. Von Storch, 2004: On the role of statistics in Climate Research, *Intern J. Climatol,* **24,** 665-680.

Tanaka, K. L., N. Ishizaki and A. Kito, 2004: Trend and interannual variability of Walker, monsoon and Hadley circulations defined by the velocity potential in the upper troposphere. *Tellus,* **56A** No.3, 250-269.

Tang, B., W. W. Hsieh, A. II. Monahan, and F. T. Tangang, 2000: Skill Comparisons between Neural Networks and Canonical Correlation Analysis in Predicting the Equatorial Pacific Sea Surface Temperatures. *J. CI im ate,* 13,287-293

Tarhule, A. and P. J. Lamb, 2003: Climate, research and Seasonal Forecasting for West Africans, Perceptions, Dissemination and Use? *Bull. Amer. Meteor. Soc.,* **84,** 1741-1759.

Terray, P., and S. Dominiak, 2005: Indian Ocean Sea Surface Temperature and El Nino Southern Oscillation, *J Climate,* 18,1351-1368

Thiessen, A.H., 1911: Precipitation averages for large areas. *Mon. Wea., Rev.,* 39, 1082-1084.

Thorn, H.C.S., 1966: Some methods of climatological analysis. *WMO Techn. note.* No. 81.

Thompson, B. W., 1957: The diurnal variation of precipitation in British East Africa. *EAMD Techn. Memo.* NO. 8, 70pp

Tomsett, J.E., 1969: Average monthly and annual rainfall of E. Africa. *EAMD Techn. Memo.* **No. 14.**

Tozuka, T., J-J. Luo, S. Mason, and T. Yamagata, 2007: Decadal Modulations of the Indian Ocean Dipole in the SINTEX-F1 Coupled GCM. *J. Climate,* **20,** 2881-2894

Trewartha, G.T., 1961: The earth problem climates, *University of Wisconsin Press, Madison,* 371PP.

Tschuck, T, F. Chauvin, B. Dong, And K. Arpe, 2004: Impact of sea-surface temperature anomalies in the equatorial Indian ocean and western pacific on the Asian summer monsoon in three general circulation models, *Int. J. Climatology,* **24,** 181-191

UNDP, 2002: The factoring of weather and climate into disaster management. *ICPAC/KMD,* lOOpp

UNEP, 1992: Preparing for Drought: *A guide book for developing countries.* 78pp.

Usman, M.T., Archer, P. Johnston and M. Tadross, 2005: A conceptual Framework for Enhancing the Utility of the Rainfall Hazard Forecasts for Agriculture in Marginal Environments; *Natural Hazards,* **34,** 111-129.

Valsala, V. K. and M. Ikeda, 2007: Pathways and Effects of the Indonesian Throughflow Water in the Indian Ocean Using Particle Trajectory and Tracers in an OGCM., *J Climate***, 20, No.13,** 2994-3017

Vialard, J., F. Vitat, M.A. Balmased, T.N. Stockdale, and D.L.T. Anderson, 2005: An Ensemble Generation Method for Seasonal Forecasting with Ocean-atmosphere coupled model. *Mon. Wea. Rev.,* 133, 441-453.

Vidyunmala, V., R. S. Nanjundiah, and J. Srinivasan, 2007: The effect of variation in sea-surface temperature and its meridional gradient on the equatorial and off-equatorial ITCZ in an Aquaplanet General Circulation model. *Journal Meteorology and Atmospheric Physics***, 95, No. 3-4,** 239-253.

Wajsowicz, R. C., 2004: Climate Variability over the Tropical Indian Ocean Sector in the NSIPP Seasonal Forecast System. *J. Climate,* **17,** 4783-4804.

:: Atlantic climate variability anH it*
/. ***Climate,*** 15, 1516-1536. * aSSoClated atmospheric circulation cells.

• A B Eltahir, 1999 Use of FNcn
Forecasting of The Nile In F ^ ^ Long- Kange

^<es. 0fE1"NIn° Changed - ^

and its ^pacts on
Asian Australian Monsoon variation. *J. Climate,* **16,** 1195-1211.

iP Chang, 2004: Effect of oceanic advection on the potential predictability of sea surface temperature. *J Climate*, **17, 3603-3615.**

J . and I H.Wanncott, 1985: Introductory statistics, *4th edition ,1985, John - Wiley **and Sons***, **New York.**

I99K Diagnosis and short-lead time prediction of summer rainfall in tropical North Africa at inter-annual and multi-decadal Timescales. *J. Climate,* **1,** 3167-3191

. and C. K Holland, 1991: Prediction of seasonal rainfall in the north nordeste of Brazil using eigenvectors of sea surface temperature. *J climatol.,* 11, 711-743.

r., A G. **Barnston,** and V. Kumar, 1999: Prediction^ of) African rainfall on the **seasonal** timescale. *J. Geophysics. Res.,* **104,** D24, 31589-31597

1 M., 2004: Asia Jet Wave guide and a do^ns^e7a!^46n^tenS*0n of ^ ^ Atlantic Oscillation, *J. Climate,* **17, No** 24, 4674-4691

35 The World Climate Research Programme Strategtc hram ctratpair Framework 2005-2015,
WRCP-123. WMO/TD-NO.1291, 59P1'

• • „f Atlantic ocean surface temperatures,
1977: Empirical Orthogonal Analysts of Atlant.c
Quart J R.Mel. Soc., 103,467-478.

9007- Dobson Circulation and solar
.. S. Dhomse. S. Dikty and J.. *SPARC saence vorksHop,*
variability in **ozone-c**.imate
Bremen, Germany, 17-19 bepien

^ ebster, P. J.} 1972: Responses of tropical atmosphere to local steady forcing. *Mon Wea Rev,* **100,** 518- 541.

W **ebster, P. J.,** A. M. Moore, J. P. Loschnigg And R. R. Leben , 1999: Coupled Ocean-Atmosphere dynamics in the Indian ocean during 1997-98., *Nature,* **401**,356-359.

Wilkinson, 1998: *Systat version 8.0 provided to all participants of ICPAC Capacity building workshops on seasonal climate prediction.*

Wilks, D. S, 2006: Statistical methods in atmospheric sciences, *Second Edition, vol. 91, International Geophysics Series, Academic Press, Elsevier,* 627pp.

W M O ,1953: World distribution of thunderstorm days: *WMO/OMM- No.21. TP.6.*

W M O ,1960: Guide to climatological practices. *WMO - No 100. TP. 44,* Geneva, Switzerland.

W M O, 1965: Guide to hydrometeorological practices. *WMO- No. 168, TP 82* .Geneva, Switzerland.

W M O , 1966: Statistical analysis and prognosis in Meteorology, *WMO - No. 178. TP. 88, Techn. note No. 71, WMO,* Geneva, Switzerland

W M O, 1970: Guide to hydrometeorological practices. *2nd edition, WMO- No. 168. TP.* 52. WMO, 1974: Guide to hydrological practices, *3rd edition, WMO - No. 168,* Geneva, Switzerland.

W M O, 1974: Guide to hydrological practices, *3rd edition, WMO - No. 168,* Geneva, Switzerland.

W M O, 1983: Guide to Climatological practices. *WMO - No. 100,* Geneva Switzerland.

W M O, 1999: The climate in the 21st century, *Cambridge Press, London.* 240pp

W M O, 2004: *Working together for a safer world.* 27pp

W M O, 2006: WMO *Regional Disaster Prevention and Mitigation Survey* pp.

Wolter, K.,1987: The Southern Oscillation in Surface Circulation and Climate over the tropical Atlantic, Eastern Pacific and Indian Ocean as captured by cluster analysis. *J. Appl. Meteor,* **26,** 540 - 558.

Wolter, K., 1989: Modes of Tropical circulation, Southern oscillation, and Sahel rainfall anomolies. *J. Climate,* 2, 149 - 172.

Wood, K. R.and J. E. Overland, 2006: Climate lessons from the first International Polar Year. *Bull. Amer. Meteorol. Soc.,* **87,** 1685-1697.

Wu, L., F. He, Z. Liu, and C. Li, 2007: Atmospheric teleconnections of tropical Atlantic variability: Interhemispheric, tropical-extratropical, and cross-basin interactions../. *Climate***, 20, No.5,** 856-870.

Wunsch, C., and P. Heimbach, 2006: Estimated Decadal Changes in the North Atlantic Meridional Overturning Circulation and Heat Flux 1993—2004. *J. Phys. Oceanography,* 36, 2012-2024

Xian, P., and R. L. Miller, 2008:Abrupt Seasonal Migration of the ITCZ into the Summer Hemisphere, *J. Almos. Sciences,* **65, No 6,** 1878-1895

Xie , S.-P., 1999: A Dynamic Ocean-Atmosphere Model of the Tropical Atlantic Decadal Variability,./ *Climate,* **12,** 64-70.

Xie, S.-P., H. Annamalai, F. A. Schott, and J. P. McCreary Jr., 2002: Structure and mechanisms of South Indian Ocean climate variability. *J. Climate,* 15, 864-878.

Yu ,L., and M. M. Rienecker, 2000: Indian ocean warming of 1997-98., *J. Geophys. Res.,* **105,** 16 923-16 939.

Zang, C., and J. Gottschalk, 2002: SST anomalies of ENSO and the Madden-Julian Oscillation in the equatorial Pacific,. *J. Climate, 15 No. 17,* 2429-2445.

Zebiak, S.E., 2003: Research Potential for Improvement in Climate Prediction. *Bull. Amer Meteorol. Soc.,* **84,** 1692-1696.

Zwiers, W. F., and H. V. Storch, 2004: On the role of statistics in climate research., *Int. J. Climatol,* **24,** 665-680